

Evaluation Results of US-APWR Fuel System Structural Response to Seismic and LOCA Loads

Non-Proprietary Version

December 2010

**© 2010 Mitsubishi Heavy Industries, Ltd.
All Rights Reserved**

Revision History

Revision	Date	Page (section)	Description
0	Mar. 2009	All	Original issued
1	Aug. 2010	<p>The following items are revised due to:</p> <ul style="list-style-type: none"> - RAI responses [UAP-HF- 08139, 08309, 09496, 09557, 09563, 10052, 10136] - Editorial changes (errata corrections) <p>Editorial changes are made.</p> <p>Description of the irradiation effect is removed.</p> <p>ii</p> <p>iii-iv (Table of content)</p> <p>The page numbers are updated. Appendix C, D, E and F are added.</p> <p>v (List of Tables)</p> <p>The page numbers are updated.</p> <p>vi-vii (List of Figures)</p> <p>The page numbers are updated.</p> <p>1-1 (1.0)</p> <p>Editorial change is made.</p> <p>Description of the irradiation effect is removed.</p> <p>References 1-2 is updated.</p> <p>2-4 (2.2)</p> <p>Editorial change is made.</p> <p>2-5 (Table 2.2-1)</p> <p>Functional Requirement for grid spacers, top and bottom nozzles is added.</p> <p>Comments for grid spacers, top and bottom nozzles and for control rod guide thimbles are replaced with the description in Table C.2.2-1 of MUAP-07034 (R3)</p> <p>2-6 (2.3)</p> <p>Description of the design philosophy is modified.</p> <p>References of the acceptance criteria are added in Table 2.3-1.</p> <p>Editorial change is made in the Table 2.3-1</p> <p>2-7 (2.4)</p> <p>References 2-1, 2-3 are updated.</p>	

1	Aug. 2010	3-1 (3.0)	Editorial change is made in the title.
		3-1 (3.1)	Editorial change is made.
		3-3 (3.2)	Editorial change is made in the title.
		3-3 (3.2.2)	Editorial change is made.
		3-4 (3.3)	Editorial changes are made.
			Explanaton for the evaluation of the core's response during a LOCA is added.
		3-4 (3.4)	Editorial changes are made.
		3-4,5 (3.4.1)	Editorial changes are made.
		3-5 (3.4.2)	Editorial change is made.
		3-6 (3.5)	List of references is added.
		4-1 (4.0)	Composition of subsections in Section 4.0 is modified.
		4-1 (4.1)	Section title is changed.
		4-1,2 (4.1.1)	Detailed explanation of response and stress analysis in the horizontal direction is added to Subsection 4.1.1.1 in R0.
		4-2 (Figure 4.1.1-1)	Figure 4.1.1-1 is added.
		4-3 (4.1.2)	Subsection 4.1.2 is modified from Subsection 4.1.1.1 for SSE and section 4.2.1 for LOCA in R0.
			Description of the FINDS model is modified.
			Editorial change is made.
		4-4 (Figure 4.1.2-1)	Figure 4.1.2-1 is re-numbered from Figure 4.1.1.1-2 in R0. Uppermost and lowermost grid spacers are added in the figure.

1	Aug. 2010	4-5 (4.1.3)	Subsection 4.1.3 is modified from Subsection 4.1.1.2 in R0.
			Treatment of the model uncertainties and the irradiation effect is added
		4-6 (Figure 4.1.3-1)	Figure 4.1.3-1 is re-numbered from Figure 4.1.1.2.1-1 in R0.
		4-7 (Figure 4.1.3-2 (a))	Figure 4.1.3-2 (a) is added.
		4-8 (Figure 4.1.3-2 (b))	Figure 4.1.3-2 (b) is added.
		4-9 (4.1.4)	Subsection 4.1.4 is modified from Subsection 4.1.1.2.2 in R0.
			Description of EOL condition is added.
		4-10 (Figure 4.1.4-1)	Figure 4.1.4-1 is re-numbered from Figure 4.1.1.2.2-2 in R0.
		4-11 (Figure 4.1.4-2)	Figure 4.1.4-2 is re-numbered from Figure 4.1.1.2.2-3 in R0.
		4-12 (Figure 4.1.4-3)	Figure 4.1.4-3 is added.
		4-13 (Figure 4.1.4-4)	Figure 4.1.4-4 is added.
		4-14 (4.1.5)	Subsection is added.
			Outline of response analysis is added.
		4-14 (4.1.6)	Subsection 4.1.6 is modified from Subsection 4.1.2 in R0.
			Description of the stress analysis is detailed
		4-14,15 (4.1.7)	Subsection is added.
		4-16 (Figure 4.1.6-1)	Figure 4.1.6-1 is re-numbered from Figure 4.1.2-1 in R0.
		4-17 (4.2)	Section 4.2 is modified from Subsection 4.1.3 in R0.

1	Aug. 2010	4-18 (Figure 4.2-1)	Figure 4.2-1 is re-numbered from Figure 4.1.3-1 in R0.
			Editorial changes are made.
		4-19 (Figure 4.2-2)	Figure 4.2-2 is re-numbered from Figure 4.1.3-2 in R0.
		4-20 (4.3)	Section 4.3 is added.
			Outline of stress analysis is added.
		4-21 (4.4)	Section 4.4 is modified from Section 4.3 in R0.
		4-21,22,23 (4.4.1)	Subsection 4.4.1 is modified from Subsection 4.3.1 in R0.
			Evaluation procedure is detailed.
		4-24 (Table 4.4.1-1) (Table 4.4.1-2) (Table 4.4.1-3)	Table 4.4.1-1 through Table 4.4.1-3 are added.
		4-25 (Table 4.4.1-4) (Table 4.4.1-5)	Table 4.4.1-4 and Table 4.4.1-5 are added.
		4-26 (Table 4.4.1-6)	Table 4.4.1-6 is added.
		4-27 (Figure 4.4.1-1)	Figure 4.4.1-1 is added.
		4-28 (Figure 4.4.1-2)	Figure 4.4.1-2 is re-numbered from Figure 4.3.1-1 in R0.
		4-29 (Figure 4.4.1-3)	Figure 4.4.1-3 is re-numbered from Figure 4.3.1-2 in R0.
		4-30 (Figure 4.4.1-4)	Figure 4.4.1-4 is re-numbered from Figure 4.3.1-3 in R0.
		4-31 (Figure 4.4.1-5)	Figure 4.4.1-5 is re-numbered from Figure 4.3.1-4 in R0.
		4-32 (Figure 4.4.1-6)	Figure 4.4.1-6 is re-numbered from Figure 4.3.1-5 in R0.
		4-33 (Figure 4.4.1-7)	Figure 4.4.1-7 is re-numbered from Figure 4.3.1-6 in R0.

1	Aug. 2010	4-34 (Figure 4.4.1-8)	Figure 4.4.1-8 is re-numbered from Figure 4.3.1-7 in R0.
		4-35 (Figure 4.4.1-9)	Figure 4.4.1-9 is re-numbered from Figure 4.3.1-8 in R0.
		4-36 (Figure 4.4.1-10)	Figure 4.4.1-10 is re-numbered from Figure 4.3.1-9 in R0.
		4-37 (Figure 4.4.1-11(1))	Figure 4.4.1-11(1) is added.
		4-38 (Figure 4.4.1-11(2))	Figure 4.4.1-11(2) is added.
		4-39 (Figure 4.4.1-12)	Figure 4.4.1-12 is added.
		4-40 (Figure 4.4.1-13)	Figure 4.4.1-13 is added.
		4-41 (4.4.2)	Subsection is added. Evaluation procedure is detailed.
		4-42 (Table 4.4.2-1)	Table 4.4.2-1 is added.
		4-43 (Table 4.4.2-2)	Table 4.4.2-2 is added.
		4-44 (Table 4.4.2-3)	Table 4.4.2-3 is added.
		4-45 (Table 4.4.2-4)	Table 4.4.2-4 is added.
		4-46 (Table 4.4.2-5)	Table 4.4.2-5 is added.
		4-47 (Table 4.4.2-6)	Table 4.4.2-6 is added.
		4-48 (4.4.3)	Subsection 4.4.3 is modified from Subsection 4.3.2 in R0.
		4-48 (Table 4.4.3-1)	Table 4.4.3-1 is re-numbered from Table 4.3.2-1 in R0. Editorial change is made.
		4-49 (Table 4.4.3-2)	Table 4.4.3-2 is modified from Table 4.3.2-2 in R0.

1	Aug. 2010	4-50 (4.5)	Section 4.5 is added for evaluation results for rod cluster control assembly insertability and reactor coolability
		4-51 (4.6)	Reference 4-1, 4-4 and 4-5 in R0 are deleted. Reference numbers are changed: 4-2 → 4-1 4-3 → 4-2 4-6 → 4-4 References are updated. Reference 4-3, 4-5 and 4-6 are added.
		5-1 (5.0)	Editorial change is made in the title.
		5-1 (5.1.1)	Editorial changes are made. The description of RCCA location is added in the last paragraph.
		5-2 (Figure 5.1.1-1)	Editorial changes are made.
		5-5 (Figure 5.1.1-4)	Editorial changes are made.
		5-6 (5.1.2)	Editorial changes are made.
		5-6 (Table 5.1.2-1)	Editorial change is made.
		5-7 (5.2)	Editorial change is made in the title.
		5-7 (5.2.1)	Subsection 5.2.1 is modified from Subsection 5.2.1 and 5.2.2 in R0.
		5-8 (Table 5.2.1-1)	Table 5.2.1-1 is modified from Table 5.2.1-1 and 5.2.2-1 in R0.
		5-9 (5.2.2)	Subsection 5.2.2 is modified from Subsection 5.2.1 and 5.2.2 in R0.
		5-9 (Table 5.2.2-1)	Table 5.2.2-1 is modified from Table 5.2.1-1 and 5.2.2-1 in R0.
		5-10 (5.2.3)	Editorial changes are made. Reference 5-2 is re-numbered from Reference 5-1 in R0.

1	Aug. 2010	5-10 (Table 5.2.3-1)	Table 5.2.3-1 is modified.
		5-11 (5.3)	Reference number is changed: 5-1 → 5-2 Reference is updated. Reference 5-1 is added.
		6-1 (6.0)	Errata correction is made in the section title. Editorial changes are made.
		App.A	A title is modified. Description of effect of Irradiation on fuel assembly vibration characteristics is removed. This issue is discussed in App.C, App.E and App.F. Description of integrity of a cluster control rod assembly is removed. Impact test result with hydrogen absorbed grid spacers is improved.
		A-2 (Table of Contents)	The page numbers are updated.
		A-3 (List of Tables)	The page numbers are updated.
		A-4 (List of Figures)	The page numbers are updated.
		A-5 (1.0)	Description is modified due to replacement of discussion for irradiated fuel assembly vibration characteristics to Appendix C, E and F.
		A-6 (A.2.0)	Section A.2.0 is brought forward from Subsection A.3.1 in R0. Editorial changes are made.
		A-6 (A.2.1)	Section A.2.1 is brought forward from Subsection A.3.1.1 in R0. Reference A-1 is added. Figure A.2.1-1 is re-numbered from Figure A.3.1.1-1 in R0. Editorial changes are made.

1	Aug. 2010	A-7 (A.2.1)	Table A.2.1-1 is re-numbered from Table A.3.1.1-1 in R0. Editorial changes are made.
		A-8 (A.2.1)	Figure A.2.1-2 through Figure A.2.1-5 are re-numbered from Figure A.3.1.1-2 through Figure A.3.1.1-5 in R0. Table A.2.1-2 and Table A.2.1-3 are re-numbered from Table A.3.1.1-2 and Table A.3.1.1-3 in R0. Reference A-2 is re-numbered from Reference A-3 in R0. Editorial change is made.
		A-9,10 (A.2.1)	Table A.2.1-1 through Table A.2.1-3 are re-numbered from Table A.3.1.1-1 through Table A.3.1.1-3 in R0.
		A-11 (A.2.1)	Figure A.2.1-1 is re-numbered from Figure A.3.1.1-1 in R0. Explanation about release angle is added in the figure.
		A-12,13 (A.2.1)	Figure A.2.1-2 through Figure A.2.1-5 are re-numbered from Figure A.3.1.1-2 through Figure A.3.1.1-5 in R0.
		A-14 (A.2.2)	Subsection A.2.2 is brought forward from Subsection A.3.1.2 in R0. Reference A-3 is renumbered from Reference A-4 in R0. Table 2.2-1 is re-numbered form Table 3.1.1-1 in R0. Figure A.2.2-1 through Figure A.2.2-5 are re-numbered form Figure A.3.1.1-1 through Figure A.3.1.1-5 in R0. Editorial change is made.
		A-15 (A.2.2)	Table 2.2-1 is re-numbered from Table 3.1.1-1 in R0. Editorial change is made in the table's title.

1	Aug. 2010	A-16-21 (A.2.2)	Figure A.2.1-1 through Figure A.2.1-6 are re-numbered from Figure A.3.1.1-1 through Figure A.3.1.1-6 in R0.
		A-22 (A.3.0)	Section A3.0 is brought forward from Subsection A.3.2 in R0. Errata collection on the section title: EMBRITTLNESS → EMBRITTLEMENT 2 nd , 3 rd , 4 th , 5 th and 7 th paragraphs are added. Reference A-4 and A-5 is added. Reference A-1 is renumbered from Reference A-5 in R0. Editorial changes are made.
		A-22 (A.3.1)	Subsection A.3.1 is brought forward from Subsection A.3.2.1 in R0. 2 nd paragraph is added. Editorial changes are made.
		A-23 (A.3.1)	Figure A.3.0-1 is added. Reference A-6 is added.
		A-24 (A.3.1)	Figure A.3.1-1 is re-numbered from Figure 3.2.1-1 in R0.
		A-25 (A.3.2)	Subsection A.3.2 is brought forward from Subsection A.3.2.2 in R0. Editorial modification.
		A-25,26 (A.3.3)	Subsection A.3.3 is brought forward from Subsection A.3.2.3 in R0. For buckling force and impact stiffness, description in 1 st and 2 nd paragraphs is modified due to additional hydrided grid spacer test result. For plastic deformation, description in 3 rd through 5 th paragraphs is modified due to additional hydrided grid spacer test result.

1	Aug. 2010	A-27 (A.3.3)	Table A.3.3-1 is re-numbered from Table A.3.2.3-1. Additional test results of hydrided grid spacers are added in Table A.3.3-1.
		A-28 (A.3.3)	Figure A.3.3-1 is re-numbered from A.3.2.3-1 in R0. Additional test results of hydrided grid spacers are added in Figure A.3.3-1.
		A-29 (A.3.3)	Figure A.3.3-2 is added.
		A-30 (A.3.3)	Figure A.3.3-3 is re-numbered from A.3.2.3-2 in R0. Additional test results of hydrided grid spacers are added in Figure A.3.3-3 in R0.
		A-31 (A.3.3)	Figure A.3.3-4 is substituted for Figure A.3.2.3-3 and A.3.2.3-4 in R0. Figure A.3.3-5 is added.
		A-32 (A.4.0)	Section A.4.0 is brought forward from Section A.6.0.
		A-33 (A.5.0)	Section A.5.0 is brought forward from Section A.7.0.
			Reference A-1, A-2 and A-3 are re-numbered from Reference A-5, A-3 and A-4 in R0, respectively. Reference A-4 through A-6 are added. Reference A-1 and A-2 in R0 are deleted.
		B-2-10 Appendix B	Appendix B is deleted and moved to Section F.5.0
		C-1-50 Appendix C	Appendix C is added.
		D-1-50 Appendix D	Appendix D is added.
		E-1-28 Appendix E	Appendix E is added.
F-1-124 Appendix F	Appendix F is added.		

2	Dec. 2010	<p>iii-iv (Table of content)</p> <p>v (List of Tables)</p> <p>vi-vii (List of Figures)</p> <p>3-4 (3.3)</p> <p>3-6 (3.5)</p> <p>4-21 (4.4.1)</p> <p>4-22 (4.4.1)</p> <p>4-23 (4.4.1)</p> <p>4-24,25 (Table 4.4.1-1 Table 4.4.1-2 Table 4.4.1-3 Table 4.4.1-4 Table 4.4.1-5)</p> <p>4-26,27 (Table 4.4.1-6, Table 4.4.1-7)</p> <p>4-28 to 4-37 (Figure 4.4.1-2 to Figure 4.4.4-11)</p>	<p>The following items are revised due to:</p> <ul style="list-style-type: none"> - Revision of the core plate acceleration data used as input to evaluate the fuel assembly response during SSE and LOCA - Editorial changes (errata corrections) <p>The page numbers are updated.</p> <p>The list of Tables is updated.</p> <p>The list of Figures is updated.</p> <p>Document revision number is updated.</p> <p>Document revision number is updated.</p> <p>The references of the acceleration time history are modified. Reference number is updated. The section numbers of the reference are deleted.</p> <p>The references of the acceleration time history are modified. The figure numbers are updated. Reference number is updated.</p> <p>The references of the acceleration time history are modified.</p> <p>The reference to the representative wave for SSE is modified. The results are updated.</p> <p>The reference to the representative waves is modified.</p> <p>The revised acceleration time histories are shown.</p>
---	-----------	---	---

2	Dec. 2010	4-38 to 4-41 (Figure 4.4.4-12 to Figure 4.4.4-13)	The figures are updated.
		4-42 (Figure 4.4.1-14)	The reference to the representative waves is modified.
		4-43 (4.4.2)	Stress results are updated.
		4-44 to 4-49 (Table 4.4.2-1 to Table 4.4.2-6)	Figures are updated.
		4-50 (4.4.3)	The reference to the representative wave for SSE is modified. Reference number is updated.
		4-50 (Table 4.4.3-1)	Results are updated.
		4-51 (Table 4.4.3-2)	Results are updated.
		4-53 (References)	Document revision number is updated. References are updated.
		5-7 (5.2.1)	The references to the representative wave for SSE and LOCA are modified.
		5-8 (Table 5.2.1-1)	Results are updated.
		5-9 (5.2.2)	Results are updated.
		5-9 (Table 5.2.2-1)	Results are updated.
		5-10 (Table 5.2.3-1)	Results are updated.
		5-11 (References)	Document revision number is updated.
		D-44 (D.3.1)	- "14B pipe rupture" is replaced by "8B pipe rupture", "equivalent to or" is removed. - The section number of the reference is updated.
		D-47 (D.3.2)	- The section number of the reference is deleted in the first paragraph

2	Dec. 2010	D-47 (D.3.2)	- One reference is added in second paragraph, -The description of PCT is modified.
		D-48 (Figure D.3.2-1)	Figure is modified.
		D-50 (D.4.0)	List of references is updated.
		E-3 (List of Tables)	List of Tables is updated.
		E-4 (E.1.0)	The references of the acceleration time history are modified.
		E-5 (E.2.1)	Results are updated.
		E-6 to E-12 (Table E.2.1-1 to Table E.2.1-2)	The results are updated.
		E-13 (E.2.2)	The results are updated.
		E-14 to E-17 (Table E.2.2-1)	The results are updated.
		E-18 to E-25 (Table 2.2-2 to Table 2.2-9)	Grid buckling results are added.
		E-26 to E-28 (Table 2.2-10)	The results are updated.
		E-29 (E.2.3)	The results are updated.
		E-30 to E-33 (Table E.2.3-2)	The results are updated.
		E-34 (E.3.1)	The results are updated.
		E-35 (Table E.3.1-1)	The results are updated.
		E-36 (E.3.2)	The results are updated.

2	Dec. 2010	E-37 (Table E.3.2-1)	The results are updated.
		E-38 (E.4.0)	The results are updated.
		F-3 to F-7 (List of Tables)	List of Tables is updated.
		F-8 (F.1.0)	Description of the most limiting case is modified.
		F-9 (F.2.1)	Reference of the SSE wave is modified.
		F-10 to F-25 (Table F.2.1-1 to Table F.2.1-4)	The results are updated.
		F-26 (F.2.2)	Reference of the SSE wave is modified.
		F-27 to F-42 (Table F.2.2-1 to Table F.2.2-4)	The results are updated.
		F-43 (F.2.3)	Reference of the SSE wave is modified.
		F-44 to F-59 (Table F.2.3-1 to Table F.2.3-4)	The results are updated.
		F-60 (F.2.4)	Reference of the LOCA wave is modified.
		F-61 to F-76 (Table F.2.4-1 to Table F.2.4-4)	The results are updated.
		F-77 (F.2.5)	Reference of the LOCA wave is modified.
		F-78 to F-93 (Table F.2.5-1 to Table F.2.5-4)	The results are updated.
		F-95 to F-114 (Table F.3-1 to Table F.3-20)	The results are updated.

2	Dec. 2010	F-116 (F.4.0)	The results are updated.
		F-117 to F-120 (Table F.4-1 to Table F.4-4)	The results are updated.
		F-121 (F.5.2)	The results are updated.
		F-122,123 (Table F.5-1, Table F.5-2)	The results are updated.
		F-124 (F.6.0)	References of the acceleration data are modified.

© 2010
MITSUBISHI HEAVY INDUSTRIES, LTD.
All Rights Reserved

This document has been prepared by Mitsubishi Heavy Industries, Ltd. ("MHI") in connection with the U.S. Nuclear Regulatory Commission's ("NRC") licensing review of MHI's US-APWR nuclear power plant design. No right to disclose, use or copy any of the information in this document, other than by the NRC and its contractors in support of the licensing review of the US-APWR, is authorized without the express written permission of MHI.

This document contains technology information and intellectual property relating to the US-APWR and it is delivered to the NRC on the express condition that it not be disclosed, copied or reproduced in whole or in part, or used for the benefit of anyone other than MHI without the express written permission of MHI, except as set forth in the previous paragraph.

This document is protected by the laws of Japan, U.S. copyright law, international treaties and conventions, and the applicable laws of any country where it is being used.

Mitsubishi Heavy Industries, Ltd.
16-5, Konan 2-chome, Minato-ku
Tokyo 108-8215 Japan

Abstract

During a seismic event, the reactor vessel is accelerated laterally and vertically and these accelerations are transmitted to the fuel assemblies via the reactor internal structures, such as the upper core plate and the lower core support plate. The fuel assemblies respond laterally and vertically due to these accelerations. The loss of coolant accident (LOCA) event can also result in a significant fuel assembly dynamic response due to the LOCA-specific accelerations and transient flow in the core. The same type of analysis input parameters and modeling applies to the evaluation of the effects of both seismic and LOCA events.

In accordance with Standard Review Plan Section 4.2 (NUREG-0800), each fuel assembly and the core must be designed to maintain a coolable geometry and allow safe shutdown of the reactor during both seismic and LOCA events. The fuel assembly will be shown to satisfy the SRP guidelines by specific stress criteria and component deformation limits. The rod cluster control assembly (RCCA) will be shown to maintain its integrity by satisfying stress limits to provide a safe shutdown of the reactor. This document describes the evaluation method and provides the evaluation results of the US-APWR fuel system structural response to seismic and LOCA loads which show that the SRP requirements are met.

Table of Contents

List of Tables	v
List of Figures	vi
1.0 INTRODUCTION	1-1
2.0 DESCRIPTION, FUNCTIONAL REQUIREMENTS AND ACCEPTANCE CRITERIA FOR THE FUEL ASSEMBLY AND ROD CLUSTER CONTROL ASSEMBLY	2-1
2.1 Description of the Fuel Assembly and Rod Cluster Control Assembly	2-1
2.2 Functional Requirements for the Fuel Assembly and the Rod Cluster Control Assembly	2-4
2.3 Design Philosophy and Acceptance Criteria.....	2-6
2.4 References	2-7
3.0 BOUNDARY CONDITIONS OF THE FUEL ASSEMBLY AND THE ROD CLUSTER CONTROL ASSEMBLY FOR SEISMIC AND LOCA EVENTS	3-1
3.1 Structures Interacting with the Fuel Assembly and the Rod Cluster Control Assembly and Resultant Loads	3-1
3.2 Behavior of the Fuel Assembly and Rod Cluster Control Assembly for Seismic Event	3-3
3.2.1 Fuel Assembly	3-3
3.2.2 RCCA	3-3
3.3 Postulated Accident - LOCA	3-4
3.4 Behavior of the Fuel Assembly and Rod Cluster Control Assembly for LOCA	3-4
3.4.1 Fuel Assembly	3-4
3.4.2 RCCA	3-5
3.5 References	3-6
4.0 RESPONSE AND STRESS ANALYSIS OF THE FUEL ASSEMBLY FOR SSE AND LOCA EVENTS	4-1
4.1 Methodology for the Fuel Assembly Response and Stress Analysis in the Horizontal Direction	4-1
4.1.1 Overall Procedure.....	4-1
4.1.2 FINDS Code	4-3
4.1.3 Non-linear Vibration Model for the US-APWR in the FINDS Code	4-5
4.1.4 In-elastic Impact Model for Grid Spacer.....	4-9
4.1.5 Response Analysis by the FINDS Code	4-14
4.1.6 Stress Analyses by the ANSYS Code	4-14
4.1.7 Determination of Grid Spacer Buckling Occurrence	4-14
4.2 Methodology for the Fuel Assembly Response and Stress Analysis in the Vertical Direction	4-17

4.3	Stress Combination in Horizontal and Vertical Directions.....	4-20
4.4	Evaluation Condition and Results for the Fuel Assembly Response and Capability for SSE and LOCA Events	4-21
4.4.1	Input Accelerations and Vibration Characteristics of the Fuel Assembly in Horizontal Response with Uncertainties.....	4-21
4.4.2	Horizontal Response during SSE and LOCA Events.....	4-43
4.4.3	Stress Evaluation Results of the Fuel Assembly under SSE and LOCA Events.....	4-50
4.5	Evaluation Results for Rod Cluster Control Insertability and Reactor Coolability....	4-52
4.6	References	4-53
5.0	STRESS ANALYSIS OF THE ROD CLUSTER CONTROL ASSEMBLY FOR SSE AND LOCA EVENTS	5-1
5.1	Stress Evaluation Methodology for Rod Cluster Control Assembly	5-1
5.1.1	Stress Analysis Model for Rod Cluster Control Assembly.....	5-1
5.1.2	Stress Categories for the Rod Cluster Control Assembly	5-6
5.2	Stress of Rod Cluster Control Assembly during SSE and LOCA Events.....	5-7
5.2.1	Stress due to Horizontal Deflection during SSE and LOCA events	5-7
5.2.2	Stress due to Vertical Acceleration during SSE and LOCA Events.....	5-9
5.2.3	Stress Evaluation Results of Rod Cluster Control Assembly for SSE and LOCA Events.....	5-10
5.3	References	5-11
6.0	CONCLUSION	6-1
Appendix A	Effect of Irradiation on Grid Spacer Impact Behavior	
Appendix B	Parametric Study on the Sensitivity of FINDS Input Uncertainty on FINDS Analysis Results (Intentionally Blank)	
Appendix C	US-APWR Fuel Assembly Test and Modeling for the FINDS Code	
Appendix D	Grid Spacer Deformation Effect on Control Rod Insertability and Coolable Geometry	
Appendix E	FINDS Results of Response Analysis for Seismic and LOCA Horizontal Direction	
Appendix F	Worst Case Results of Response Analysis for Seismic and LOCA Horizontal Direction	

List of Tables

Table 2.2-1 Functional Requirements for the Fuel Assembly and Rod Cluster Control Assembly	2-5
Table 2.3-1 Acceptance Criteria during SSE and LOCA events.....	2-6
Table 4.4.1-1 Response Analysis Results for 560-100 with EOL Condition.....	4-24
Table 4.4.1-2 Response Analysis Results for 560-100 with EOL Condition including the Uncertainty of SSE wave	4-24
Table 4.4.1-3 Response Analysis Results for 560-100 with EOL Condition including the Uncertainty of Fuel Assembly Vibration.....	4-24
Table 4.4.1-4 Response Analysis Results for CLB 8B 102%LF with EOL Condition	4-25
Table 4.4.1-5 Response Analysis Results for CLB 8B 102%LF with EOL Condition including the Uncertainty of Fuel Assembly Vibration.....	4-25
Table 4.4.1-6 Analysis Cases per Row in FINDS for the US-APWR Fuel Assembly Horizontal Response	4-26
Table 4.4.2-1 Best Estimated Bending Stress for SSE and LOCA Horizontal Direction (Control Rod Guide Thimble).....	4-44
Table 4.4.2-2 Best Estimated Bending Stress for SSE and LOCA Horizontal Direction (Fuel Cladding)	4-45
Table 4.4.2-3 Bending Stress for SSE and LOCA Horizontal Direction (Control Rod Guide Thimble) including Uncertainties.....	4-46
Table 4.4.2-4 Bending Stress for SSE and LOCA Horizontal Direction (Fuel Cladding) including Uncertainties	4-47
Table 4.4.2-5 Buckled Grid Spacer Number for Each Fuel Assembly Position (Best Estimate Results)	4-48
Table 4.4.2-6 Buckled Grid Spacer Number for Each Fuel Assembly Position Including Uncertainties.....	4-49
Table 4.4.3-1 Peak Vertical Load for Fuel Assembly under SSE (560-100, 900-200) and LOCA (CLB 8B 102%LF) Events.....	4-50
Table 4.4.3-2 Stress for the Fuel Assembly under SSE (560-100) and LOCA (CLB 8B 102%LF) Events at Most Limiting Conditions (EOL with Uncertainties).....	4-51
Table 5.1.2-1 Stress Categories	5-6
Table 5.2.1-1 Stresses of Control Rod due to Horizontal Deflection during SSE and LOCA Events.....	5-8
Table 5.2.2-1 Stresses of Control Rod due to Vertical Acceleration during SSE and LOCA Events.....	5-9
Table 5.2.3-1 Stress Evaluation Results for Control Rod	5-10

List of Figures

Figure 2.1-1	Structural Schematic for the US-APWR Fuel Assembly	2-2
Figure 2.1-2	Structural Schematic for the US-APWR Rod Cluster Control Assembly	2-3
Figure 3.1-1	US-APWR Reactor Vessel Structures	3-2
Figure 4.1.1-1	Stress Evaluation for SSE and LOCA Response in the Horizontal Direction (Example: Control Rod Guide Thimble)	4-2
Figure 4.1.2-1	Fuel Assembly Vibration Response Analysis Model in the Horizontal Direction	4-4
Figure 4.1.3-1	Non-linear Mechanisms in a Fuel Assembly Structure	4-6
Figure 4.1.3-2 (a)	Amplitude Dependence of the US-APWR Fuel Assembly's Frequency and Damping at BOL Operating Conditions	4-7
Figure 4.1.3-2 (b)	Amplitude Dependence of the US-APWR Fuel Assembly's Frequency and Damping at EOL Operating Conditions	4-8
Figure 4.1.4-1	Comparison of Analyzed and Measured Impact Force (As-Built)	4-10
Figure 4.1.4-2	Comparison of Analyzed and Measured Plastic Deformation (As-Built)	4-11
Figure 4.1.4-3	Comparison of Analyzed and Measured Impact Force (Relaxed Spring Force)	4-12
Figure 4.1.4-4	Comparison of Analyzed and Measured Plastic Deformation (Relaxed Spring Force)	4-13
Figure 4.1.6-1	Fuel Assembly Stress Analysis Model in the Horizontal Direction	4-16
Figure 4.2-1	Stress Evaluation for SSE and LOCA Response in the Vertical Direction	4-18
Figure 4.2-2	Fuel Assembly Stress Analysis Model for Vertical Response	4-19
Figure 4.4.1-1	Limiting Input Acceleration and FA Condition for Horizontal Response ...	4-27
Figure 4.4.1-2	Acceleration Time History of the Core Plates for 270-200	4-28
Figure 4.4.1-3	Acceleration Time History of the Core Plates for 270-500	4-29
Figure 4.4.1-4	Acceleration Time History of the Core Plates for 560-100	4-30
Figure 4.4.1-5	Acceleration Time History of the Core Plates for 560-200	4-31
Figure 4.4.1-6	Acceleration Time History of the Core Plates for 560-500	4-32
Figure 4.4.1-7	Acceleration Time History of the Core Plates for 900-100	4-33
Figure 4.4.1-8	Acceleration Time History of the Core Plates for 900-200	4-34
Figure 4.4.1-9	Acceleration Time History of the Core Plates for 2032-100	4-35
Figure 4.4.1-10	Acceleration Time History of the Core Plates for LOCA (CLB 8B 102%LF)	4-36
Figure 4.4.1-11	Acceleration Time History of the Core Plates for LOCA (HLB 10B 102%LF)	4-37
Figure 4.4.1-12	Fuel Assembly Time History Response (SSE 560-100) (0 – 8 sec)	4-38

Figure 4.4.1-13 Fuel Assembly Time History Response (LOCA CLB 8B 102%LF)	4-41
Figure 4.4.1-14 Uncertainty Consideration for SSE Frequency and FA Vibration Characteristics	4-42
Figure 5.1.1-1 Stress Evaluation for the Control Rod Assembly due to Fuel Assembly Horizontal Deflection during SSE and LOCA Events.....	5-2
Figure 5.1.1-2 Axial Positions of RCCA for Stress Evaluation.....	5-3
Figure 5.1.1-3 Analysis Model for RCCA.....	5-4
Figure 5.1.1-4 Stress Evaluation for the Control Rod Assembly due to Vertical Acceleration during SSE and LOCA Events.....	5-5

1.0 INTRODUCTION

The US-APWR fuel assembly (referred to simply as 'FA' below), is an important structural component of the core. The array of fuel assemblies is contained by a core support structure placed within the reactor vessel, and during operation is subject to coolant flow at high temperature and pressure. With respect to the Standard Review Plan, Section 4.2 (NUREG-0800) ⁽¹⁻¹⁾, the fuel assembly must be able to maintain core coolability (coolable geometry) and the control rod insertion for safe reactor shutdown during both seismic and loss of coolant accident (LOCA) events. The fuel assembly must be designed to fulfill those functions.

The US-APWR rod control cluster assembly (referred to simply as 'RCCA' below) is also an important structural component of the core. It is almost fully withdrawn from the fuel assembly during normal operation, but needs to be inserted rapidly into the fuel assembly to shut down the reactor. The RCCAs must be designed to maintain their insertion function during seismic and LOCA events.

Based on Reference 1-2, this report describes the functional requirements for the fuel assembly and the RCCA, the design philosophy, the acceptance criteria, the evaluation methodologies to demonstrate that the functional requirements for the fuel assembly and the rod cluster control assembly are maintained in the seismic and LOCA events, and the evaluation results.

References

- (1-1) U.S. Nuclear Regulatory Commission, Standard Review Plan (NUREG-0800) Section 4.2, March 2007
- (1-2) "Mitsubishi Fuel Design Criteria and Methodology", MUAP-07008-P(R2) (Proprietary) and MUAP-07008-NP(R2) (Non-Proprietary), July 2010

2.0 DESCRIPTION, FUNCTIONAL REQUIREMENTS AND ACCEPTANCE CRITERIA FOR THE FUEL ASSEMBLY AND ROD CLUSTER CONTROL ASSEMBLY

2.1 Description of the Fuel Assembly and Rod Cluster Control Assembly

The structure of the US-APWR fuel assembly is shown in Figure 2.1-1. The fuel assembly is comprised of a 17 x 17 square array of 264 fuel rods, 24 control rod guide thimbles, and one guide tube for in-core instrumentation, as well as eleven grid spacers, one top nozzle and one bottom nozzle. As shown in Figure 2.1-2, the RCCA consists of one spider and 24 control rods attached to the spider.

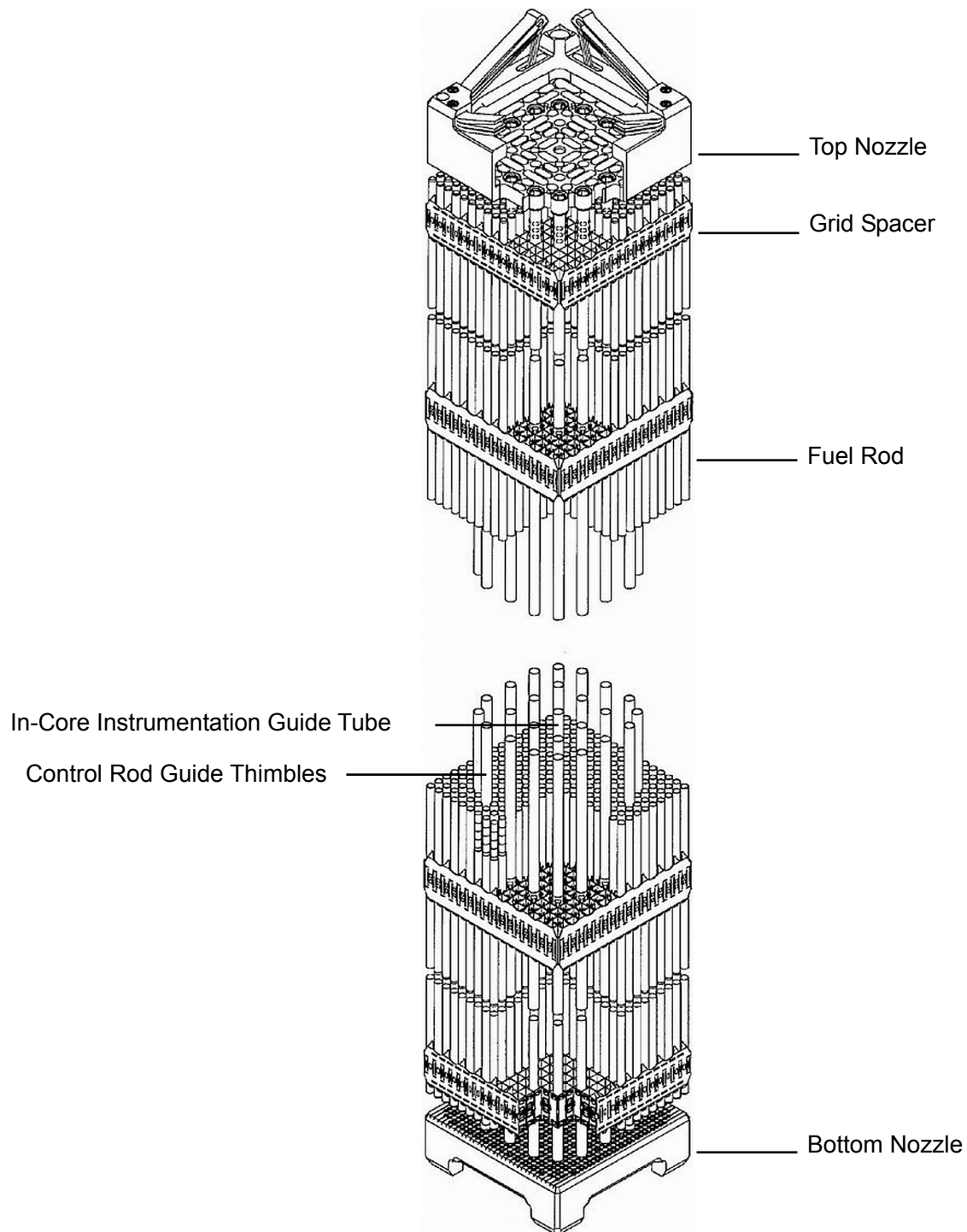


Figure 2.1-1 Structural Schematic for the US-APWR Fuel Assembly

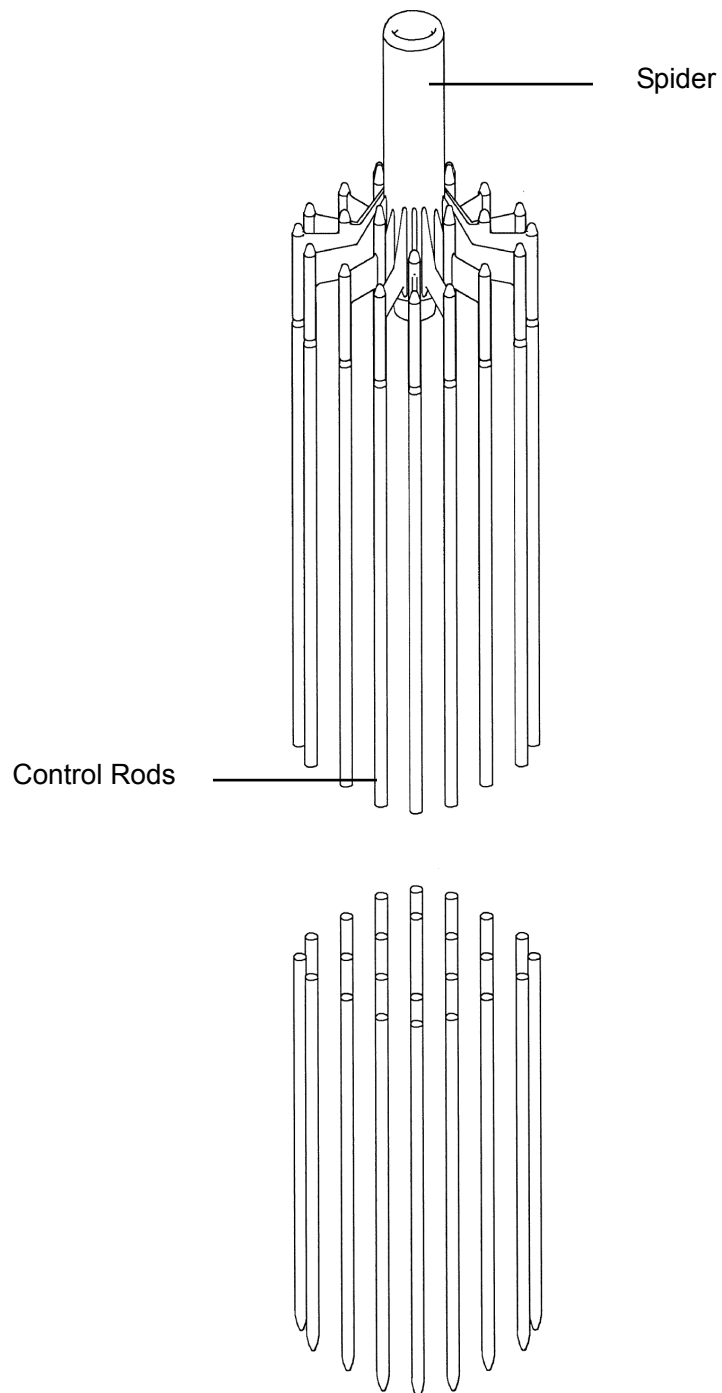


Figure 2.1-2 Structural Schematic for the US-APWR Rod Cluster Control Assembly

2.2 Functional Requirements for the Fuel Assembly and the Rod Cluster Control Assembly

In Section 3.7.1 of Reference 2-1, it is stated that the Operating Basis Earthquake (OBE) accelerations are assumed to be limited to 1/3 of the Safe Shutdown Earthquake (SSE) accelerations and therefore, in accordance with Appendix S of 10 CFR 50⁽²⁻²⁾, it is not required to perform an explicit response or design analysis for the OBE.

The evaluation for the fuel assembly and the RCCA during an SSE event is described in this report. The functional requirements for the fuel assembly and the rod cluster control assembly during an SSE are described in this section and in Reference 2-3.

In accordance with SRP Section 4.2⁽²⁻⁴⁾, the fuel assembly and the RCCA must be designed to maintain a coolable geometry of the core and maintain control rod insertion function to shut down the reactor safely during both SSE and LOCA events. The safety functions of the US-APWR fuel assembly and the RCCA components, to ensure this capability, are listed in Table 2.2-1.

Table 2.2-1 Functional Requirements for the Fuel Assembly and Rod Cluster Control Assembly

Component	Functional Requirements	Comments
Grid spacers, top and bottom nozzles	Maintaining coolable geometry of the core	These bundle the fuel cladding to prevent major damage to the fuel and maintain the structure of the fuel assembly.
	Safe reactor shutdown	These maintain the arrangement of the control rod guide thimbles to retain adequate control rod insertion capability.
Control rod guide thimbles	Maintaining coolable geometry of the core	Connect the top and bottom nozzles and the grid spacers; also maintain the core shape by supporting the fuel rods via the grid spacers.
	Safe reactor shutdown	Maintaining the path for insertion of the control rod into the fuel assembly.
Fuel cladding	Maintaining coolable geometry of the core	Fuel cladding fragmentation must not occur.
Control rod cladding and top end plug	Safe reactor shutdown	Maintain geometry of RCCA to allow insertion of control rods into the fuel assembly.

2.3 Design Philosophy and Acceptance Criteria

To maintain the functions listed in Table 2.2-1, each component must be designed to have the required strength.

There are, however, no specific acceptance criteria regarding the strength requirements for these components during SSE and LOCA events in the ASME Code Section III ⁽²⁻⁵⁾ or SRP Section 4.2 ⁽²⁻⁴⁾ except for fuel cladding. Therefore, the basis for the acceptance criteria defined in the ASME Code Section III Subsection NG ⁽²⁻⁵⁾ for core support structures, which have the same safety functions as the fuel assembly and the RCCA, will be applied to these components.

For the control rod guide thimbles, an acceptance criterion related to buckling under vertical load is included to assure that the effects of this deformation mechanism will not interfere with control rod insertion. For the grid spacers, which maintain the spacing of the control rod guide thimbles and fuel rods, there are additional acceptance criteria with regard to maintaining the coolable geometry of the core and control rod insertability.

The specific acceptance criteria are presented in Table 2.3-1.

Table 2.3-1 Acceptance Criteria during SSE and LOCA events

Structural Component	Acceptance Criteria		Reference
	Primary General Membrane Stress	Primary Membrane Stress + Primary Bending Stress	
Control Rod Guide Thimble Top and Bottom Nozzles	Min. (2.4 Sm, 2/3 Su) *1	Min. (3.6 Sm, Su)	*2
Fuel Cladding	90% of the irradiated yield stress		*3
Control Rod Guide Thimble	Shall not buckle when subjected to vertical compressive load		*4
Grid Spacer	No excessive deformation shall occur due to horizontal load		*5
Cladding and top end plug of control rod	Min. (2.4 Sm, 2/3 Su)	Min. (3.6 Sm, Su)	*2

*1: Sm is the allowable stress intensity value; Su is ultimate tensile stress.

*2: Paragraph F-1331.1 of Appendix F in Section III of ASME code ⁽²⁻⁵⁾.

*3: Subsection IV.1 and IV.2 of SRP Section 4.2 Appendix A ⁽²⁻⁴⁾.

*4: Subsection 1.B.viii of SRP Section 4.2 ⁽²⁻⁴⁾.

*5: Subsection III.2 of SRP Section 4.2 Appendix A ⁽²⁻⁴⁾.

2.4 References

- (2-1) "US-APWR Design Control Document", MUAP-DC003 Revision 2, October 2009
- (2-2) Earthquake Engineering Criteria for Nuclear Power Plants, Domestic Licensing of Production and Utilization Facilities, Energy. Title 10 Code of Federal Regulations Part 50, Appendix S, Part IV(a)(1)(i), U.S. Nuclear Regulatory Commission, Washington, DC.
- (2-3) "Mitsubishi Fuel Design Criteria and Methodology", MUAP-07008-P (Proprietary) and MUAP-07008-NP (Non-Proprietary) Revision 2, July 2010
- (2-4) U.S. Nuclear Regulatory Commission, Standard Review Plan (NUREG-0800) Section 4.2, March 2007
- (2-5) American Society of Mechanical Engineers Boiler and Pressure Vessel Code Section III

3.0 BOUNDARY CONDITIONS OF THE FUEL ASSEMBLY AND THE ROD CLUSTER CONTROL ASSEMBLY FOR SEISMIC AND LOCA EVENTS

3.1 Structures Interacting with the Fuel Assembly and the Rod Cluster Control Assembly and Resultant Loads

The fuel assembly is placed inside the reactor vessel as shown in Figure 3.1-1. The reactor vessel also contains structures that support the fuel assemblies, guide the control rods, and form paths for coolant flow. The upper core plate, the lower core support plate, the core support columns, and other such structures that support the fuel assemblies are referred to as the core support structures. The fuel assembly is supported within the core barrel by the upper core plate and the lower core support plate, and is laterally positioned by pins attached to the upper core plate and the lower core support plate. It is also surrounded by neutron reflector plates that constrain the periphery of the core.

During normal operating conditions, the RCCA drive rod is engaged with the control rod drive mechanism (CRDM) at about its mid-point and with the RCCA spider hub at its bottom. The drive rod and RCCA spider/rods are supported laterally, above the upper core plate by a series of guide plates within the upper internals guide columns when the RCCA is withdrawn from the fuel assembly. Only the tip of the control rod is in the fuel assembly during normal operation.

During normal reactor operation, the hydraulic lift force, gravity and buoyant force act on the fuel assembly in addition to the mechanical force from the fuel assembly holddown springs to prevent liftoff of the fuel assembly. During a seismic event, the motion of the reactor vessel results in loads on the fuel assembly. During a LOCA event pressure fluctuations and hydraulic flow fluctuations occur in the reactor vessel which result in reactor internals motion and loads on the fuel assemblies.

For the RCCA, the vibration of the reactor vessel due to a seismic event is transmitted to the RCCA by way of the upper internals guide column's guide plates. When a LOCA occurs, the loads that accompany pressure fluctuations and hydraulic flow fluctuations in the reactor vessel act on the RCCA. The motions of the RCCA during seismic and LOCA events must not prevent safe shutdown of the reactor.

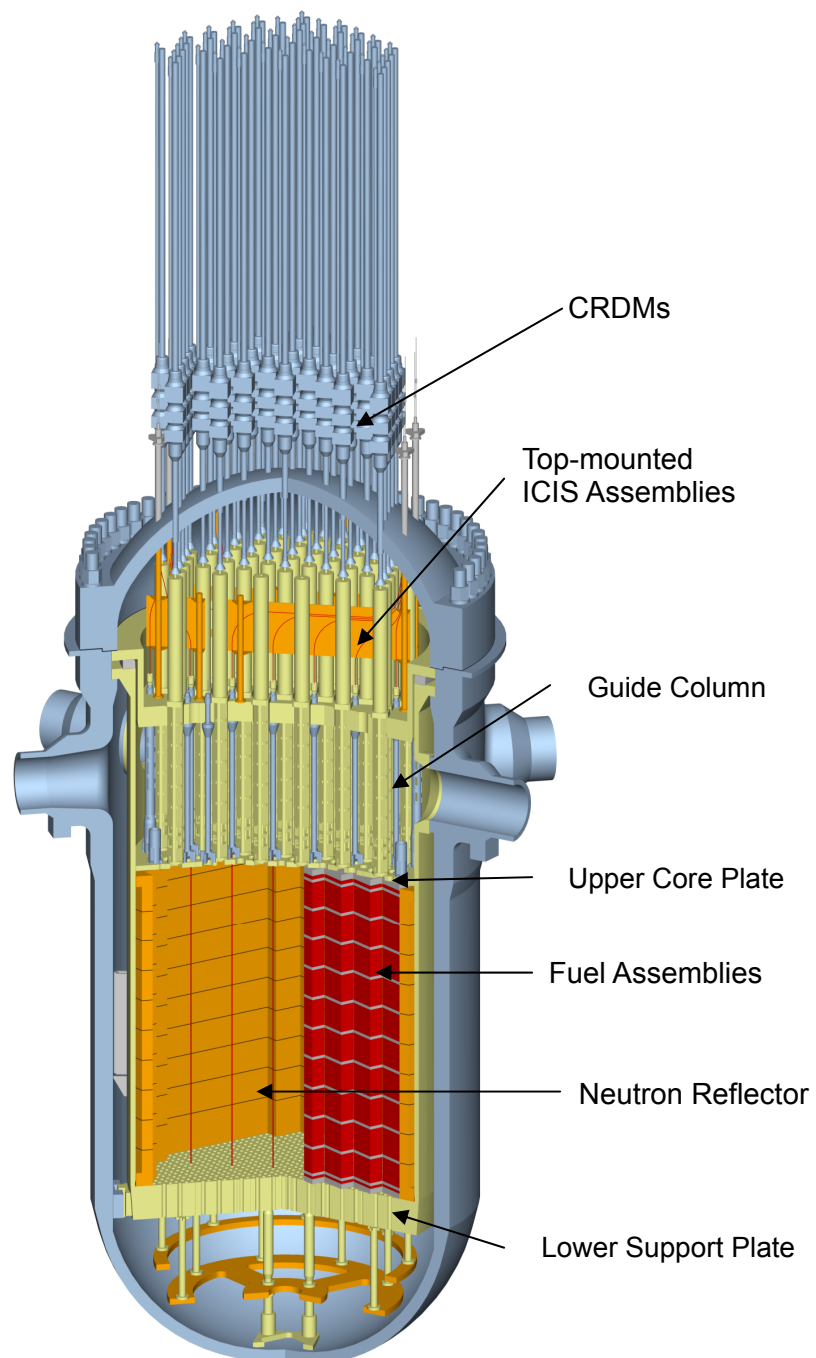


Figure 3.1-1 US-APWR Reactor Vessel Structures

3.2 Behavior of the Fuel Assembly and Rod Cluster Control Assembly for Seismic Event

The source of vibration and resultant loads on the fuel assembly and the RCCA during a seismic event are described below.

3.2.1 Fuel Assembly

- The seismic event starts with the ground motion (accelerations) resulting in vibration of the reactor building which leads to the vibration of the reactor vessel.
- The vibration of the reactor vessel is accompanied by vibration of the upper core plate and the lower core support plate that support the ends of the fuel assemblies.
- The upper core and the lower core support plates vibrate in both the vertical and horizontal directions, resulting in vibration of the fuel assemblies supported by the plates. The neutron reflector plates act as rigid beams with the top and bottom ends connected/moving with the upper core plate and lower core support plate, respectively.
- The magnitude and phase of the acceleration that act on every fuel assembly (through the upper core plate and lower core support plate core pins) are the same due to the horizontal rigidity of the upper core and lower core support plates. Therefore, the ends of all fuel assemblies move synchronously. If the vibration is large, the displacement of the outermost fuel assemblies is limited by the neutron reflector or the gap between adjacent assemblies. Therefore collisions may occur with the neutron reflector plates or adjacent fuel assemblies at the grid spacers, which affect the horizontal vibration behavior of each fuel assembly.
- Vertical vibration of the upper core plate and the lower core support plate act on the fuel assembly in the form of a compressive load due to the variation of distance between these plates. If the vertical acceleration of the lower core support plate is large, it may cause the fuel assembly to lift off the lower core support plate and impact back into contact with the lower core support plate. As the transient subsides, the fuel assembly will come back into contact with the lower core support plate in its original alignment.

3.2.2 RCCA

- Vibration of the reactor building caused by the seismic event leads to the vibration of the reactor vessel.
- The vibration of the reactor vessel is accompanied by vibration of the CRDMs and the guide plates in the upper internals guide columns that support the RCCAs.
- The horizontal vibration is transmitted to the RCCAs by way of the guide plates and the vertical vibration is transmitted by way of the CRDMs.
- The horizontal displacement of the RCCA control rod caused by the guide plate vibration is limited by the short span between the guide plates.
- During RCCA insertion into the fuel assembly, either by CRDM stepping or scram, the RCCA is kept in alignment by the guide plates in the guide column and by the fuel assembly guide thimbles. The shape of the portion of the RCCA control rod in the fuel assembly guide thimble is essentially the same as that of the fuel assembly during the seismic event.

3.3 Postulated Accident - LOCA

Of the postulated design basis accidents, LOCA event involves a large fluctuation of pressure and hydraulic flow inside the reactor, which result in significant loads on the fuel assembly and the RCCA.

In a LOCA event caused by failure of a coolant pipe, a decompression wave is generated at the point of failure which envelopes the core barrel vertically and circumferentially. This creates a time differential in the arrival of the decompression wave around the core that gives rise to loads, thus inducing vibration in the core. The detailed explanation of the evaluation of the core's response during a LOCA event is provided in technical report MUAP-09002-P(R2)⁽³⁻¹⁾.

The acceleration history of the core plates during a LOCA event is input to the FINDS code for analyzing the fuel assemblies' response. To generate the LOCA acceleration history, an analysis of the reactor coolant system's (RCS) thermal hydraulic transient and an analysis of the reactor vessel and reactor internal's dynamic responses are needed. The RCS thermal hydraulic transient during the blowdown stage of LOCA is analyzed using the MULTIFLEX code, which is described in Subsection 3.9.1.2.1 of Reference 3-2. The abrupt RCS pressure reduction, due to the pipe break results in the propagation of a high speed pressure wave in the RCS. The time required for the propagation of the wave around the core barrel creates a pressure differential across the core barrel. This pressure differential results in the vibration of the reactor internals and core barrel. The 3-dimensional dynamic response of the reactor vessel and reactor internals (due to the pressure fluctuations inside the reactor vessel analyzed by the MULTIFLEX code) are analyzed by the ANSYS FEM code. The horizontal time history displacements of the upper and lower core support plates and the vertical loads between the core plates and the fuel assembly nozzles are calculated in this FEM analysis.

3.4 Behavior of the Fuel Assembly and Rod Cluster Control Assembly for LOCA

The fuel assembly and the RCCA behavior during LOCA event are described below.

3.4.1 Fuel Assembly

- Because the upper core plate and the lower core support plate vibrate in both the horizontal and vertical directions due to the LOCA event, the fuel assemblies supported by them are vibrated by the LOCA event as well. The neutron reflector plates act as rigid beams with the top and bottom ends connected/moving with the upper core plate and lower core support plate, respectively.
- The horizontal vibration of the upper core and the lower core support plates during LOCA event is at the fundamental frequency of the core barrel. Because the primary vibration component is near 10 Hz, the fuel assemblies respond in a tertiary mode near their natural frequency. As with the seismic response in Section 3.2, the magnitude and phase of the acceleration that act on the fuel assemblies due to the vibration of the upper and lower support points are the same, and therefore the ends of all fuel assemblies vibrate synchronously. If the vibration is large, however, the displacement of the outermost fuel assemblies is limited by the neutron reflector or the gap between adjacent assemblies. Therefore collisions may occur with the neutron reflector plates or adjacent fuel assemblies at the position of the grid spacers, which affects the horizontal vibration behavior of each fuel assembly.

- The vertical response of the fuel assembly is analyzed in a similar manner to the seismic event analysis in terms of the internals response, but there are also significant transient axial flow effects that act on the fuel assembly that may cause it to lift off the lower core support plate and impact back into contact with the lower core support plate. As the flow subsides during the LOCA event the fuel assembly will come back into contact with the lower core support plate in its original alignment.

3.4.2 RCCA

- The horizontal acceleration is transmitted to the RCCAs by way of the guide plates in the upper internals guide columns and the vertical acceleration is transmitted by way of the CRDMs into the RCCA drive rods.
- As with the seismic response in Section 3.2, the displacement of the RCCA in the horizontal direction caused by the upper internals guide column guide plate vibration is limited by the short span between the guide plates.
- The vertical acceleration of the CRDM results in axial stresses in the control rod cladding, the control rod top end plug, and the RCCA spider assembly components.
- During RCCA insertion into the fuel assembly, either by CRDM stepping or scram, the RCCA is kept in alignment by the guide plates in the guide column and by the fuel assembly guide thimbles. The shape of the portion of the RCCA control rod in the fuel assembly guide thimble is essentially the same as that of the fuel assembly during the LOCA event.

3.5 References

- (3-1) "Summary of Seismic and Accident Load Conditions for Primary Components and Piping", MUAP-09002-P (Proprietary) Revision 2, December 2010
- (3-2) "US-APWR Design Control Document", MUAP-DC003 Revision 2, October 2009

4.0 RESPONSE AND STRESS ANALYSIS OF THE FUEL ASSEMBLY FOR SSE AND LOCA EVENTS

Individual responses of the fuel assembly in the horizontal and vertical directions are analyzed for SSE and LOCA events, and followed by stress analyses. The independently calculated fuel assembly stresses for SSE and LOCA events in the horizontal and vertical directions are combined by SRSS. The SRSS stress value is added to the stress due to normal operation and the result is compared to the acceptance limit.

4.1 Methodology for the Fuel Assembly Response and Stress Analysis in the Horizontal Direction

4.1.1 Overall Procedure

- (1) For determining the US-APWR fuel assembly's response to SSE and LOCA events, there are several kinds of upper core and lower core support plate accelerations available. Response to the input accelerations depends on specific fuel assembly vibration characteristics such as BOL and EOL conditions. Therefore, the combination of input accelerations, independently for SSE and LOCA events, and the fuel assembly condition which results in the maximum horizontal response of the fuel assembly is defined as a "base" case input. The base case input then has applied to it a range of other parameters to determine the combination of the limiting base case with the parameter that produces a further more limiting result.
- (2) The influence of frequency uncertainty for the limiting SSE acceleration above is investigated. Several accelerations whose frequency is varied from the original SSE acceleration are analyzed using the limiting fuel assembly condition (BOL or EOL) and the most limiting result is used to define the frequency uncertainty of SSE acceleration.
- (3) As part of the above two stages, best estimate vibration characteristics of the fuel assembly such as amplitude dependency of frequency and damping ratio are used. As described in Appendix C, however, there are uncertainties in the amplitude dependency of frequency and damping ratio for the fuel assembly, and combinations of best estimate, upper bound and lower bound of the each dependence are parametrically analyzed using the base case input. The most limiting result is used to define the uncertainty with respect to the fuel assembly vibration characteristics.
- (4) After determining the limiting base case input for SSE and LOCA accelerations, the limiting fuel assembly condition (BOL/EOL), the limiting fuel assembly amplitude dependency (frequency and damping ratio) and the limiting SSE frequency uncertainty, a series of SSE and LOCA analyses are conducted, as schematically shown in Figure 4.1.1-1⁽⁴⁻¹⁾. The fuel assembly horizontal response to SSE and LOCA events, such as the displacement of the fuel assembly and the impact force at grid spacers (between fuel assemblies and neutron reflectors) are independently analyzed modeling {
The horizontal displacements obtained are used in the fuel assembly stress analyses. The maximum bending stress results in the horizontal X and Z directions for each axial position of each fuel assembly during both events are combined by the Square Root of the Sum of the Squares (SRSS) method. The process described above is explained in the following subsections, with the example being for the control rod guide thimble. The bending stresses of the fuel rod cladding are obtained in the same manner.

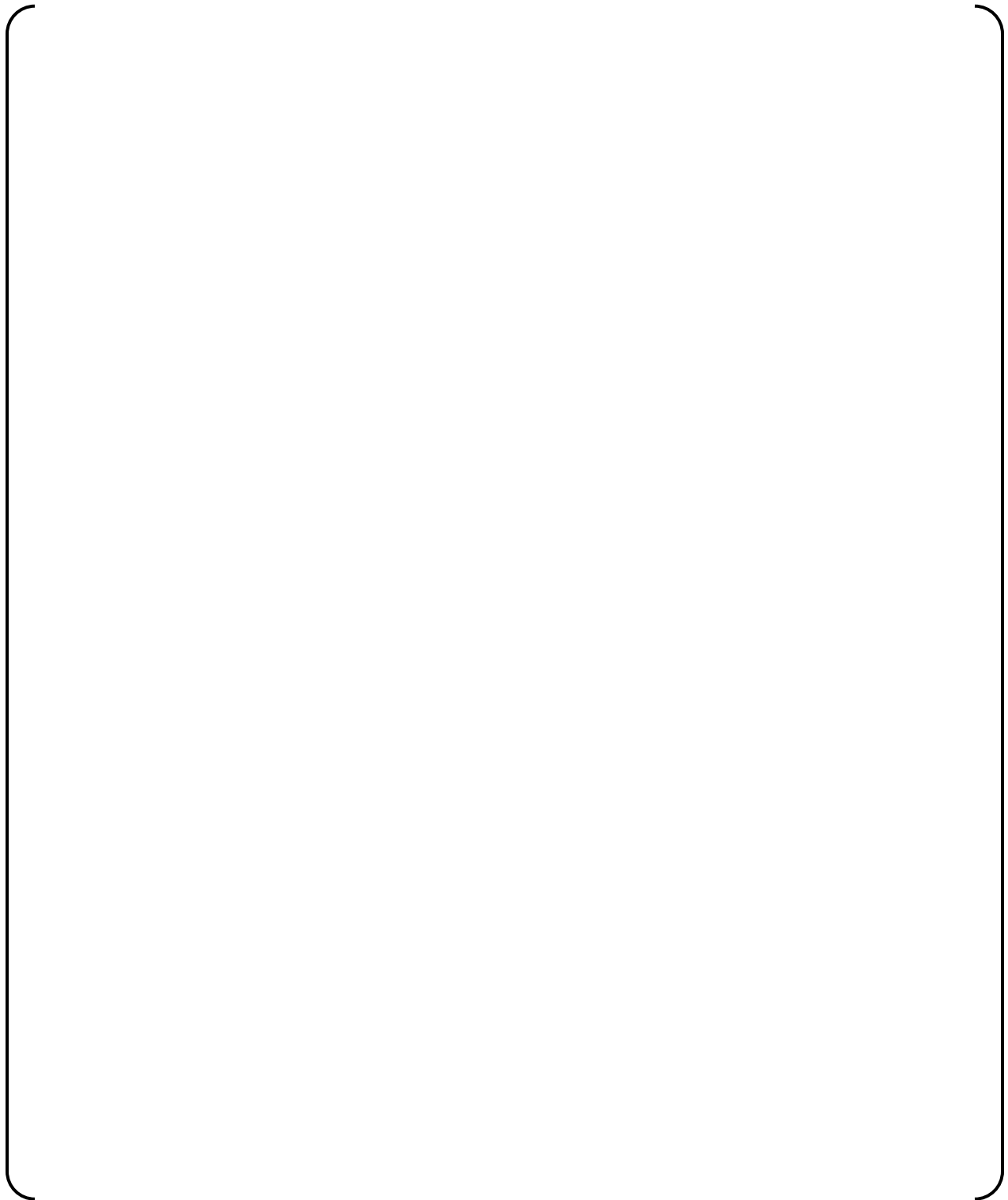


Figure 4.1.1-1 Stress Evaluation for SSE and LOCA Response in the Horizontal Direction (Example: Control Rod Guide Thimble)

4.1.2 FINDS Code

The FINDS code ⁽⁴⁻¹⁾ is used for the analysis of the fuel assembly horizontal response. The FINDS code was originally developed by MHI for seismic response analysis of an array of fuel assemblies and can also be applied to the analysis for LOCA event since the models necessary to determine the fuel assemblies' horizontal response under LOCA event is the same as for the SSE event, as described in Section 3.4. The vibration model of the fuel assembly in the FINDS is based on empirically-confirmed models for not only the 1st mode response but also higher vibration modes in term of natural frequencies and vibration mode shapes. The deformation characteristics obtained by grid spacer impact tests are included in the model and determine the collision characteristics of the grid spacers.

The FINDS code was verified and validated in compliance with the MHI quality assurance program as described in Appendix D of Reference 4-2.

The analysis model for the case with 17 fuel assemblies in a row, the maximum for the US-APWR, is shown in Figure 4.1.2-1 ⁽⁴⁻¹⁾. The individual fuel assembly is modeled with beam elements using the finite element method (FEM). Spring elements that correspond to the stiffness of the grid spacers and damping elements to model rebound characteristics are placed at the grid spacer positions to obtain the collision behavior. The upper and lower ends of the beam models are connected to the upper core and the lower core support plates which are modeled as laterally rigid. The neutron reflector located adjacent to the outermost fuel assemblies, is modeled as a rigid wall. The effect of the coolant inside the core is taken into account as an additional mass to the actual mass of the fuel assembly, and the resultant vibration characteristics (the specific frequency of the fuel assembly and the attenuation constant) are used in the analyses.

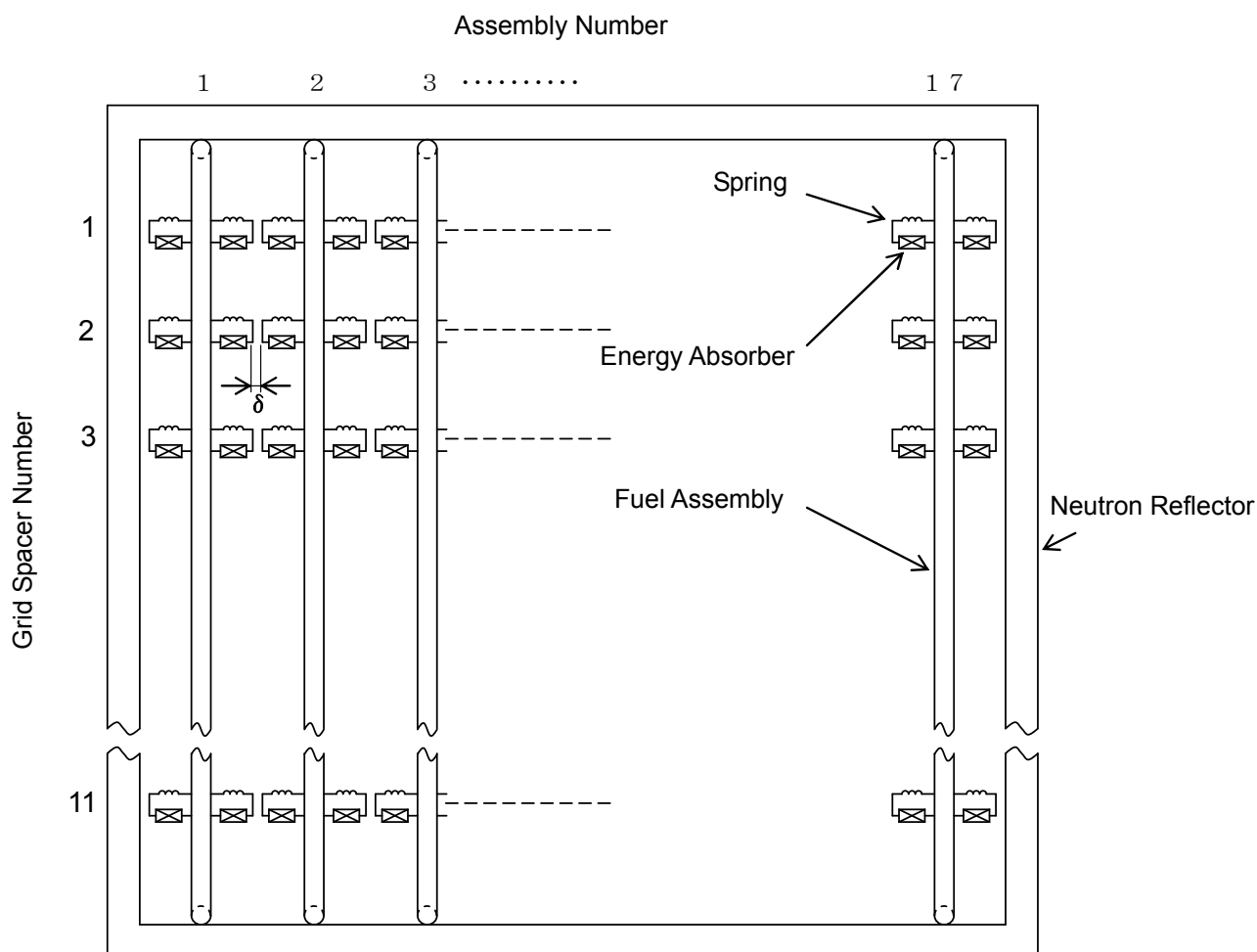


Figure 4.1.2-1 Fuel Assembly Vibration Response Analysis Model in the Horizontal Direction

4.1.3 Non-linear Vibration Model for the US-APWR in the FINDS Code

The FINDS code is characterized by its ability to account for the non-linearity of the fuel assembly's vibration characteristics and the grid spacer impact behavior. A description of these behaviors for the US-APWR fuel assembly, used in the FINDS analysis, is described in this section. In the response analysis of the FINDS code, the uncertainty band on the FINDS results for the expected range of damping and frequency sensitivities is evaluated. Moreover, the variation of the fuel assembly vibration characteristics and the impact characteristics of the grid spacers, resulting from irradiation, are also conservatively considered in the model by choosing the most limiting combination of inputs for evaluation considering the varying characteristics of the fuel assembly over its lifetime.

There are strong amplitude dependencies for a PWR fuel assembly, especially for the 1st mode vibration damping and frequency. These characteristics are due to the contact mechanism between the fuel rods and grid spacers as shown in Figure 4.1.3-1. Since the fuel rods are axially supported only by the friction interaction with the grid spacers, the axial and lateral slippage and/or the lift-off of fuel rods from the supporting grid spacer springs and dimples becomes increasingly significant as the deflection of the fuel assembly increases. The friction effects result in an energy loss during each vibration cycle of the fuel assembly, and are a primary cause of the damping variation. The softening of the fuel assembly lateral stiffness at larger deflections is due to a reduced contribution of fuel rod stiffness to the overall fuel assembly stiffness as more rods are slipping. This reduced overall fuel assembly stiffness causes a decrease in the natural frequency.

The amplitude dependence of the natural frequency and damping is considered in the FINDS analysis. The relationship can be determined based on the results from the fuel assembly lateral pluck test in air and water. By using these test data, a vibration model at the BOL condition for the US-APWR fuel assembly in the FINDS code is determined. Test procedures, results and the model tuning process are discussed in Appendix C of this report.

The vibration characteristics of the fuel assembly can change due to relaxation of the grid spacer springs. Therefore, {

The process is also discussed in Appendix C of this report.

The amplitude dependency of frequency and damping for the US-APWR models at BOL and EOL operating conditions are shown in Figure 4.1.3-2 (a) and (b).

The US-APWR BOL and EOL models are used in the FINDS code analysis for a spectrum of SSE and LOCA acceleration histories and the most limiting model determined is used in the stress analyses.

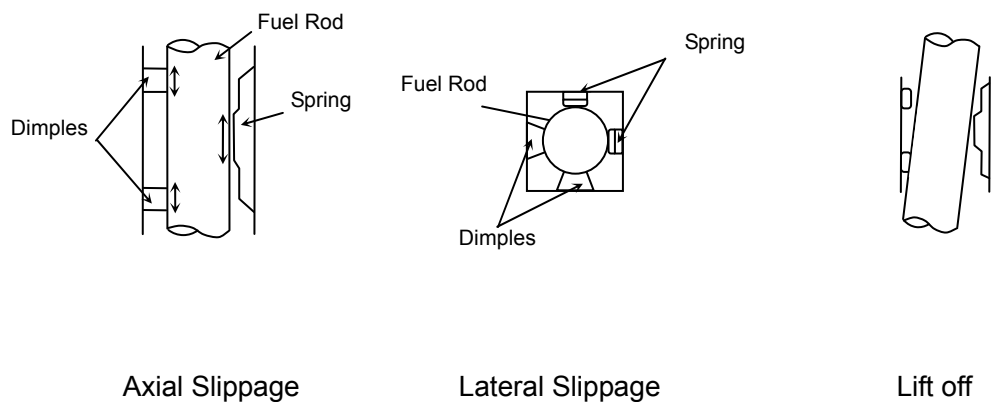
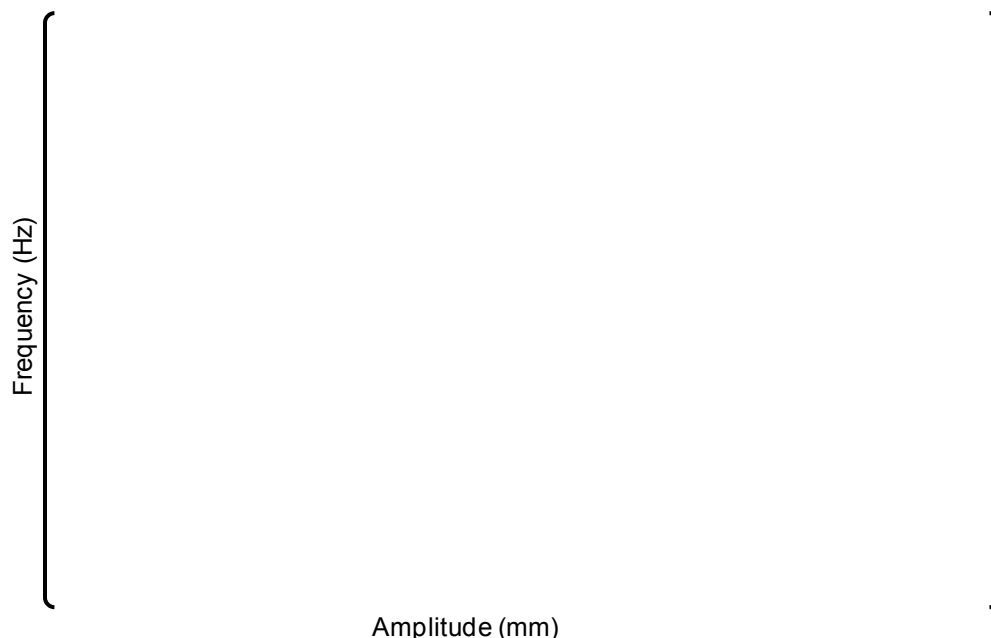
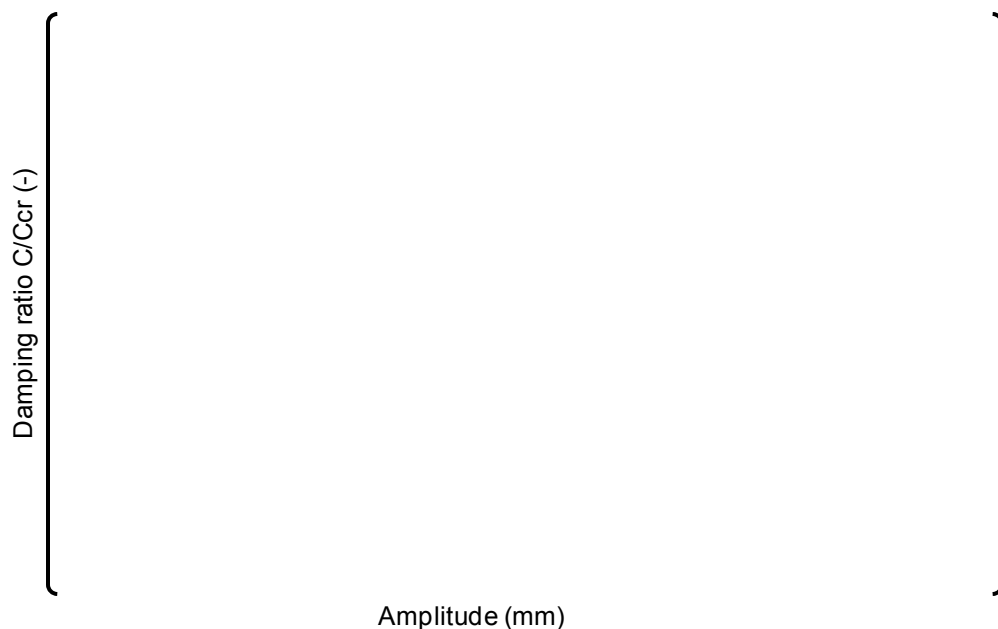


Figure 4.1.3-1 Non-linear Mechanisms in a Fuel Assembly Structure

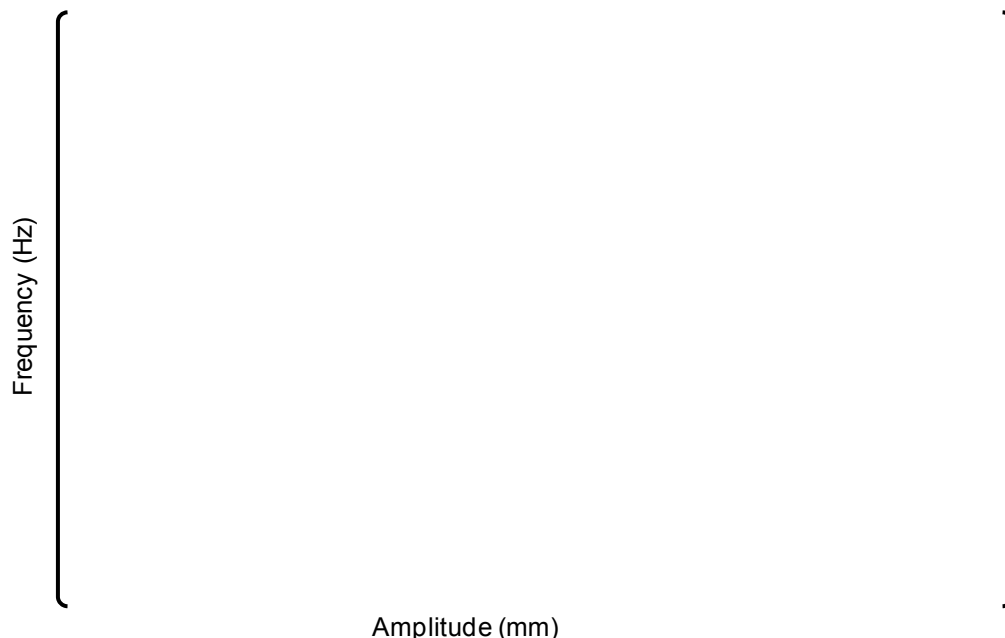


(i) Natural Frequency – BOL 1st Mode

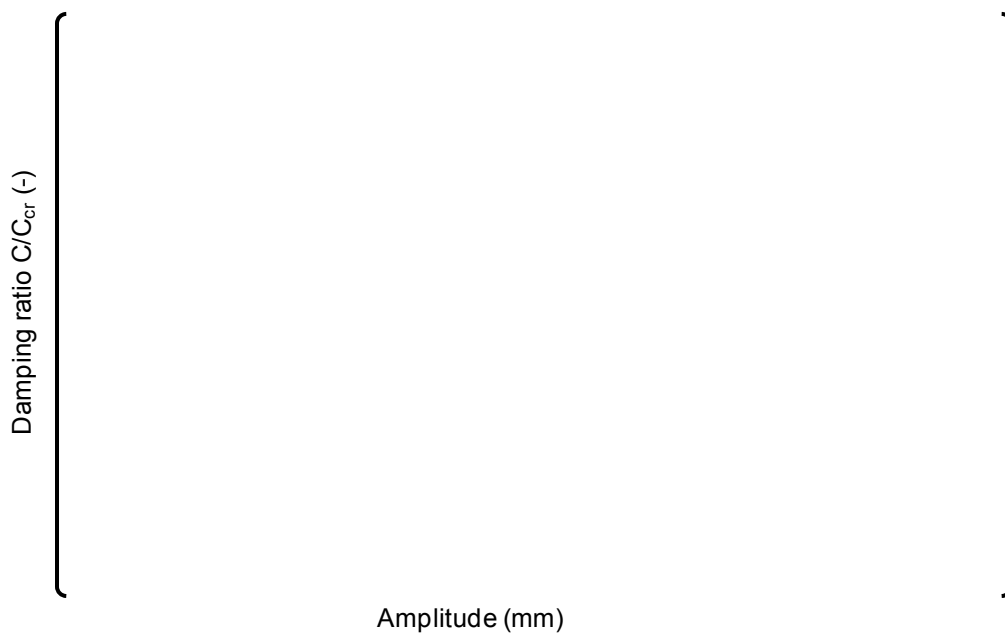


(ii) Damping Ratio – BOL 1st Mode

Figure 4.1.3-2 (a) Amplitude Dependence of the US-APWR Fuel Assembly's Frequency and Damping at BOL Operating Conditions



(i) Natural Frequency – EOL 1st Mode



(ii) Damping Ratio – EOL 1st Mode

Figure 4.1.3-2 (b) Amplitude Dependence of the US-APWR Fuel Assembly's Frequency and Damping at EOL Operating Conditions

4.1.4 In-elastic Impact Model for Grid Spacer

In order to solve for the multi-fuel assembly impacting interaction, one grid spacer is modeled by a spring and a damper element pair, located on both sides of the beam because impacting needs to be considered to occur on both sides of the fuel assembly.

When the impact force at the grid spacer exceeds its buckling load, the plastic deformation due to buckling occurs in one row of grid spacer cells and propagates to the next row depending on the impact force generated in later impacts. As mentioned above, semi-empirical rules are used in the FINDS code to express the grid spacer deformation progress. They are derived from the experimental results obtained by the "pendulum and grid spacer" type impact and deformation tests as described in Appendix A of this report. Therefore, two types of grid spacers, ones with as-built spring force and ones with relaxed spring force, are impact tested to generate FINDS in-elastic models for the US-APWR at BOL and EOL conditions, respectively. The test results and tuned FINDS in-elastic model results for the BOL condition are shown in Figure 4.1.4-1 and Figure 4.1.4-2, for the impact force versus test sequence and the plastic deformation versus test sequence, respectively. In the same way as for the BOL condition, the results for the EOL condition are shown in Figure 4.1.4-3 and Figure 4.1.4-4. These figures are for test grid spacers identified as As-Built 5, As-Built 6, Relaxed_7 and Relaxed_8, which are the as-built and relaxed spring grid spacers which were tested to determine the post-buckling force versus deformation characteristics, as explained in Appendix A of this report.

The US-APWR fuel assembly in-elastic models for BOL and EOL conditions are added to the FINDS code beam models.

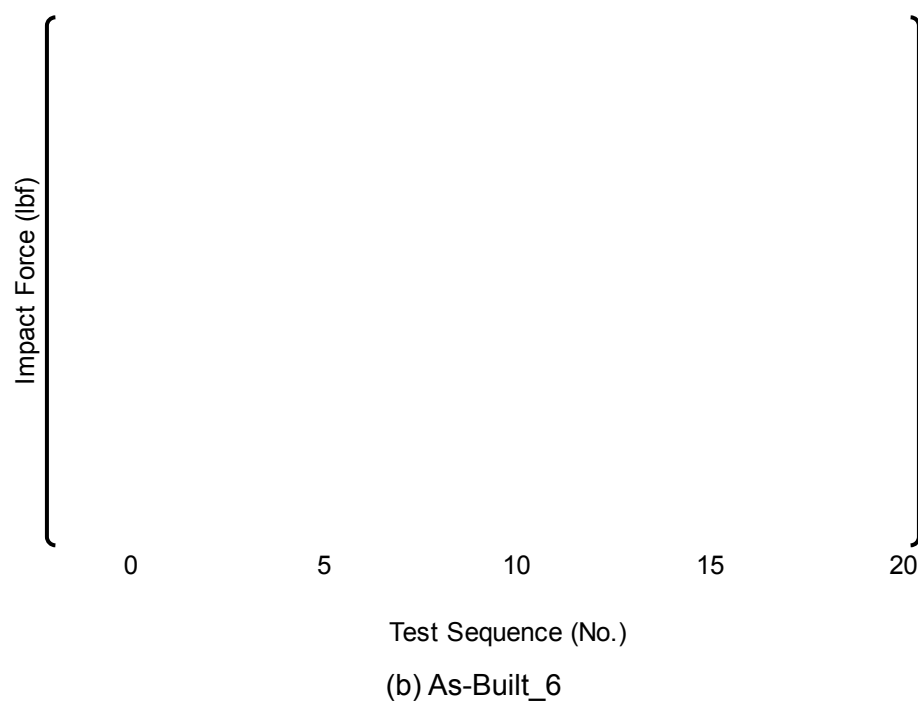
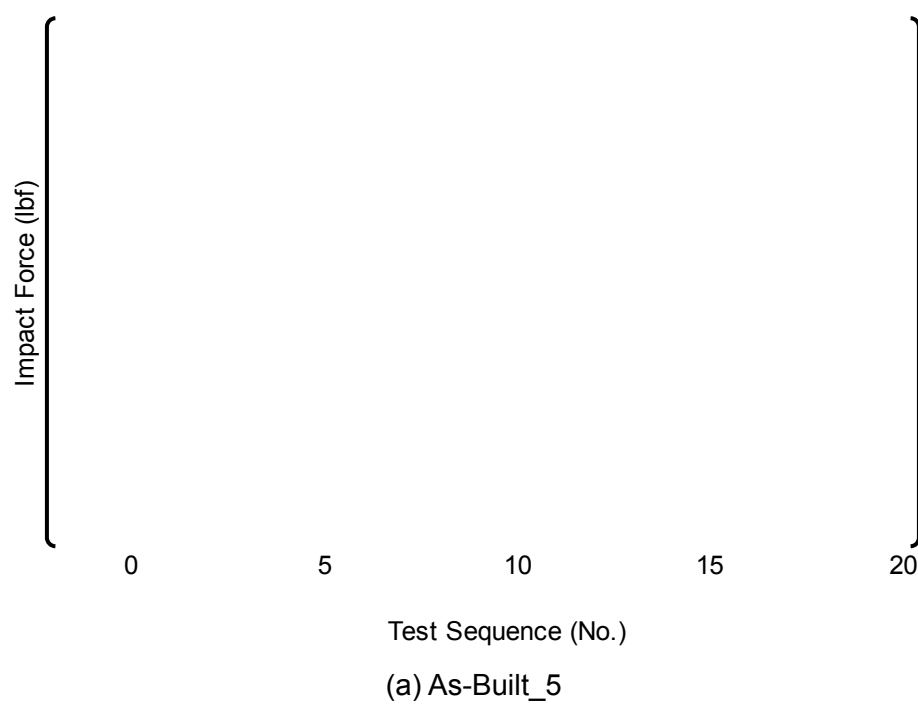


Figure 4.1.4-1 Comparison of Analyzed and Measured Impact Force (As-Built)

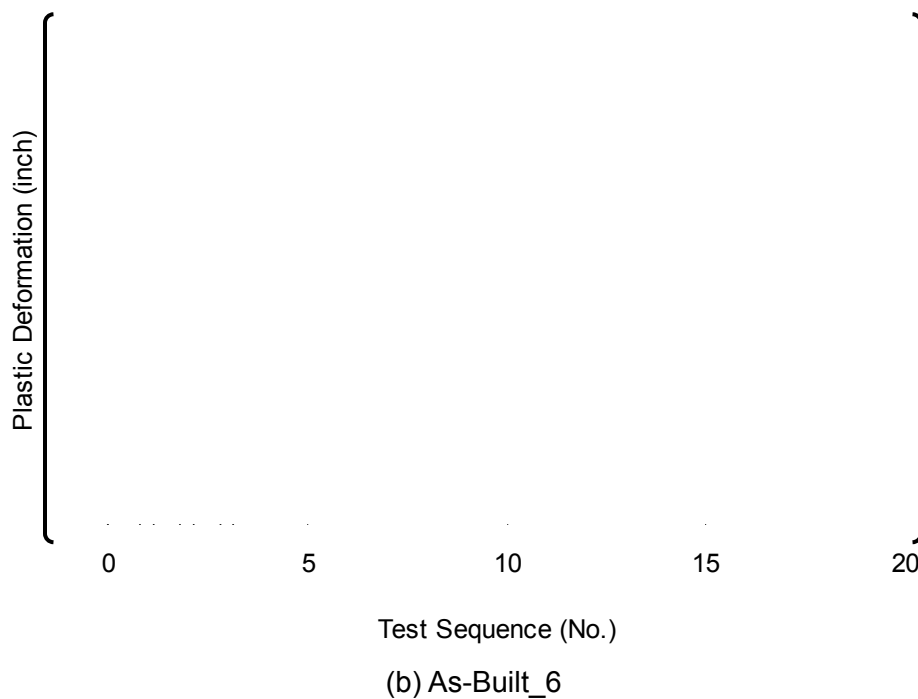
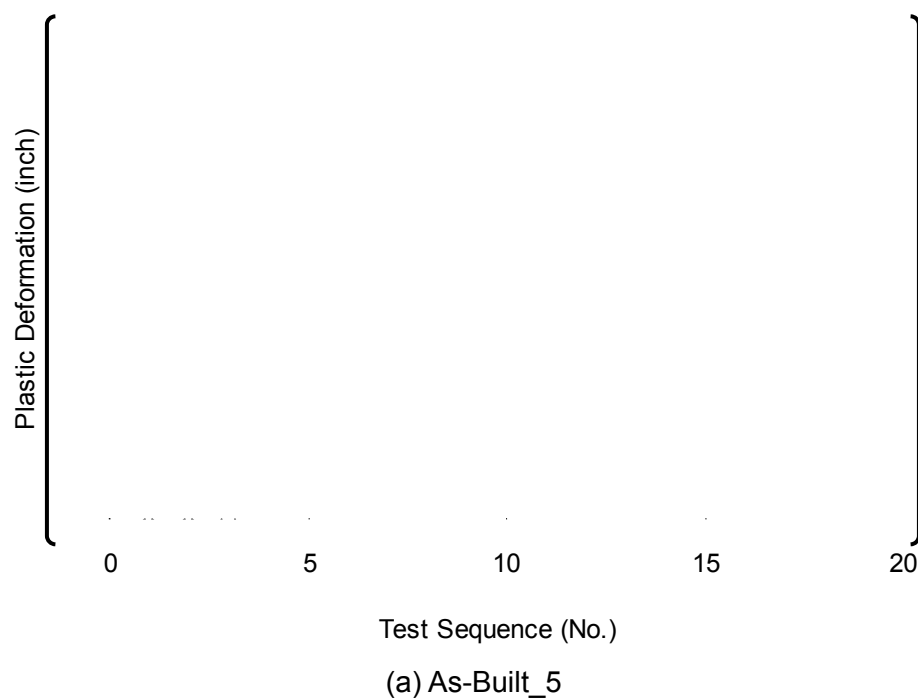
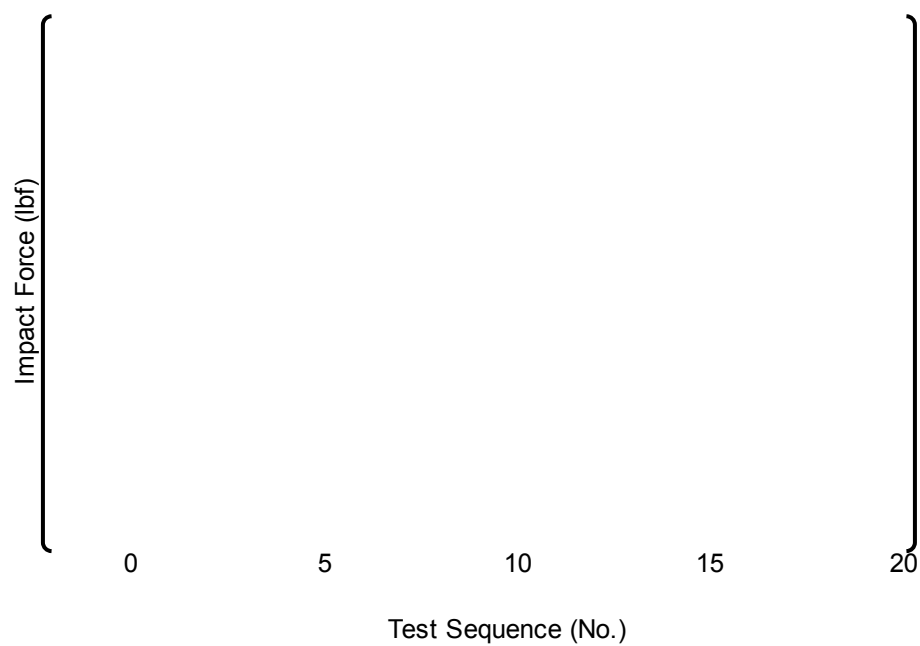
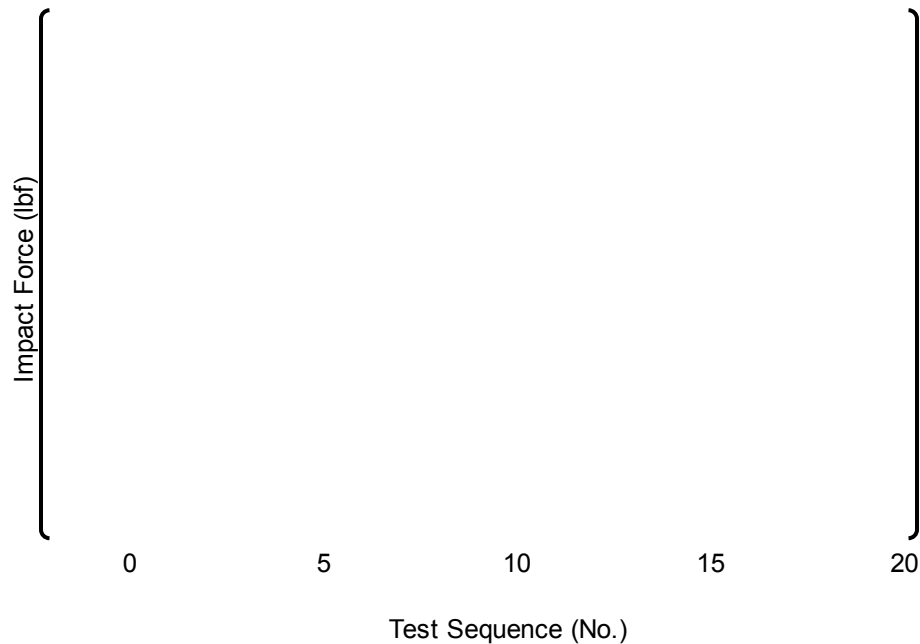


Figure 4.1.4-2 Comparison of Analyzed and Measured Plastic Deformation (As-Built)

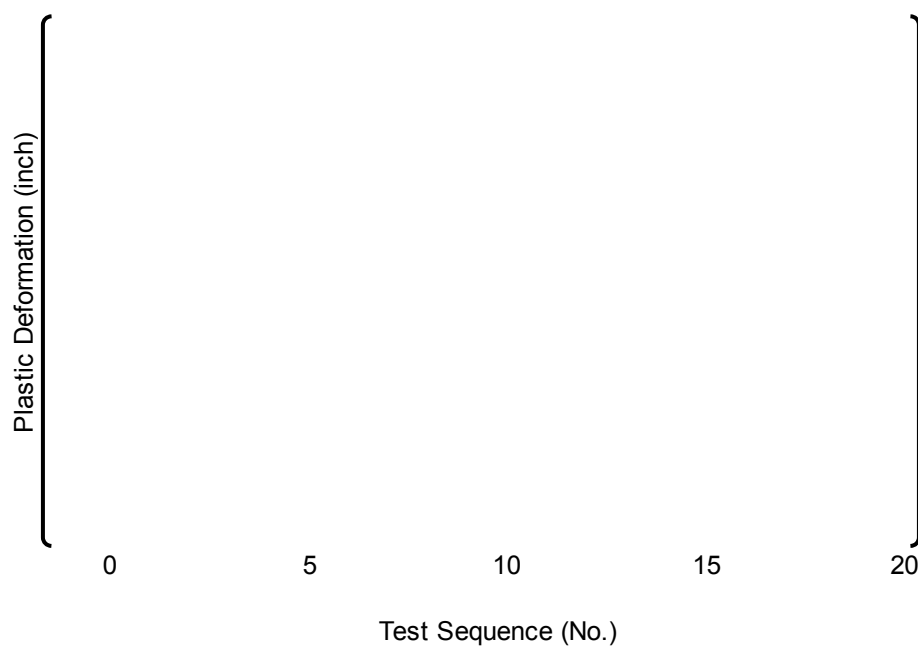


(a) Relaxed_7

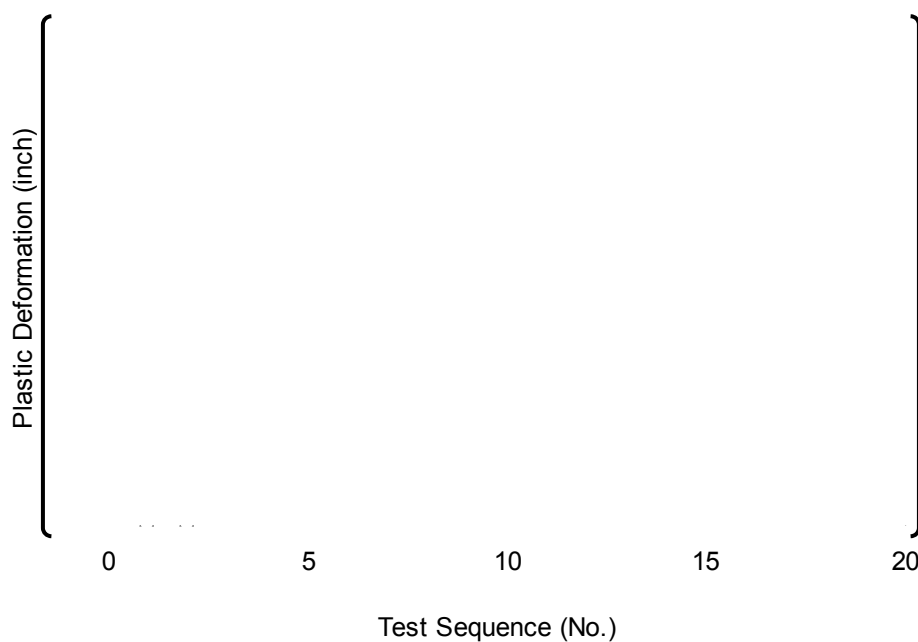


(b) Relaxed_8

**Figure 4.1.4-3 Comparison of Analyzed and Measured Impact Force
(Relaxed Spring Force)**



(a) Relaxed_7



(b) Relaxed_8

**Figure 4.1.4-4 Comparison of Analyzed and Measured Plastic Deformation
(Relaxed Spring Force)**

4.1.5 Response Analysis by the FINDS Code

The fuel assembly model in the FINDS code analyzes horizontal response in one direction, as previously shown in Figure 4.1.2-1. Accordingly, a time-dependent response analysis is independently performed on an array of fuel assemblies forming a single row and vibrating along the row, using the accelerations in the x and z direction obtained from the reactor internal's response analysis as inputs (

4.1.6 Stress Analyses by the ANSYS Code

The fuel assembly stress analysis model is shown in Figure 4.1.6-1⁽⁴⁻¹⁾. (

As described in Subsection 4.4.3, this bending stress due to horizontal response is combined with membrane stress resulting from vertical response of the fuel assembly by SRSS, added to normal operation stresses, and then compared to the acceptance limit.

4.1.7 Determination of Grid Spacer Buckling Occurrence

The methodology from the FINDS analysis results for determining whether grid spacer buckling

has occurred is explained in Appendix D of this report.

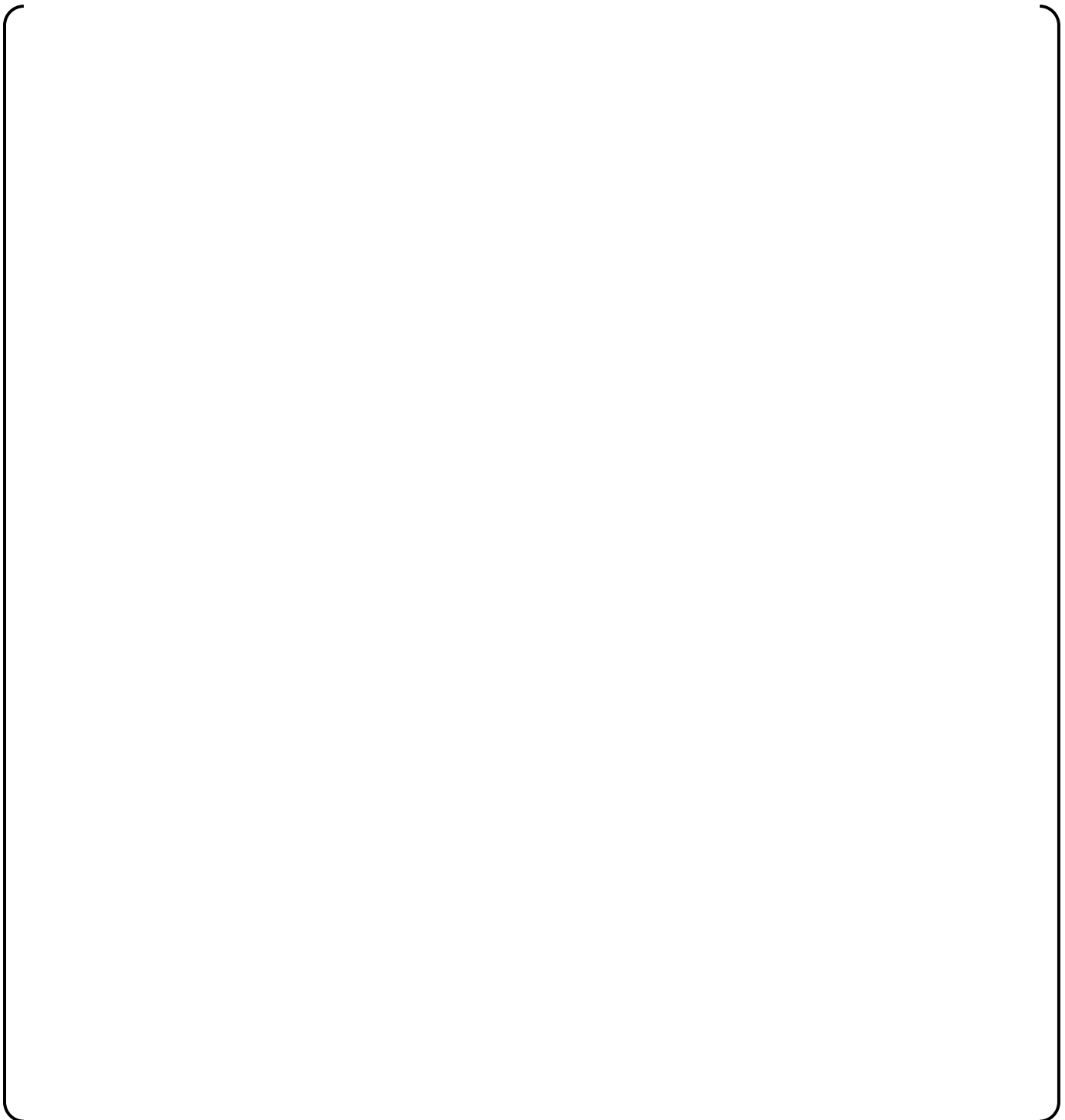


Figure 4.1.6-1 Fuel Assembly Stress Analysis Model in the Horizontal Direction

4.2 Methodology for the Fuel Assembly Response and Stress Analysis in the Vertical Direction

For the membrane stress evaluation in the vertical direction of the fuel assembly, all assemblies are assumed to be independent, so that the limiting fuel assembly is determined by the relative movement of the upper core plate and lower core support plate at that core location. There are negligible lateral interactive effects among the fuel assemblies and neutron reflectors.

Consistent with the analyses in the horizontal direction, the stress analyses in the vertical direction for the SSE and LOCA events are performed individually. The procedure is schematically shown in Figure 4.2-1⁽⁴⁻¹⁾.

The fuel assembly stress analysis model for the vertical response is shown in Figure 4.2-2⁽⁴⁻¹⁾.

} In addition, three-dimensional solid elements are used for the detailed stress analyses of the top and bottom nozzles.

The peak vertical load on the fuel assembly, obtained by the reactor internal response analyses, is directly used as input for the stress analyses models for the fuel assembly components, including the top and bottom nozzles. In addition, for the control rod guide thimbles, the vertical load is also used in the buckling evaluation of the control rod guide thimbles. When the fuel assembly lifts off from the lower core support plate, the relative velocity between the bottom nozzle and the lower core support plate is used as input for the transient analysis with the fuel assembly stress analysis model.

The above stress analyses are individually carried out for the SSE and LOCA events. The membrane stresses in the fuel cladding and the control rod guide thimbles resulting from the SSE analysis are combined with those for LOCA by the SRSS method.

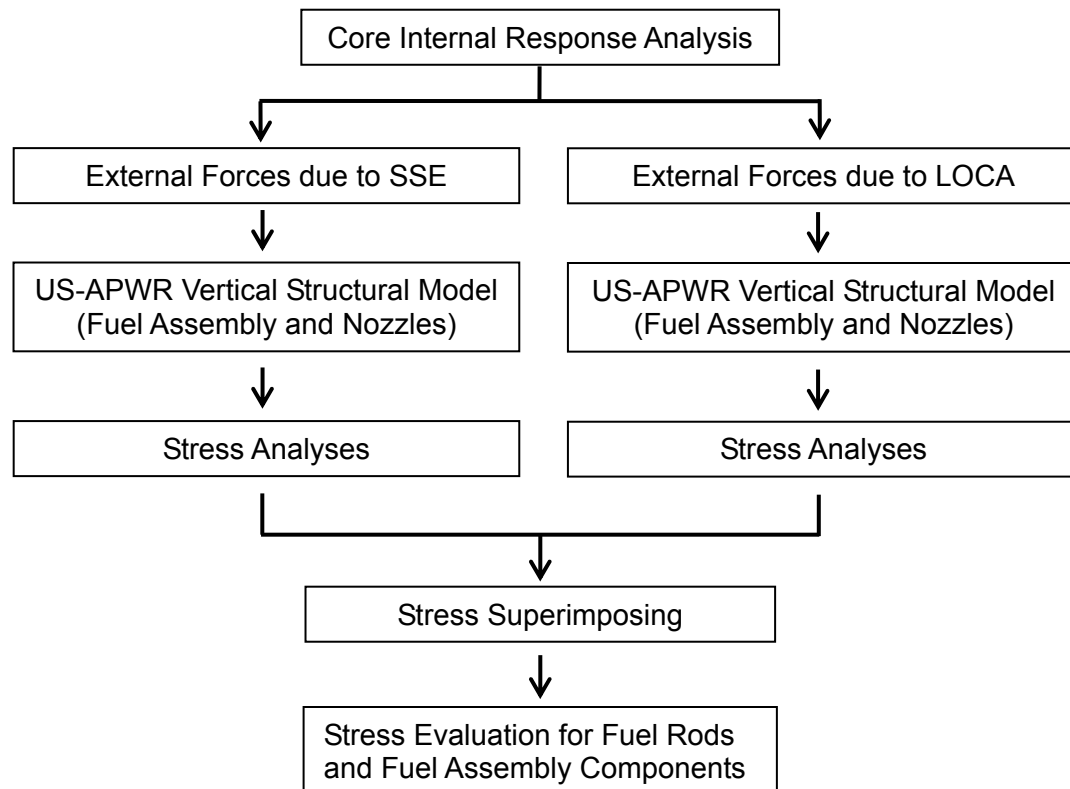


Figure 4.2-1 Stress Evaluation for SSE and LOCA Response in the Vertical Direction

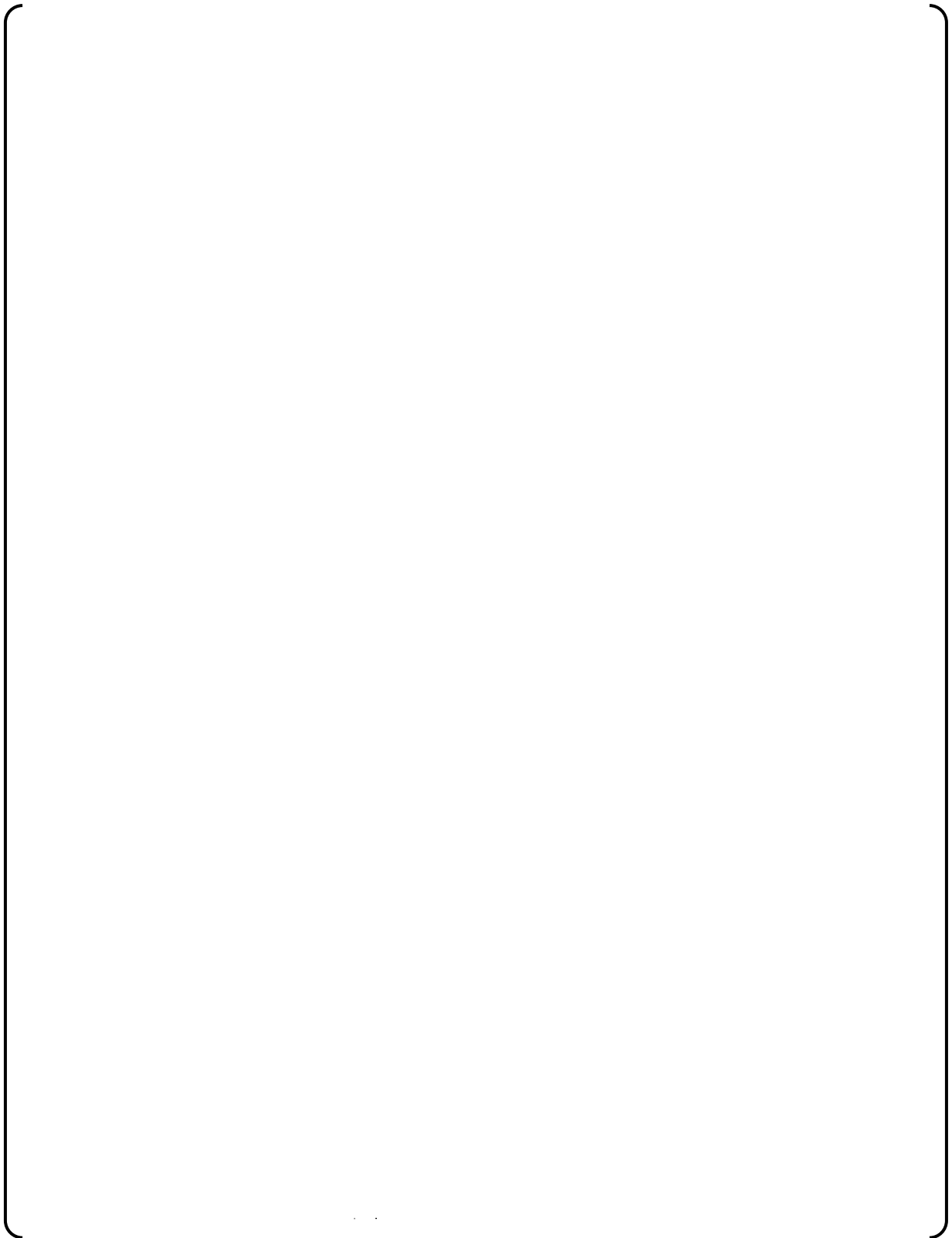


Figure 4.2-2 Fuel Assembly Stress Analysis Model for Vertical Response

4.3 Stress Combination in Horizontal and Vertical Directions

The stress due to the SSE and LOCA response is obtained by combining the bending stress of the control rod guide thimbles and fuel rods in each of 257 fuel assemblies, obtained from the horizontal response described in Section 4.1, and the membrane stress resulting from the vertical response described in Section 4.2, by the SRSS method and then by simple addition of membrane stress due to normal operation. All of the local stresses in the control rod guide thimble and the fuel rod are combined node by node in each fuel assembly and the resulting stresses are compared to the acceptance limit for each stress category such as (Primary Membrane Stress) and (Primary Membrane Stress + Primary Bending Stress + Local Membrane Stress) according to the ASME code ⁽⁴⁻³⁾.

4.4 Evaluation Condition and Results for the Fuel Assembly Response and Capability for SSE and LOCA Events

4.4.1 Input Accelerations and Vibration Characteristics of the Fuel Assembly in Horizontal Response with Uncertainties

Using the FINDS code, the most limiting horizontal response with uncertainty is determined in terms of input acceleration, fuel assembly condition (BOL/EOL) and the fuel assembly's amplitude dependency in frequency and damping ratio.

(1) Limiting input acceleration and fuel assembly condition

As shown in Figure 4.4.1-1, the procedure to determine the limiting combination for SSE and LOCA acceleration input and limiting fuel assembly condition is discussed.

The FINDS code horizontal direction response analyses due to the SSE and LOCA events are conducted using the following acceleration ^{(4-4),(4-5)} data calculated by the dynamic response analyses of the reactor vessel and reactor internals. There are eight SSE and two LOCA acceleration histories to be considered for the US-APWR.

Safe shutdown earthquake (SSE)*:

- 270-200
- 270-500
- 560-100
- 560-200
- 560-500
- 900-100
- 900-200
- 2032-100

LOCA**:

- CLB 8B 102%LF
- HLB 10B 102%LF

*The first three digits refers to the Category(initial Vs(30 m)) and the last three digits refers to the Depth to Rock(ft).

* CLB is cold leg break, HLB is hot leg break,
8B or 10B is the diameter of the pipe which is assumed to break at LOCA.
102% refers to reactor power.

LF means the vibration force of the loop is considered in the dynamic response analyses of the reactor vessel and reactor internals.

The above eight categories of SSE acceleration data are used to evaluate the capability of the US-APWR standard plant as described in Reference 4-4, and the responses of the upper core plate and lower core support plate are calculated by the dynamic response analyses of the reactor vessel and reactor internals.

For LOCA event, the diameters of the pipe which break at LOCA event are determined as 8 inches for cold leg break and as 10 inches for hot leg break, as described in Reference 4-5. The

Reference 4-4. The detailed procedure to calculate the response of the upper core plate and the lower core support plate is described in Section 3.3 of this report.

The acceleration time history of the upper core plate and lower core support plate are shown in Figure 4.4.1-2 through 4.4.1-9 for SSE acceleration histories and Figure 4.4.1-10 through 4.4.1-11 for LOCA acceleration histories, respectively. The x direction corresponds to the plant's N-S direction and the z direction corresponds to the plant's E-W direction.

All of the FINDS code analysis results for the conditions described in Subsection 4.4.1 are shown in Sections E2.1, E2.2, E3.1 and E3.2 of Appendix E.

As a result of the analyses, the following combination is determined to be the limiting for input acceleration and fuel assembly condition in terms of resulting maximum fuel assembly displacement.

- Safe shutdown earthquake (SSE):
 - 560-100 X and Z
- LOCA:
 - CLB 8B 102%LF X and Z
- Fuel assembly vibration characteristic
 - EOL condition

The time history responses of the fuel assembly for EOL conditions are shown in Figure 4.4.1-12 for SSE event and Figure 4.4.1-13 for LOCA event. Figure 4.4.1-12 shows the response for the 560-100 case as the representative SSE event and Figure 4.4.1-13 shows the response for the CLB 8B 102%LF case as the representative LOCA event.

(2) Uncertainties of SSE frequency and vibration characteristics

Uncertainties of SSE frequency and fuel assembly frequency and damping ratio are investigated, as shown in Figure 4.4.1-14.

The maximum responses obtained in these analyses are summarized in Table 4.4.1-1 through Table 4.4.1-3 for SSE events and Table 4.4.1-4 and Table 4.4.1-5 for LOCA events.

- SSE frequency uncertainty:

In addition, as described in Appendix C, there are uncertainties in the amplitude dependency of frequency and damping ratio for the fuel assembly, influence of uncertainty in amplitude dependency of fuel assembly frequency and damping ratio is investigated, as shown in Figure 4.4.1-13.

As a result, it is determined that {

- Combination of fuel assembly frequency and damping ratio uncertainty

(3) The most limiting stress of the components and impact force of the grid spacer

As discussed above, on a row by row basis the most limiting control rod guide thimbles and fuel cladding stress and grid spacer impact force is determined as shown in Table 4.4.1-6.

The time independent maximum displacement of each beam in each row is obtained from the FINDS analyses above. {

{ More detail is provided in Section F3.0 and F4.0 of Appendix F.

Table 4.4.1-1 Response Analysis Results for 560-100 with EOL Condition

Wave	Units	SSE 560-100 with EOL BE/BE* Condition	
Direction		x	z
Fuel Assembly Number	-		
Maximum Displacement	inch (mm)		
Time	s		
Grid number	-		

* Combination of best estimate frequency and damping ratio

Table 4.4.1-2 Response Analysis Results for 560-100 with EOL Condition including the Uncertainty of SSE wave

Wave	Units	SSE 560-100() Frequency with EOL BE/BE* Condition	
Direction		x	z
Fuel Assembly Number	-		
Maximum Displacement	inch (mm)		
Time	s		
Grid number	-		

* Combination of best estimate frequency and damping ratio

Table 4.4.1-3 Response Analysis Results for 560-100 with EOL Condition including the Uncertainty of Fuel Assembly Vibration

Wave	Units	SSE 560-100 with EOL () Condition	
Direction		x	z
Fuel Assembly Number	-		
Maximum Displacement	inch (mm)		
Time	s		
Grid number	-		

Table 4.4.1-4 Response Analysis Results for CLB 8B 102%LF with EOL Condition

Wave	Units	CLB 8B 102%LF with EOL BE/BE* Condition	
Direction		x	z
Fuel Assembly Number	-		
Maximum Displacement	inch (mm)		
Time	s		
Grid number	-		

* Combination of best estimate frequency and damping ratio

**Table 4.4.1-5 Response Analysis Results for CLB 8B 102%LF with EOL Condition
including the Uncertainty of Fuel Assembly Vibration**

Wave	Units	CLB 8B 102%LF with EOL () Condition	
Direction		x	z
Fuel Assembly Number	-		
Maximum Displacement	inch (mm)		
Time	s		
Grid number	-		

[illegible]



**Figure 4.4.1-1 Limiting Input Acceleration and
FA Condition for Horizontal Response**

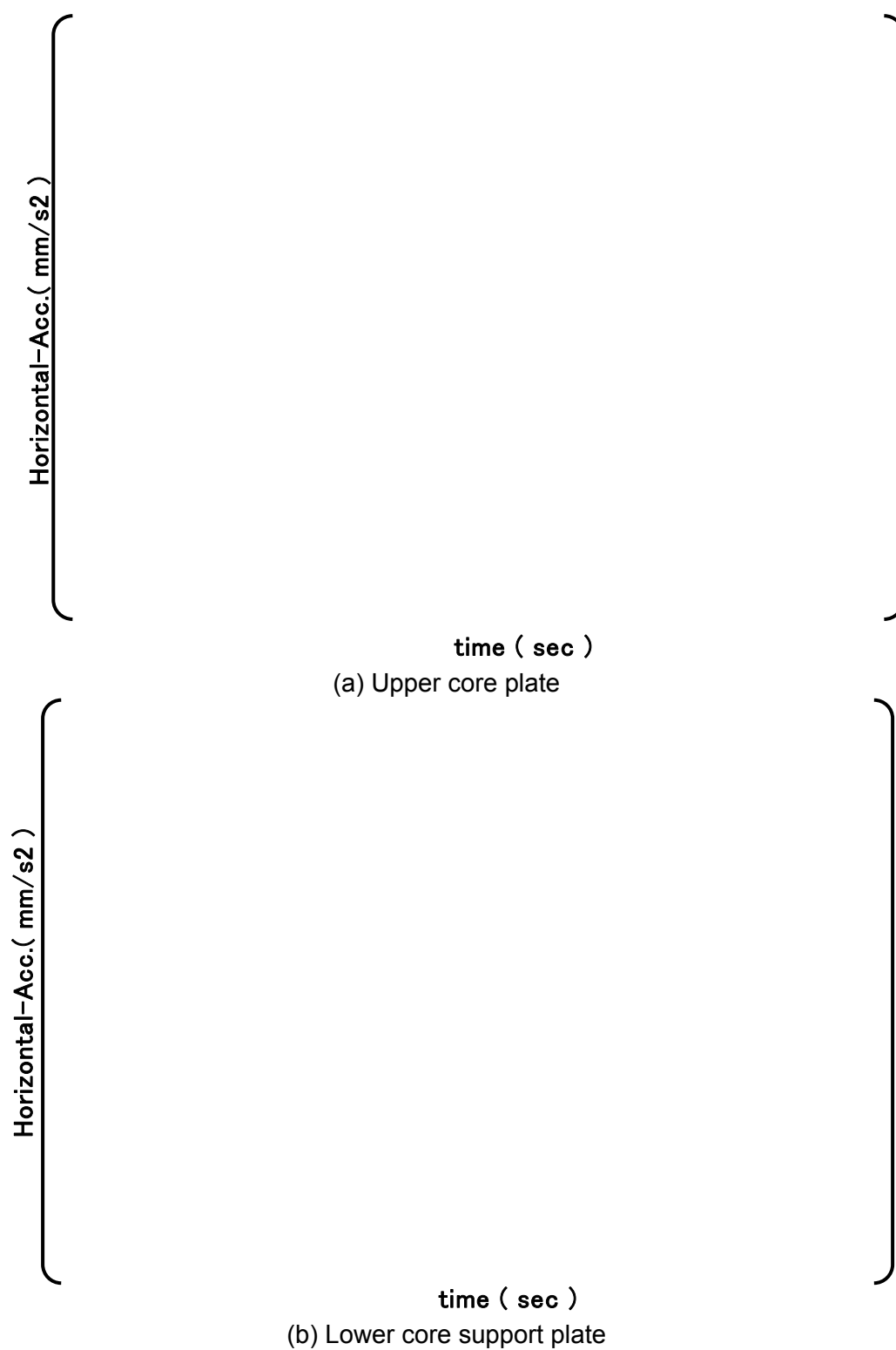
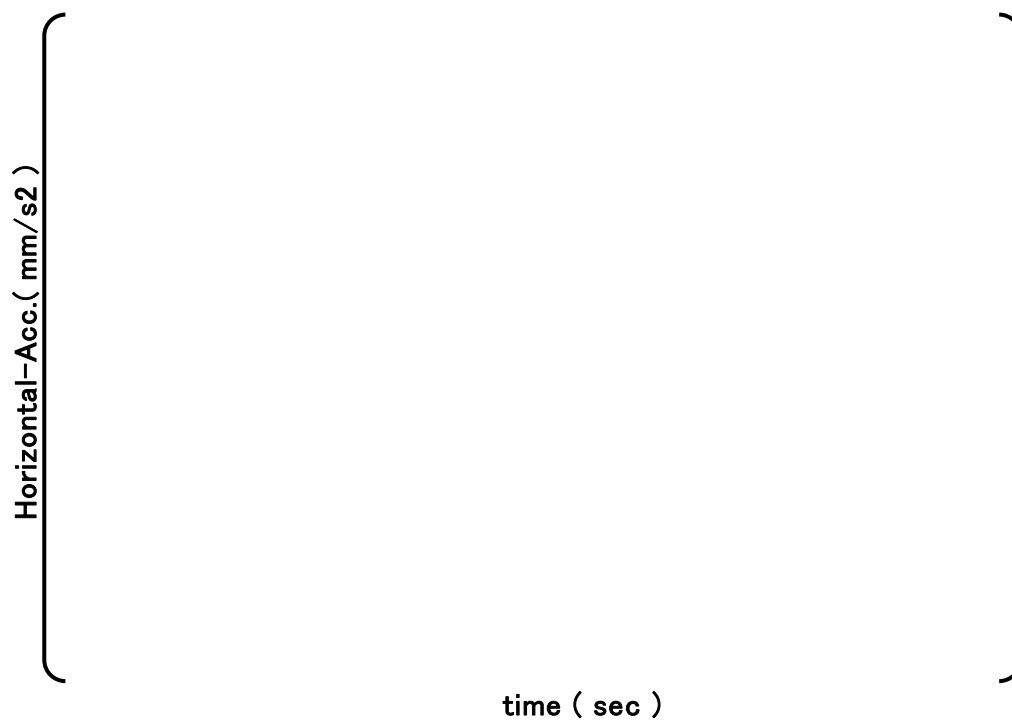
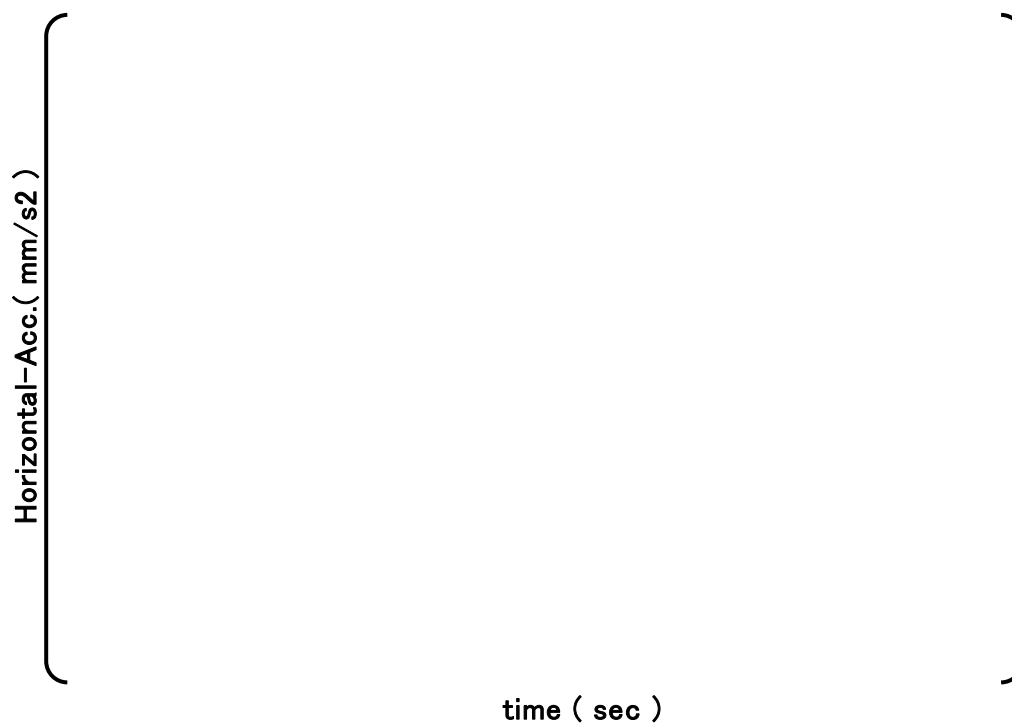


Figure 4.4.1-2 Acceleration Time History of the Core Plates for 270-200

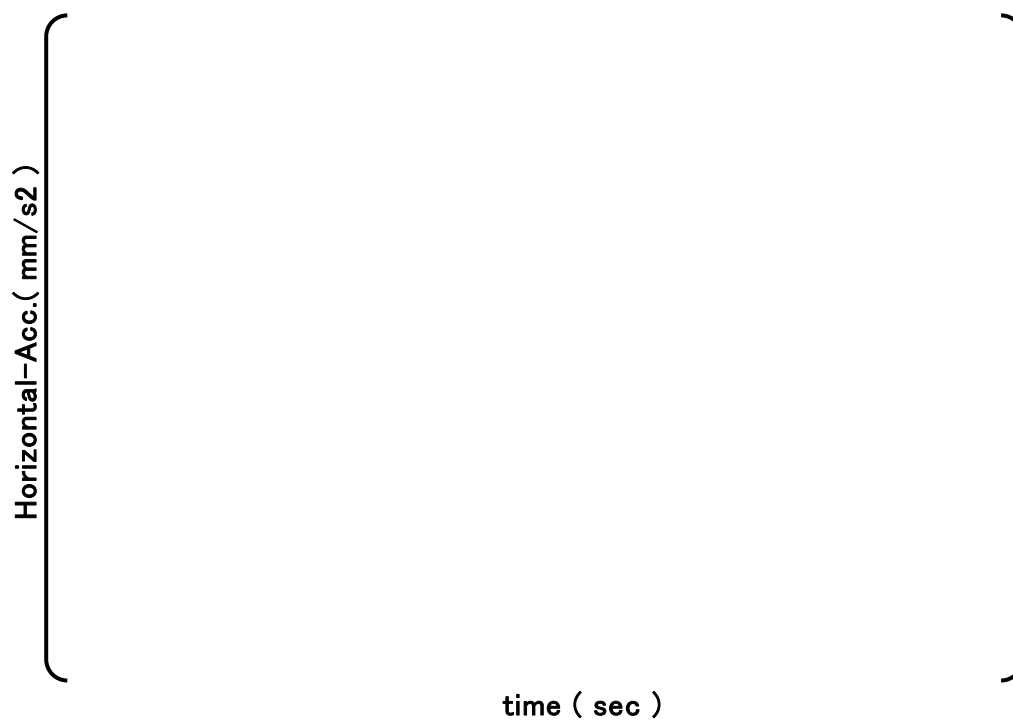


(a) Upper core plate

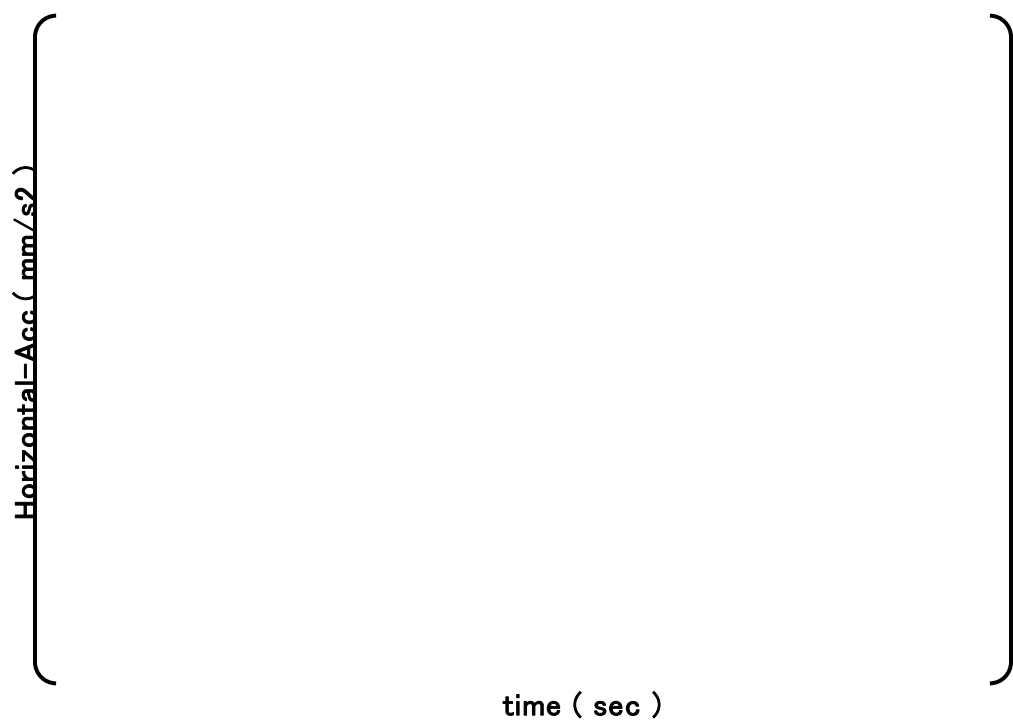


(b) Lower core support plate

Figure 4.4.1-3 Acceleration Time History of the Core Plates for 270-500



(a) Upper core plate



(b) Lower core support plate

Figure 4.4.1-4 Acceleration Time History of the Core Plates for 560-100

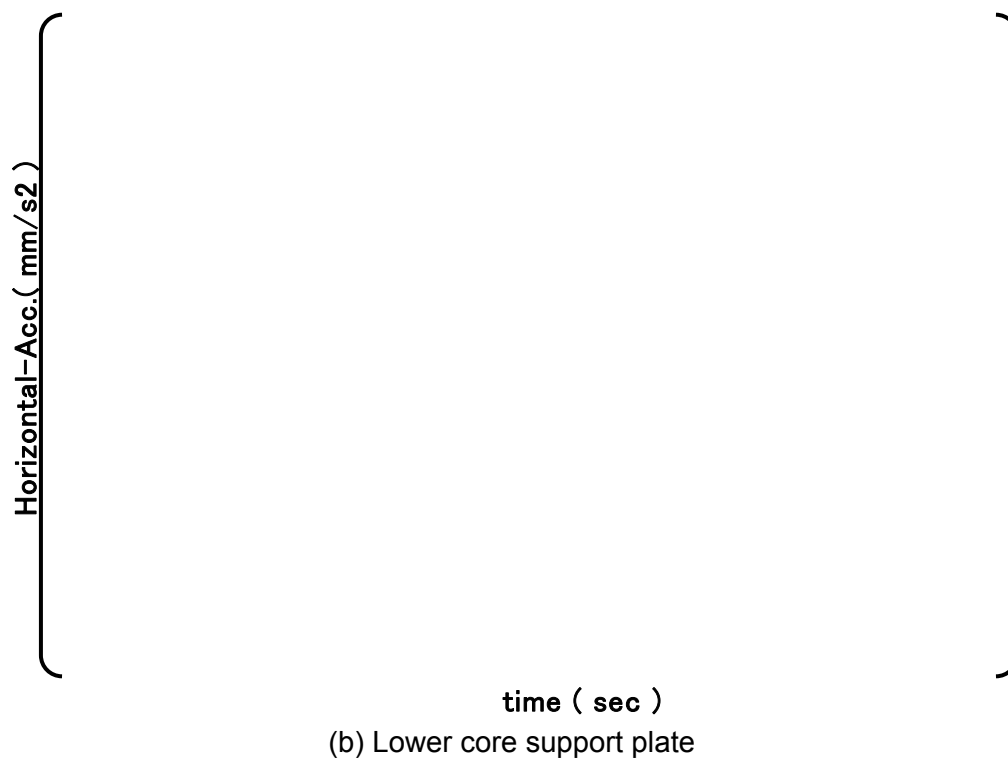
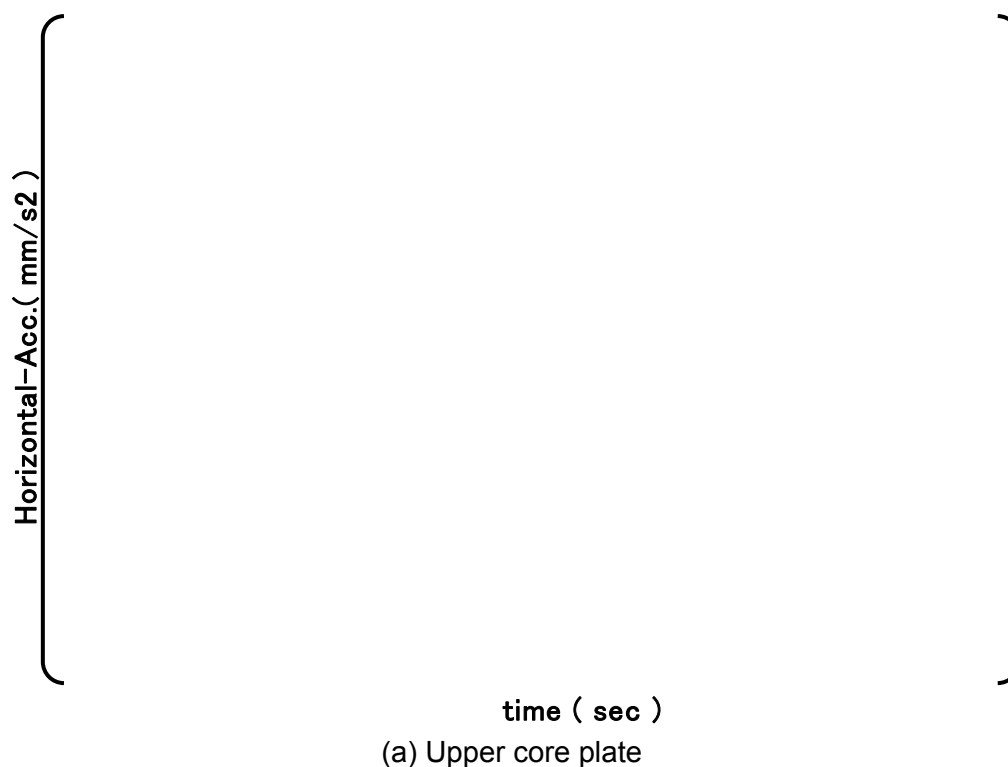


Figure 4.4.1-5 Acceleration Time History of the Core Plates for 560-200

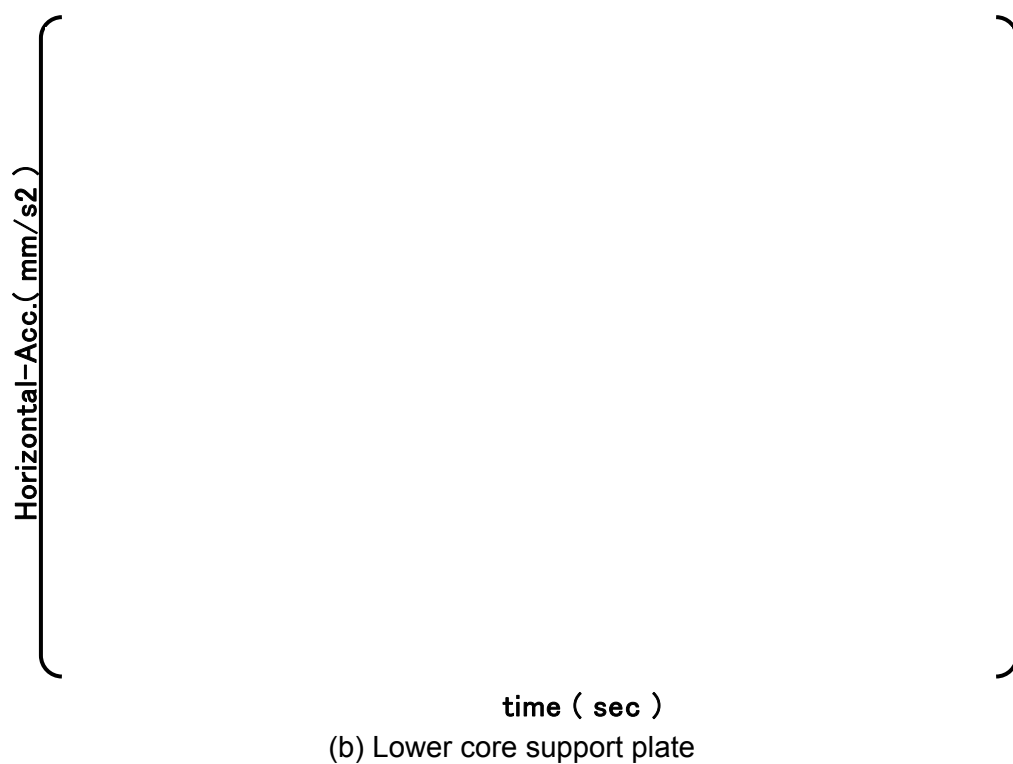
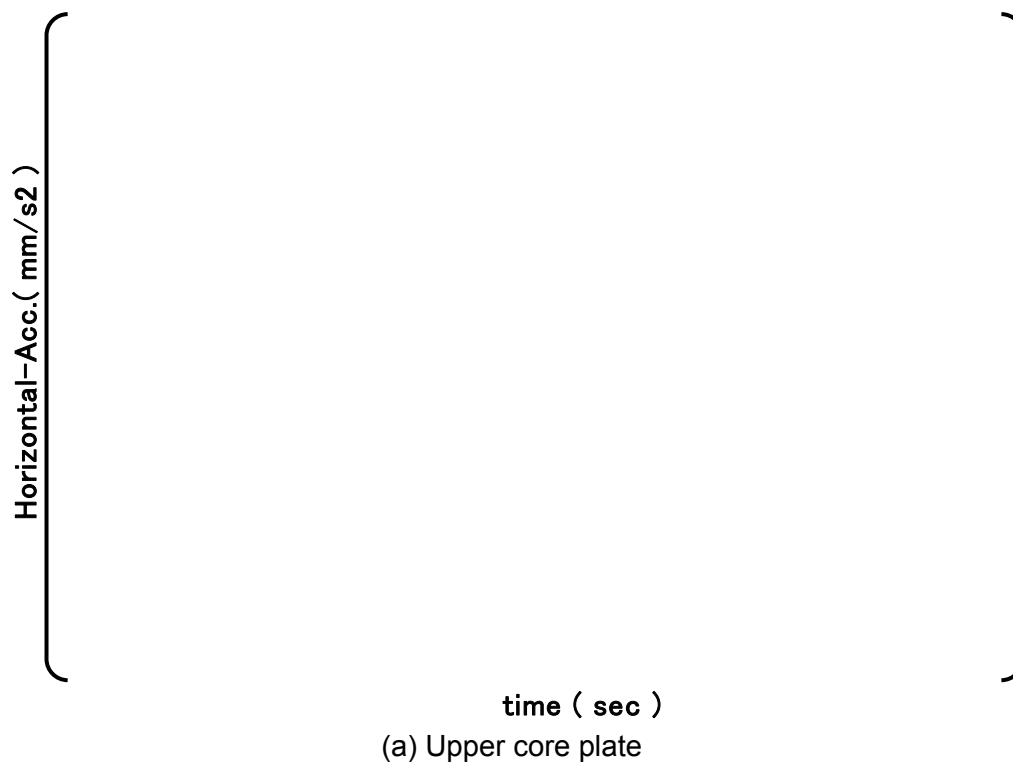


Figure 4.4.1-6 Acceleration Time History of the Core Plates for 560-500

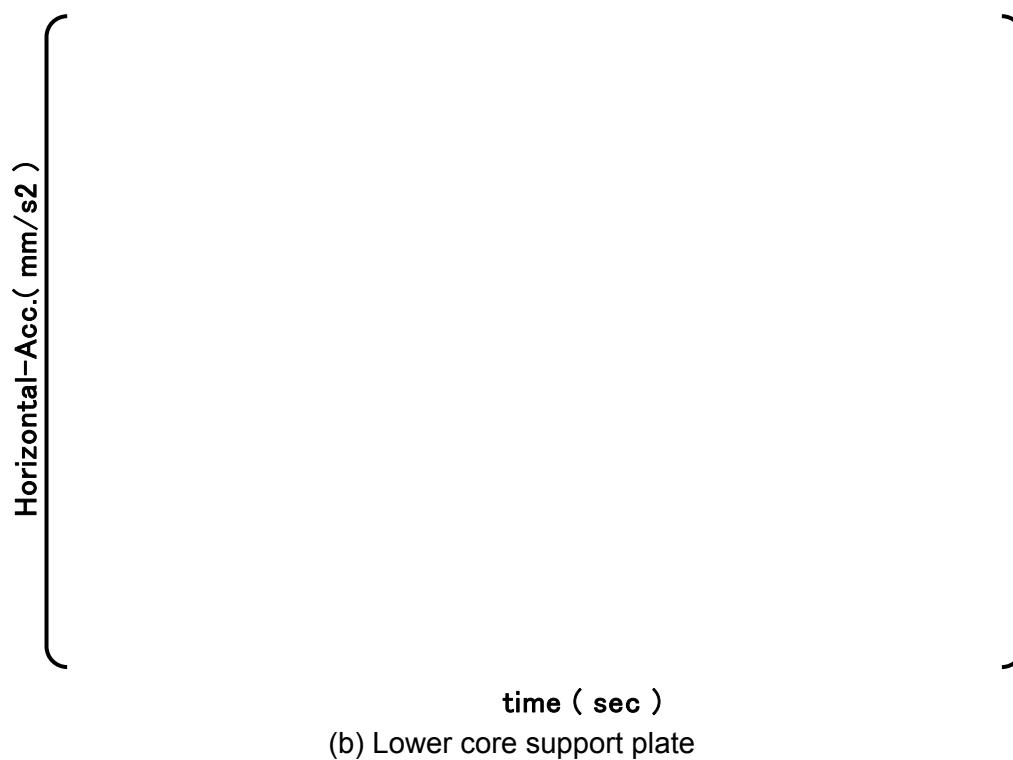
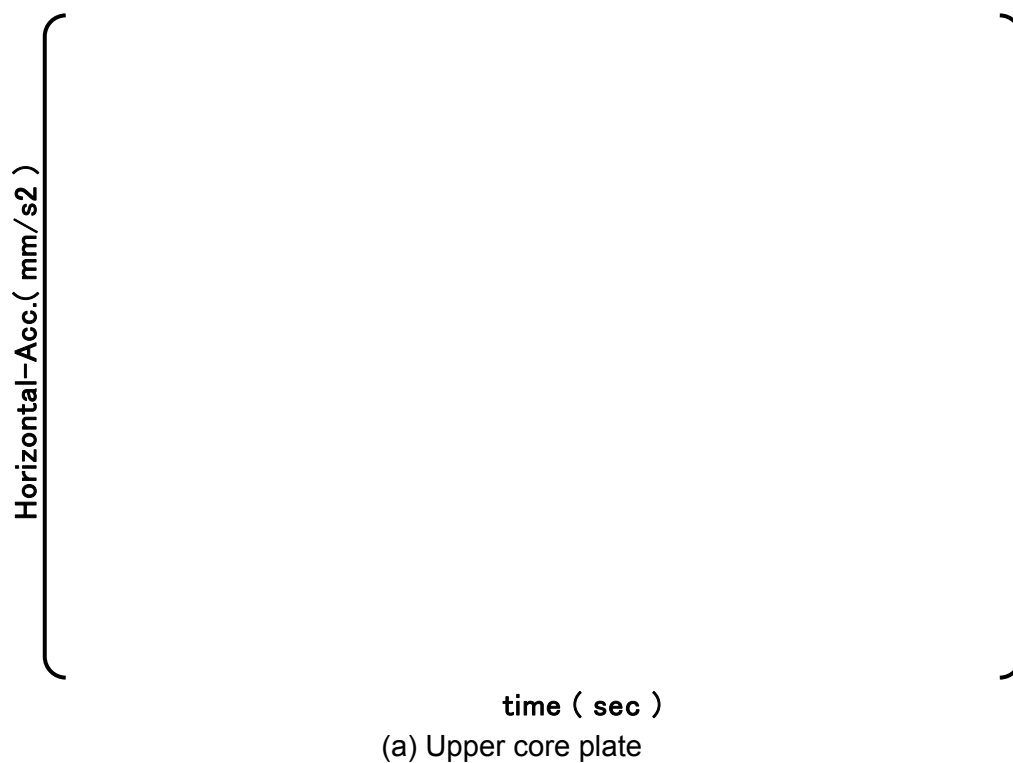


Figure 4.4.1-7 Acceleration Time History of the Core Plates for 900-100

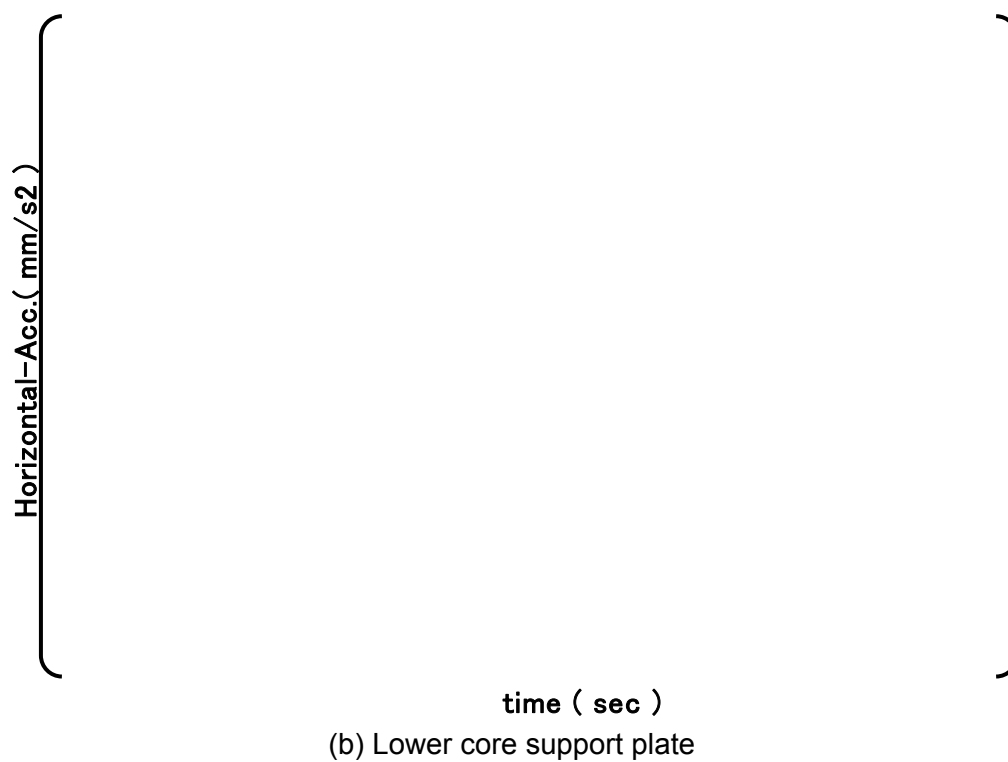
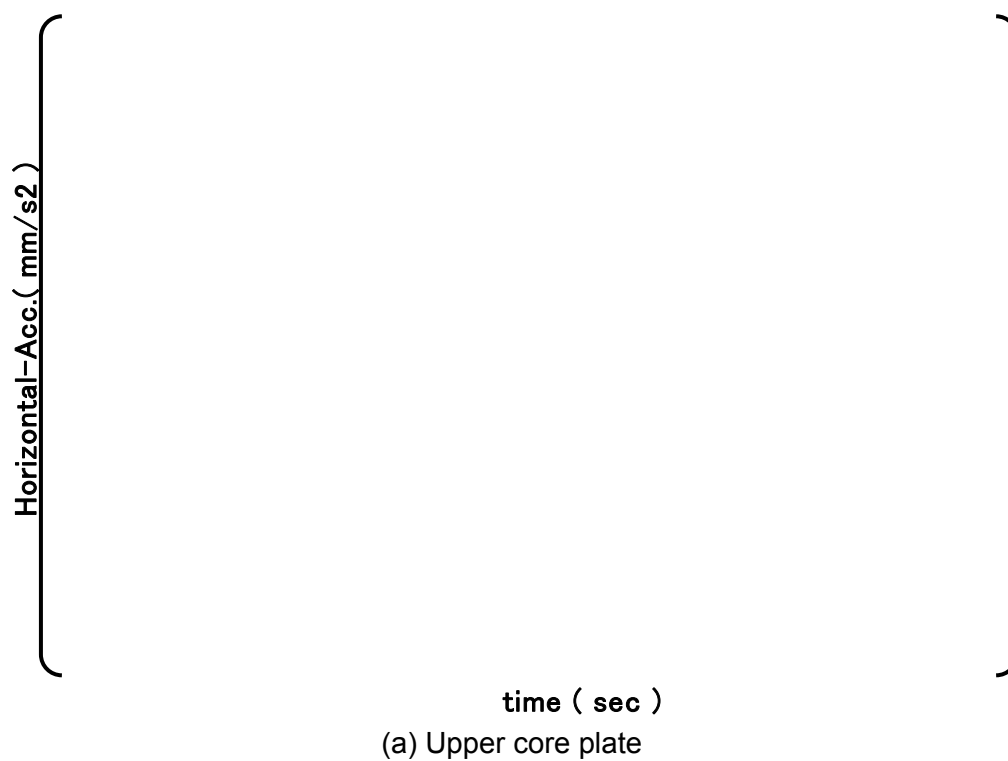


Figure 4.4.1-8 Acceleration Time History of the Core Plates for 900-200

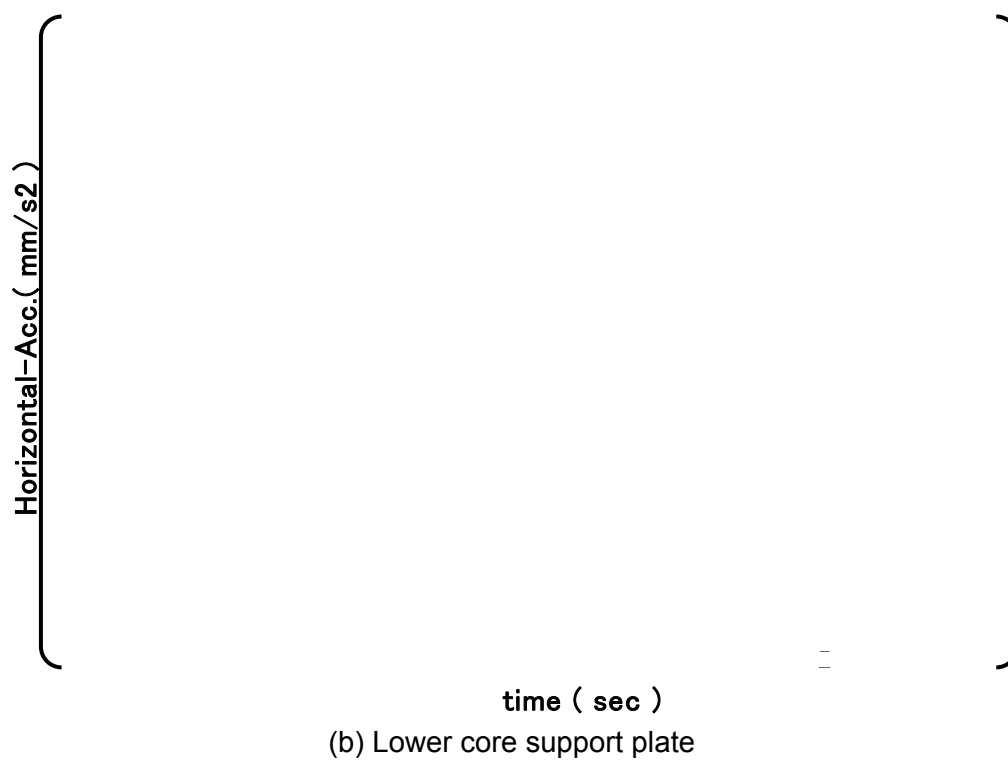
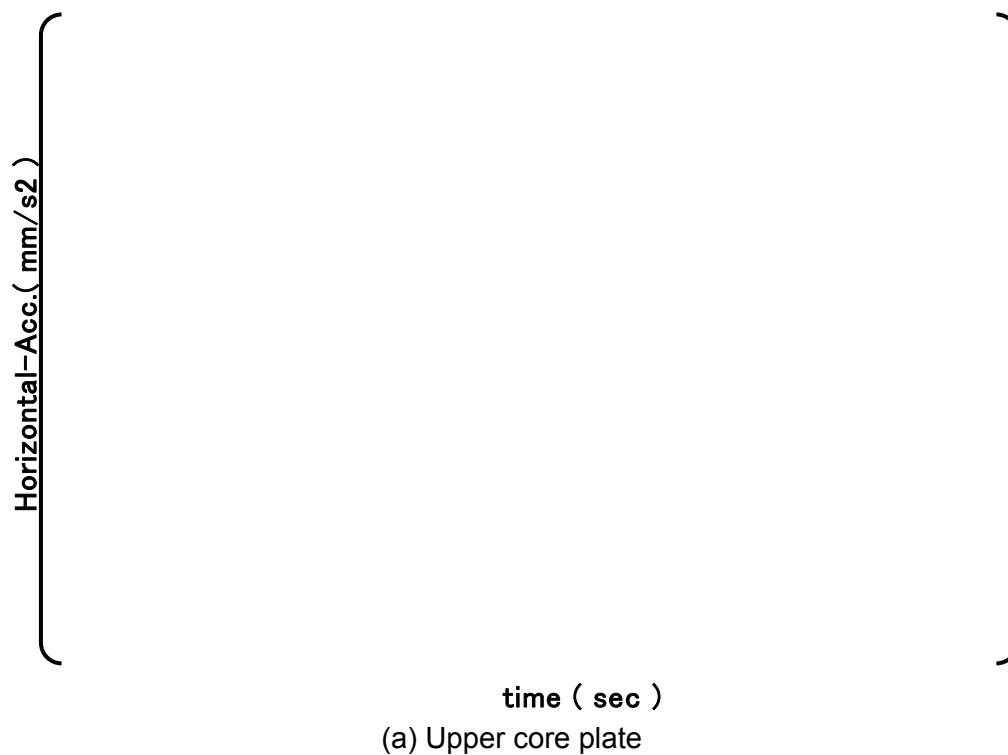
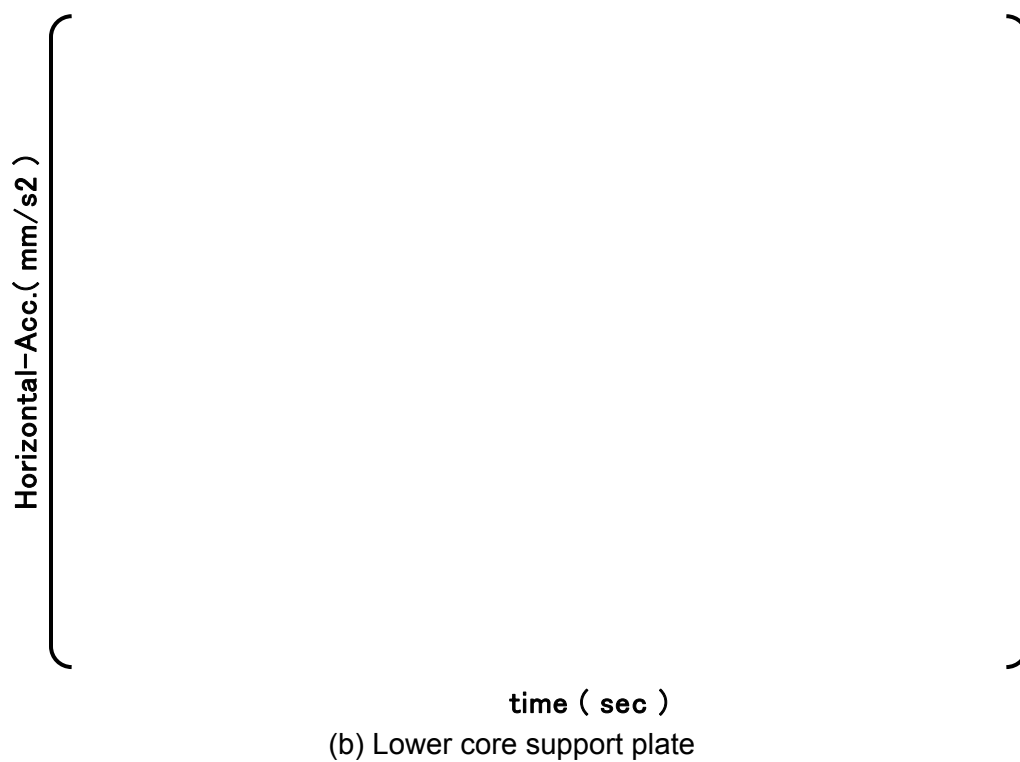
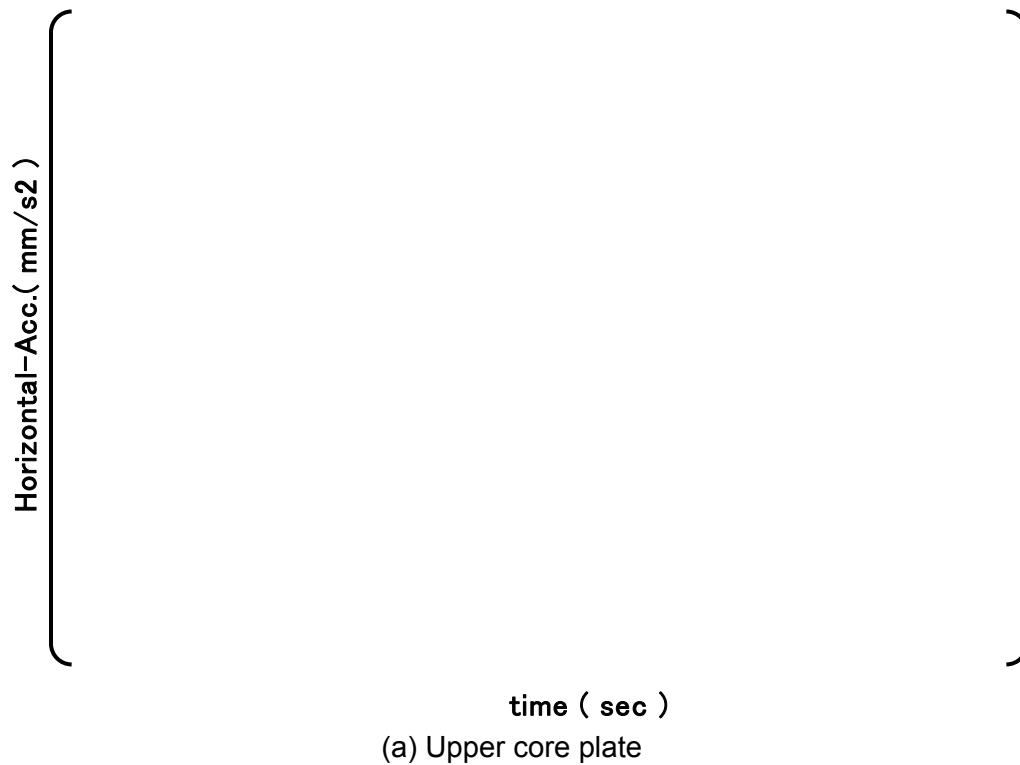
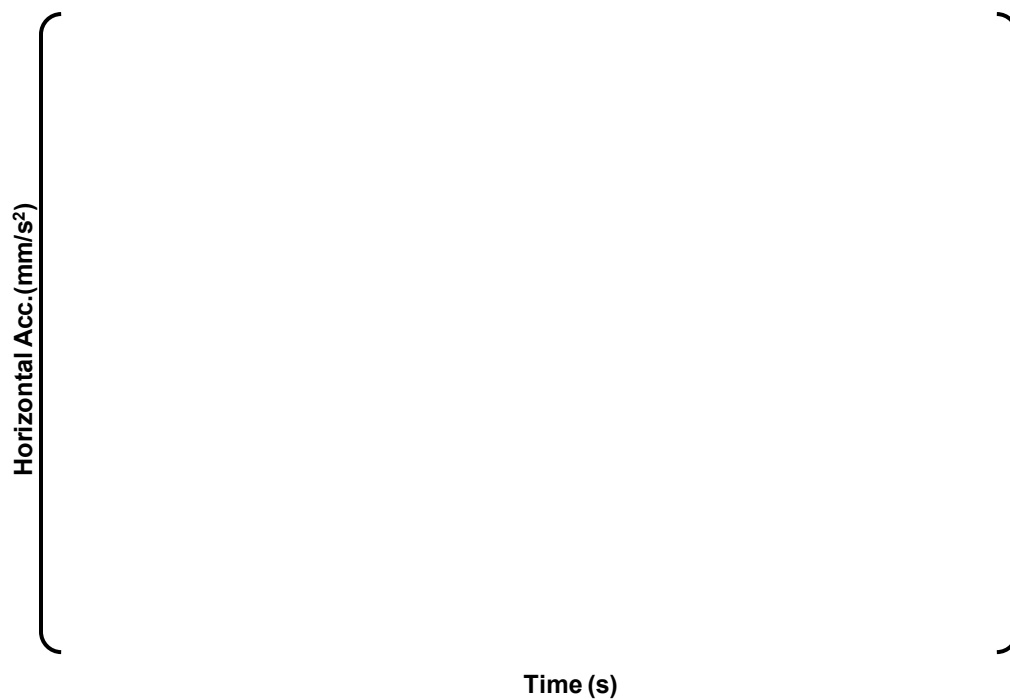


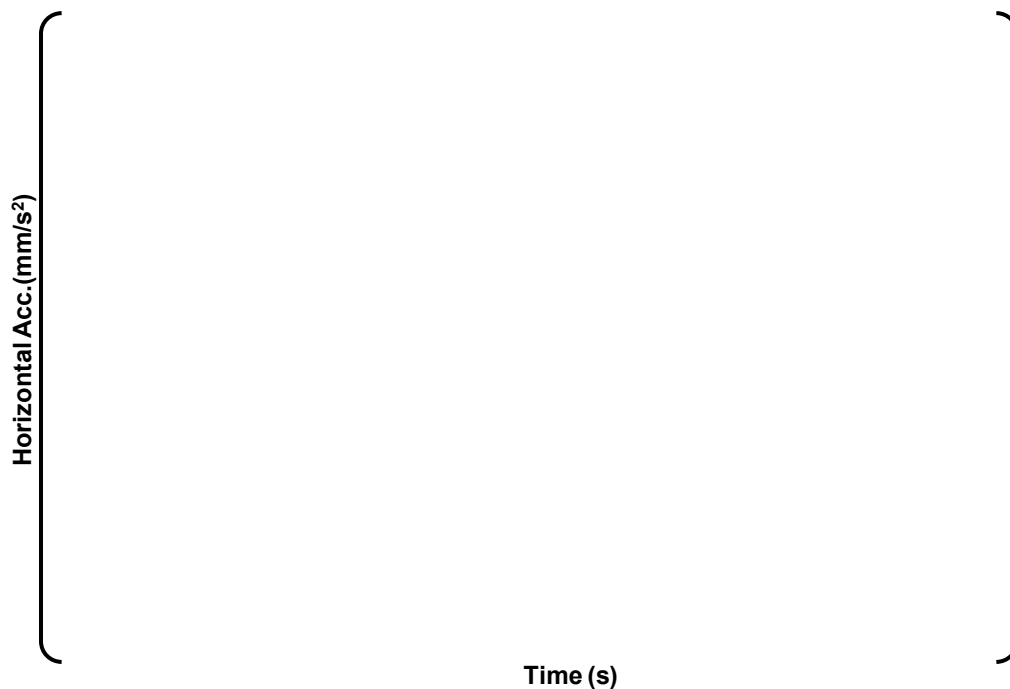
Figure 4.4.1-9 Acceleration Time History of the Core Plates for 2032-100



**Figure 4.4.1-10 Acceleration Time History of the Core Plates for LOCA
(CLB 8B 102%LF)**



(a) Upper core plate

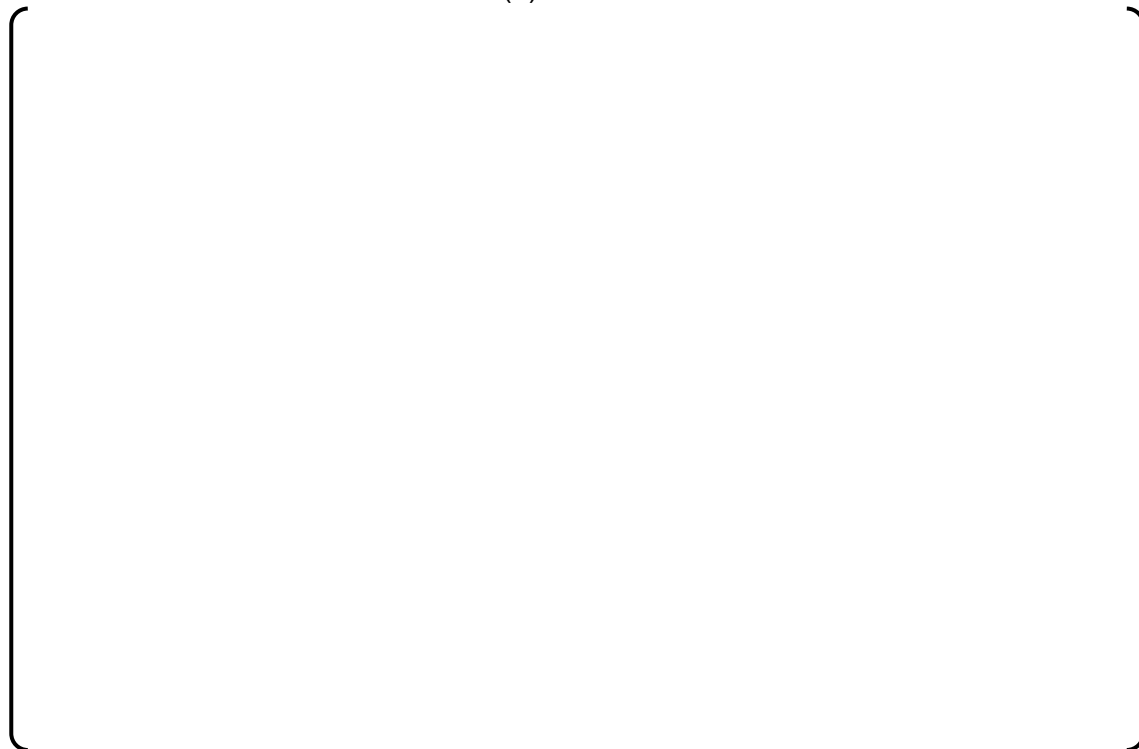


(b) Lower core support plate

**Figure 4.4.1-11 Acceleration Time History of the Core Plates for LOCA
(HLB 10B 102%LF)**



(a) x direction

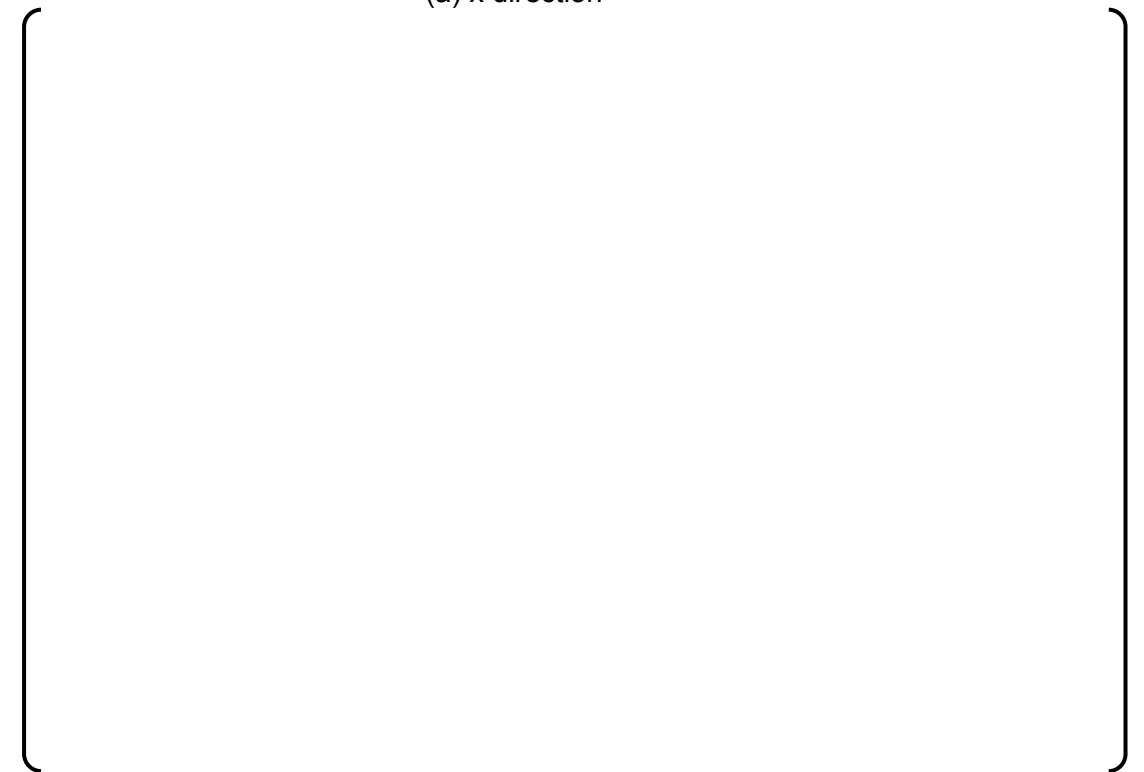


(b) z direction

**Figure 4.4.1-12(1) Fuel Assembly Time History Response (SSE 560-100)
(0 – 8 sec)**



(a) x direction



(b) z direction

Figure 4.4.1-12(2) Fuel Assembly Time History Response (SSE 560-100)
(8– 16 sec)

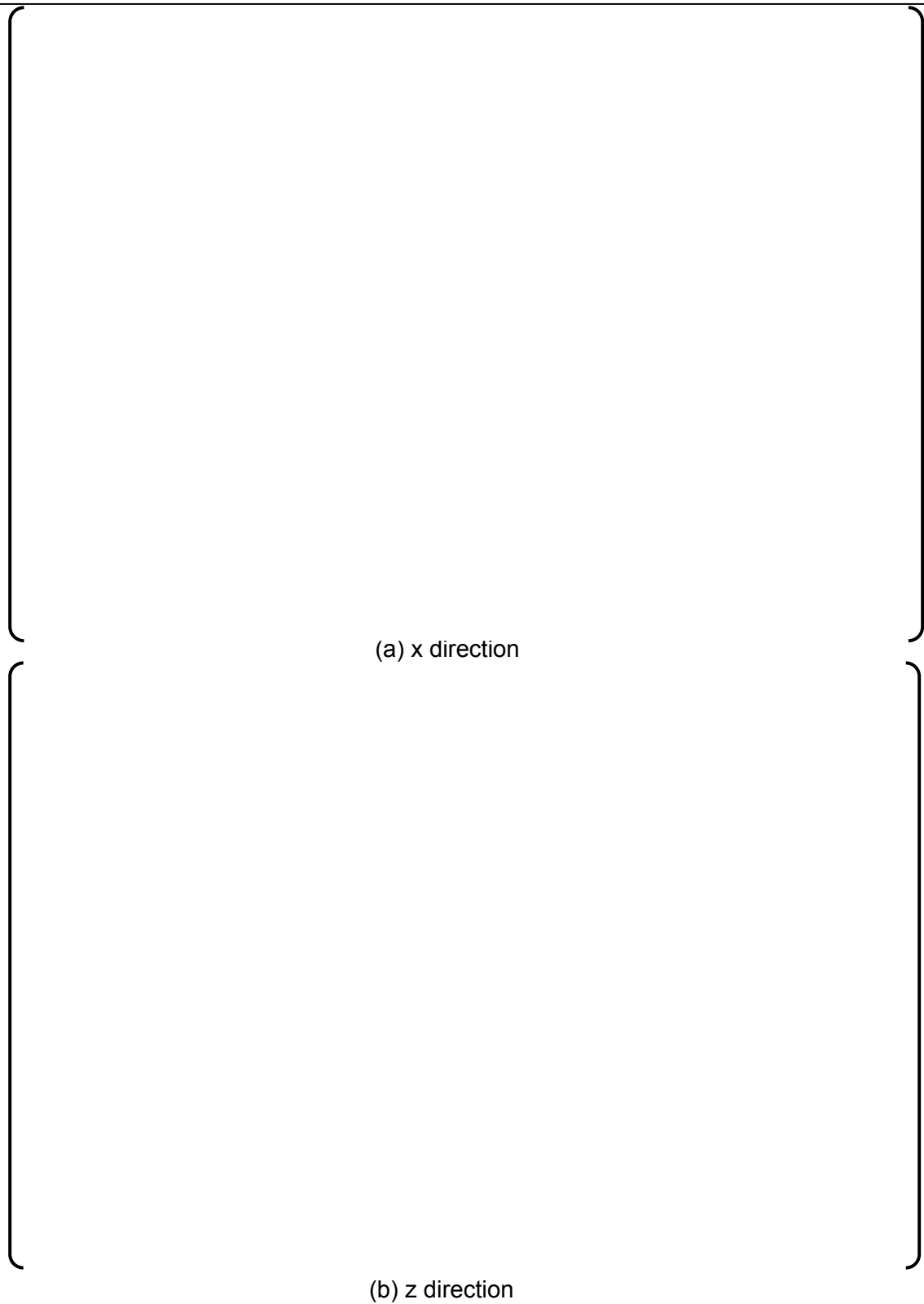


**Figure 4.4.1-12(3) Fuel Assembly Time History Response (SSE 560-100)
(16– 22 sec)**

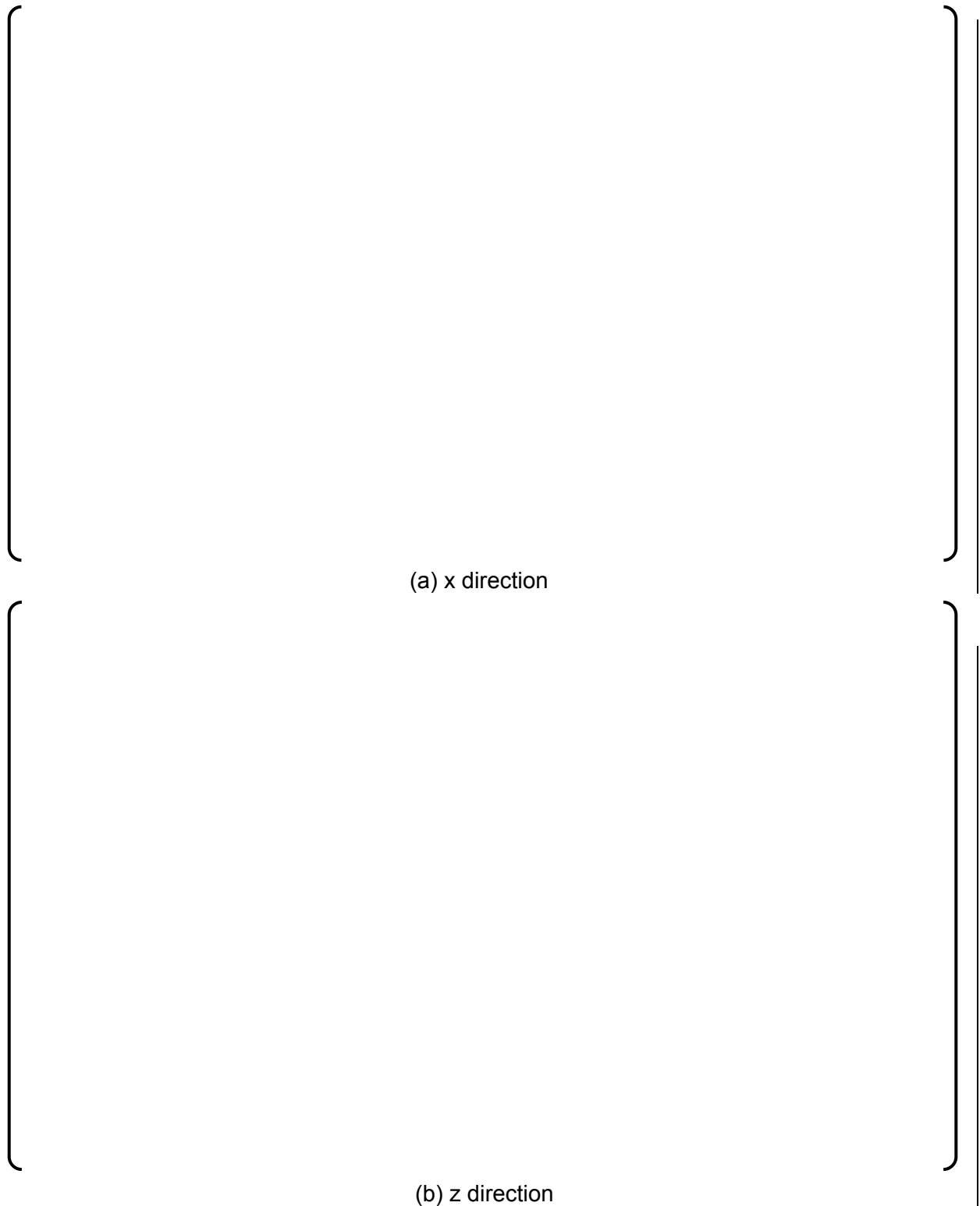


Figure 4.4.1-13 Fuel Assembly Time History Response (LOCA CLB 8B 102%LF)

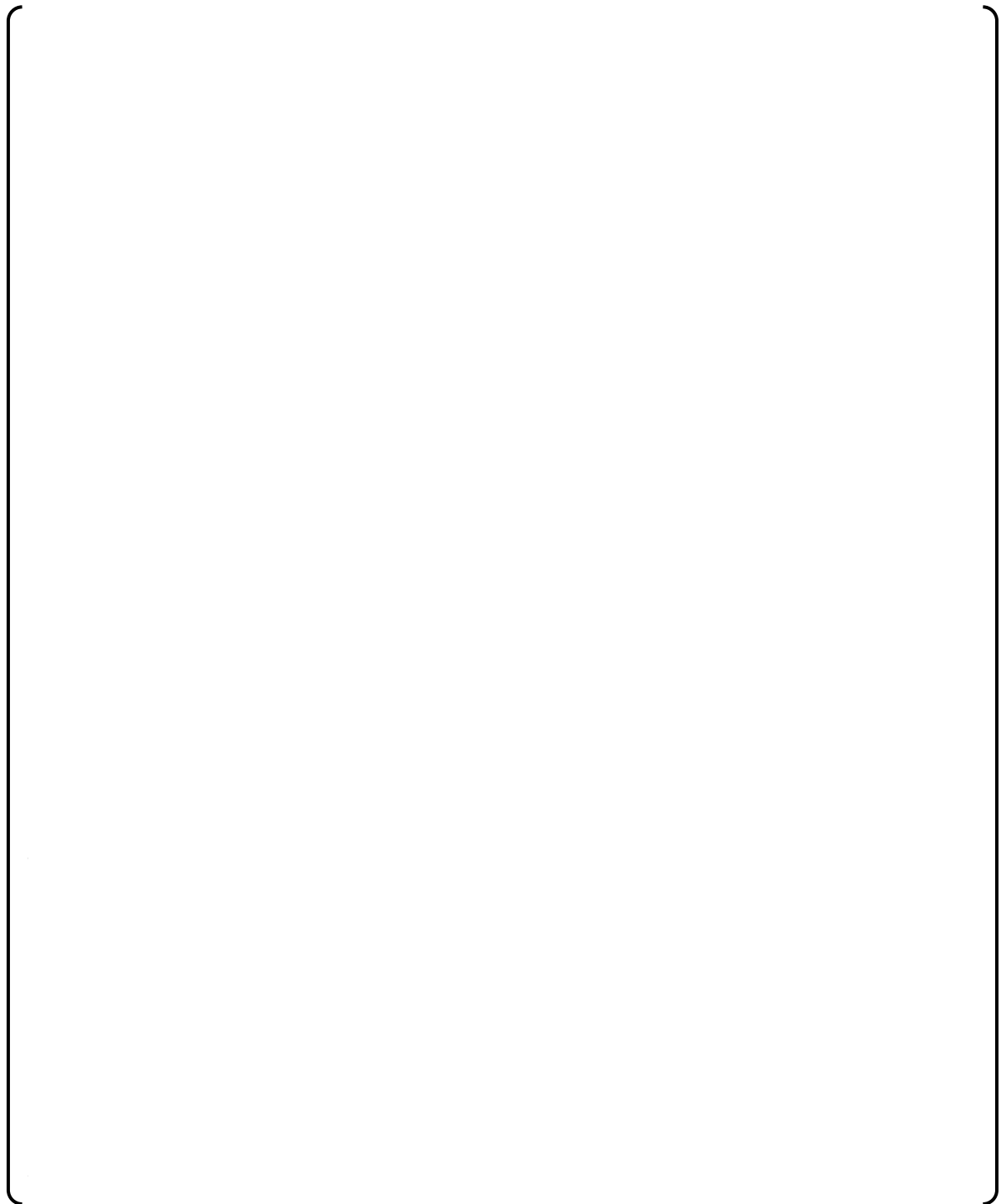


Figure 4.4.1-14 Uncertainty Consideration for SSE Frequency and FA Vibration Characteristics

4.4.2 Horizontal Response during SSE and LOCA Events

Using the methods to determine the most limiting control rod guide thimble and fuel cladding stress and grid spacer impact force as described in Subsection 4.4.1, the FINDS code analysis { } performed in order to determine the stress in the control rod guide thimbles and fuel rods in each of the 257 fuel assemblies. All of the results are shown in Appendix F.

The procedure to obtain bending stresses from the FINDS code analysis is illustrated in the flow chart shown in Figure 4.1.1-1. The method to evaluate the effects of uncertainty is described in Section F.4.0 of Appendix F.

The maximum bending stress of the control rod guide thimble and fuel cladding without uncertainties at each core location is shown in Table 4.4.2-1 and Table 4.4.2-2, respectively. As shown in both tables, { }

The maximum bending stress of the control rod guide thimble and fuel cladding with uncertainties at each core location is shown in Table 4.4.2-3 and Table 4.4.2-4. As shown in the both tables, { }

{ } In order to determine maximum stress, the maximum bending stress is combined with stress due to the vertical response and stress due to normal operation in each axial position along the fuel assembly axis, as described in Section 4.4.3 below.

The impact force of the grid spacer is also determined per the flow chart shown in Figure D.1.0-1 of Appendix D and the number of buckled grid spacers, including uncertainties, in each of 257 fuel assemblies is obtained as described in Section F.3.0 of Appendix F.

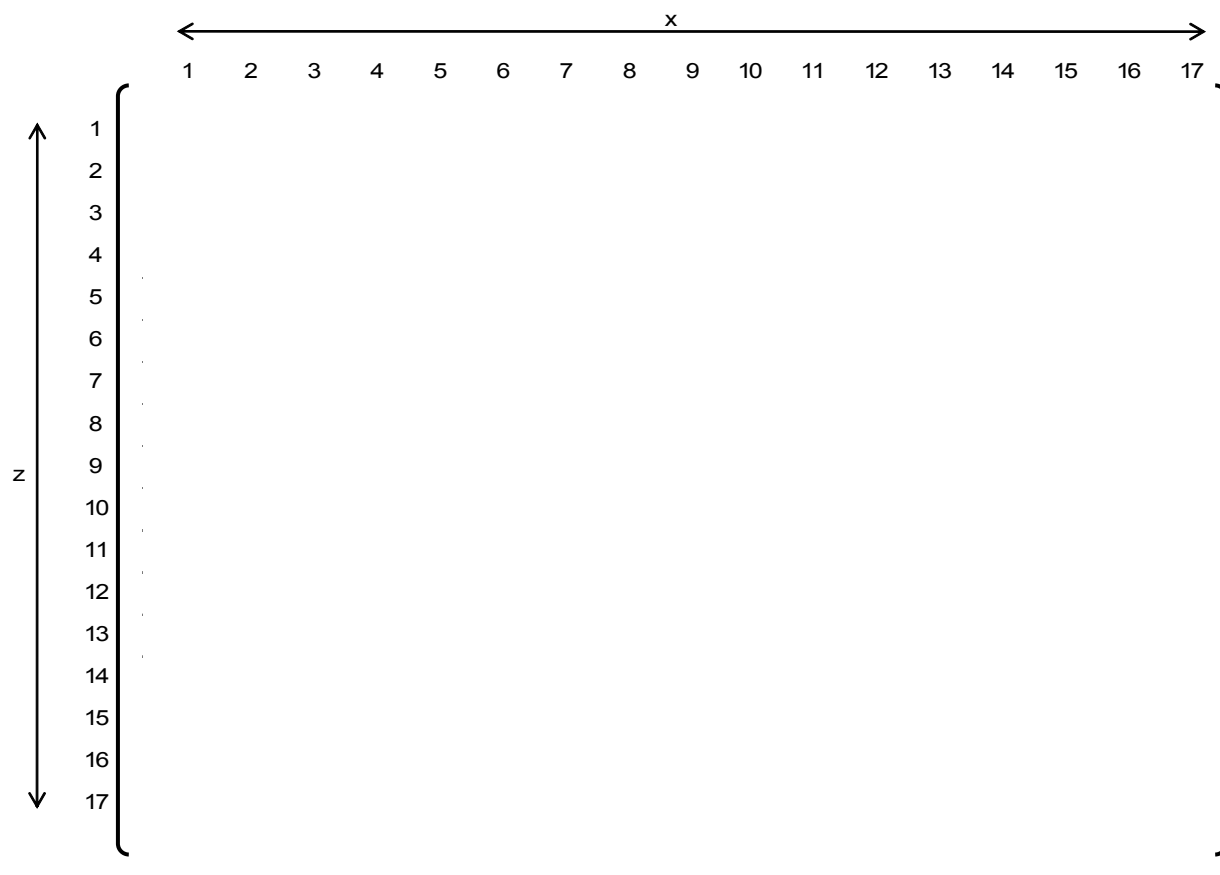
Table 4.4.2-5 shows the best estimate number of buckled grid spacers. { }

When uncertainties are included, the number of buckled grid spacers increases to that shown in Table 4.4.2-6. Although the impact force of the grid spacer calculated by FINDS code is relatively conservative, as shown in Appendix C, these more conservative results are used in the RCCA insertability and reactor coolability evaluation which are discussed in Section 4.5 and Appendix D.

Since the grid spacer deformation due to the buckling causes control rod guide thimble and fuel cladding distortion, the stress caused by the plastic deformation is calculated and superimposed on the stress due to fuel assembly deflection by the SRSS method. The results shown in Table 4.4.2-1 through Table 4.4.2-5 include the stress resulting from this deformation.

**Table 4.4.2-1 Best Estimated Bending Stress for SSE and LOCA
Horizontal Direction (Control Rod Guide Thimble)**

(Unit: MPa)



: Maximum value

**Table 4.4.2-2 Best Estimated Bending Stress for SSE and LOCA
Horizontal Direction (Fuel Cladding)**

(Unit: MPa)

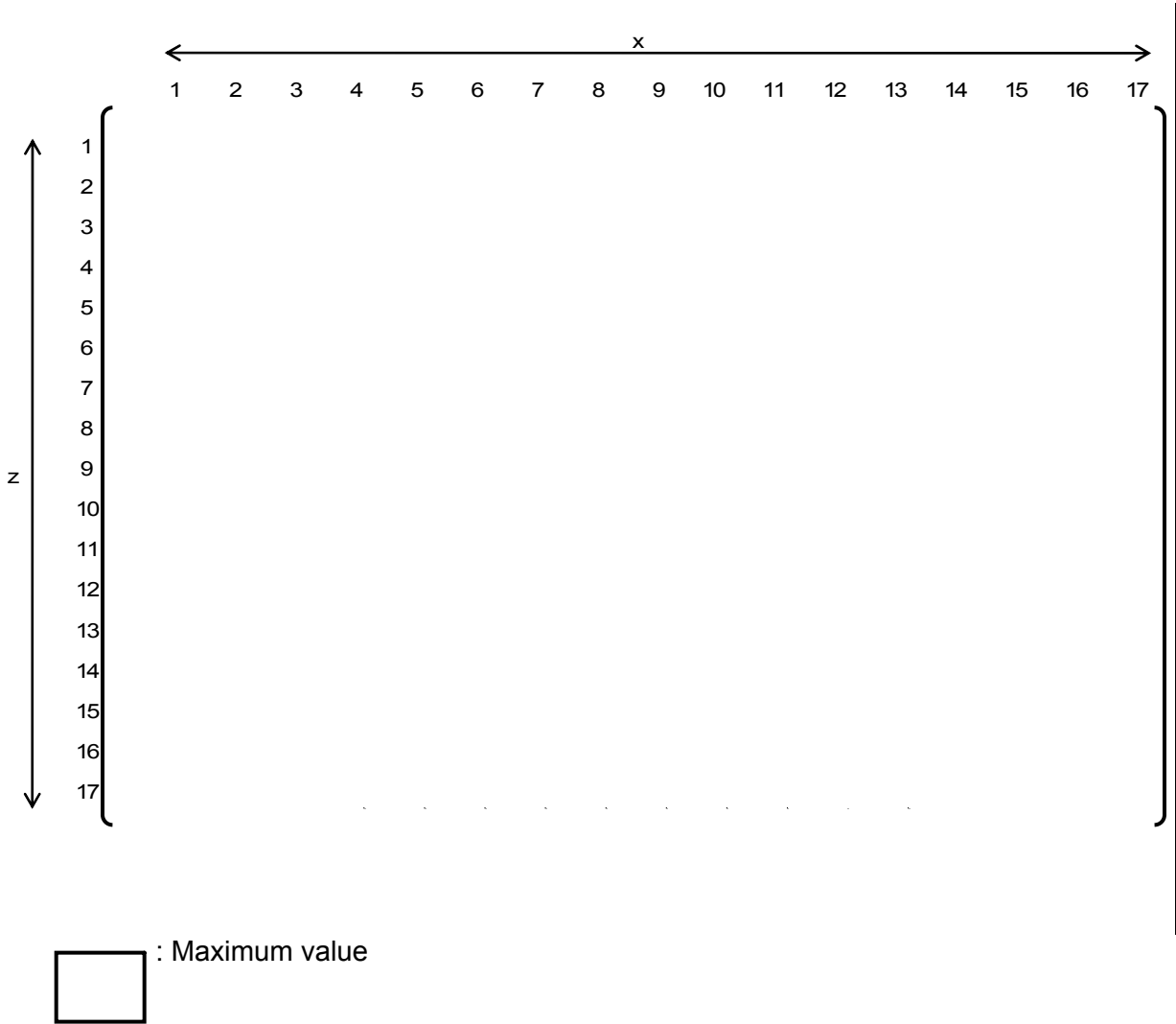
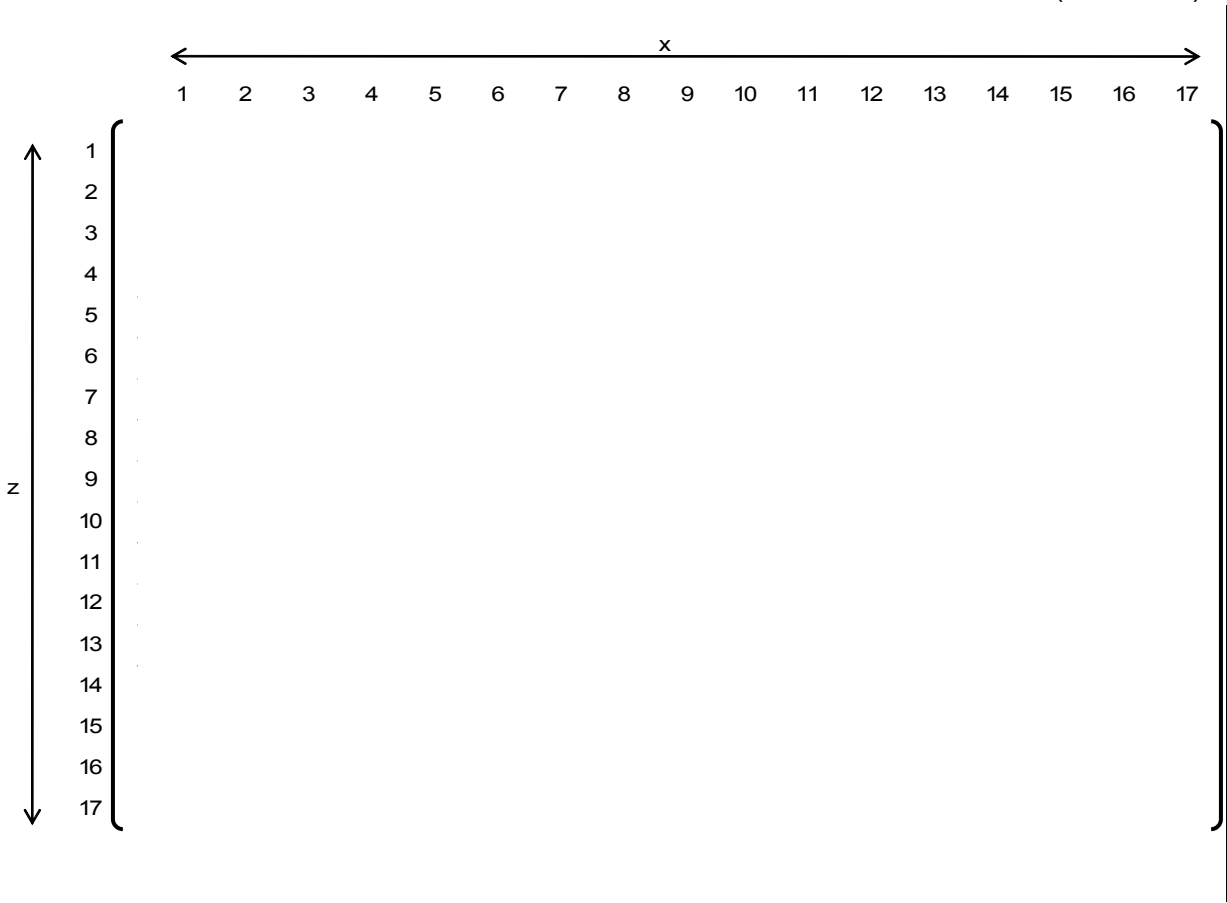


**Table 4.4.2-3 Bending Stress for SSE and LOCA Horizontal Direction
(Control Rod Guide Thimble) including Uncertainties**

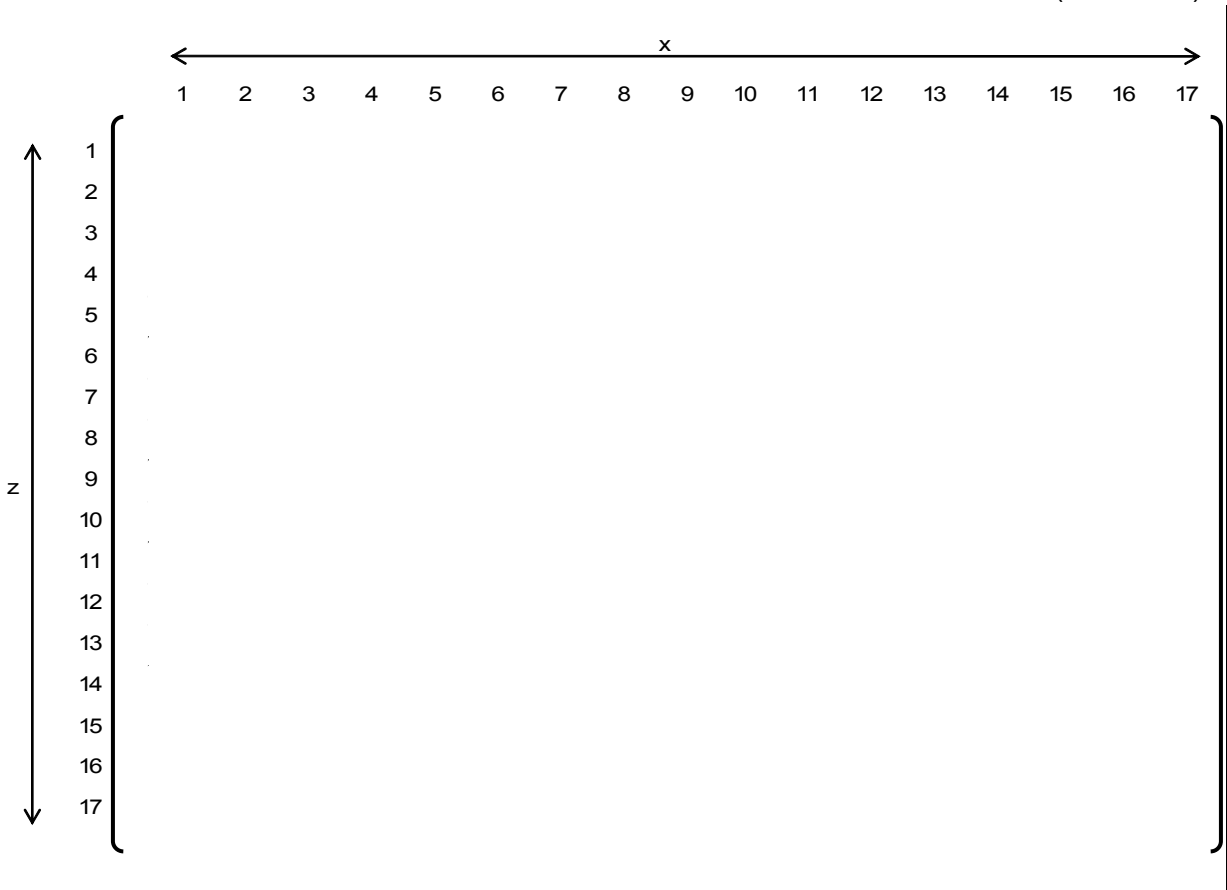
(Unit: MPa)




☐ : Maximum value

**Table 4.4.2-4 Bending Stress for SSE and LOCA Horizontal Direction
(Fuel Cladding) including Uncertainties**

(Unit: MPa)



 : Maximum value

**Table 4.4.2-5 Buckled Grid Spacer Number for Each Fuel Assembly Position
(Best Estimate Results)**

		x																
		1	2	3	4	5	6	7	8	9	10	11	12	13	14	15	16	17
z	1																	
	2																	
	3																	
	4																	
	5																	
	6																	
	7																	
	8																	
	9																	
	1																	
	1																	
	1																	
	1																	
	14																	
	15																	
	16																	
	17																	

Table 4.4.2-6 Buckled Grid Spacer Number for Each Fuel Assembly Position Including Uncertainties

		x																
		1	2	3	4	5	6	7	8	9	10	11	12	13	14	15	16	17
z	1																	
	2																	
	3																	
	4																	
	5																	
	6																	
	7																	
	8																	
	9																	
	10																	
	11																	
	12																	
	13																	
	14																	
	15																	
	16																	
	17																	

4.4.3 Stress Evaluation Results of the Fuel Assembly under SSE and LOCA Events

As described in Section C.5.0 in Reference 4-1, the stress due to the combined SSE and LOCA response is obtained by combining the bending stress of the control rod guide thimbles and fuel cladding in each of the 257 fuel assemblies, obtained from the horizontal response, and the membrane stress resulting from the vertical response by the SRSS method and then by simple addition of the stress due to normal operation (NO).

The bending stresses of the fuel assembly due to lateral displacement are obtained by the response to the 560-100 wave and the response to the CLB 8B 102%LF as described in Subsection.4.3.1.

The membrane stresses of the fuel assembly due to vertical acceleration are calculated based on the analysis results which are obtained by the reactor internal response analyses to SSE and LOCA events. The relative velocity between the bottom nozzle and the lower core support plate is used as input for the transient analysis model shown in Figure 4.2-2 because fuel assembly lift-off from the lower core support plate occurs in the SSE and LOCA events and the fuel assembly then impacts onto the lower core support plate. The load on the fuel assembly and the impact velocity of the fuel assembly onto the lower core support plate are given in Table 4.4.3-1.

For normal operation, holddown spring force, hydraulic lift force, buoyancy force, self-weight and reaction force from the lower core support plate are considered in calculating membrane stress. The details are explained in Section 4.0 of Reference 4-7.

The maximum stress obtained by combining the stresses for NO, SSE event and LOCA event is shown in Table 4.4.3-2.

As shown in Table 4.4.3-2, the resulting stress is lower than the acceptance limit and it is therefore confirmed that each component has the required strength.

No benefit from the increase of strength due to irradiation is assumed, which provides additional conservatism (margin) to the acceptance limit.

Table 4.4.3-1 Peak Vertical Load for Fuel Assembly under SSE (560-100, 900-200) and LOCA (CLB 8B 102%LF) Events

Item	Units	SSE 560-100	SSE 900-200*	CLB 8B 102%LF
Holddown Spring Reaction Force	lbf (N)			
Impact Velocity**	inch/s (mm/s)			

* This case shows the maximum membrane stress.

* Impact velocity is the relative velocity between the bottom nozzle and the lower core support plate.

Table 4.4.3-2 Stress for the Fuel Assembly under SSE (560-100) and LOCA (CLB 8B 102%LF) Events at Most Limiting Conditions (EOL with Uncertainties)

(a) Control rod guide thimble

				Unit: ksi (MPa)
Stress Category	NO	SSE & LOCA	NO + SSE & LOCA	BOL Acceptance limit at { } deg.F
Primary Membrane Stress	{			}
Primary Membrane Stress + Primary Bending Stress				
* Stress due to vertical load				
** Stress due to vertical load and horizontal displacement and distortion caused by the grid deformation				

(b) Top nozzle

				Unit: ksi (MPa)
Stress Category	NO	SSE & LOCA	NO + SSE & LOCA	BOL Acceptance limit at { } deg.F
Primary Membrane Stress + Primary Bending Stress				
* Stress due to the vertical load				

(c) Bottom nozzle

				Unit: ksi (MPa)
Stress Category	NO	SSE & LOCA	NO + SSE & LOCA	BOL Acceptance limit at { } deg.F
Primary Membrane Stress + Primary Bending Stress				
* Stress due to the vertical load				

(d) Buckling of control rod guide thimble

Unit: lbf (N)	
Maximum force	Acceptance limit

(e) Fuel cladding

Unit: ksi (MPa)		
Stress Category	NO +SSE & LOCA	BOL Acceptance limit*
Primary Membrane Stress		
Primary Membrane Stress + Primary Bending Stress		
Primary Membrane Stress + Local Membrane Stress		

* Acceptance limit at the fuel cladding temperature

4.5 Evaluation Results for Rod Cluster Control Insertability and Reactor Coolability

Rod Cluster Control (RCC) Insertability and reactor coolability are required to be maintained during SSE and LOCA events. The US-APWR fuel assemblies responses are analyzed to four SSE acceleration waves and five LOCA acceleration waves which are required RCC insertability, as described in Section 4.4.1 of this report. As results of comparison of the combined impact force during SSE and LOCA events by using SRSS calculation with the 95% lower bound based on the true mean for buckling force of grid spacers, plastic deformations due to buckling were judged to occur in some grid spacers of fuel assemblies. These grid spacer deformations are likely to influence RCC insertability and reactor coolability since RCC guide thimbles are misaligned from original positions and each fuel rod cell pitch decreases.

The following conclusions are obtained as further analysis is shown in Appendix D.

Even if the maximum credible deformation is assumed for the grid spacers judged to be buckled when the SSE and LOCA events are combined, grid spacer deformation in the US-APWR fuel assemblies is concluded;

to have little effect on the rod cluster control insertability, as results of comparing with experimental results of grid spacer deformation with control rod guide thimble misalignment and fuel assembly vibration, and

to have little effect on reactor coolability, since the deformation of the grid spacer does not alter the basic pin-coolant-channel-to-pin-coolant-channel arrangement (fuel rod bundle geometry) for the fuel assemblies containing the deformed grid spacers which decrease the fuel rod pitch, and the core flow area is unchanged from the original configuration, and PCT (peak cladding temperature) evaluation during the LOCA event demonstrates that consequence of the accident is substantially identical to that obtained by assuming no grid spacer deformation.

4.6 References

- (4-1) "FINDS: Mitsubishi PWR Fuel Assemblies Seismic Analysis Code", MUAP-07034-P (Proprietary) and MUAP-07034-NP (Non-Proprietary) Revision 3, July 2010
- (4-2) MHI's Responses to the NRC's Requests for Additional Information on Topical Report MUAP-07034-P "FINDS: Mitsubishi PWR Fuel Assemblies Seismic Analysis Code", UAP-HF-08139-P (Proprietary) and MUAP-08139-NP (Non-Proprietary), August 2008
- (4-3) American Society of Mechanical Engineers Boiler and Pressure Vessel Code Section III
- (4-4) "Seismic Design Bases of the US-APWR Standard Plant", MUAP-10001-P (Proprietary) and MUAP-10001-NP (Non-Proprietary) Revision 1, May 2010
- (4-5) "Summary of Stress Analysis Results for the US-APWR Reactor Coolant Loop Branch Piping", MUAP-09011-P (Proprietary) and MUAP-09011-NP (Non-Proprietary) Revision 2, December 2010
- (4-6) U.S. Nuclear Regulatory Commission, Regulatory Guide 1.122, "Development of Floor Response Spectra for Seismic Design of Floor-Supported Equipment or Components", February 1978
- (4-7) "US-APWR Fuel System Design Evaluation", MUAP-07016-P (Proprietary) and MUAP-07016-NP (Non-Proprietary) Revision 3, August 2010

5.0 STRESS ANALYSIS OF THE ROD CLUSTER CONTROL ASSEMBLY FOR SSE AND LOCA EVENTS

5.1 Stress Evaluation Methodology for Rod Cluster Control Assembly

5.1.1 Stress Analysis Model for Rod Cluster Control Assembly

During normal operation, the RCCA drive rod is engaged with the CRDM near its middle and with the RCCA spider hub at the bottom. The RCCA is supported laterally over short span lengths by the guide plates of the upper internals control rod guide tube.

In the reactor shutdown state, the RCCA is fully inserted into the fuel assembly. In SSE or LOCA events, the fuel assembly deflects laterally and the control rods deform laterally as well as during insertion. The flow chart, shown in Figure 5.1.1-1, is used to determine the control rod stresses associated with the lateral deformations generated in both SSE and LOCA events.

The stresses of the control rod are evaluated at three representative axial positions 1) fully withdrawn from the fuel assembly, 2) half inserted and 3) fully inserted into the fuel assembly, as shown in Figure 5.1.1-2. The resulting stress of the control rod when fully withdrawn is very small, due to the reason described in Section 5.2, and is negligible compared with the acceptance limit. In the half inserted and fully inserted positions, the stresses of the control rod are evaluated by an FEM model considering the fuel assembly deflections in the SSE and LOCA events. The stress due to LOCA event is combined with the stress due to an SSE event using the SRSS method. The stresses of the cladding and the reduced diameter portion of the control rod top end plug are evaluated in the analysis.

The FEM analysis model for the RCCA consists of several elastic beams which represent each component of the RCCA, as shown in Figure 5.1.1-3.

The stresses due to the vertical response of the RCCA in the SSE and LOCA events are calculated using the same model as shown in Figure 5.1.1-3, considering the maximum vertical acceleration of the CRDM which is obtained by the dynamic response analysis of the reactor vessel and reactor internals. The flow chart for this stress evaluation is shown in Figure 5.1.1-4. The stress due to LOCA event is combined with the stress due to an SSE event using the SRSS method.

The RCCAs of the US-APWR are located inside the outermost ring of assemblies, as shown in Figure 4.3-4 of DCD chapter 4.3⁽⁵⁻¹⁾. The determination of RCCA maximum stresses is based on the deflections and deformations of the fuel assembly in this inner region of the core.

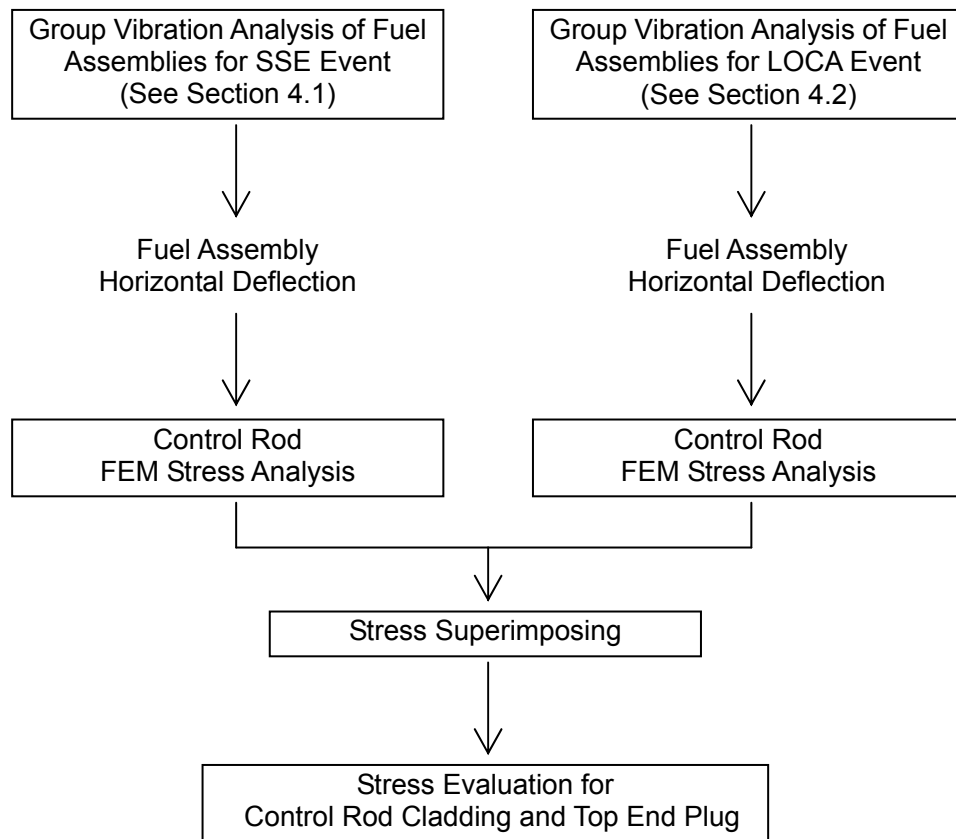


Figure 5.1.1-1 Stress Evaluation for the Control Rod Assembly due to Fuel Assembly Horizontal Deflection during SSE and LOCA Events

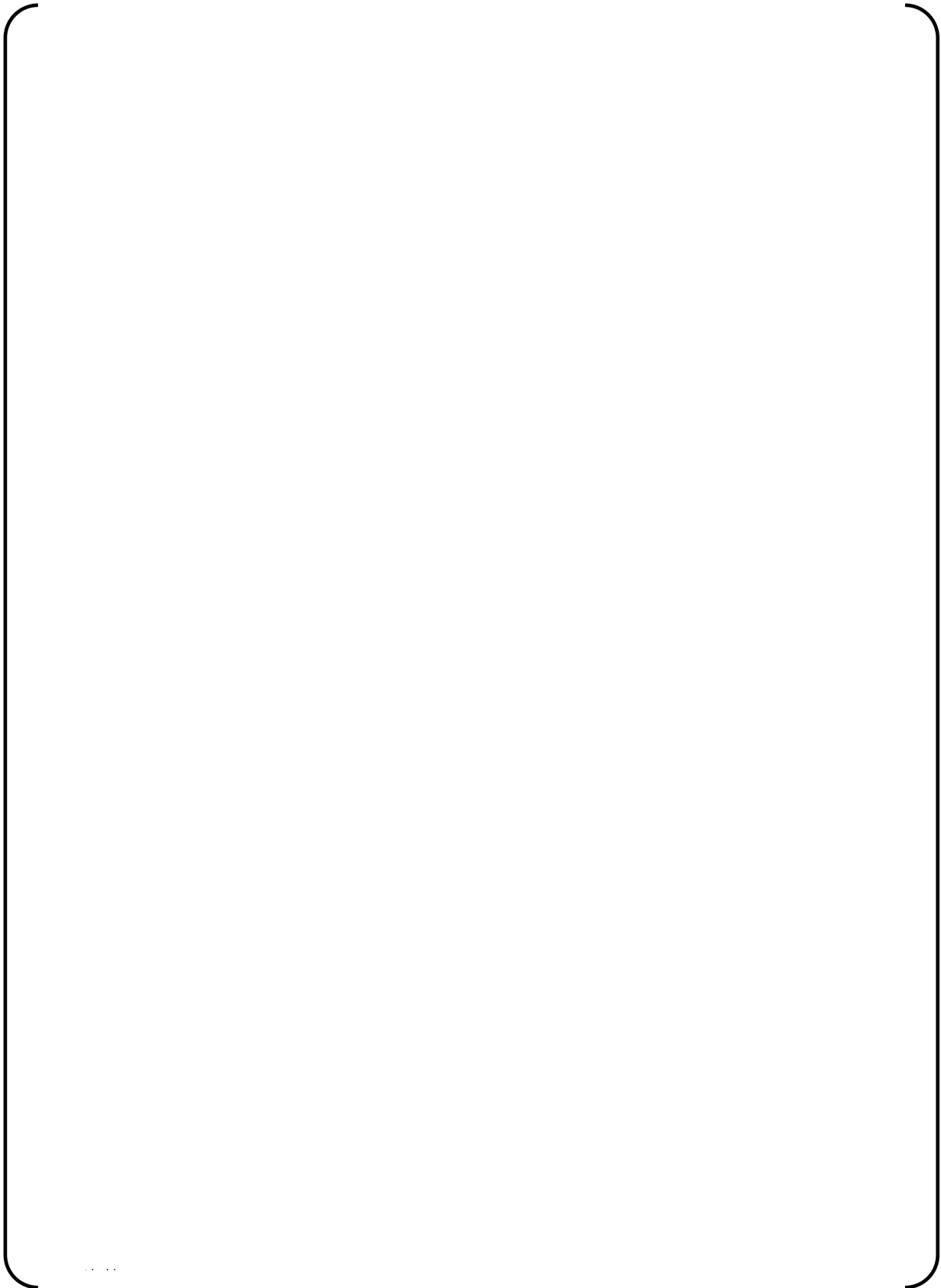


Figure 5.1.1-2 Axial Positions of RCCA for Stress Evaluation



Figure 5.1.1-3 Analysis Model for RCCA

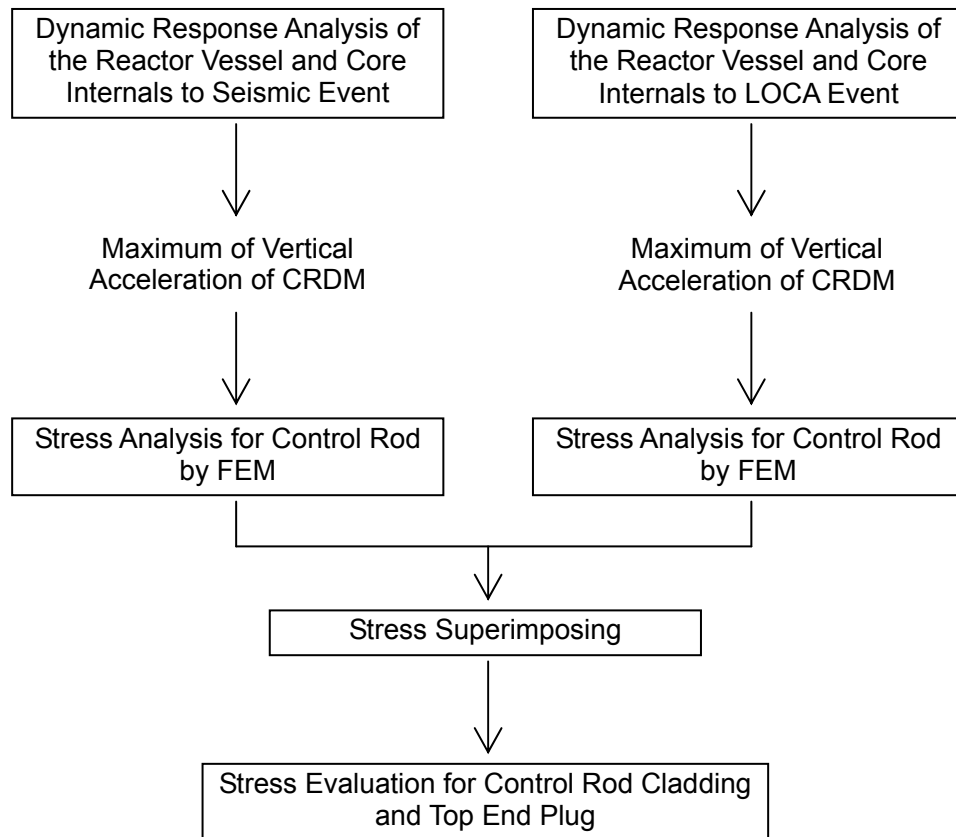


Figure 5.1.1-4 Stress Evaluation for the Control Rod Assembly due to Vertical Acceleration during SSE and LOCA Events

5.1.2 Stress Categories for the Rod Cluster Control Assembly

The stresses due to the horizontal deflection and vertical acceleration are combined using the SRSS method. In addition to the above stresses, the effect of the CRDM stepping loads or the scram impact load is taken into account in the half inserted and fully inserted cases, respectively. All of these stresses are additive.

The stress due to the pressure differential (system pressure versus control rod internal pressure) is also evaluated and added to the stresses calculated above.

The stress categories used in evaluating the integrity of the control rod assembly are summarized in Table 5.1.2-1.

Table 5.1.2-1 Stress Categories

Loading Conditions	Stress Category	Classification
Lateral deformation due to deflection of fuel assembly during SSE and LOCA	Primary Bending Stress	Pb
Vertical acceleration during SSE and LOCA	Primary Membrane Stress	Pm
Stepping Load of CRDM or RCCA Scram Impact Load	Primary Membrane Stress	Pm
Inner-outer differential pressure	Primary Membrane Stress	Pm

5.2 Stress of Rod Cluster Control Assembly during SSE and LOCA Events

5.2.1 Stress due to Horizontal Deflection during SSE and LOCA events

As described in Section 2.2 of the report, the stresses of the RCCA cladding and the reduced diameter portion of the top end plug of the control rod are evaluated.

Of the three representative axial positions of the RCCA relative to the fuel assembly, the resulting stress when the RCCA is fully withdrawn is very small because the lateral deformation of the control rod guide tube during SSE and LOCA events is very small and the control rod is supported by the guide plates over short span lengths, of about () inch () mm) or less. Therefore, the deflection of the control rod is small and the resulting stresses of the control rod at the fully withdrawn position during SSE and LOCA events are negligible compared with the acceptance limit. On the other hand, in the half inserted and fully inserted axial positions, the stress of the control rod is evaluated because it is affected by the deflection of the fuel assembly. The deflection of the fuel assembly giving the maximum stress of the control rod guide thimble for SSE and LOCA events is obtained from the response analysis described in Subsection 4.3.1. The analysis result for the 560-100 and CLB 8B 102%LF with EOL condition is used for the stress analysis of the control rod because the deflection of the fuel assembly is the largest compared with the other conditions and therefore results in a conservative evaluation. The lateral displacements of each fuel assembly's grid spacers determine the shape of the control rod used in the model shown in Figure 5.1.1-3 to estimate the stress of the control rod. Since the grid spacer deformation causes control rod guide thimble distortion, the stress caused by the grid spacer deformation is calculated and superimposed on the stress due to fuel assembly deflection by the SRSS method in the same way as fuel assembly stress evaluation.

The calculated stress of the control rod due to lateral deflection is shown in Table 5.2.1-1. The uncertainty of fuel assembly deflection is considered in the same way as fuel assembly stress evaluation described in Subsection 4.4.1.

**Table 5.2.1-1 Stresses of Control Rod due to Horizontal Deflection during
SSE and LOCA Events**

Unit: ksi (MPa)			
	Stress category	Cladding of control rod	Top end plug of control rod (Reduced diameter portion)
Half inserted	Primary Bending Stress	[]
Fully inserted	Primary Bending Stress		

5.2.2 Stress due to Vertical Acceleration during SSE and LOCA Events

The stress due to the vertical acceleration is calculated considering the maximum acceleration obtained from the dynamic analysis of the reactor vessel and reactor internals of () inch/s² () mm/s² for SSE event and () inch/s² () mm/s² for LOCA event. Applying the acceleration to the model shown in Figure 5.1.1-3 vertically, the stresses of the limiting components are evaluated.

The calculated stress of the control rod assembly due to vertical acceleration is shown in Table 5.2.2-1.

Table 5.2.2-1 Stresses of Control Rod due to Vertical Acceleration during SSE and LOCA Events

Unit: ksi (MPa)			
	Stress category	Cladding of control rod	Top end plug of control rod (Reduced diameter portion)
Half inserted	Primary Membrane Stress		
Fully inserted			

5.2.3 Stress Evaluation Results of Rod Cluster Control Assembly for SSE and LOCA Events

In addition to the stress due to SSE and LOCA events, the effect of the CRDM stepping loads described in Table 5.1-2 of Reference 5-2 is considered in the evaluation for a half withdrawn RCCA. For a fully inserted RCCA, the RCCA scram impact load of [] lbf ([] N) is used as described in Subsection 4.1.2.2.1 of Reference 5-2.

Also, the effect of differential pressure (system pressure versus control rod internal pressure) is taken into account. The maximum system pressure of [] ksi ([] MPa) is used and an internal pressure of [] psi ([] MPa) at cold condition is used for conservatism.

The evaluation results are summarized in Table 5.2.3-1 to confirm the RCCA integrity in the combined SSE and LOCA events.

Table 5.2.3-1 Stress Evaluation Results for Control Rod

(a) Cladding of control rod

		Unit: ksi (MPa)	
	Stress Category	Stress	Acceptance Limit @ [662] * deg.F ⁽⁵⁻²⁾
Half inserted	Primary Membrane Stress	[]	[]
	Primary Membrane Stress +Primary Bending Stress		
Fully inserted	Primary Membrane Stress		
	Primary Membrane Stress +Primary Bending Stress		

* Obtained from thermal analysis performed for the control rod

(b) Top end plug of control rod (reduced diameter portion)

		Unit: ksi (MPa)	
	Stress Category	Stress	Acceptance Limit @ [617] ** deg.F ⁽⁵⁻²⁾
Half inserted	Primary Membrane Stress	[]	[]
	Primary Membrane Stress +Primary Bending Stress		
Fully inserted	Primary Membrane Stress		
	Primary Membrane Stress +Primary Bending Stress		

** Outlet temperature of the core

5.3 References

- (5-1) MHI, "Design Control Document for the US-APWR", MUAP-DC004, Rev.2 October, 2009
- (5-2) "US-APWR Fuel System Design Evaluation", MUAP-07016-P (Proprietary) and MUAP-07016-NP (Non-Proprietary) Revision 3, August 2010

6.0 CONCLUSION

This report describes the functional requirements and acceptance criteria of the US-APWR fuel system, namely the fuel assembly and the rod cluster control assembly, for SSE and LOCA events. Also, the evaluation results for the dynamic response and integrity of the fuel system are included in the report to confirm that the required functions are maintained during these events.

The effects of irradiation on the fuel system response for SSE and LOCA events were also discussed in the report to show that the integrity of the fuel system is maintained under irradiated conditions.

Appendix A

EFFECT OF IRRADIATION ON GRID SPACER IMPACT BEHAVIOR

December 2010

**© 2010 Mitsubishi Heavy Industries, Ltd.
All Rights Reserved**

Table of Contents

List of Tables	A-3
List of Figures	A-4
A.1.0 INTRODUCTION	A-5
A.2.0 EFFECT OF GRID SPACER'S SPRING RELAXATION	A-6
A.2.1 Impact Test of Grid Spacers with Relaxed Spring Force	A-6
A.2.2 In-elastic Impact Model of the Grid Spacer with Relaxed Spring Force	A-14
A.3.0 EFFECT OF IRRADIATION EMBRITTLEMENT	A-22
A.3.1 Tested Grid Spacers	A-22
A.3.2 Test Procedure	A-25
A.3.3 Test Results	A-25
A.4.0 CONCLUSION	A-32
A.5.0 REFERENCES	A-33

List of Tables

Table A.2.1-1	Free Vibration Pendulum Test Results.....	A-9
Table A.2.1-2	Buckling Force of the As-built Grid Spacers.....	A-10
Table A.2.1-3	Buckling Force of the Relaxed Grid Spacers	A-10
Table A.2.2-1	Test Sequence for Deformation Progression (pre-buckling included)....	A-15
Table A.3.3-1	Buckling Force and Dynamic Stiffness of the As-built, Relaxed and Hydrided Grid Spacers.....	A-27

List of Figures

Figure A.2.1-1	Grid Spacer Pendulum Type Impact Test	A-11
Figure A.2.1-2	Impact Force versus Impact Velocity (As-built Grid Spacers)	A-12
Figure A.2.1-3	Impact Force versus Impact Velocity (Relaxed Grid Spacers)	A-12
Figure A.2.1-4	Coefficient of Restitution vs Impact Velocity (As-built Grid Spacers) ...	A-13
Figure A.2.1-5	Coefficient of Restitution vs Impact Velocity (Relaxed Grid Spacers) ..	A-13
Figure A.2.2-1(a)	Impact Force (As-Built_5)	A-16
Figure A.2.2-1(b)	Impact Force (As-Built_6)	A-16
Figure A.2.2-2(a)	Plastic Deformation (As-Built_5)	A-17
Figure A.2.2-2(b)	Plastic Deformation (As-Built_6)	A-17
Figure A.2.2-3(a)	Coefficient of Restitution (As-Built_5)	A-18
Figure A.2.2-3(b)	Coefficient of Restitution (As-Built_6)	A-18
Figure A.2.2-4(a)	Impact Force (Relaxed_7)	A-19
Figure A.2.2-4(b)	Impact Force (Relaxed_8)	A-19
Figure A.2.2-5(a)	Plastic Deformation (Relaxed_7)	A-20
Figure A.2.2-5(b)	Plastic Deformation (Relaxed_8)	A-20
Figure A.2.2-6(a)	Coefficient of Restitution (Relaxed_7)	A-21
Figure A.2.2-6(b)	Coefficient of Restitution (Relaxed_8)	A-21
Figure A.3.0-1	Effect of Hydrogen Content on Zircaloy-4 Material Properties	A-23
Figure A.3.1-1	Autoclave for Full-Sized Grid Spacer's Hydrogen Absorption	A-24
Figure A.3.3-1	Impact Force of Hydrided, As-built and Relaxed Grid Spacers	A-28
Figure A.3.3-2	Pendulum Release Angle versus Weight Impact Velocity	A-29
Figure A.3.3-3	Deformation Progression of Hydrided, As-built, and Relaxed Grid Spacers	A-30
Figure A.3.3-4	Top View of the Hydrided_3 Grid Spacer (After the 5 th Impact, at a 17° Release Angle)	A-31
Figure A.3.3-5	Side View of the Hydrided_3 Grid Spacer (After the 5 th Impact, at a 17° Release Angle)	A-31

A.1.0 INTRODUCTION

The spring force of the grid spacer decreases during irradiation, primarily due to irradiation induced stress relaxation. The reduced grid spring force can affect the grid spacer's impact behavior during seismic or LOCA events. In this Appendix, the effect of the relaxation of the grid spacer spring force on the grid spacer's impact behavior is determined by testing.

The effect of the reduced ductility of the grid spacer material (due to irradiation hardening) on the grid spacer's buckling load and deformation behavior is also described in this Appendix.

A.2.0 EFFECT OF GRID SPACER'S SPRING RELAXATION

A Zr-4 grid spacer's spring force typically relaxes significantly during irradiation, which may have an effect on the grid spacer's impact behavior. To investigate the influence of this grid spring force relaxation, grid spacer impact tests were performed with grid spacers whose spring force was relaxed in a furnace to simulate end of life (EOL) condition.

A.2.1 Impact Test of Grid Spacers with Relaxed Spring Force

(1) Tested Grid Spacers

The following Z3 type of Zircaloy-4 grid spacers, which are intended to be used in the US-APWR fuel assembly, were tested.

- Grid spacers with as-built spring force (As-built grid spacers) ---- 6 Grid Spacers
- Grid spacers with relaxed spring force (Relaxed grid spacers) ---- 8 Grid Spacers

The process of reducing the spring force begins with inserting short solid stainless steel rods, of a larger diameter than the fuel rod cladding, into all of the fuel rod cells. To relax the spring force, the grid spacers are then placed in a furnace at [] deg. F ([] deg. C) for [] hours. The permanent cell size increase occurs due to yielding of the Zr-4 material and thermal creep at the elevated temperature. The temperature, time in the furnace and the diameter of the stainless steel rod were empirically determined to enlarge the cell size so that the spring force after the relaxation process corresponded to approximately [] % of the as-built spring force, as described in Subsection 4.4 of Reference A-1. Short sections of 17x17 fuel rod clad replaced the stainless steel rods when the grid spacers were used in the impact tests.

(2) Test Procedure

The impact tests for the grid spacers were performed by a pendulum impact test apparatus as shown in Figure A.2.1-1. A furnace is placed around the grid spacer to heat it to the test temperature. To perform the impact test the furnace is quickly removed and replaced with the weight. The weight at the end of the pendulum arm impacts with the grid spacer that is attached to a rigid wall. Considering reactor operating temperatures the grid spacer is heated up to [] deg. F ([] deg. C). Grid spacer temperatures during heat-up and at impact are monitored by thermocouples.

A load cell on the rigid wall and an accelerometer on the weight are used to determine impact force and load-displacement characteristics. An angular transducer at the top end of the pendulum arm senses the release angle and rebound angle needed to calculate the coefficient of restitution. The swinging weight is prevented from re-impacting the grid spacer after achieving its maximum rebound angle.

The impact test is repeatedly performed at increasing release angles and continues to and beyond the buckling load of the grid spacer.

(3) Data reduction

Physical data obtained by the test are reduced as follows.

<Weight velocity at the impact>

Before the grid impact test is performed, a free vibration test is conducted to obtain the relationship between pendulum arm release angle and the velocity of the weight at the moment of grid impact. The weight's velocity dependence on release angle is calculated by following equation.

$$V(\theta_0) = 2PL_0 \sin(\theta_0/2)$$

where

$V(\theta_0)$: Weight's velocity (m/sec) at grid impact when release angle is θ_0 .

θ_0 : Release angle (degrees)

P : P is obtained by the following equation as a function of the pendulum period and the first order elliptic integral.

$$P = \frac{1}{T} K(k^2)$$

where

T : Quarter cycle of the pendulum period (sec), T is determined by the pendulum arm's displacement history which is measured by the angular transducer in the free vibration tests of the pendulum.

$K(k^2)$: The first order elliptic integral for $k = \sin(\theta_0/2)$

P is calculated in Table A.2.1-1 and the averaged value of [] is used in the velocity calculation.

L_0 : Pendulum arm length, 1 (m)

<Buckling Load>

Since the impact force tends to be lower after buckling, the buckling force is defined as the highest impact force measured at the step before the impact force begins to decrease.

<Dynamic Stiffness>

Using the method of least squares, the slope "a" (F/V) is obtained for a linear relationship between the impact velocity of the weight, V and the impact force, F before buckling.

In addition, the following relationship between the impact velocity of the weight and the impact force before buckling is used.

$$F = \sqrt{M_{eq} K} V$$

where

K : Dynamic stiffness of the grid spacer
M_{eq} : Equivalent mass of the weight
F : Impact force measured by load cell sensor
V : Impact velocity of the weight

The dynamic stiffness of the grid spacer is calculated by using the equation " $a = \sqrt{M_{eq}K}$ " and solving for K.

< Coefficient of Restitution >

The coefficient of restitution is defined as ratio of the rebound angle to the release angle of the pendulum arm. The angle is measured by the angular transducer.

(4) Test results

Figure A.2.1-2 and Figure A.2.1-3 show the relationship between impact force and impact velocity for the as-built and the relaxed grid spacers, respectively. In addition, Figure A.2.1-4 and Figure A.2.1-5 illustrate the relationship between the coefficient of restitution and impact velocity of both types of grid spacers, respectively.

Although it can be seen in Figure A.2.1-2 that the impact force of the as-built grid spacer increases again after the 20 inch/sec velocity, the buckling force is defined as the impact force at around 17 inch/sec because the coefficient of restitution for the as-built grid spacers is predominantly decreasing after about 17 inch/sec. On the other hand, the trend of the buckling force of the relaxed grid spacers continually decreases after buckling at around 17 inch/sec, as seen in Figure A.2.1-3.

The buckling force for both conditions of the grid spacers is summarized in Table A.2.1-2 and Table A.2.1-3. Based on the comparison of the average buckling load, the decrease in the buckling load due to the relaxed spring force is calculated to be () %.

Using the test data for the buckling forces of the grid spacers, the 95% confidence values of the true mean are calculated, consistent with Reference A-2, for grid spacers with as-built spring force and relaxed spring force. The calculated 95% confidence values are shown in Table A.2.1-2 for the grid spacer with as-built spring force, and in Table A.2.1-3 for the grid spacer with relaxed spring force. Based on the comparison of the lower bound buckling force, the decrease in the buckling load due to the relaxed spring force is calculated to be () %.

Table A.2.1-1 Free Vibration Pendulum Test Results

Release Angle : θ_0 (degree)	$\sin(\theta_0/2) : k$	k^2	$K(k^2)$	1/4 Cycle : T (sec)	$P=K(k^2)/T$ (1/sec)
2					
4					
6					
8					
10					
12					
14					
16					
18					
20					

Table A.2.1-2 Buckling Force of the As-built Grid Spacers

Grid Spacer No.	Buckling Force		Dynamic Stiffness	
	(lbf)	(kN)	(lbf/inch)	(kN/mm)
As-Built_1				
As-Built_2				
As-Built_3				
As-Built_4				
As-Built_5				
As-Built_6				
Ave.				
Std.				
95% confidence*				

Table A.2.1-3 Buckling Force of the Relaxed Grid Spacers

Grid Spacer No.	Buckling Force		Dynamic Stiffness	
	(lbf)	(kN)	(lbf/inch)	(kN/mm)
Relaxed_1				
Relaxed_2				
Relaxed_3				
Relaxed_4				
Relaxed_5				
Relaxed_6				
Relaxed_7				
Relaxed_8				
Ave.				
Std.				
95% confidence*				

* 95% confidence level based on the true mean of the test results

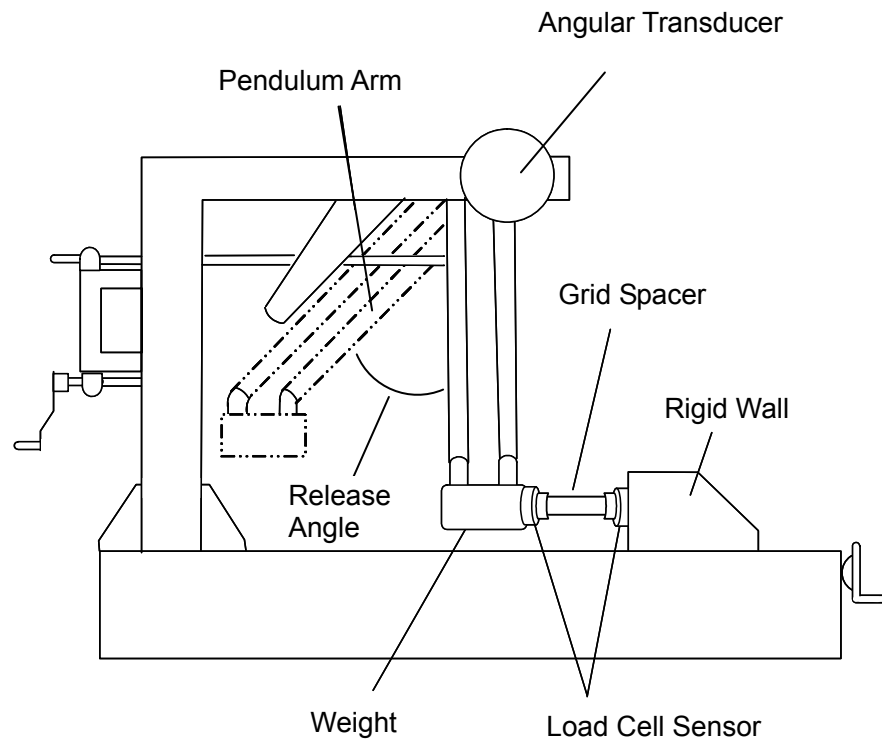


Figure A.2.1-1 Grid Spacer Pendulum Type Impact Test

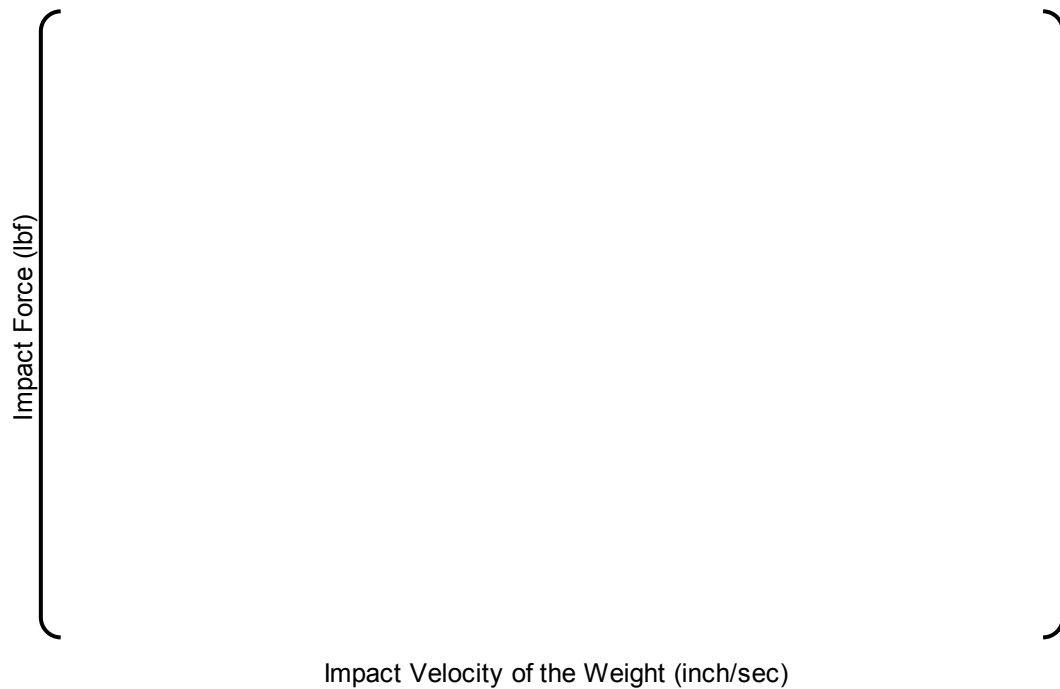


Figure A.2.1-2 Impact Force versus Impact Velocity (As-built Grid Spacers)

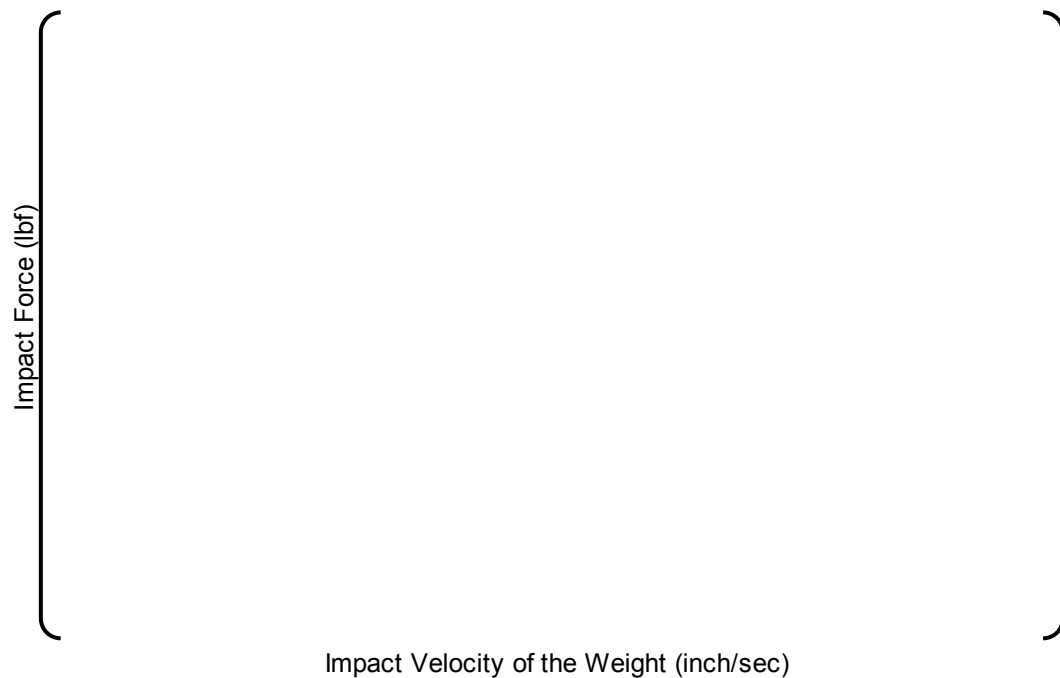


Figure A.2.1-3 Impact Force versus Impact Velocity (Relaxed Grid Spacers)

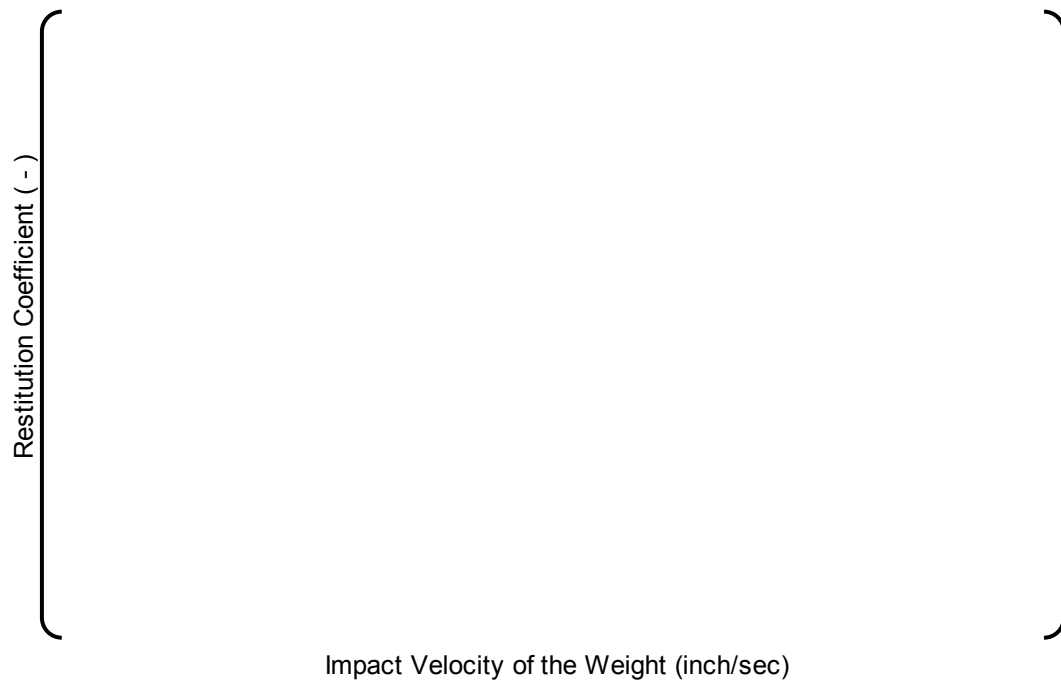


Figure A.2.1-4 Coefficient of Restitution vs Impact Velocity (As-built Grid Spacers)



Figure A.2.1-5 Coefficient of Restitution vs Impact Velocity (Relaxed Grid Spacers)

A.2.2 In-elastic Impact Model of the Grid Spacer with Relaxed Spring Force

As part of the grid impact test series, two each of the as-built and the relaxed grid spacers were used to perform a deformation progression test in order to develop the in-elastic models of the grid spacers in both conditions for use in the FINDS code.

As described in Subsection 3.7.3 in Reference A-3, the deformation progression test is used to obtain the characteristics of the grid spacer's energy storage capacity in the post-buckling phase. Basically the grid impact test is sequentially continued with the same or increased release angles until the grid spacer shows significant plastic deformation. During the test series, the plastic deformation is defined by the reduction in the grid spacer's envelope as measured by a vernier caliper. As-Built_5, As-Built_6, Relaxed_7 and Relaxed_8 were used in the deformation progression test. The test sequence is shown in Table A.2.2-1. The tests were performed with the temperature of the grid spacer at [] deg. F ([] deg. C).

Impact force, plastic deformation and the coefficient of restitution obtained by the deformation progression tests are used to adjust the grid spacer's in-elastic models used in the FINDS code, as described in Subsection 4.2 of Reference A-3. A comparison between analytical and experimental results for the as-built grid spacers are shown in the following figures.

- Figure A.2.2-1(a) Impact Force (As-Built_5)
- Figure A.2.2-1(b) Impact Force (As-Built_6)
- Figure A.2.2-2(a) Plastic Deformation (As-Built_5)
- Figure A.2.2-2(b) Plastic Deformation (As-Built_6)
- Figure A.2.2-3(a) Coefficient of Restitution (As-Built_5)
- Figure A.2.2-3(b) Coefficient of Restitution (As-Built_6)

Although the buckling of the as-built grid spacers is regarded as having occurred in test sequence No.3, the increase in impact force until test sequence No.9 or No.10 in Figure A.2.2-1(a) and (b) is simulated by the FINDS code model.

Plastic deformation of the as-built grid spacer is conservatively modeled as shown in the Figure A.2.2-2(a) and (b).

The same comparisons as in Figure A.2.2-1 thorough Figure A.2.2-3, but for the relaxed grid spacers, are shown in Figure A.2.2-4 thorough Figure A.2.2-6. The impact force for the relaxed grid spacers is well simulated by the empirically adjusted model, as shown in Figure A.2.2-4(a) and (b). There is a little difference in the plastic deformation between the two tested grid spacers, however, and the FINDS code conservatively models the plastic deformation, as seen in Figure A.2.2-5(a) and (b).

Since the as-built and the relaxed grid spacer models developed here are for full-sized grid spacers, the models are adapted to the two half-sized grid spacers used in the FINDS code according to the procedure described in Subsection 4.2.2 in Reference A-3.

**Table A.2.2-1 Test Sequence for Deformation Progression
(pre-buckling included)**

Test Sequence (No.)	Pendulum Release Angle (Degree)	
	Grid spacers As-Built_5 and As-Built_6	Grid spacers Relaxed_7 and Relaxed_8
1		
2		
3		
4		
5		
6		
7		
8		
9		
10		
11		
12		
13		
14		
15		
16		
17		
18		
19		

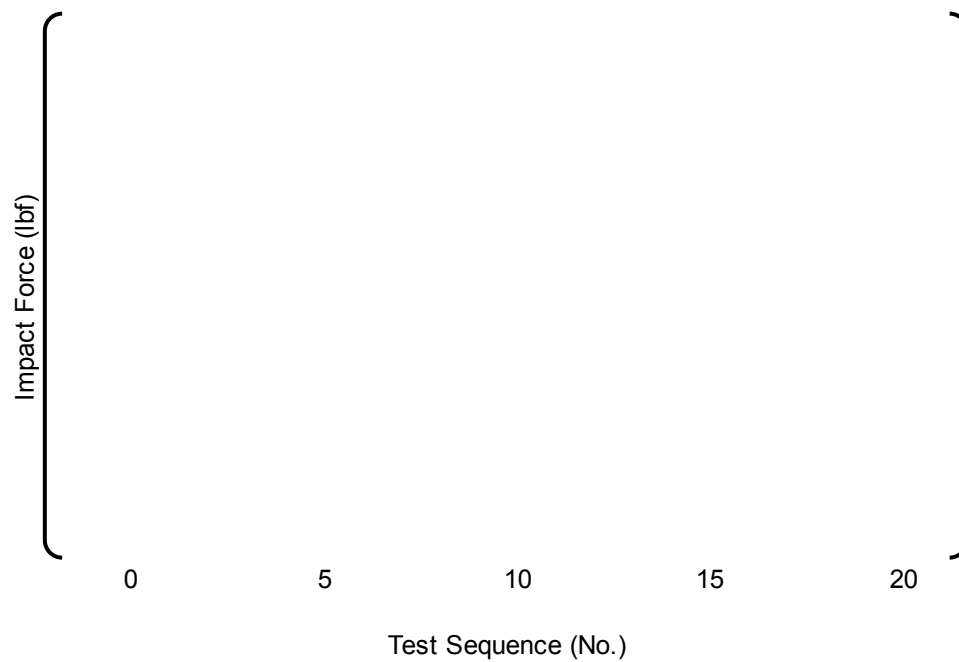


Figure A.2.2-1(a) Impact Force (As-Built_5)

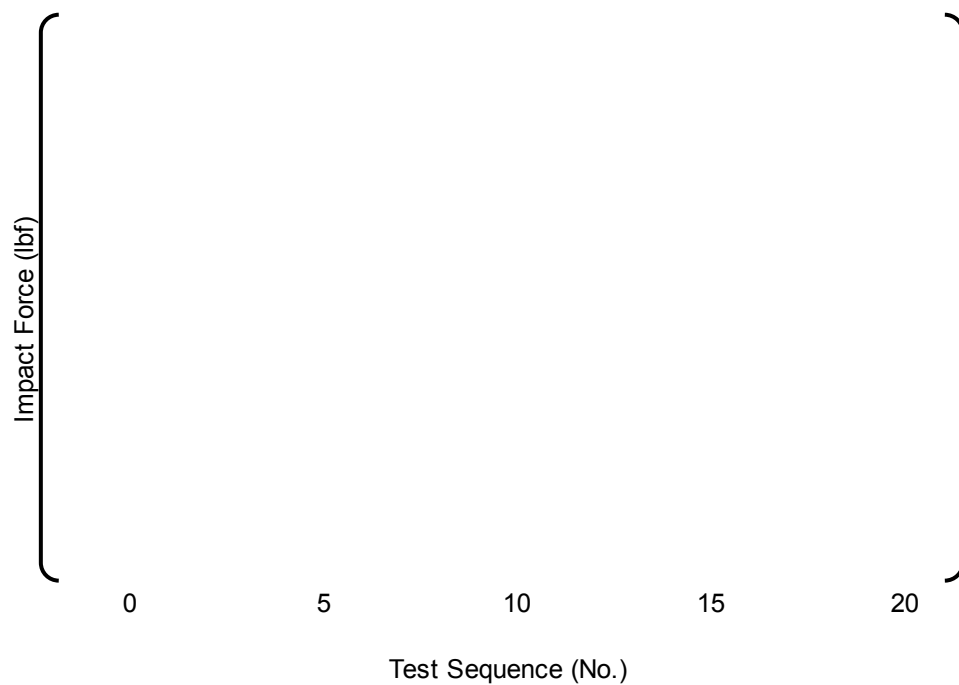


Figure A.2.2-1(b) Impact Force (As-Built_6)

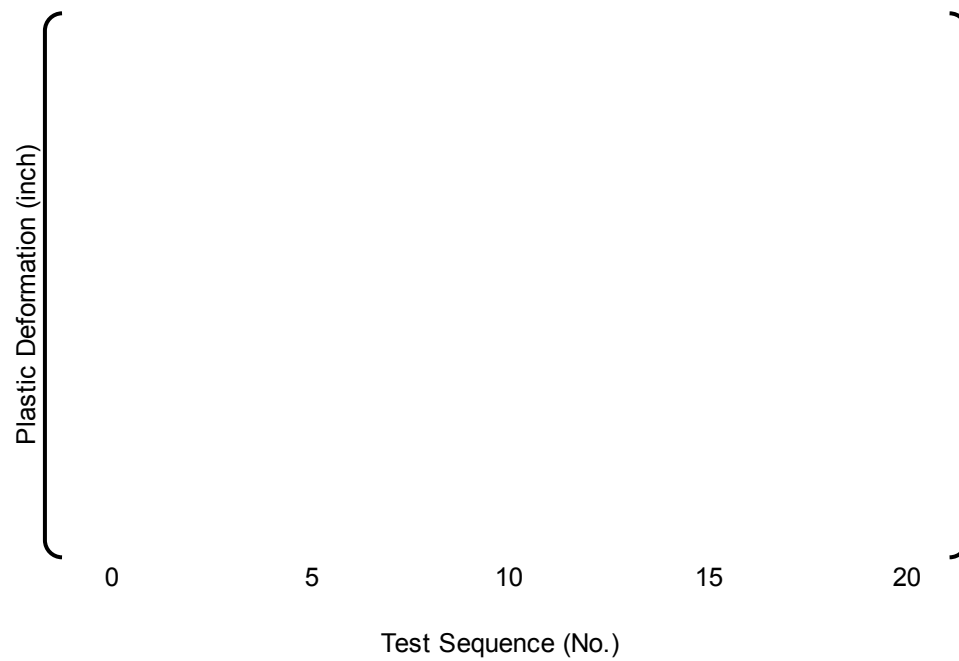


Figure A.2.2-2(a) Plastic Deformation (As-Built_5)

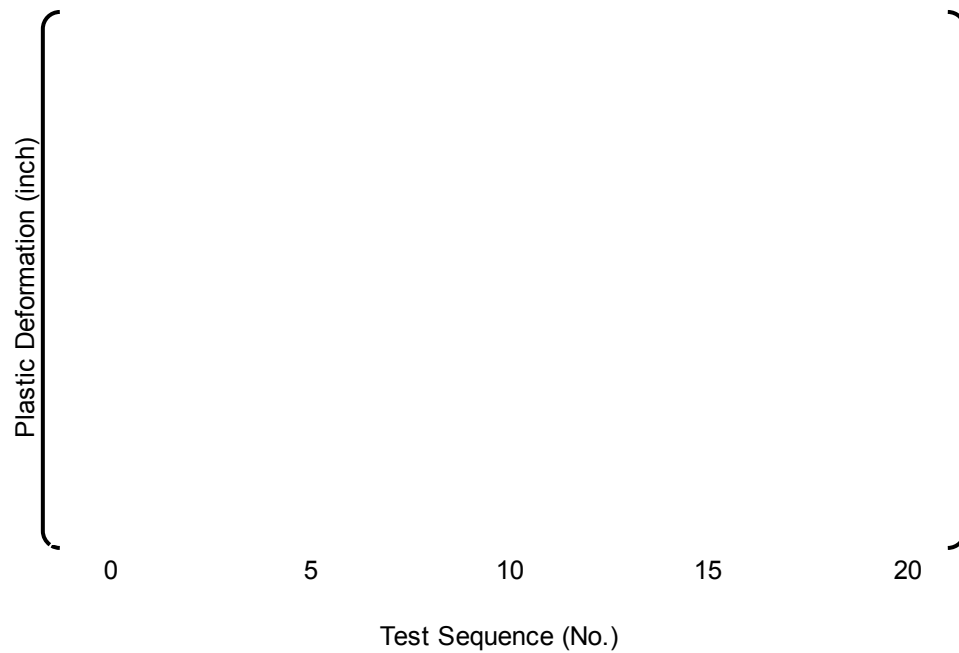


Figure A.2.2-2(b) Plastic Deformation (As-Built_6)

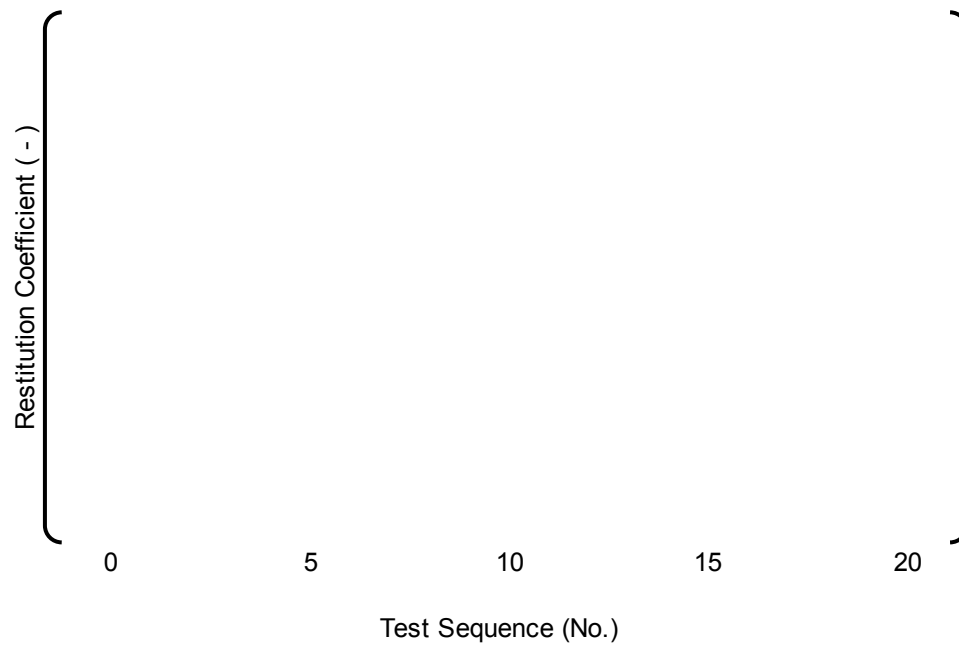


Figure A.2.2-3(a) Coefficient of Restitution (As-Built_5)

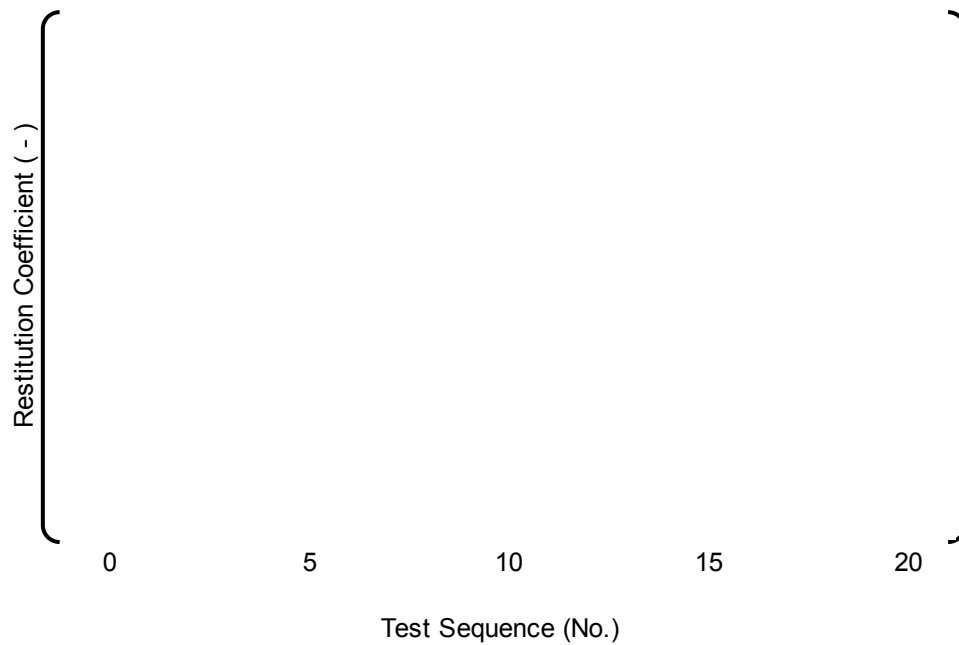


Figure A.2.2-3(b) Coefficient of Restitution (As-Built_6)

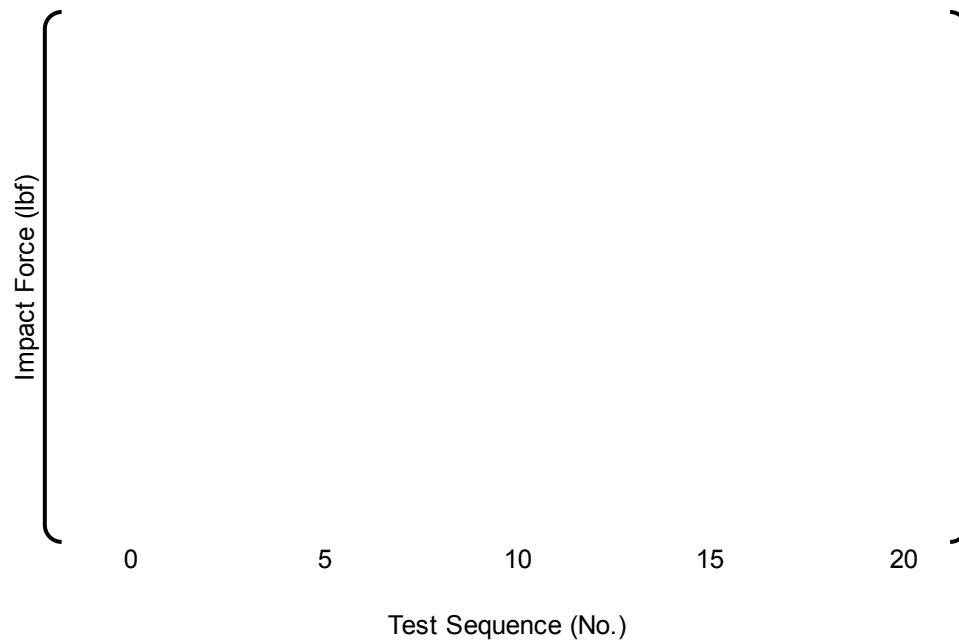


Figure A.2.2-4(a) Impact Force (Relaxed_7)

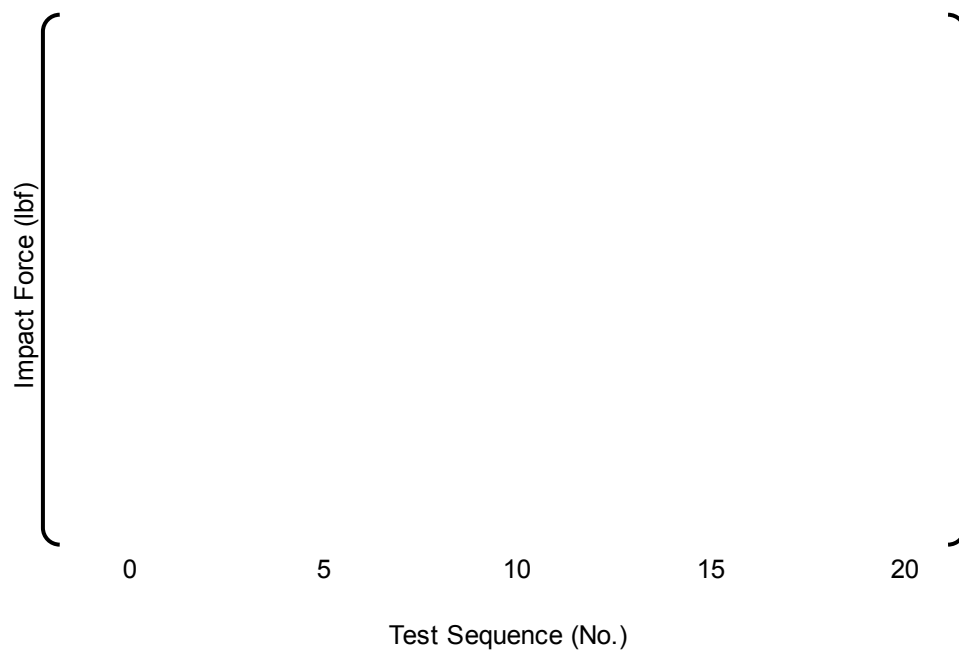


Figure A.2.2-4(b) Impact Force (Relaxed_8)

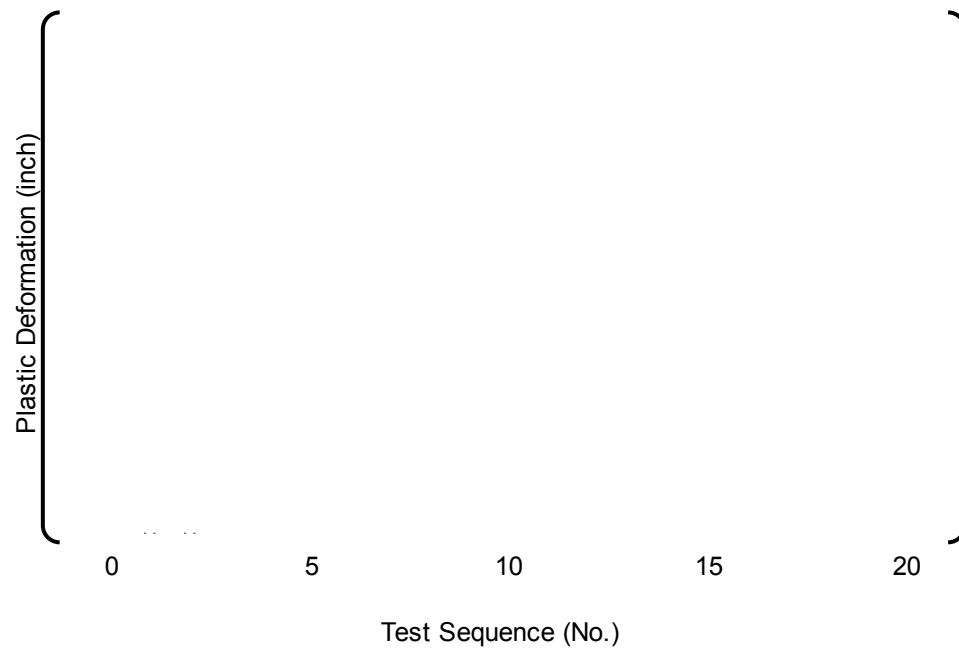


Figure A.2.2-5(a) Plastic Deformation (Relaxed_7)

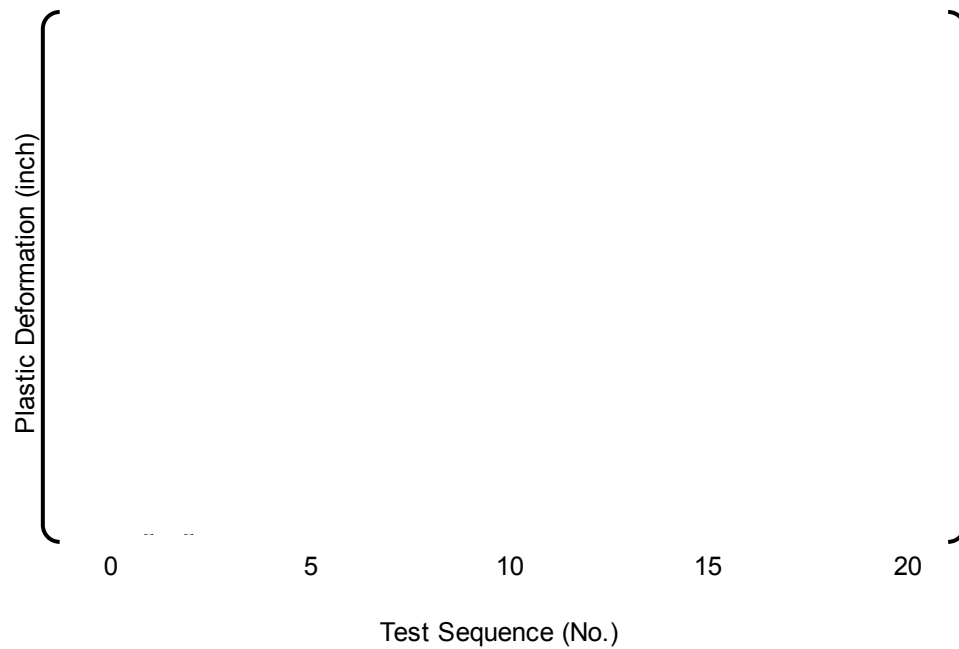


Figure A.2.2-5(b) Plastic Deformation (Relaxed_8)

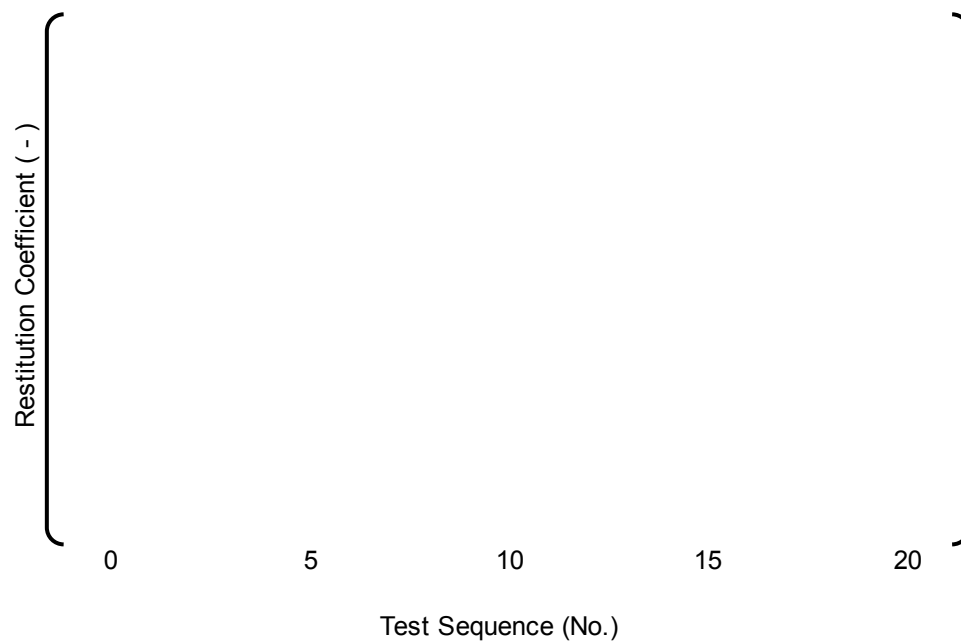


Figure A.2.2-6(a) Coefficient of Restitution (Relaxed_7)

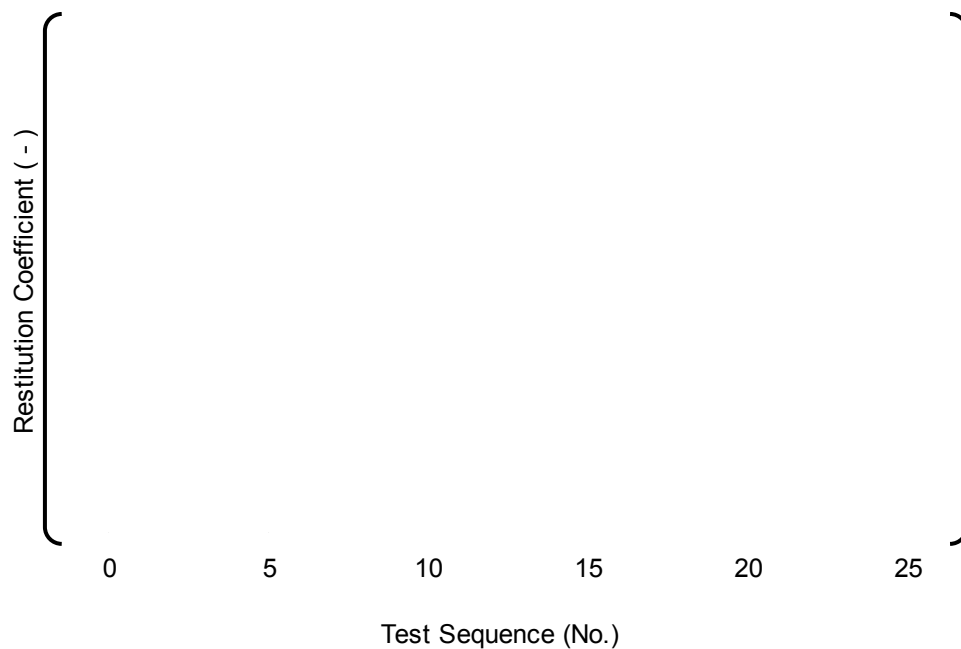


Figure A.2.2-6(b) Coefficient of Restitution (Relaxed_8)

A.3.0 EFFECT OF IRRADIATION EMBRITTLEMENT

Embrittlement of Zircaloy-4 due to irradiation and hydrogen absorption in a reactor may have an influence on grid spacer impact behavior.

Fast neutron exposure produces lattice defects in Zircaloy-4. The mechanical properties of Zircaloy-4 are influenced by the irradiation induced defects, which limit the movement of dislocations. In general, it is believed that the lattice defect obstacles to the movement of the dislocations result in a reduction of the ductility, such that the ductility decreases with irradiation. In addition, the hydrogen absorption due to waterside corrosion with irradiation results in hydrogen precipitates in the Zircaloy-4 near the grain boundaries and the ductility also decreases with increased hydrogen content. Since the high exposure irradiated specimens have high hydrogen contents, tensile tests of high exposure irradiated samples show the effects of both irradiation and hydrogen content on the ductility.

The ductility of Zircaloy-4 decreases due to fast neutron exposure and increased hydrogen content for stress relief annealed (SRA) Zircaloy-4, as shown in Figures B.3.3.3-1 and B.3.3.5-1, respectively, of Reference A-4.

Similarly, for re-crystallized annealed (RXA) Zircaloy-4 these effects are shown in Figure B.1.3.6-1 of Reference A-1 and Figure A.3.0-1 of this appendix.

These figures show that although the ductility of Zircaloy-4 generally decreases with irradiation and hydrogen content, sufficient ductility remains at reactor operating temperatures and predicted hydrogen content. Reference A-5 also supports the above results.

To investigate the influence of the loss of ductility, impact tests with hydrogen-absorbed grid spacers were performed.

After the test results of the hydrogen charged grid spacer "Hydrided_1" were obtained, it was found that during the grid spacer's spring force reduction process { } and before its hydrogen absorption in the autoclave, the grid spacer cell sizes had increased excessively which resulted in unintended gapped cells. Therefore, MHI has performed additional impact tests with 5 hydrogen absorbed grid spacers with properly relaxed spring forces. The grid spacers identified as "Hydrided_2" through "Hydrided_6" are the additional ones tested

A.3.1 Tested Grid Spacers

The grid spacers absorbed hydrogen in an autoclave filled with a lithium hydroxide solution, as shown in Figure A.3.1-1. The hydrogen content of the tested grid spacers was increased to { } ppm to simulate the in-reactor embrittlement due to both hydrogen absorption and irradiation.

The grid spacers "Hydrided_2" through "Hydrided_6" cell sizes have been approximately adjusted to EOL conditions with an average grid spring deflection of { } in ({ } mm), whereas "Hydrided_1" contained cells sized to an average gap of { } in ({ } mm).

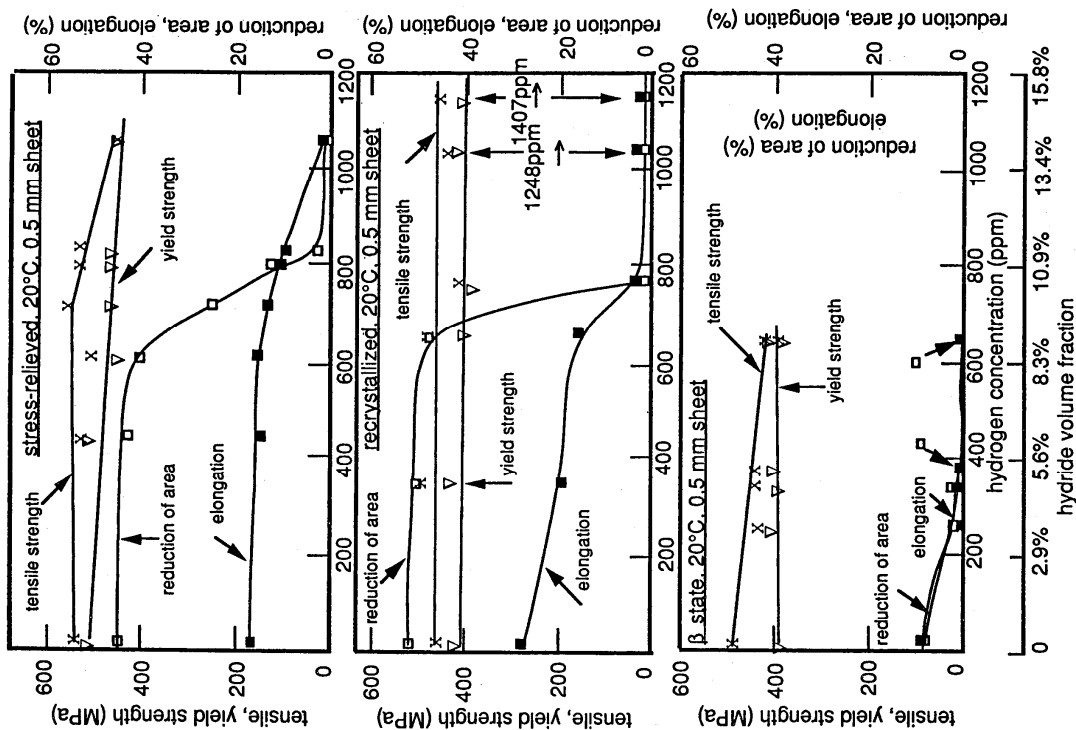


Fig.3: Influence of hydrogen concentration on the mechanical properties of Zircalloy-4 at room temperature.

Figure A.3.0-1 Effect of Hydrogen Content on Zircalloy-4 Material Properties (Reference A-6)

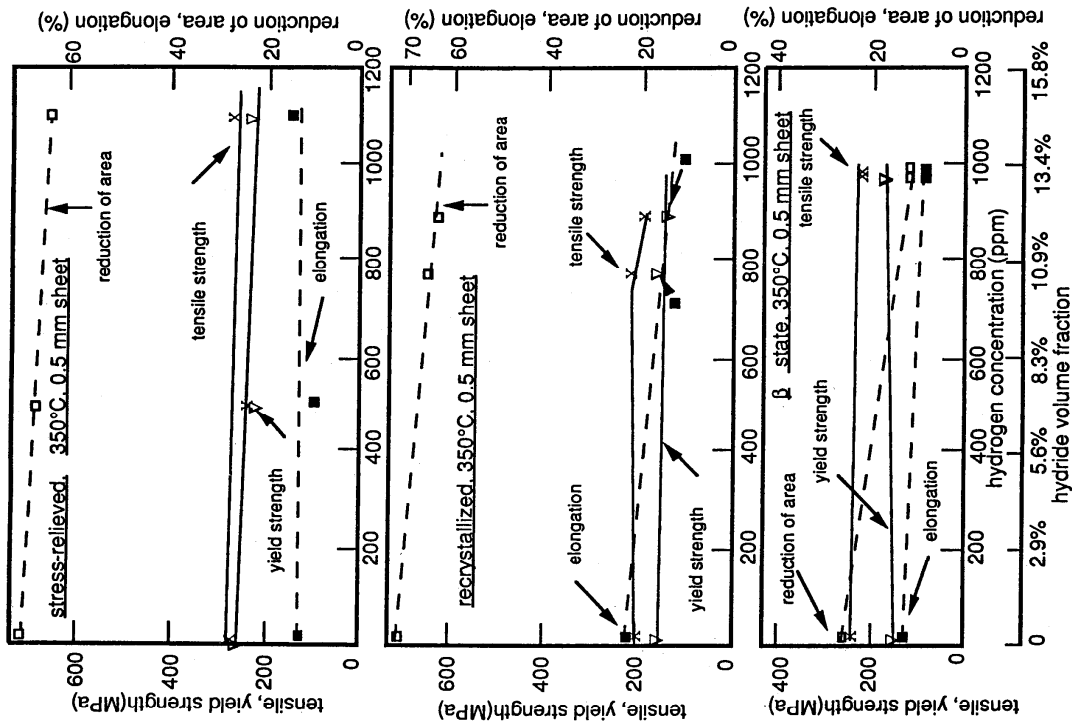


Fig.4: Influence of hydrogen concentration on the mechanical properties of Zircalloy-4 at 350°C.

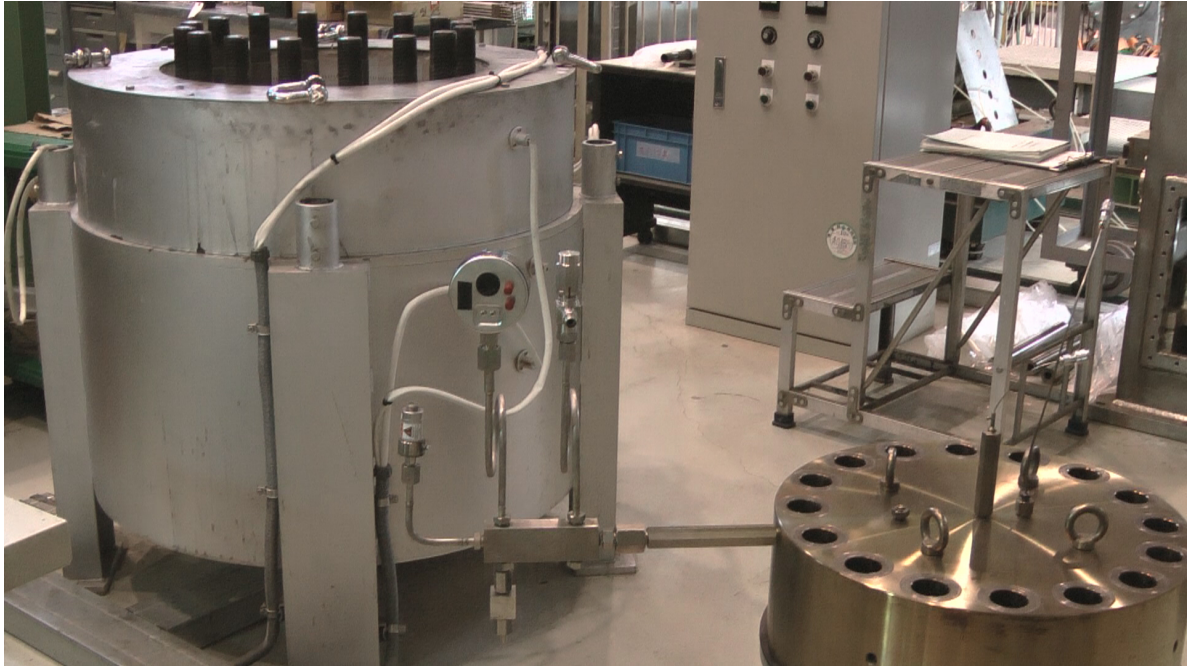


Figure A.3.1-1 Autoclave for Full-Sized Grid Spacer's Hydrogen Absorption

A.3.2 Test Procedure

The test procedures for the hydrogen-absorbed grid spacer are the same as those used for the grid spacers with relaxed spring force, as described in Section A.2.2. Considering the temperature in an operating reactor, the temperature of the tested grid spacer is () deg. F (() deg. C). Short pieces of 17x17 fuel rod cladding are inserted in each cell of the hydrided grid spacer before the grid spacer impact tests. The impact test is repeatedly performed with increasing pendulum release angles. The deformation progression after buckling of the hydrided grid spacer was also investigated to confirm the effect of the embrittlement on the post-buckling deformation versus load behavior.

A.3.3 Test Results

(1) Buckling force and impact stiffness

Figure A.3.3-1 shows the relationship between impact force and the pendulum's release angle for the hydrided grid spacer, as-built grid spacers and grid spacers with relaxed spring force. The relationship between release angle and impact velocity is also shown in Figure A.3.3-2. All of the grid spacers were tested with short pieces of cladding in the grid spacer cells.

As shown in Table A.3.3-1, the average buckling load of the hydrided grid spacer is () lbf (() kN) which is about () % higher than the () lbf (() kN) as-built grid spacers' buckling load. In addition, the average dynamic stiffness of the hydrided grid spacer is () lbf/inch (() kN/mm) which is also higher than the () lbf/inch (() kN/mm) dynamic stiffness of the as-built grid spacers.

(2) Plastic deformation

The deformation progression test has been performed using the same hydrided grid spacers (except Hydrided_5 and Hydrided_6) to investigate the effect of material embrittlement on the deformation behavior. Figure A.3.3-3 shows the relationship between the plastic deformation and pendulum release angle. The test results show that the "Hydrided_2" through "Hydrided_6" grid spacers exhibit higher buckling load compared to the as-built grid spacers. Moreover, "Hydrided_2" through "Hydrided_4", which were measured for plastic deformation, showed much less plastic deformation progression than the as-built grid spacers, as shown in Figure A.3.3-3. The hydrided grid spacer buckling load is higher since the definition of buckling load is based on the load just before measurable permanent deformation occurs. The hydrided grid spacers are able to recover (remain elastic) from higher loads than as-built grid spacers due to a characteristic reduction in impact stiffness sufficiently below when permanent deformation occurs which is not characteristic of as-built grid spacers.

Figure A.3.3-4 shows a top view of the deformation modes of the Hydrided_3 grid spacer after the 5th impact, from a 17° release angle. Figure A.3.3-5 shows the corresponding side view of the deformation of the outer strap at the most deformed region of the grid spacer. No cracks were observed in the strap.

Therefore, it is expected that buckling will be less likely to occur and that reduced plastic deformation would be predicted when the FINDS code considers the impact characteristics of the hydrided grid spacers. However, for conservatism, the FINDS in-elastic impact model, used for the most limiting condition in the seismic and LOCA response analyses, will be based on the

Relaxed_7 and Relaxed_8 grid spacer test results.

Table A.3.3-1 Buckling Force and Dynamic Stiffness of the As-built, Relaxed and Hydrided Grid Spacers

Category	Buckling force		Dynamic Stiffness	
	(lbf)	(kN)	(lbf/inch)	(kN/mm)
As-built				
Relaxed				
Hydrided				

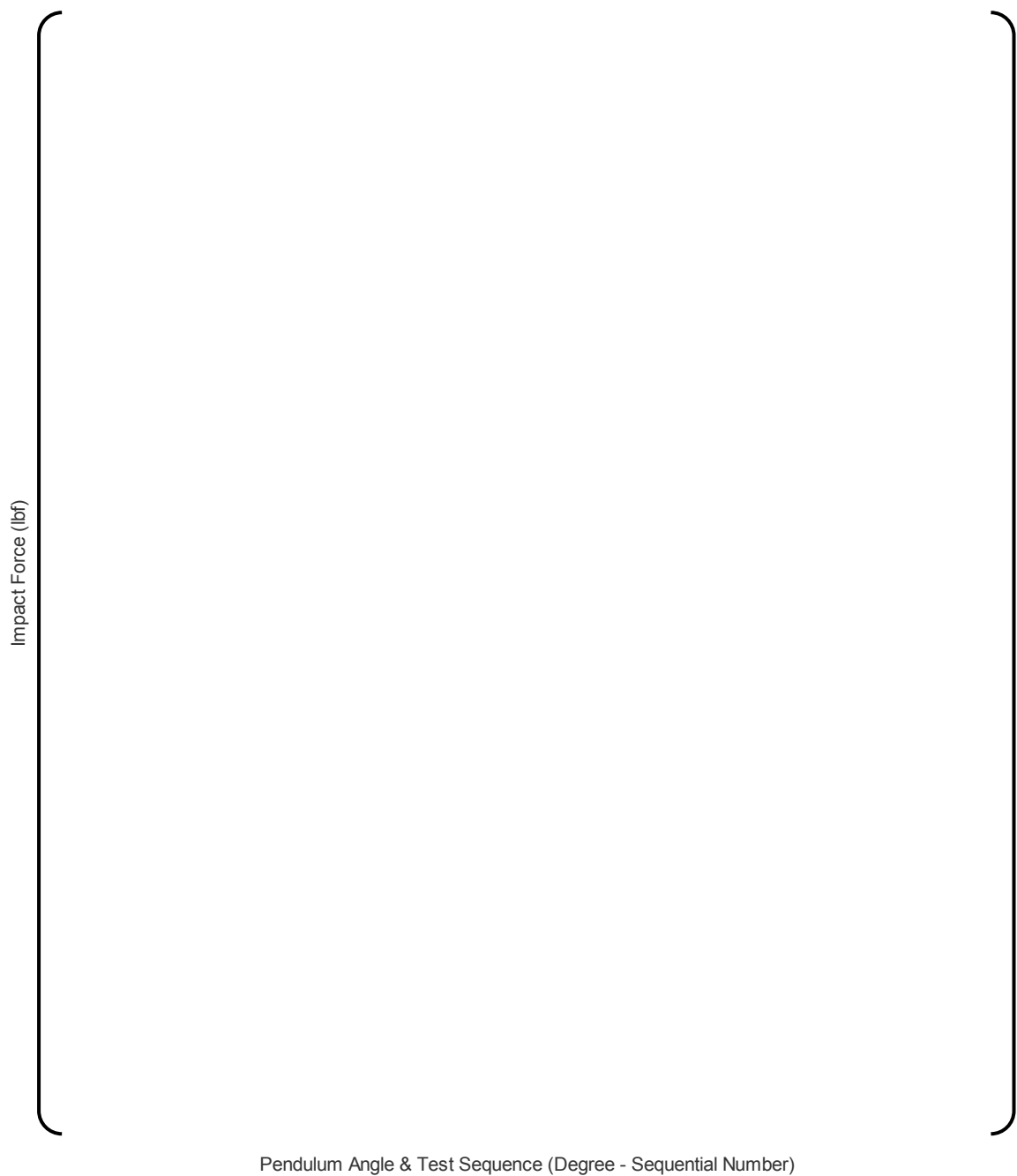
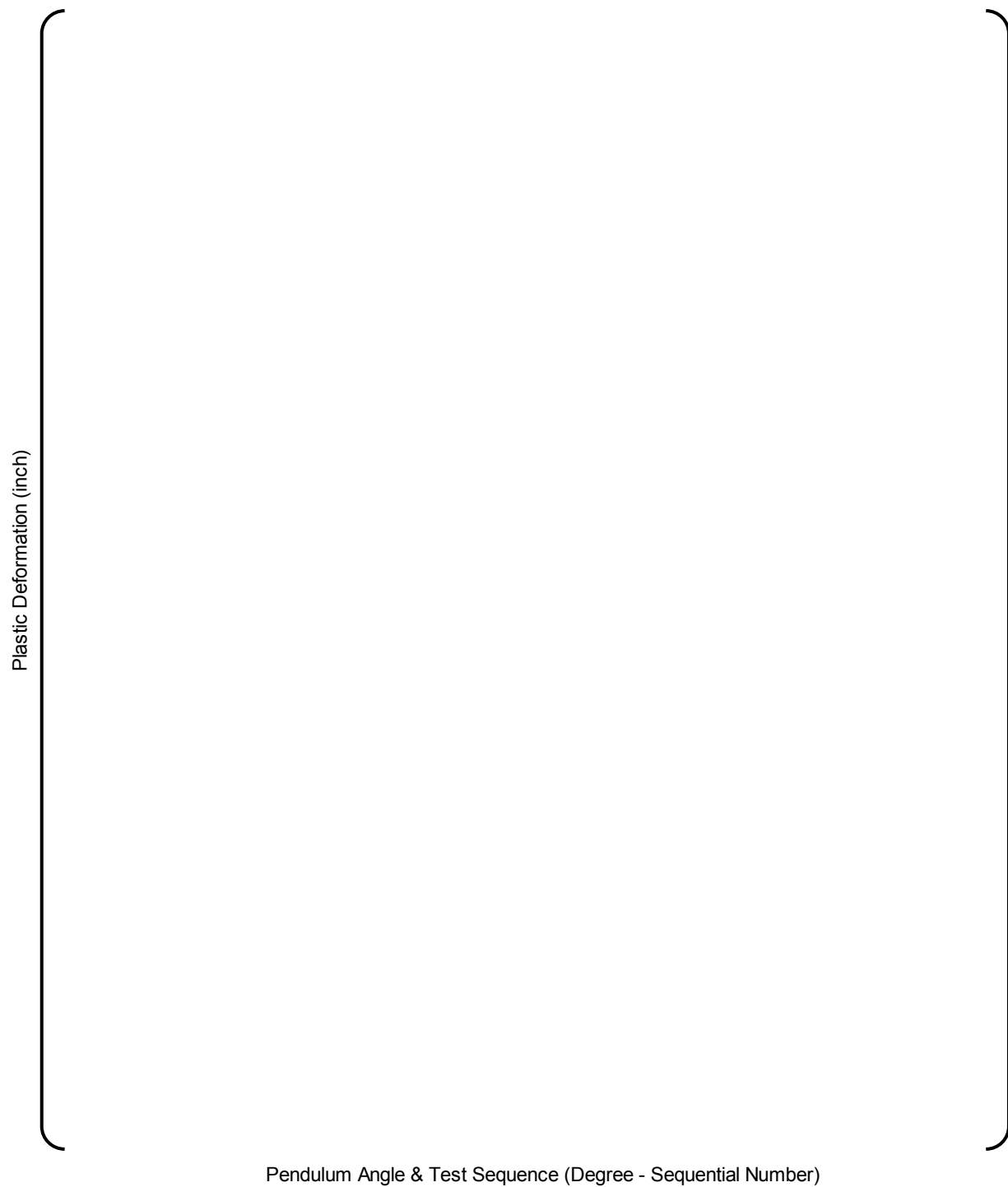


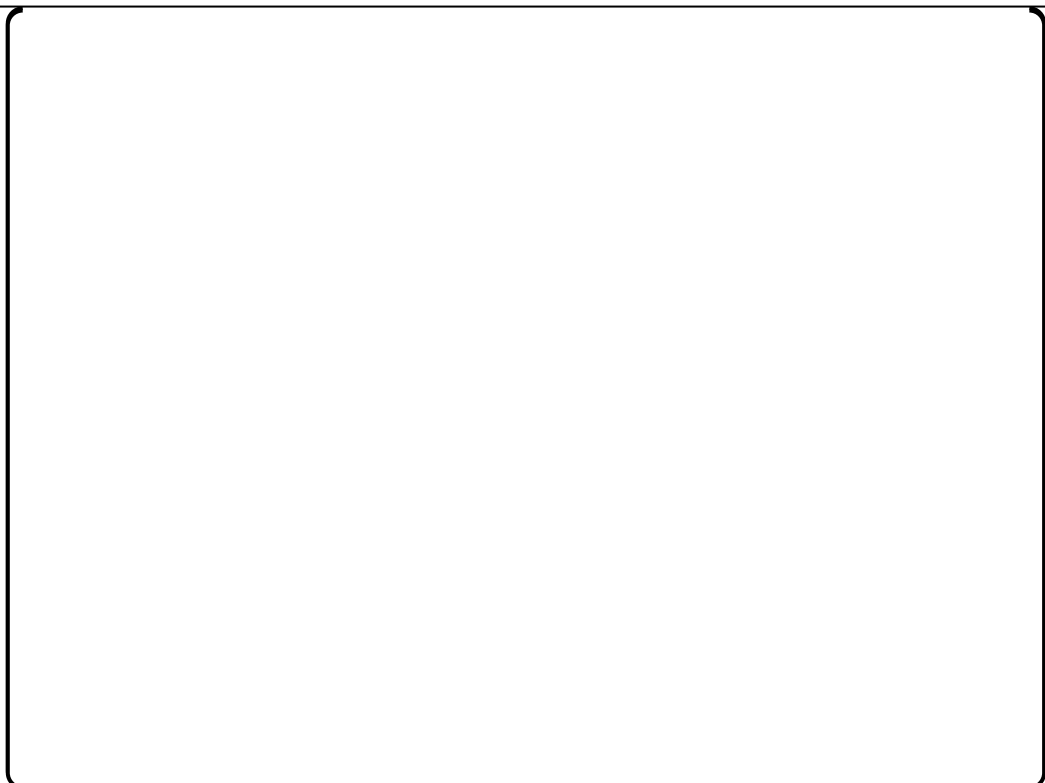
Figure A.3.3-1 Impact Force of Hydrided, As-built and Relaxed Grid Spacers




Figure A.3.3-2 Pendulum Release Angle versus Weight Impact Velocity



**Figure A.3.3-3 Deformation Progression of Hydrided, As-built, and Relaxed
Grid Spacers**



**Figure A.3.3-4 Top View of the Hydrided_3 Grid Spacer
(After the 5th Impact, at a 17° Release Angle)**



**Figure A.3.3-5 Side View of the Hydrided_3 Grid Spacer
(After the 5th Impact, at a 17° Release Angle)**

A.4.0 CONCLUSION

The effects of grid spacer spring relaxation, due to irradiation, on the grid spacer impact behavior are described in this appendix.

The effect of the reduced ductility of the grid spacer material (due to irradiation hardening) on the grid spacer's buckling load and deformation behavior is also described in this Appendix and it is shown that the lower ductility does not adversely effect the impact behavior.

The FINDS in-elastic impact model used for the most limiting condition in the seismic and LOCA response analyses is based on the relaxed grid spacer test results.

A.5.0 REFERENCES

- (A-1) "US-APWR Fuel System Design Evaluation", MUAP-07016-P (Proprietary) and MUAP-07016-NP (Non-Proprietary) Revision 3, Aug 2010
- (A-2) U.S. Nuclear Regulatory Commission, Standard Review Plan (NUREG-0800) Section 4.2, March 2007
- (A-3) "FINDS: Mitsubishi PWR Fuel Assemblies Seismic Analysis Code", MUAP-07034-P (Proprietary) and MUAP-07034-NP (Non-Proprietary) Revision 3, July 2010
- (A-4) "Mitsubishi Fuel Design Criteria and Methodology", MUAP-07008-P (Proprietary) and MUAP-07008-NP (Non-Proprietary) Revision 2, July 2010
- (A-5) Yagnik, S.K., Hermann, A., and Kuo, R.-C., "Ductility of Zircaloy-4 Fuel Cladding and Guide Tubes at High Fluences", Journal of ASTM International, Vol.2, No5 (2005)
- (A-6) J. Bai, et. al., "Effect of hydrides on the ductile-brittle transition in stress-relieved, recrystallised and beta-treated Zircaloy-4", International Topical Meeting on LWR Fuel Performance, Avignon, France, April 21 – 24, 1991.

Appendix B

PARAMETRIC STUDY ON THE SENSITIVITY OF FINDS INPUT UNCERTAINTY ON FINDS ANALYSIS RESULTS

Moved to Section F.5.0 in Appendix F of this report

December 2010

**© 2010 Mitsubishi Heavy Industries, Ltd.
All Rights Reserved**

Appendix C

US-APWR FUEL ASSEMBLY TEST AND MODELING FOR THE FINDS CODE

December 2010

**© 2010 Mitsubishi Heavy Industries, Ltd.
All Rights Reserved**

Table of Contents

List of Tables	C-4
List of Figures	C-4
C.1.0 INTRODUCTION	C-6
C.2.0 GENERAL DESCRIPTION	C-7
C.2.1 Test Facility	C-7
C.2.2 Fuel Assembly	C-7
C.3.0 LATERAL VIBRATION TEST (AIR AND WATER)	C-9
C.3.1 Objective	C-9
C.3.2 Experimental Details	C-9
C.3.2.1 Test Arrangement	C-9
C.3.2.2 Test Procedure	C-15
C.3.3 Test and Analysis Results	C-16
C.3.3.1 Pluck Test	C-16
C.3.3.2 Forced Vibration Test	C-21
C.3.4 Summary of the Lateral Vibration Test	C-26
C.4.0 LATERAL IMPACT TEST	C-27
C.4.1 Objective	C-27
C.4.2 Experimental Details	C-27
C.4.2.1 Test Arrangement	C-27
C.4.2.2 Test Procedure	C-27
C.4.3 Comparison of the Test and the Analysis Results	C-30
C.4.3.1 1 Point Tensile Condition Test	C-30
C.4.3.2 3 Point Tensile Condition Test	C-30
C.4.4 Summary of the Lateral Impact Test	C-33
C.5.0 MODELING OF US-APWR FUEL ASSEMBLY FOR FINDS CODE	C-34
C.5.1 BOL Condition	C-34
C.5.2 EOL Condition	C-35
C.5.3 Uncertainty Evaluation for US-APWR Fuel Assembly FINDS Model at BOL Conditions	C-41
C.5.3.1 Introduction	C-41
C.5.3.2 Evaluation	C-42
C.5.4 Uncertainty Evaluation for US-APWR Fuel Assembly FINDS model at EOL	

Condition.....	C-45
C.5.4.1 Uncertainty Evaluation for Frequency	C-45
C.5.4.2 Uncertainty Evaluation for Damping Ratio	C-45
C.6.0 CONCLUSION.....	C-47
C.7.0 REFERENCES	C-50

List of Tables

Table C.3.3.2-1	US-APWR Fuel Assembly Non-damped Natural frequency (Forced Vibration Test in Air)	C-22
Table C.5.3-1	Required Cases for FINDS Analysis	C-41

List of Figures

Figure C.2.2-1	US-APWR Prototype Fuel Assembly Setup (Bottom view)	C-8
Figure C.2.2-2	Shaker Attached to the 6 th Grid Spacer	C-8
Figure C.3.2.1-1	Schematic View of Fuel Assembly Pluck Test in Air (3 Point Tensile Type)	C-11
Figure C.3.2.1-2	Schematic View of Fuel Assembly Pluck Test in Air (1 Point Tensile)	C-12
Figure C.3.2.1-3	Schematic View of Fuel Assembly Pluck Test in Water	C-13
Figure C.3.2.1-4	Schematic View of Fuel Assembly Lateral Forced Vibration Test in Air	C-14
Figure C.3.3.1-1	Displacement Time History at the 6 th Grid Spacer during Free Vibration in Air	C-17
Figure C.3.3.1-2	Frequency Dependency on Amplitude for the US-APWR Mockup Fuel Assembly	C-18
Figure C.3.3.1-3	Damping Ratio Dependency on Amplitude for the US-APWR Mockup Fuel Assembly	C-18
Figure C.3.3.1-4(1)	Frequency Dependency on Amplitude for US-APWR Fuel Assembly in First Mode (Lateral Pluck Test in Air)	C-19
Figure C.3.3.1-4(2)	Frequency Dependency on Amplitude for US-APWR Fuel Assembly in First Mode (Lateral Pluck Test in Water)	C-19
Figure C.3.3.1-5(1)	Damping Ratio Dependency on Amplitude for US-APWR Fuel Assembly in First Mode (Lateral Pluck Test in Air)	C-20
Figure C.3.3.1-5(2)	Damping Ratio Dependency on Amplitude for US-APWR Fuel Assembly in First Mode (Lateral Pluck Test in Water)	C-20
Figure C.3.3.2-1	Frequency Dependency on Amplitude in Higher Modes (Forced Vibration Test and FINDS Analysis)	C-23
Figure C.3.3.2-2	Damping Ratio Dependency on Amplitude in Higher Modes (Forced Vibration Test)	C-23
Figure C.3.3.2-3	US-APWR Fuel Assembly Mode Shape (1st ~ 4th Mode) from Forced Vibration Test	C-24
Figure C.3.3.2-4	US-APWR Fuel Assembly Mode Shape (5th ~ 7th Mode) from Forced Vibration Test	C-25
Figure C.4.2.1-1	Fuel Assembly Lateral Impact Test (1 point tensile condition)	C-28

Figure C.4.2.1-2	Fuel Assembly Lateral Impact Test (3 point tensile condition).....	C-29
Figure C.4.3-1	Impact Force versus Impact Velocity (As-built Grid Spacers at Room Temperature)	C-31
Figure C.4.3.1-1	Maximum Impact Force versus Initial Displacement at No.6 Grid Spacer for the 1 Point Tensile Condition Test.....	C-32
Figure C.4.3.2-2	Maximum Impact Force versus Initial Displacement at No.6 Grid Spacer for the 3 Point Tensile Condition Test.....	C-32
Figure C.5.2-1	Influence of Grid Spacer Spring Relaxation on Frequency and Damping Ratio	C-37
Figure C.5.2-2	Comparison of the US-APWR and 12ft Fuel Assemblies Amplitude Dependency in the in-Air Pluck Test	C-38
Figure C.5.2-3	Fuel Assembly Stress Analysis Model in the Horizontal Direction	C-39
Figure C.5.2-4	Amplitude Dependence of the 14ft Fuel Assembly's Frequency Using ANSYS FEM Analysis (Operating Condition).....	C-40
Figure C.5.3-1(a)	Frequency for in Air Pluck Test	C-43
Figure C.5.3-1(b)	Frequency for in Water Pluck Test.....	C-43
Figure C.5.3-2(a)	Damping Ratio for in Air Pluck Test	C-44
Figure C.5.3-2(b)	Damping Ratio for in Water Pluck Test	C-44
Figure C.6.0-1	Amplitude Dependency of Frequency and Damping for US-APWR Model at BOL Operating Conditions	C-48
Figure C.6.0-2	Amplitude Dependency of Frequency and Damping for US-APWR Model at EOL Operating Conditions	C-49

C.1.0 INTRODUCTION

This appendix documents the results of the mechanical tests which were performed on a US-APWR mockup fuel assembly to develop a fuel assembly model for the FINDS code.

Lateral vibration test using the fuel assembly in air and cold water at room temperature (hereinafter called cold water) was performed to obtain vibration characteristics, such as the damping and frequency dependence on amplitude.

Based on the experimentally obtained vibration characteristics, the fuel assembly vibration model for BOL and EOL at operationing condition was developed. In the modeling, the upper and lower bounds for the amplitude dependence of frequency and damping ratio in the model were also considered.

For confirming validity of the fuel assembly vibration and grid spacer impact model, the fuel assembly model with grid spacer impact model was supplied to analysis simulating lateral impact test of the US-APWR fuel assembly. The test procedure, test result and comparison with analysis result are discussed in this appendix.

C.2.0 GENERAL DESCRIPTION

C.2.1 Test Facility

Structural test facilities for full scale prototype fuel assembly are located at the NDC (Nuclear Development Corporation). The fuel assembly structural test facility is used to investigate the static and dynamic properties of fuel assembly. The facility is located in an underground pit to provide rigid and vibration-free test boundary conditions.

C.2.2 Fuel Assembly

The test are performed on a prototype fuel assembly that is mechanically the same as the actual US-APWR 14 ft fuel assembly : Inconel-718 top and bottom grid spacers, 9 Zircaloy-4 intermediate grid spacers, 264 fuel rods, 24 control rod guide thimbles and 1 instrumentation tube. The fuel rods were filled with lead-antimony pellets to simulate the overall fuel rod weight. The rods contained a preloaded coil spring in the plenum. Figure C.2.2-1 shows the fuel assembly set up with strain gage leads in the test fixture and Figure C.2.2-2 shows the attached shaker for the vibration studies.



Figure C.2.2-1 US-APWR Prototype Fuel Assembly Setup (Bottom view)



Figure C.2.2-2 Shaker Attached to the 6th Grid Spacer

C.3.0 LATERAL VIBRATION TEST (AIR AND WATER)

C.3.1 Objective

The objective of the lateral vibration test is to determine the lateral vibration characteristics of the US-APWR fuel assembly, which are the basis of the model in the FINDS code. The first and higher mode vibration characteristics such as mode shapes, natural frequencies and damping ratio of the US-APWR fuel assembly, that are important in the structural response analysis to seismic and LOCA events, are determined in the tests.

C.3.2 Experimental Details

C.3.2.1 Test Arrangement

The top and bottom nozzles are engaged by fuel-guide pins on corresponding upper and lower core plate simulators and the top nozzle hold-down springs are compressed, consistent with cold in-core conditions. The targets for the displacement transducers are placed on each grid spacer and the displacement transducers set accordingly.

(1) Free Vibration Test (pluck test)

- In air

Two methods are used. One consists of an initial displacement to only the middle grid spacer (1 point tensile test). In this case, the resulting triangular initial shape of the fuel assembly results in the superposition of higher vibration modes which tends to introduce unwanted vibration characteristics into the desired pure first mode. The second method consists of simulating the first mode vibration shape by the appropriate lateral displacement of the 4th, 6th and 8th grid spacers (3 point tensile test) as shown in Figure C.3.2.1-1.

A clamping device surrounds the grid spacers to be excited and is attached to an adjustable lateral deflection device. The two test set-ups are:

- Grid spacer No.6 for the 1 point tensile test condition, as shown in Figure C.3.2.1-2
- Grid spacers No.4, No.6 and No.8 for the 3 point tensile test condition to create the first mode deflected shape, as shown in Figure C.3.2-1. The initial lateral displacement of each grid spacer was determined from vibration analysis using the US-APWR FEM model in the ANSYS code.

The in air pluck test is performed at room temperature.

- In water

As shown in Figure C.3.2.1-3, the fuel assembly was set in a tank filled with still water and supported in the same manner as in the in-air test. Only the 1 point tensile test is performed in water because the apparatus needed for the 3 point tensile test could not be used in this more complex test arrangement.

(2) Forced Vibration Test

The forced vibration is provided by an electro-magnetic shaker acting on the grid spacer that corresponds to the desired vibration mode. The shaker device is positioned at No.6 grid spacer or at the appropriate grid spacer, as shown in Figure C.3.2.1-4. The test is conducted in air and water at room temperature.

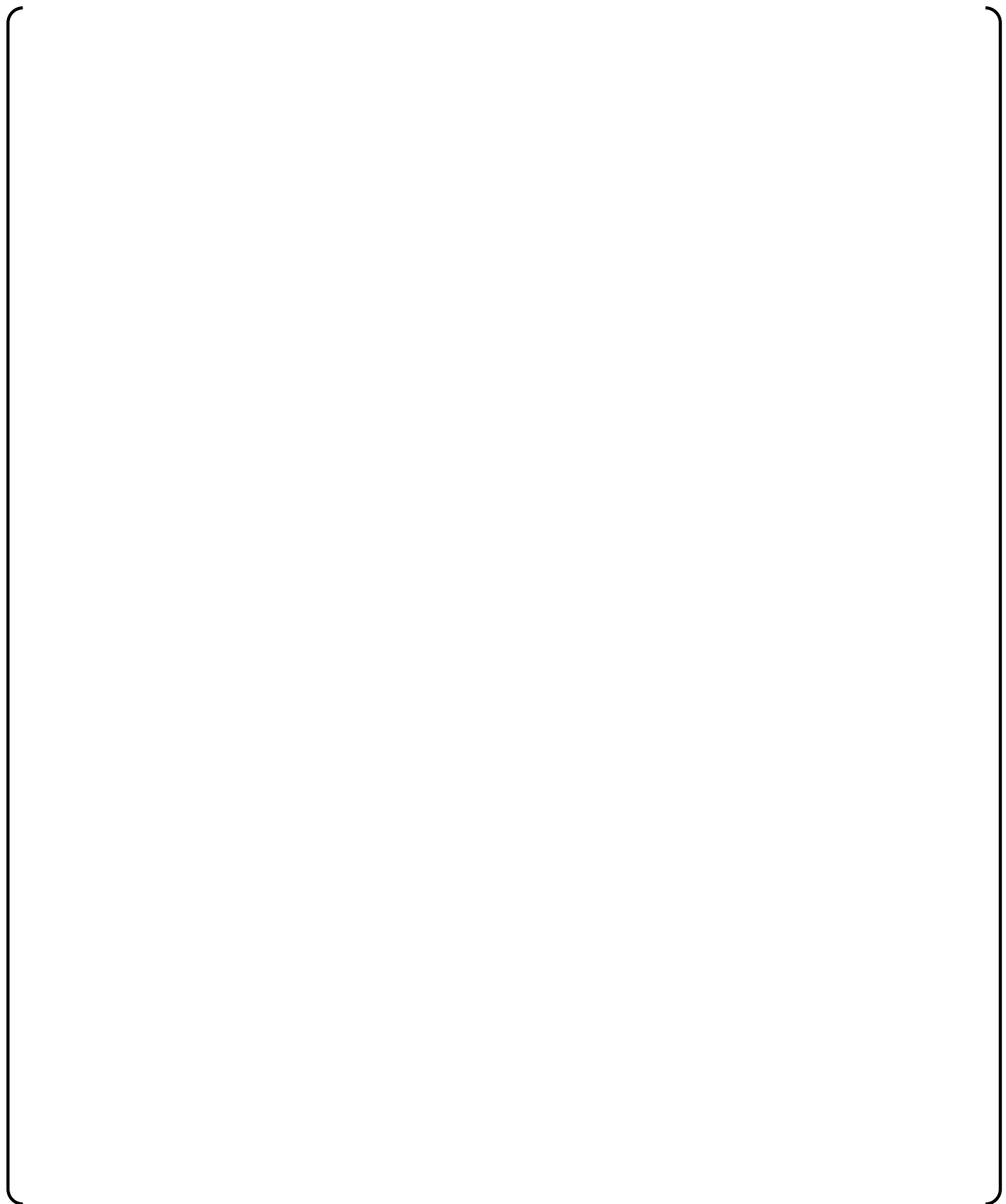


**Figure C.3.2.1-1 Schematic View of Fuel Assembly Pluck Test in Air
(3 Point Tensile Type)**

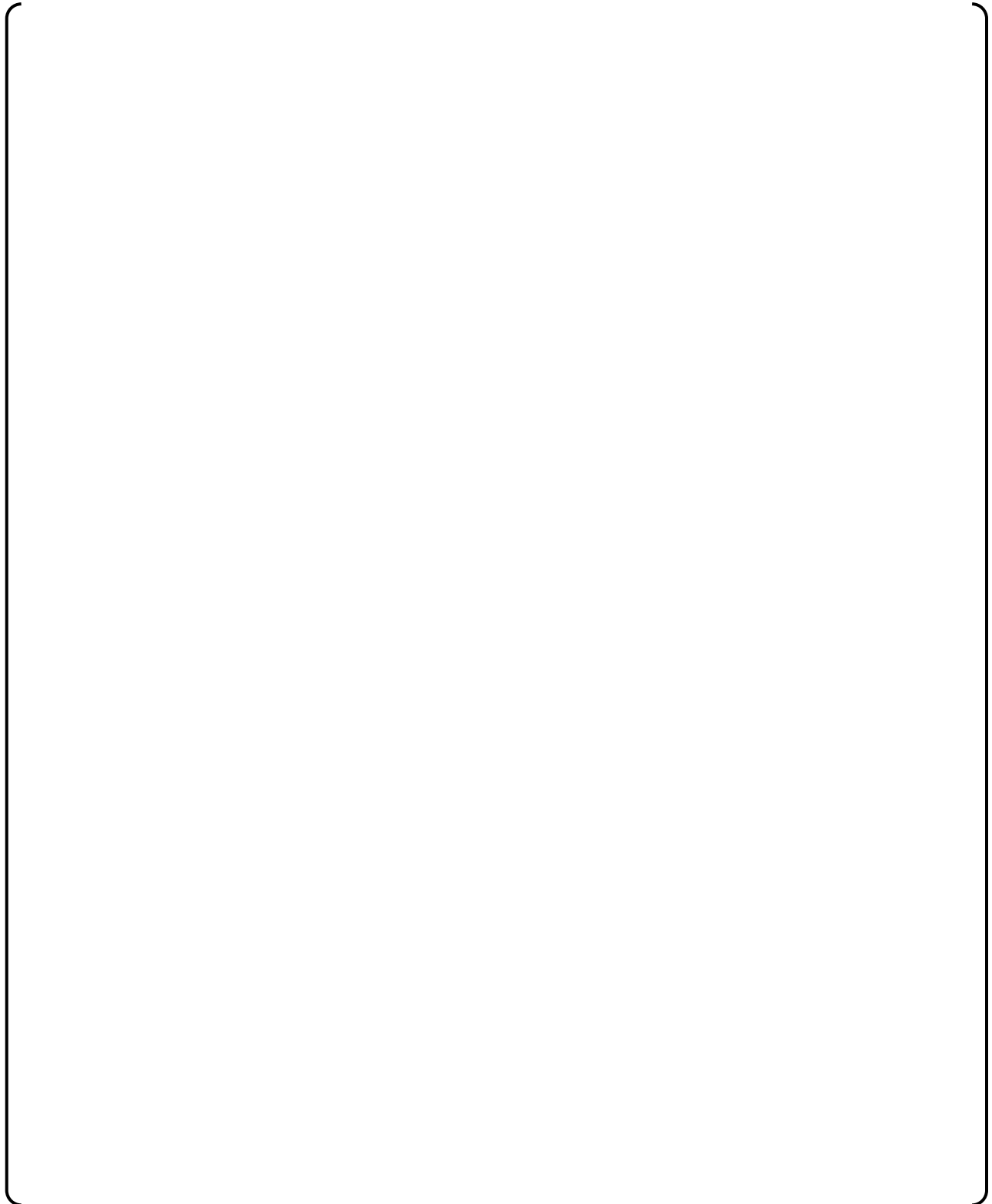


Figure C.3.2.1-2 Schematic View of Fuel Assembly Pluck Test in Air (1 Point Tensile)

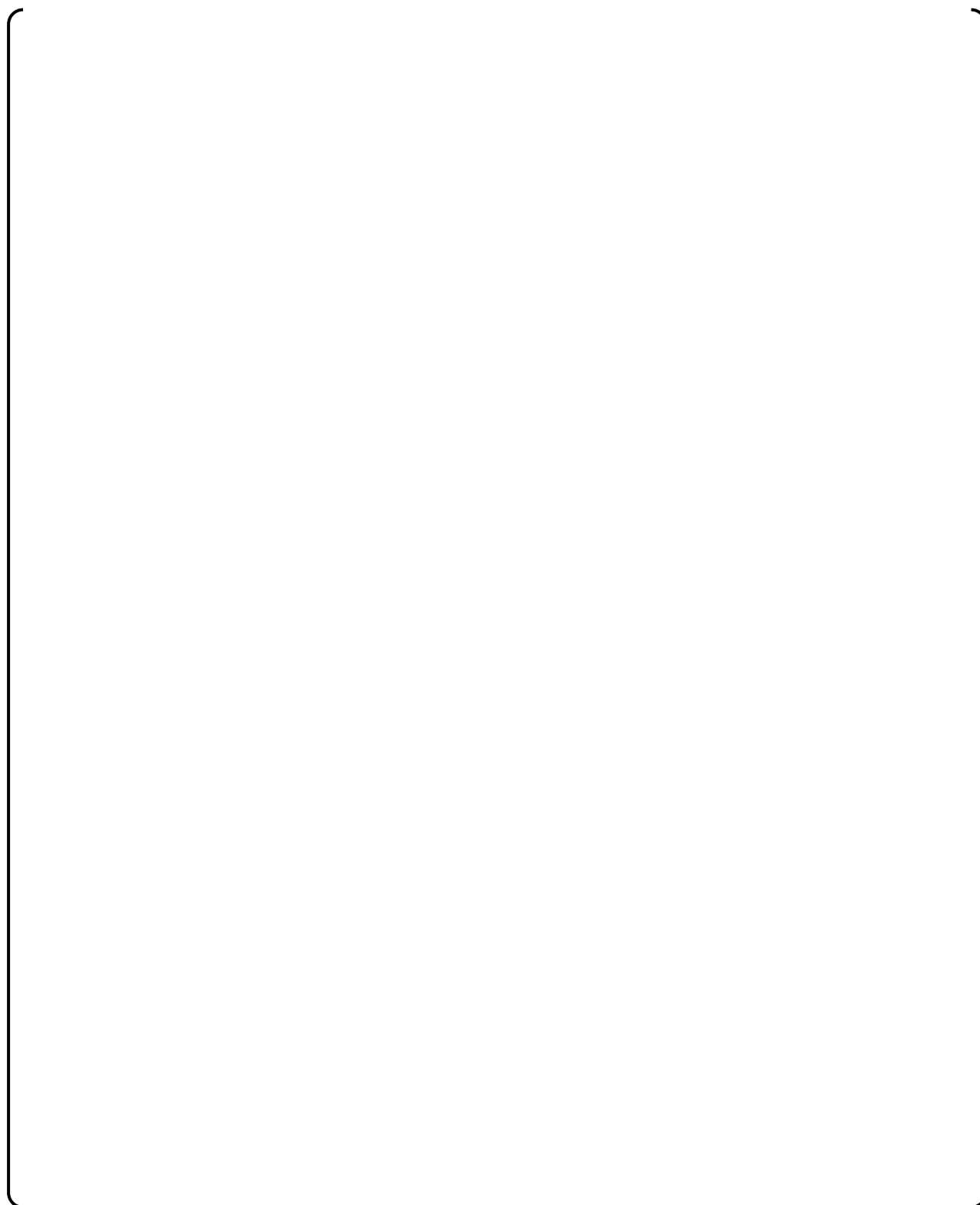


Figure C.3.2.1-3 Schematic View of Fuel Assembly Pluck Test in Water

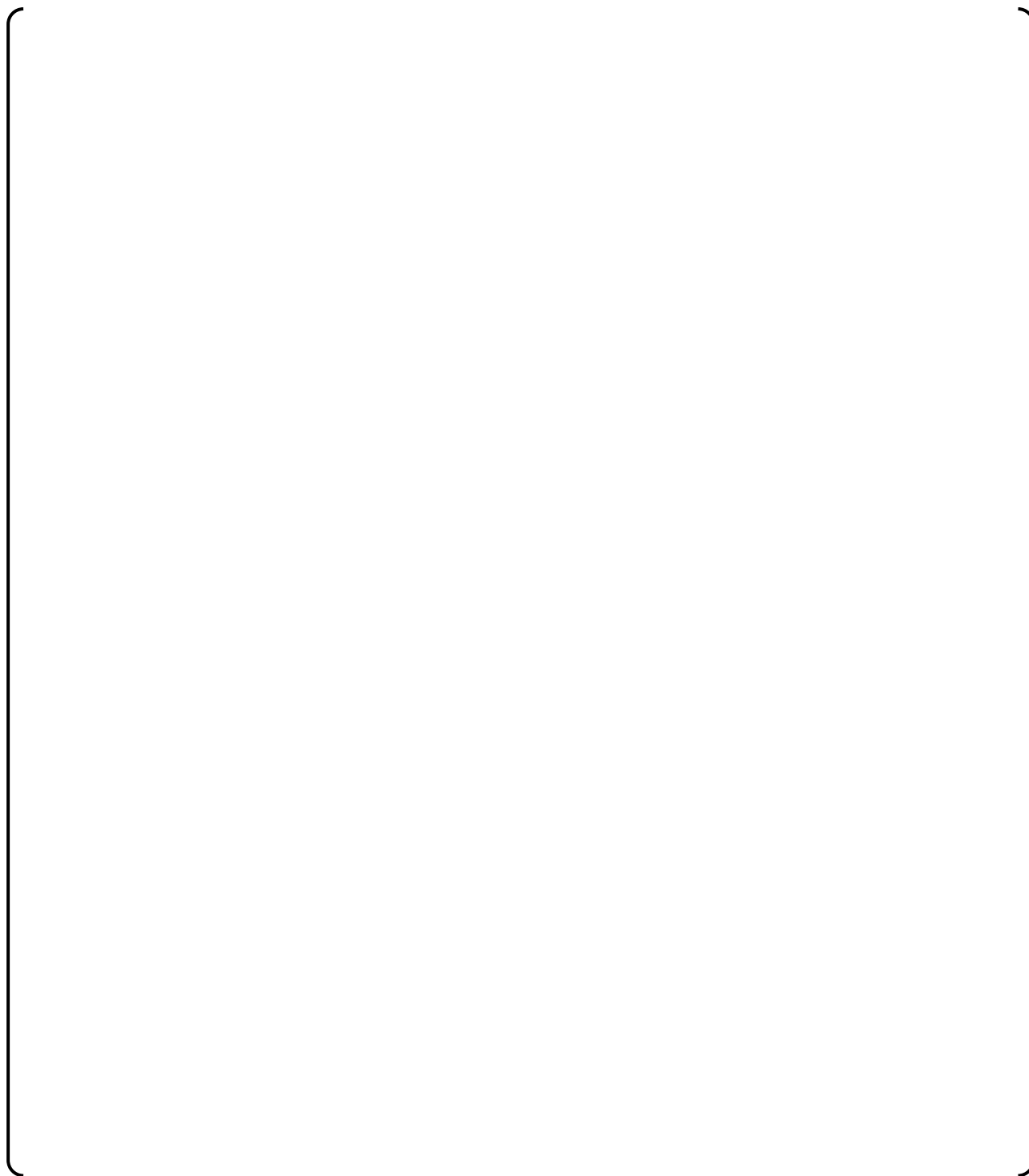


Figure C.3.2.1-4 Schematic View of Fuel Assembly Lateral Forced Vibration Test in Air

C.3.2.2 Test Procedure

(1) Free Vibration Test (pluck test)

The initial lateral deflection of the fuel assembly is obtained by laterally displacing the grid spacers a specific distance. The grid spacer is quickly released, which allows the fuel assembly to vibrate freely during which its deflection time history is recorded. The initial deflection is increased step by step and the procedure is repeated. The amplitude dependency of natural frequencies and damping ratio is obtained from this test.

For the 3 point tensile test, the initial shape of the fuel assembly simulates the 1st mode vibration shape by laterally pulling grid spacers No.4, No.6 and No.8 by the appropriate amount. As previously mentioned, the initial lateral displacement of each grid spacer is determined from modal analysis using the FEM model for the US-APWR fuel assembly. The displacement value at grid spacer No.6 is increased from () mm to () mm by () mm increments.

In the 1 point tensile test, the initial displacement is applied only to the 6th grid spacer. The displacement value is increased from () mm to () mm by () mm increments. The procedure is the same for the in air and in water tests.

(2) Forced Vibration Test

The following three types of forced vibration are used.

- Wide range frequency sweep vibration: a sinusoidal wave sweep is performed over a wide range of frequency. Natural vibrations from the 1st to the 7th modes are excited to obtain their approximate frequencies.
- Narrow range frequency sweep vibration: a sinusoidal wave sweep in the range of each natural frequency is used to obtain a resonance curve confirming the precise natural frequency value. From the resonance curve, the damping ratio at each frequency is determined by the half-power method. Vibration amplitudes are varied resulting in resonance curves which provide the amplitude dependency of natural frequency and damping ratio.
- Fixed frequency vibration: a sinusoidal wave vibration at a frequency corresponding to each of the natural frequencies determined above is applied and the vibration amplitude at each grid spacer is recorded to obtain precise mode shapes.

The forced vibration tests are repeated for each mode to obtain the amplitude dependency of frequency and damping ratio, by increasing the acceleration force provided by the shaker.

C.3.3 Test and Analysis Results

C.3.3.1 Pluck Test

A typical displacement time history of the No.6 grid spacer, obtained with a () mm initial displacement (grid spacer No.4, No.6, and No.8, 3 point tensile type), is shown in Figure C.3.3.1-1. () mm of maximum Initial displacement in the pluck test covers the maximum displacement in the FINDS code analysis, as shown in Appendix F.

The amplitude dependency of frequency and damping ratio obtained by the test are shown in Figures C.3.3.1-2 and C.3.3.1-3, respectively. In both figures, the 1 point tensile in air and the 1 point tensile in water data contained within the dotted line rectangles show the discontinuity which resulted from the influence of the initial triangular shape on the 1 point tensile test where higher mode shapes superpose, as stated previously.

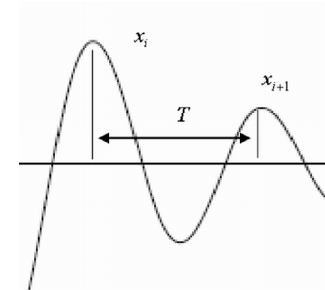
It should be noted that the horizontal axis in the figures, expressed as peak-averaged amplitude, is the average of the absolute values of two adjacent peaks per the equation below.

$$\bar{x} = (x_i + x_{i+1}) / 2 : \text{Peak - averaged amplitude}$$

$$f = 1 / T : \text{Frequency}$$

$$\zeta = 1 / \sqrt{1 + (2\pi / \delta)^2} : \text{Damping factor}$$

$$\delta = \ln(x_i / x_{i+1}) : \text{Logarithmic damping factor}$$



The amplitude dependence of the natural frequency and damping ratio modeled in the FINDS code are adjusted to obtain a good match with the experimental curves as shown in Figure C.3.3.1-4 (1), (2) and Figure C.3.3.1-5 (1), (2).

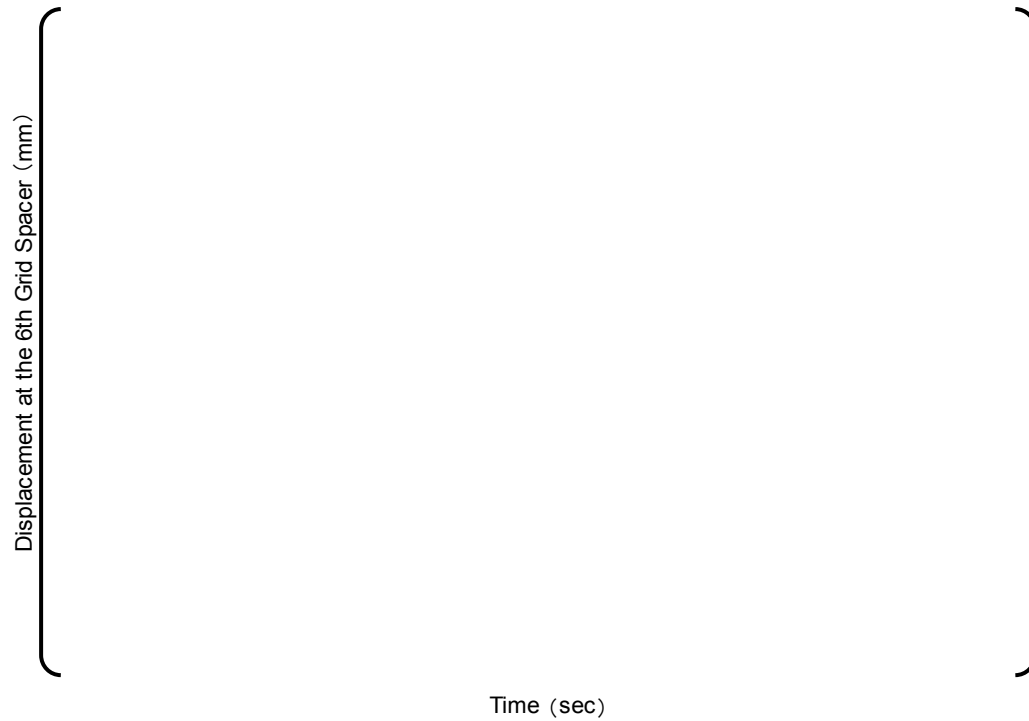


**Figure C.3.3.1-1 Displacement Time History at the 6th Grid Spacer
during Free Vibration in Air**

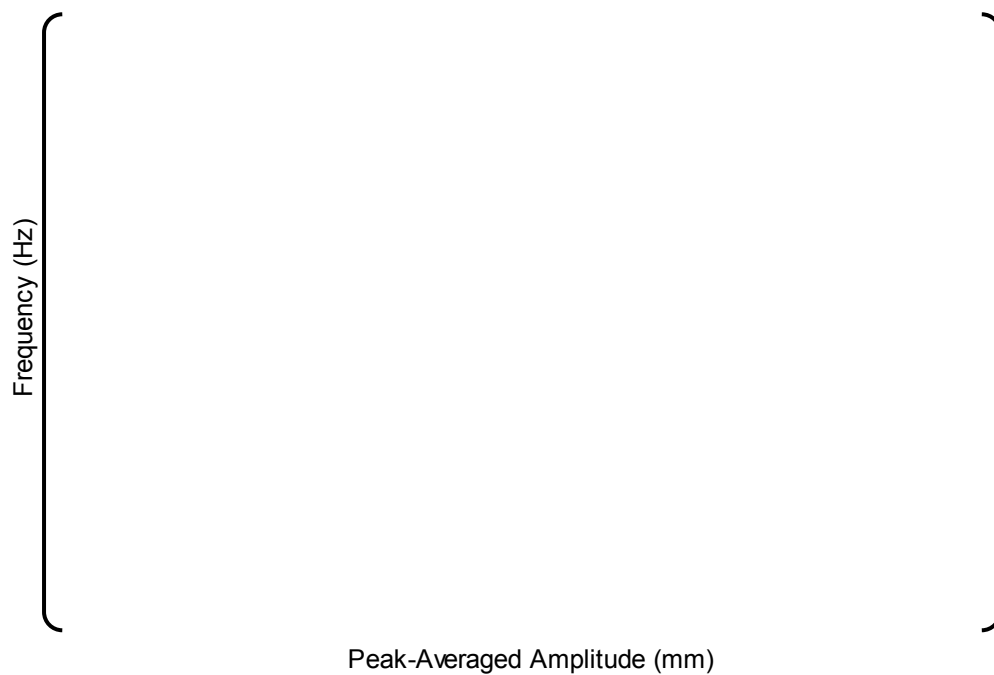


Figure C.3.3.1-2 Frequency Dependency on Amplitude for the US-APWR Mockup Fuel Assembly

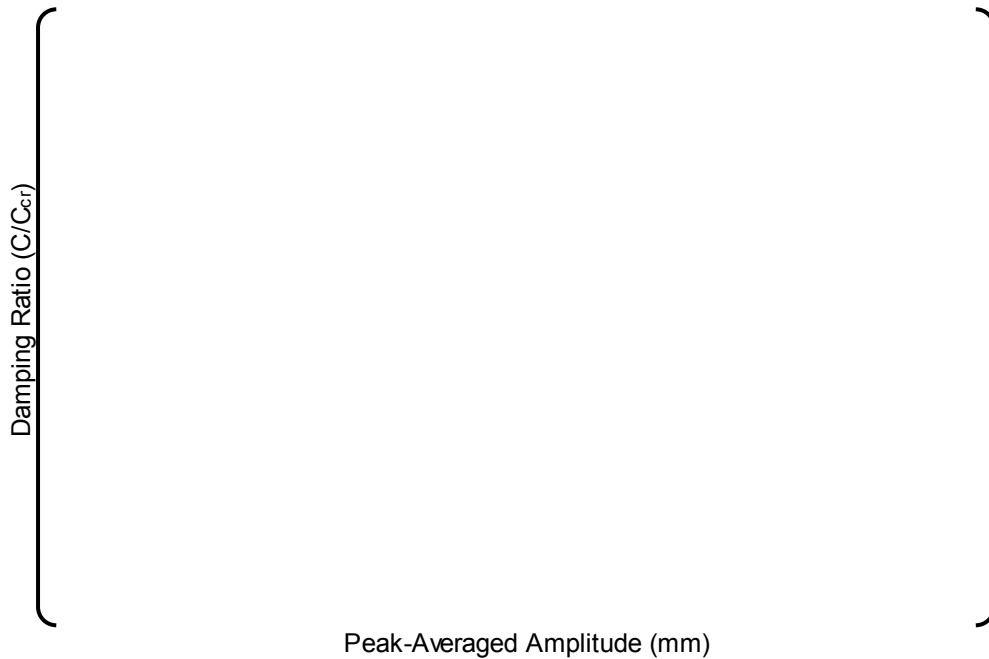
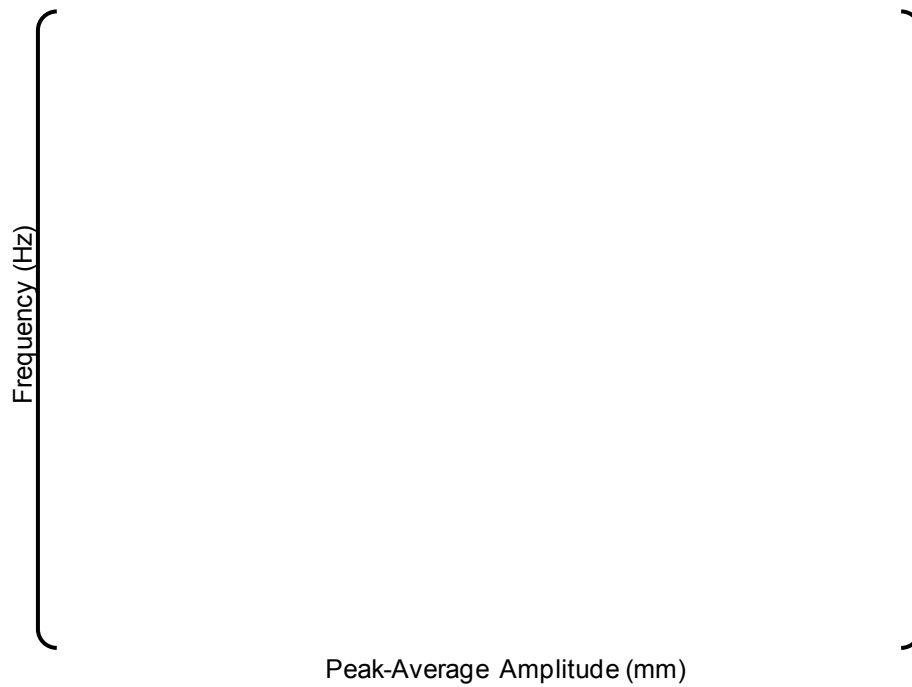
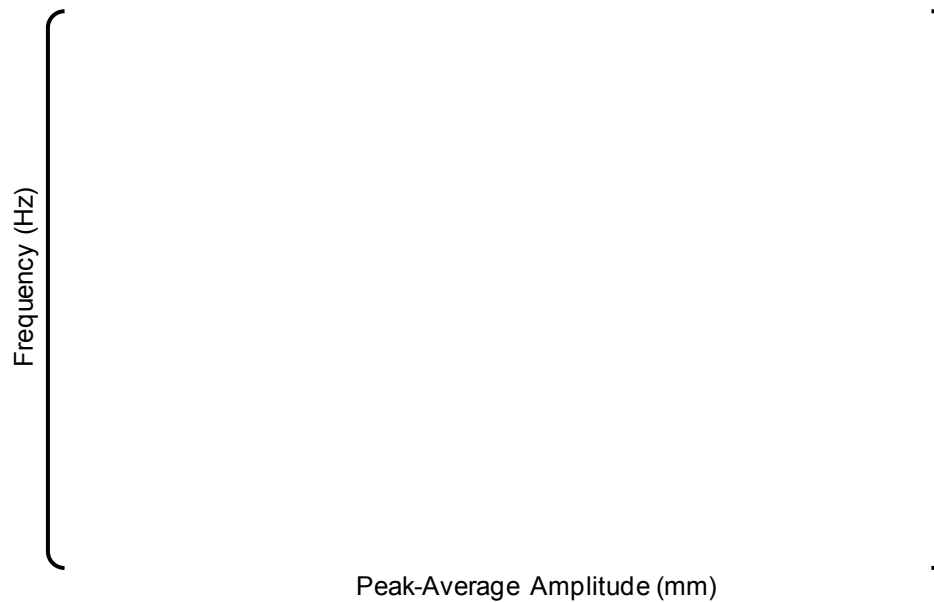


Figure C.3.3.1-3 Damping Ratio Dependency on Amplitude for the US-APWR Mockup Fuel Assembly



**Figure C.3.3.1-4(1) Frequency Dependency on Amplitude for US-APWR Fuel Assembly
in First Mode (Lateral Pluck Test in Air)**



**Figure C.3.3.1-4(2) Frequency Dependency on Amplitude for US-APWR Fuel Assembly
in First Mode (Lateral Pluck Test in Water)**

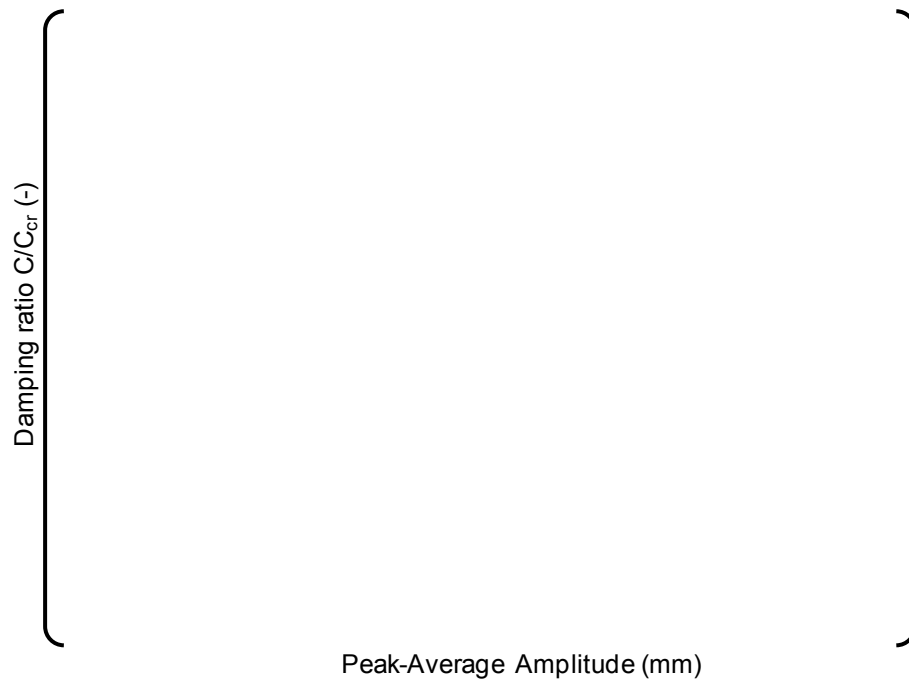


Figure C.3.3.1-5(1) Damping Ratio Dependency on Amplitude for US-APWR Fuel Assembly in First Mode (Lateral Pluck Test in Air)

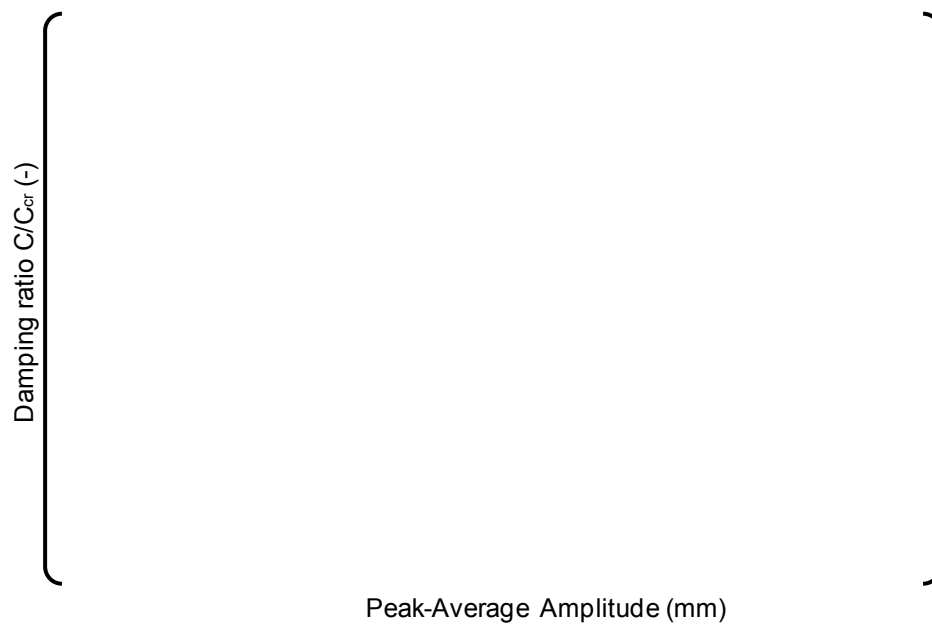


Figure C.3.3.1-5(2) Damping Ratio Dependency on Amplitude for US-APWR Fuel Assembly in First Mode (Lateral Pluck Test in Water)

C.3.3.2 Forced Vibration Test

The amplitude dependency of the frequency and damping ratio for the higher modes are presented on Figure C.3.3.2-1 and Figure C.3.3.2-2.

The US-APWR fuel assembly non-damped natural frequencies obtained with FINDS modal analysis are shown in Table C.3.3.2-1. The comparison with the non-damped natural frequencies extrapolated from the amplitude dependency in the forced vibration test, which is shown in Figure C.3.3.2-1, shows good agreement between the model's results and the experimental results. The mode shapes obtained by the FINDS model and the experimental result also agree very well, as shown in Figure C.3.3.2-3 and Figure C.3.3.2-4.

**Table C.3.3.2-1 US-APWR Fuel Assembly Non-damped Natural frequency
(Forced Vibration Test in Air)**

(Unit: Hz)

	Test	FINDS
1st mode		
2nd mode		
3rd mode		
4th mode		
5th mode		
6th mode		
7th mode		

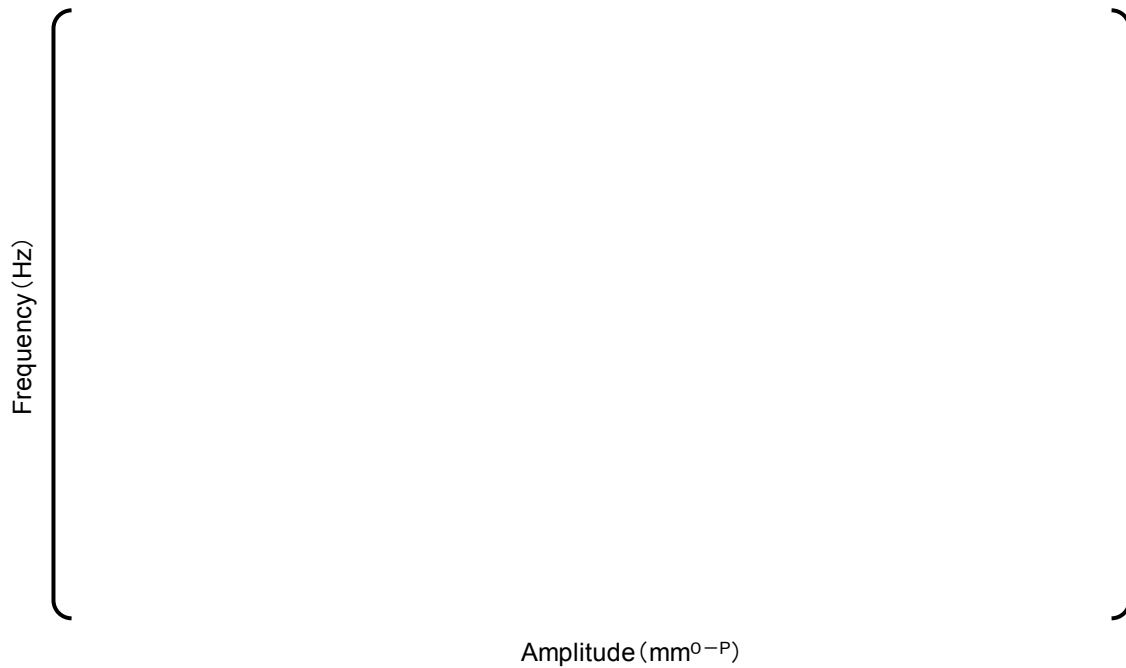


**Figure C.3.3.2-1 Frequency Dependency on Amplitude in Higher Modes
(Forced Vibration Test and FINDS Analysis)**

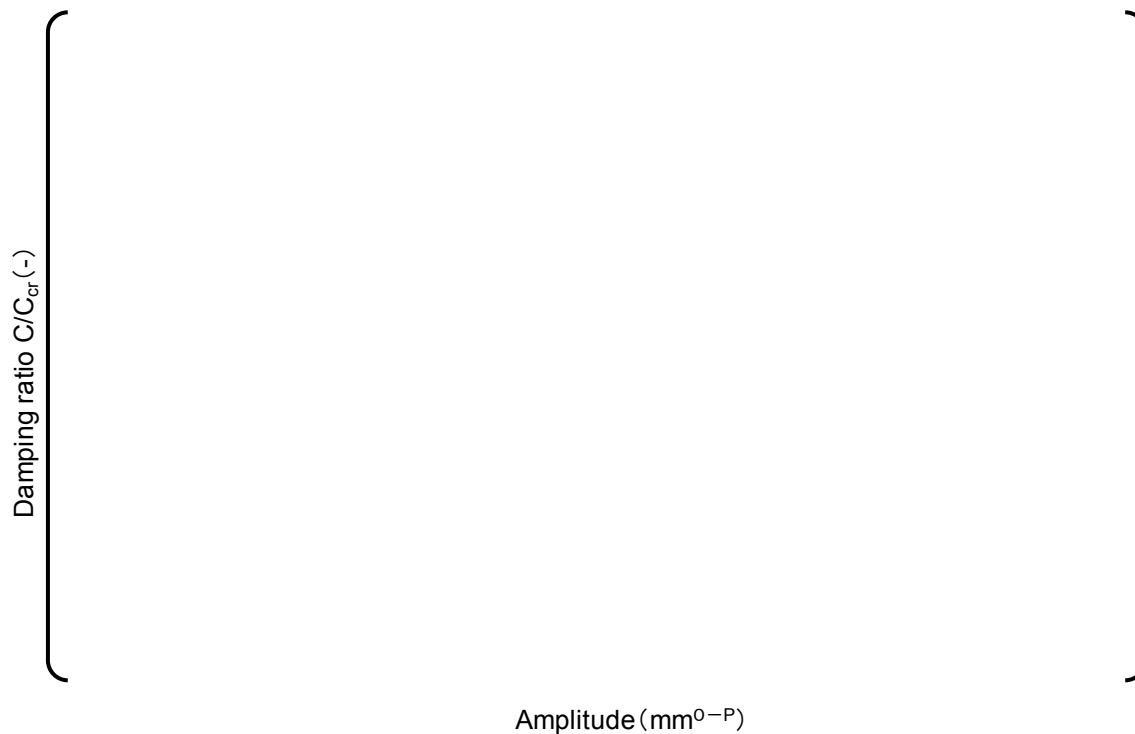


**Figure C.3.3.2-2 Damping Ratio Dependency on Amplitude in Higher Modes
(Forced Vibration Test)**

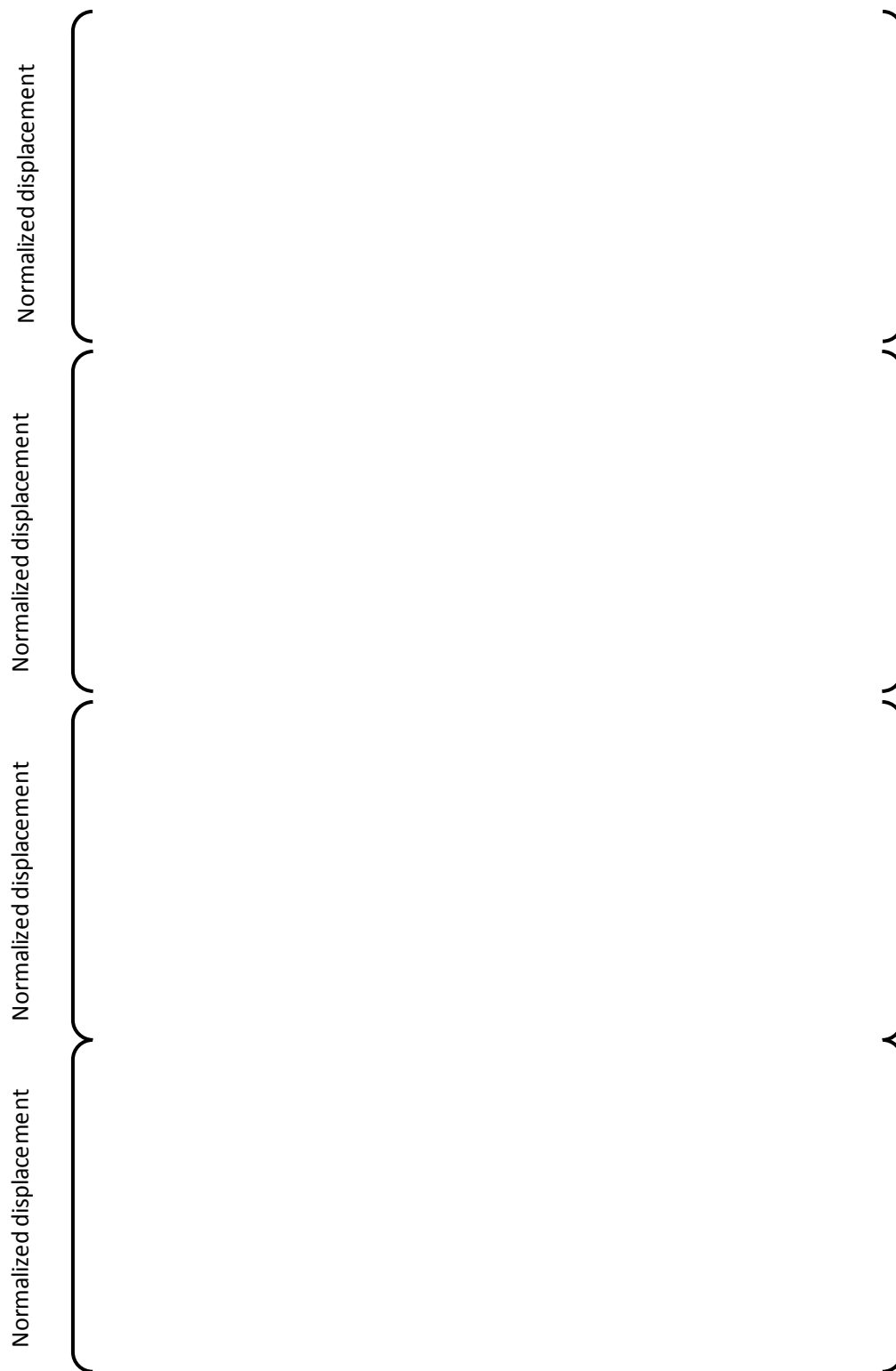


**Figure C.3.3.2-3 US-APWR Fuel Assembly Mode Shape (1st ~ 4th Mode)
from Forced Vibration Test**

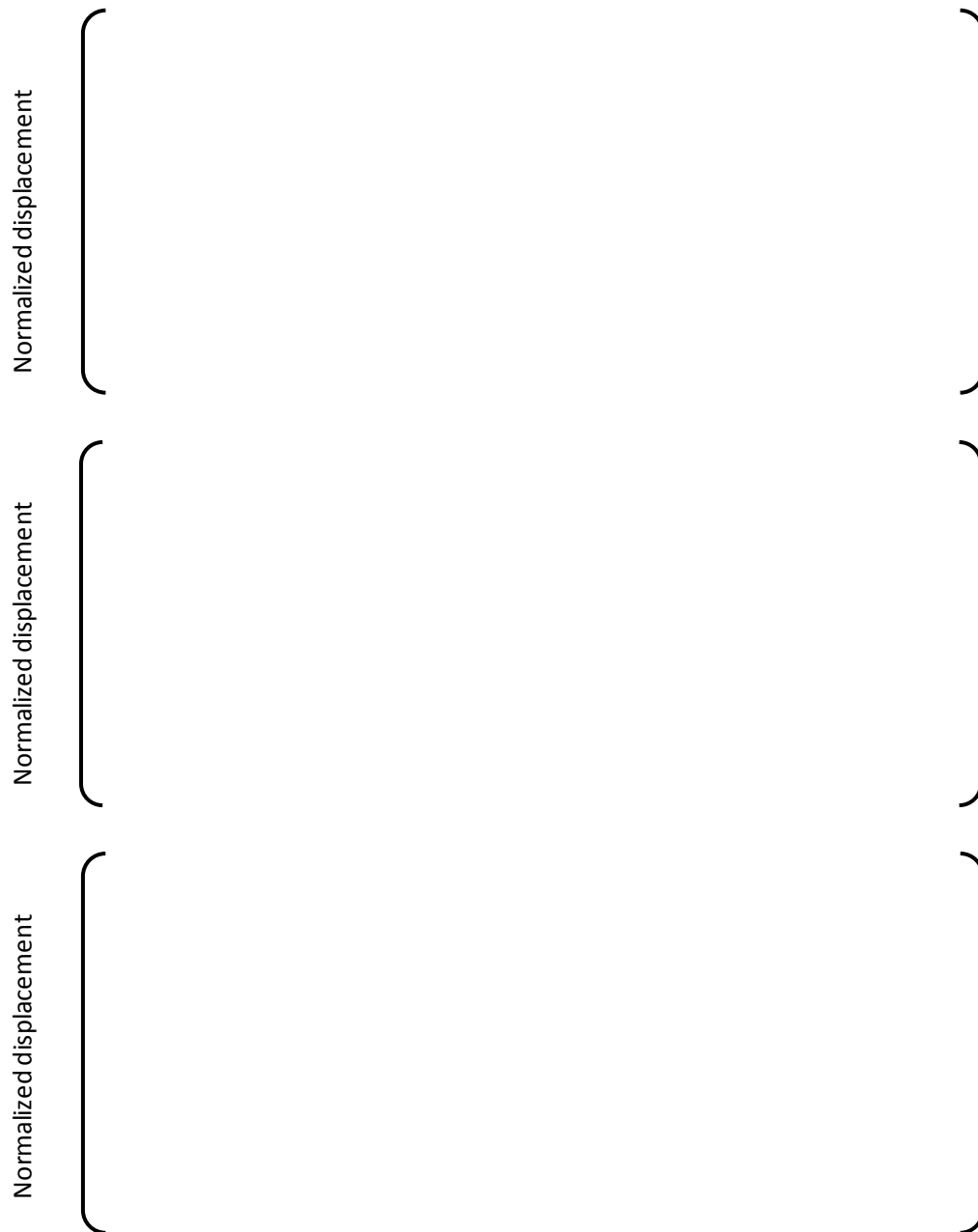


**Figure C.3.3.2-4 US-APWR Fuel Assembly Mode Shape (5th ~ 7th Mode)
from Forced Vibration Test**

C.3.4 Summary of the Lateral Vibration Test

The lateral vibration characteristics of the US-APWR fuel assembly, which is the basis of the model in the FINDS code, were obtained. For the seismic and LOCA response evaluations of the US-APWR fuel assembly, the data obtained from the lateral pluck test in air and water at room temperature are appropriately adjusted for application to in-reactor conditions, as described in Section C.5.0 and C.6.0.

C.4.0 LATERAL IMPACT TEST

C.4.1 Objective

The test is performed to confirm the US-APWR fuel assembly vibration and lateral impact behavior, and the stiffness of the connection between the fuel rod and the grid spacer used in the US-APWR fuel assembly model of the FINDS code for seismic and LOCA response.

C.4.2 Experimental Details

C.4.2.1 Test Arrangement

The fuel assembly is supported as it was in the free vibration test. The assembly is positioned vertically in the test fixture and engaged by the upper and lower core plate fuel-guide pins. The hold-down spring is deflected by approximately () mm which corresponds to the BOL cold in core condition. Load cells, attached to a rigid wall at the same elevation as the grid spacers, are used to measure impact loads. The gap between each grid spacer and load cell is () mm.

Two types of tests are performed: the 1 point tensile condition test in which only the middle grid is initially displaced, as shown in Figure C.4.2.1-1, and the 3 point tensile condition test in which grid spacers No.4, No.6 and No.8 are appropriately displaced to approximate the first mode vibration shape, as shown in Figure C.4.2.1-2.

After measuring the fuel assembly initial gap at each grid spacer location, the fuel assembly is displaced by a lateral deflection adjusting device. The appropriate grid spacers are laterally displaced a specified distance and then, when quickly released, allowed to impact against the rigid wall equipped with load cells corresponding to the grid spacer locations. The fuel assembly lateral translation, measured by displacement transducers mounted at each grid spacer elevation, results in the impact of the grid spacers with their corresponding load cells.

The load cells and displacement transducers are connected to the data processing system to record load and velocity of the grid spacers at impact.

C.4.2.2 Test Procedure

The initial displacement of the No.6 grid spacer started at () mm and was then increased in () mm increments as the tests were repeated. The impact force and deflection were recorded as a function of time.

The test was performed in air at room temperature.

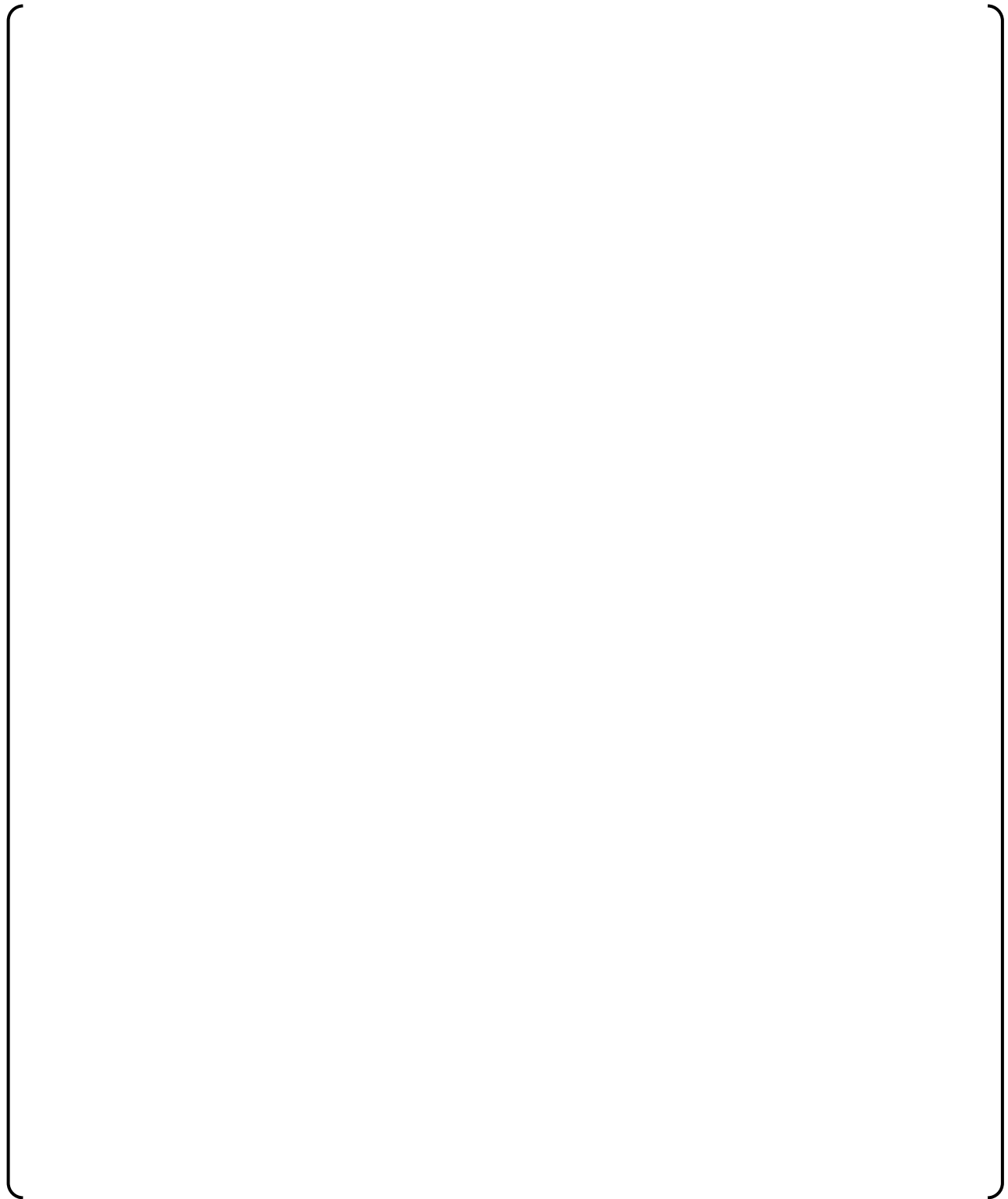


Figure C.4.2.1-1 Fuel Assembly Lateral Impact Test (1 point tensile condition)

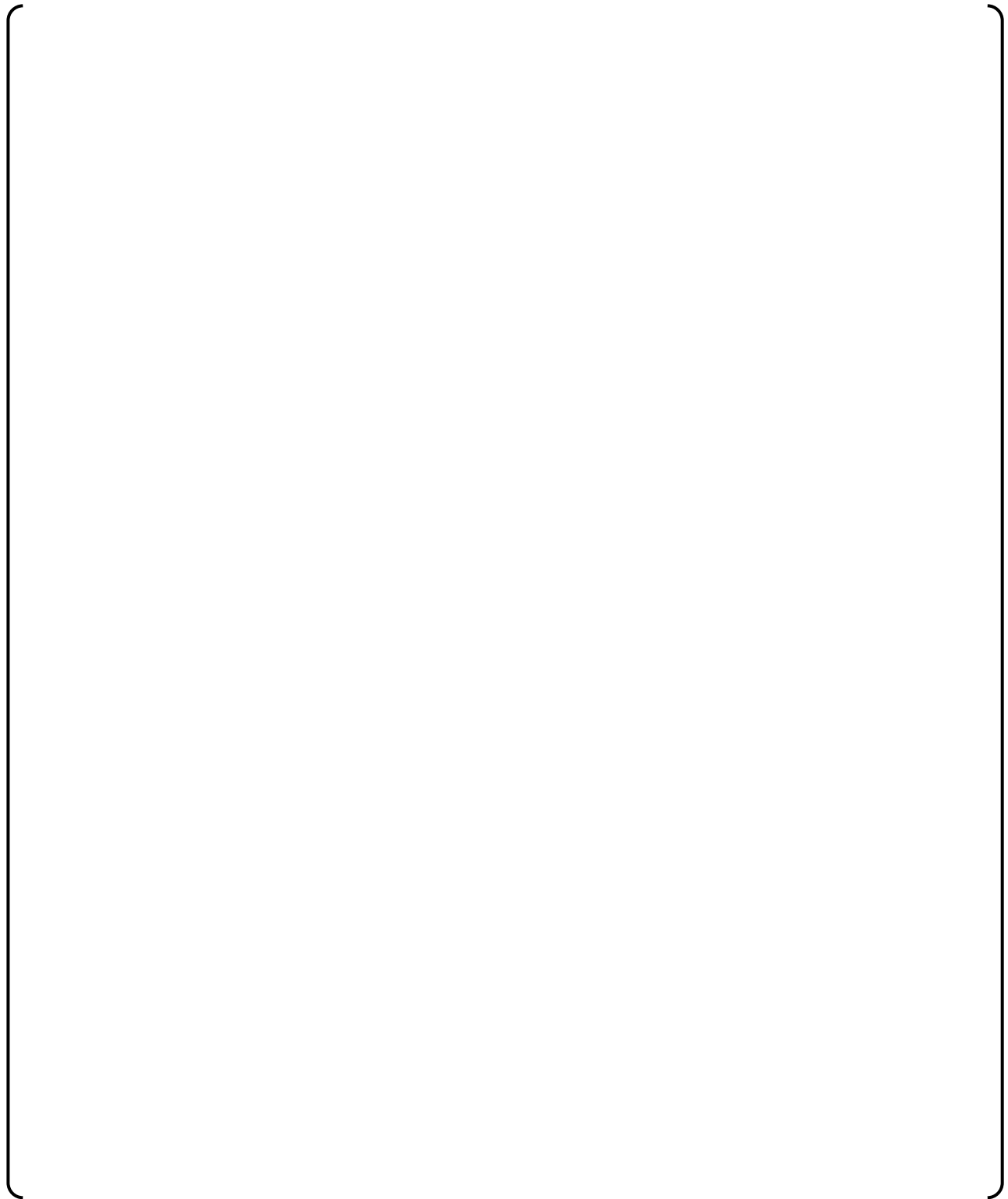


Figure C.4.2.1-2 Fuel Assembly Lateral Impact Test (3 point tensile condition)

C.4.3 Comparison of the Test and the Analysis Results

The fuel assembly residual deflection accumulation in the series of impact tests was considered in the analysis by inputting to FINDS an effective initial deflection which was the actual initial displacement of the assembly minus the residual deflection of the assembly after each test sequence.

The FINDS model based on the pluck-test results for the in-air condition described in C.4.2 is used for the impact test analysis.

Dynamic stiffness used in the grid spacer impact model was determined from relationship between impact force and impact velocity of the weight which was obtained from pendulum type of grid spacer impact test using two as-built grid spacers at room temperature. The relationship is shown in Figure C.4.3-1.

C.4.3.1 1 Point Tensile Condition Test

Figure C.4.3.1-1 shows the comparison between the maximum impact force at the 6th grid spacer obtained by the FINDS code analysis and the maximum impact force at the 6th grid test results. As shown in Figure C.4.3.1-1, the analysis conservatively over-predicts the impact force.

C.4.3.2 3 Point Tensile Condition Test

Figure C.4.3.2-2 shows the comparison between the maximum impact force at the 6th grid spacer obtained by the FINDS code analysis and the maximum impact force at the 6th grid test results. As shown in Figure C.4.3.2-2, the analysis conservatively over-predicts the impact force.



**Figure C.4.3-1 Impact Force versus Impact Velocity
(As-built Grid Spacers at Room Temperature)**

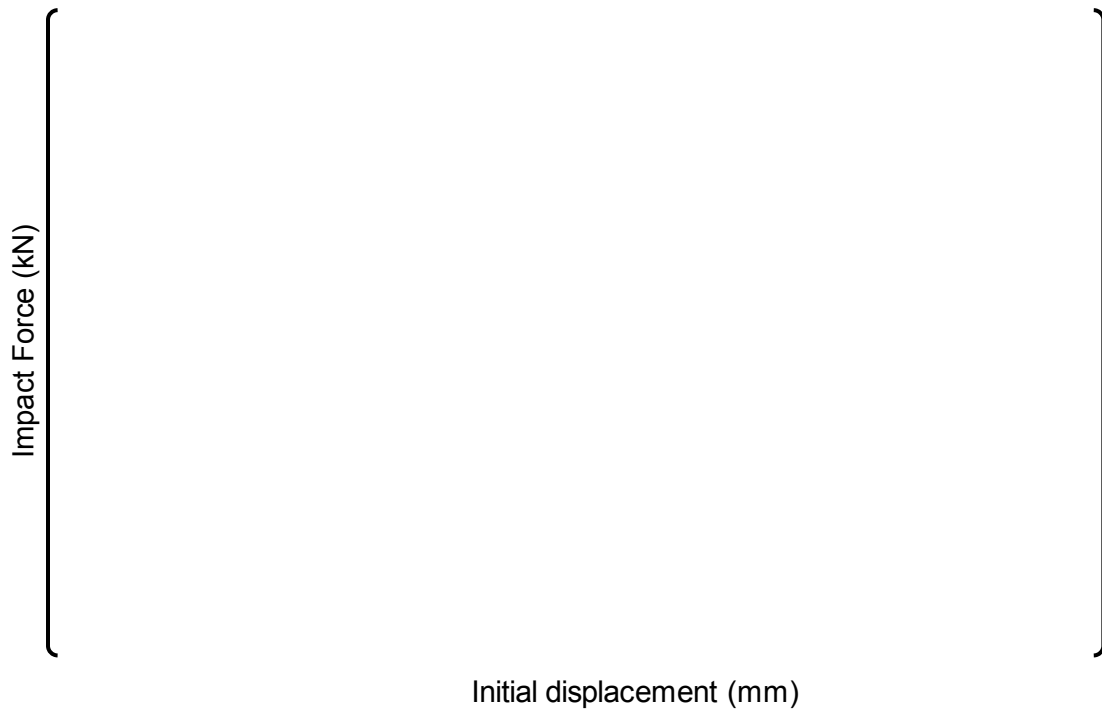


Figure C.4.3.1-1 Maximum Impact Force versus Initial Displacement at No.6 Grid Spacer for the 1 Point Tensile Condition Test

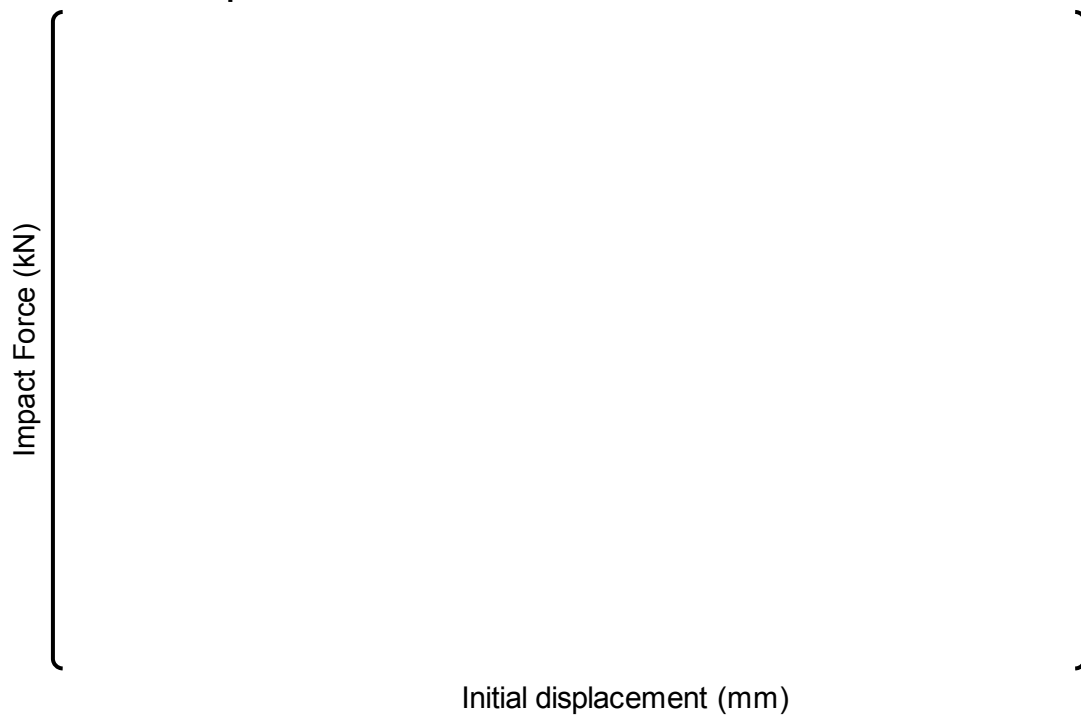


Figure C.4.3.2-2 Maximum Impact Force versus Initial Displacement at No.6 Grid Spacer for the 3 Point Tensile Condition Test

C.4.4 Summary of the Lateral Impact Test

The adequacy of the grid spacer impact model, described in Appendix A of this report, and the lateral vibration model, described in Section C.3.0, used in the FINDS code for the US-APWR fuel assembly and the conservatism for the impact force evaluation have been confirmed by the lateral impact test results.

C.5.0 MODELING OF US-APWR FUEL ASSEMBLY FOR FINDS CODE

C.5.1 BOL Condition

Based on the lateral vibration test, the FINDS model for BOL operating conditions is developed by considering the temperature difference and the effect of the hot coolant as described in Section 4.3 of Reference C-1.

(1) Added mass

For in water conditions, the added mass due to the coolant is included. (

[

]

(2) Young's modulus of beam model

[

]

(3) Vibration damping ratio

[

]

(4) Grid spacer impact characteristics

The grid spacer impact model was developed by, the grid spacer impact test at operating temperature. Therefore, the additional treatment for impact stiffness, impact damping and deformation of the grid spacer is not needed.

C.5.2 EOL Condition

The experimentally obtained amplitude dependency of frequency and damping ratio are shown in Figure C.5.2-1(a) and (b) for 12ft fuel assemblies with as-built and relaxed spring force, respectively.

The frequency of the fuel assembly with relaxed spring forces is lower than that of the fuel assembly with the as-built spring forces because with relaxed springs slippage at the contact points between the fuel rods and grid spacers starts at a relatively small fuel assembly lateral amplitude. For the same reason, the damping ratio of the fuel assembly with the relaxed spring force is larger over this small amplitude range compared with that with the beginning of life spring force. In the large amplitude range, the damping ratio of the fuel assembly with the relaxed spring force is smaller than that of the fuel assembly with the BOL spring force, because the energy loss due to friction at the contact points of the relaxed spring is relatively small.

Concerning the damping ratio, the data in Figure C.5.2-2 shows the similarity in the amplitude dependency of the damping ratio between the US-APWR fuel assembly and the 12ft fuel assembly with as-built spring forces. Damping ratio of the US-APWR fuel assembly is a little lower than that of 12ft fuel assembly. Since both of the data are provided from 1 point tensile type of pluck test, influence of higher mode superposing in 12ft fuel assembly is more than that in the US-APWR fuel assembly due to difference of the grid spacer number and overall length of the fuel assembly. Due to the close similarity of grid spacer designs of the US-APWR fuel assembly and the 12ft fuel assembly, it can be concluded that the similarity remains after the grid spacer spring is relaxed. The amplitude dependence of the damping ratio for US-APWR fuel assembly is determined as described in the Subsection C.5.4.2 below, based on the experimentally obtained amplitude dependency of the 12ft fuel assembly with relaxed spring force shown in Figure C.5.2-1.

Concerning the frequency, the effect of reduced grid spacer spring force on the amplitude dependent frequency is evaluated using the ANSYS FEM code. The analysis model is shown in Figure C.5.2-3.



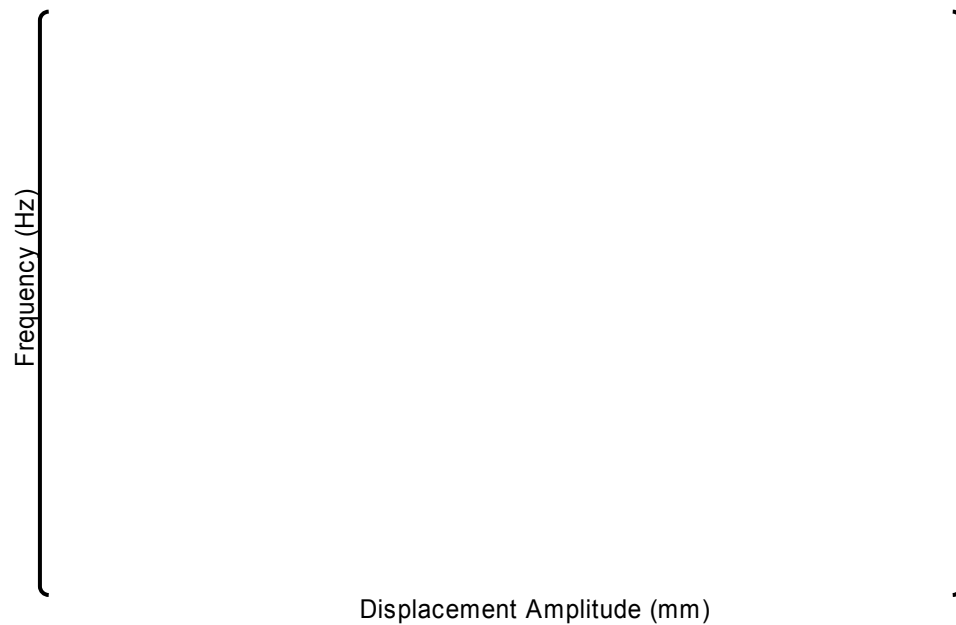


For the analysis model with relaxed grid spring force, the forces are determined to be { } percent of the initial value for the top grid spacer, { } percent for the middle grid spacers and { } percent for the bottom grid spacer, to simulate an irradiated fuel assembly at a burn-up of 60 GWd/MtU. The detail is described in Subsection 4.4 of Reference C-2.

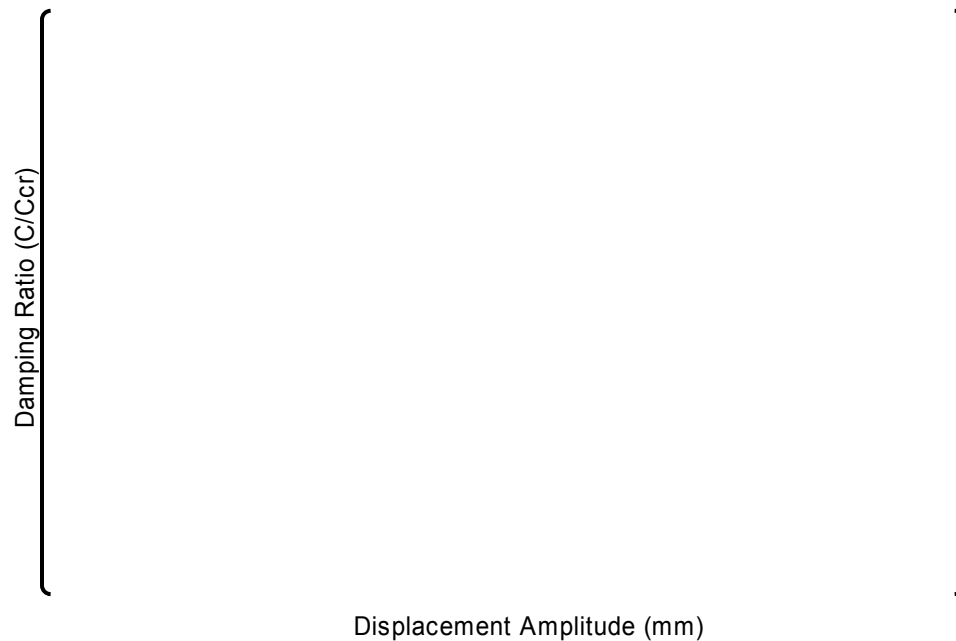
Both the as-built spring force and relaxed spring force models have the top and bottom ends restrained when the centermost middle grid spacer is initially displaced, and then quickly released. The maximum initial displacements were { } inch ({ } mm) for the as-built spring force model and { } inch ({ } mm) for the relaxed grid spring force model. The larger initial displacement has been given to the relaxed spring force model because the larger deflection has been calculated in the seismic analysis described in Appendix E of this report. Based on the time history displacement data, the amplitude dependence of frequency of the fuel assembly with the relaxed spring force is calculated as shown in Figure C.5.2-4. The analyses are conducted for operating conditions.

The amplitude dependence of the frequency is due to the contact and slippage mechanism between the fuel rods and grid spacers. As the vibration amplitude increases, the natural frequency decreases in the same way as for the BOL condition.





(a) Frequency



(b) Damping Ratio

Figure C.5.2-1 Influence of Grid Spacer Spring Relaxation on Frequency and Damping Ratio

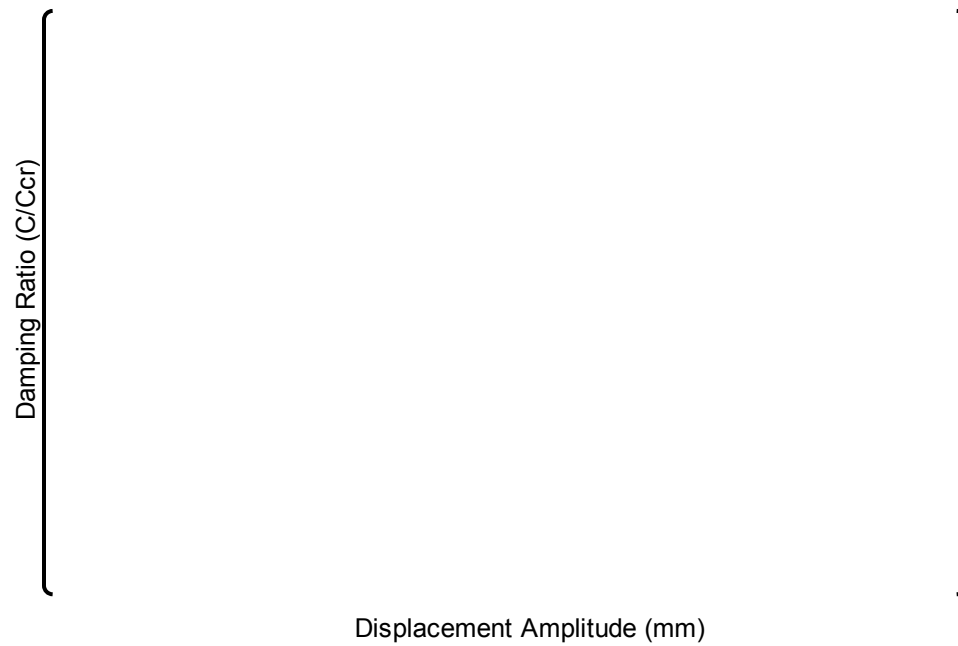


**Figure C.5.2-2 Comparison of the US-APWR and 12ft Fuel Assemblies
Amplitude Dependency in the in-Air Pluck Test**

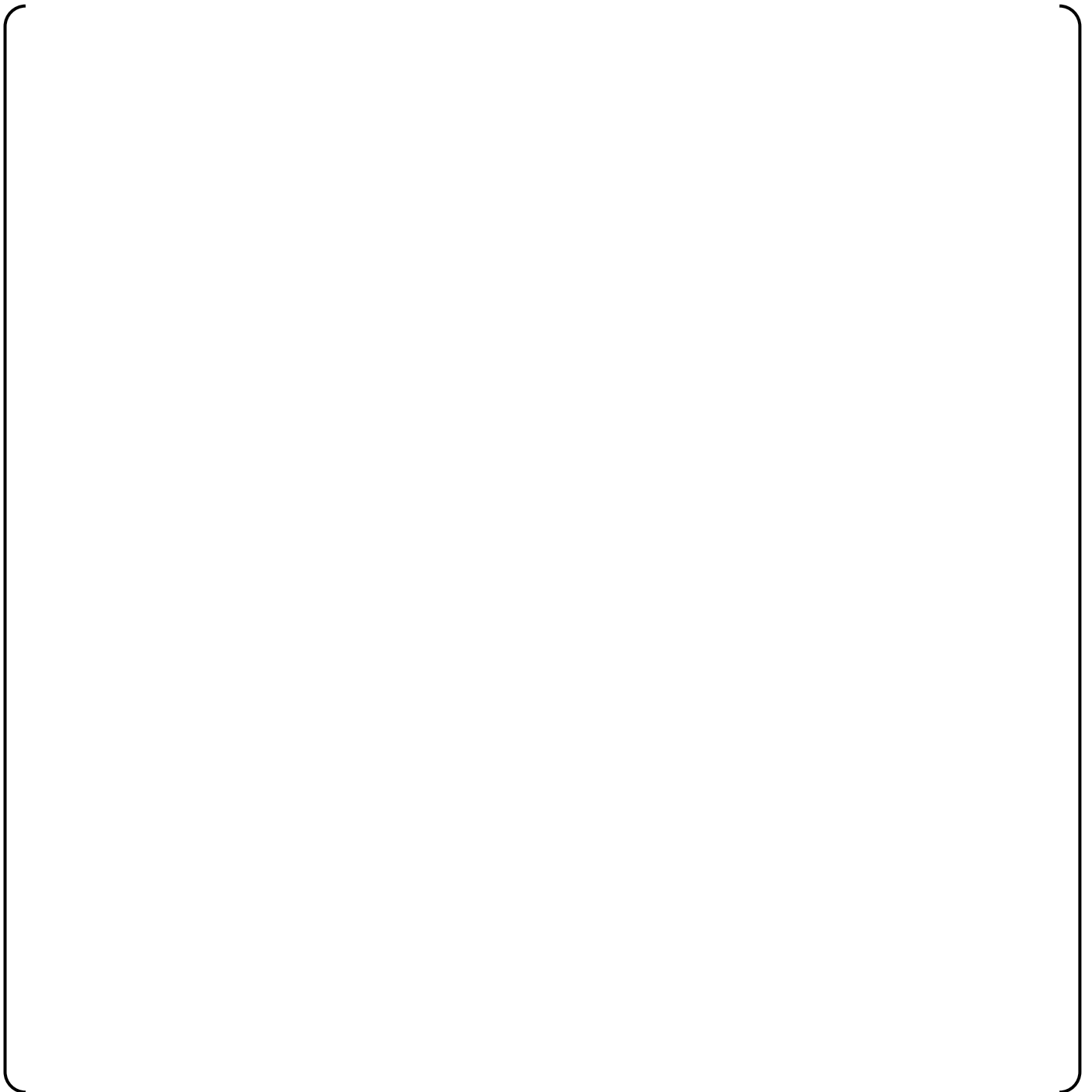


Figure C.5.2-3 Fuel Assembly Stress Analysis Model in the Horizontal Direction



Figure C.5.2-4 Amplitude Dependence of the 14ft Fuel Assembly's Frequency Using ANSYS FEM Analysis (Operating Condition)

C.5.3.1 Introduction

$$\left[\begin{array}{c} \\ \\ \\ \end{array} \right]$$

C.5.3.2 Evaluation

Frequency and damping ratio are not independent during fuel assembly vibration. As seen in the comparisons of Figure C.5.3-1(a) with Figure C.5.3-2(a), and of Figure C.5.3-1(b) with Figure C.5.3-2(b), for the US-APWR fuel assembly higher damping results in lower frequencies and, in contrast, lower damping results in higher frequencies. Therefore, MHI regards combining lower bound frequency with lower bound damping as unrealistic.

However, this dual combination has been analyzed with the FINDS code to provide results of all combinations in Table C.5.3-1.

The upper and lower bounds for the amplitude dependence of frequency and damping ratio are determined from the experimental data obtained from pluck tests in air and in cold water. The procedure is as follows.



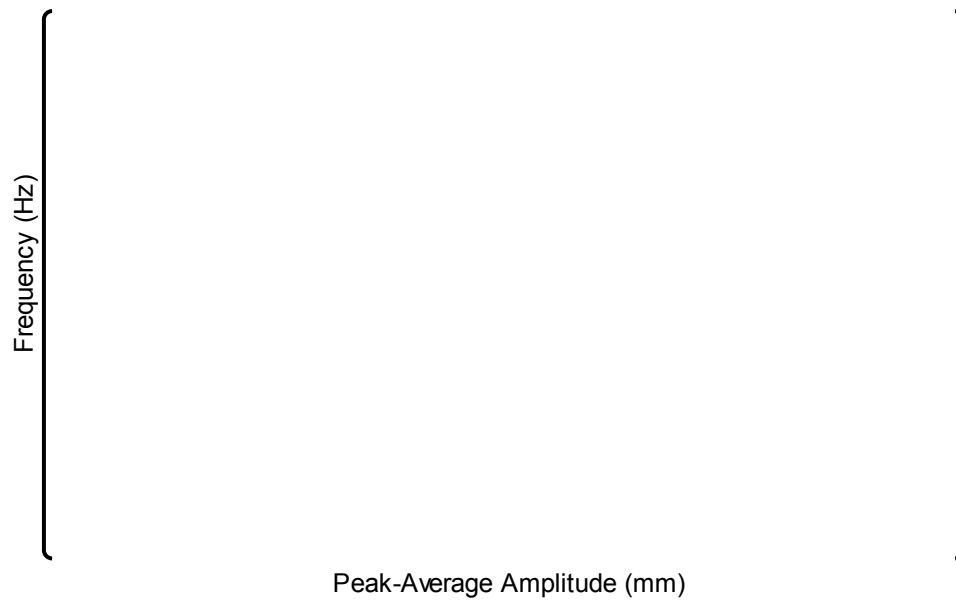


Figure C.5.3-1(a) Frequency for in Air Pluck Test

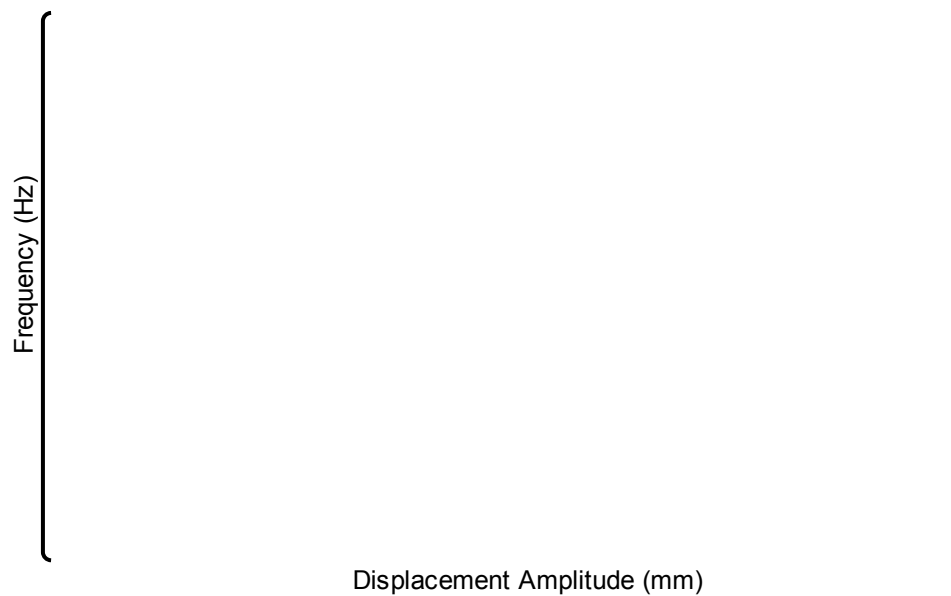


Figure C.5.3-1(b) Frequency for in Water Pluck Test

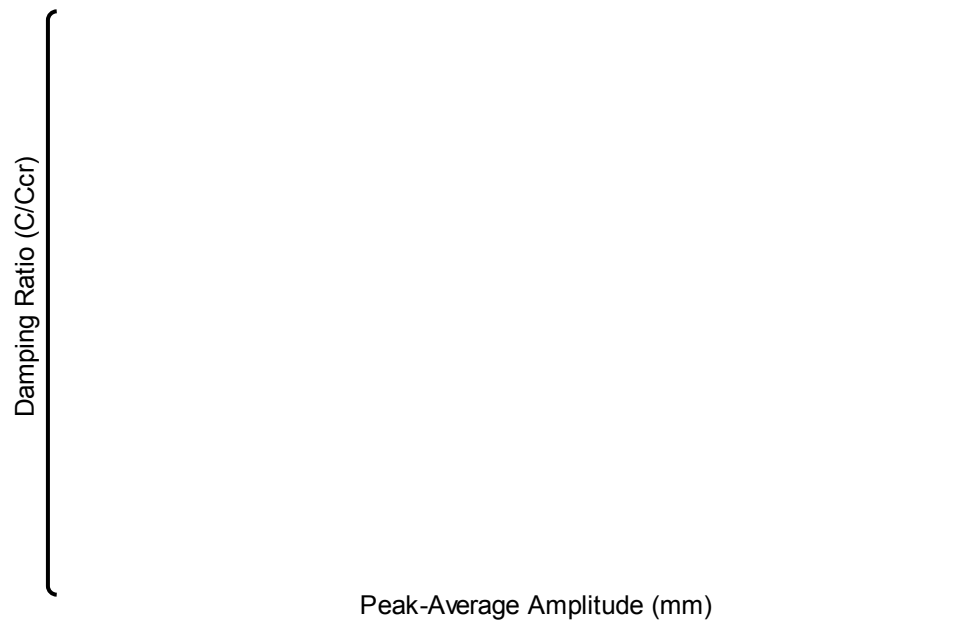


Figure-2 (a) Damping in Air Pluck Test

Figure C.5.3-2(a) Damping Ratio for in Air Pluck Test



Figure-2 (b) Dampng in Cold-Water Pluck Test

Figure C.5.3-2(b) Damping Ratio for in Water Pluck Test

C.5.4 Uncertainty Evaluation for US-APWR Fuel Assembly FINDS model at EOL Condition

C.5.4.1 Uncertainty Evaluation for Frequency

The best estimate amplitude dependency of the frequency in the US-APWR fuel assembly under reactor operating conditions at EOL is obtained from the ANSYS code analysis with the US-APWR fuel assembly model as described in Section C.5.2.

C.5.4.2 Uncertainty Evaluation for Damping Ratio



C.6.0 CONCLUSION

The results of the mechanical tests performed on a prototype fuel assembly to develop the US-APWR FINDS model and confirm the adequacy of the US-APWR fuel assembly model for response analysis during seismic and LOCA events are reported in this Appendix.

Based on the lateral vibration test of the US-APWR mockup fuel assembly, vibration model for BOL and EOL at operating condition were developed. In the modeling, uncertainty of the frequency and damping dependency on amplitude was considered.

The amplitude dependency of frequency and damping ratio for the US-APWR models at BOL and EOL are shown in Figure C.6.0-1 and Figure C.6.0-2, respectively.

The developed fuel assembly vibration model together with the grid spacer impact model was supplied to analysis simulating the fuel assembly lateral impact test and confirmed its validity by comparison between analysis and test results.

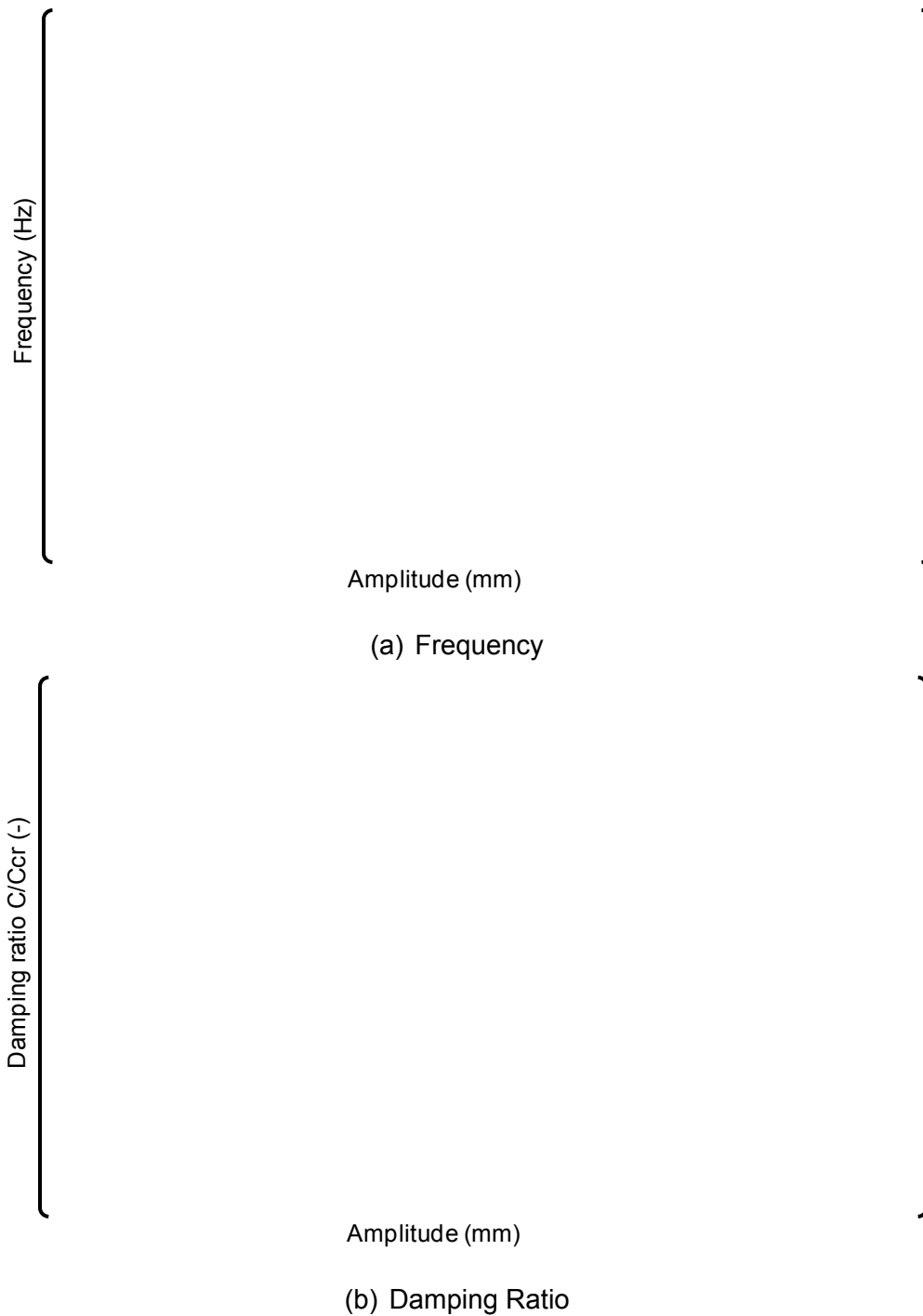
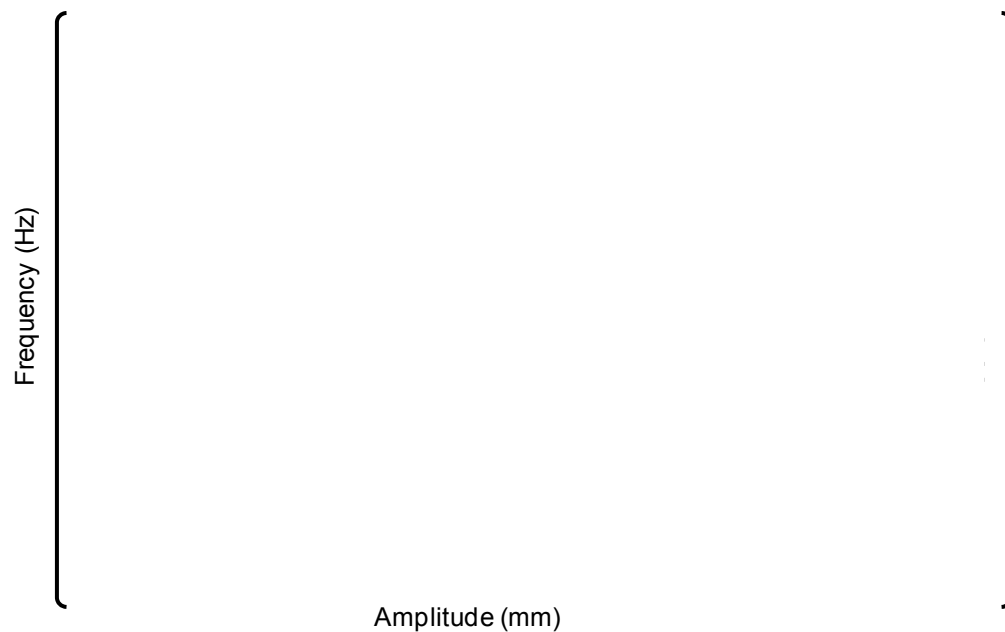
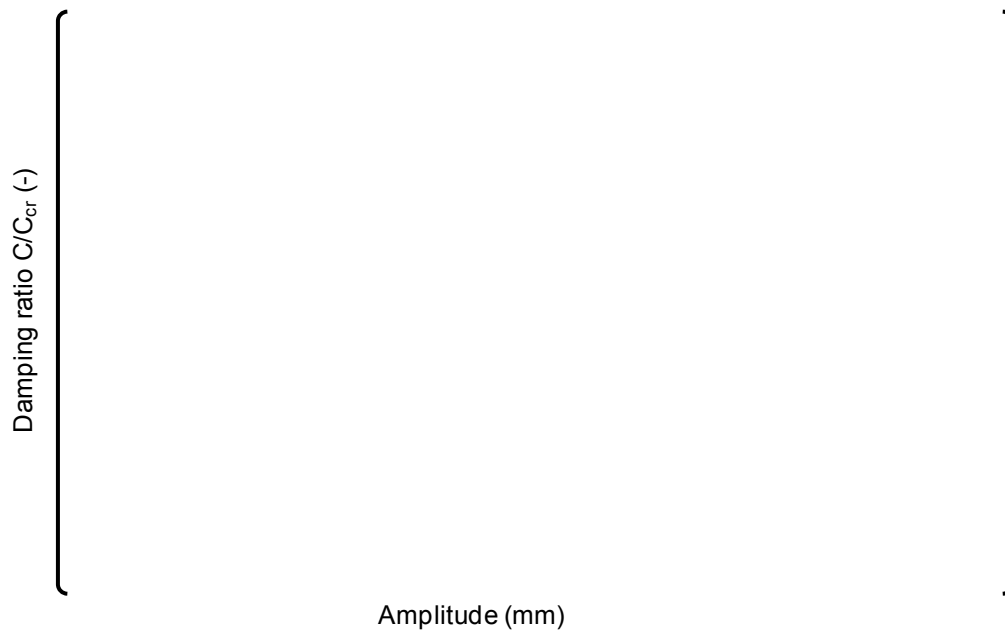


Figure C.6.0-1 Amplitude Dependency of Frequency and Damping for US-APWR Model at BOL Operating Conditions



(a) Frequency



(b) Damping Ratio

Figure C.6.0-2 Amplitude Dependency of Frequency and Damping for US-APWR Model at EOL Operating Conditions

C.7.0 REFERENCES

- (C-1) "FINDS: Mitsubishi PWR Fuel Assemblies Seismic Analysis Code", MUAP-07034-P Rev.3 (Proprietary) and MUAP-07034-NP Rev.3 (Non-Proprietary), July 2010
- (C-2) "US-APWR Fuel System Design Evaluation", MUAP-07016-P (Proprietary) and MUAP-07016-NP (Non-Proprietary) Revision 3, Aug 2010

Appendix D

GRID SPACER DEFORMATION EFFECT ON CONTROL ROD INSERTABILITY AND COOLABLE GEOMETRY

December 2010

**© 2010 Mitsubishi Heavy Industries, Ltd.
All Rights Reserved**

Table of Contents

List of Tables	D-3
List of Figures	D-4
D.1.0 INTRODUCTION	D-6
D.2.0 GRID DEFORMATION EFFECT ON CONTROL ROD INSERTABILITY	D-9
D.2.1 Determination of Grid Spacer Buckling	D-9
D.2.2 Maximum Credible Deformation of the Grid Spacer	D-13
D.2.2.1 Buckled Cell Rows and Possible Grid Spacer Deformation Patterns	D-13
D.2.2.2 Most limiting Deformation of the Grid Spacer for Control Rod Insertability ..	D-20
D.2.2.3 Geometrical Pattern of the Axially Adjacent Grid Spacers	D-27
D.2.3 Summary of Control Rod Drop Test Results Considering the Effects of Fuel Assembly Grid Spacer Deformation	D-33
D.2.3.1 Introduction	D-33
D.2.3.2 Test Model	D-33
D.2.3.3 Test Procedure	D-33
D.2.3.4 Test Results	D-40
D.2.4 Conclusion for Grid Spacer Deformation Effect on Control Rod Insertability	D-43
D.3.0 GRID DEFORMATION EFFECT ON MAINTAINING COOLABLE GEOMETORY .	D-44
D.3.1 Analysis Condition	D-44
D.3.2 Analysis Result	D-47
D.3.3 Conclusion for Grid Spacer Deformation Effect on Maintaining Coolable Geometry	D-49
D.4.0 REFERENCES	D-50

List of Tables

Table D.2.2.1-1	Geometrical Patterns of Grid Spacer's Plastic Deformation.....	D-14
Table D.2.2.2-1	Comparison of Average Relative Displacement per Thimble in the Direction Perpendicular to the Impact Direction.....	D-21
Table D.2.3.3-1	List of Test Conditions	D-35
Table D.2.3.3-2	Distribution of Grid Spacer Deformation in Fuel Assembly	D-36

List of Figures

Figure D.1.0-1	Evaluation Flow Chart for Grid Spacer Deformation Effect on RCC Insertability and PCT Using FINDS Analyses Results	D-7
Figure D.2.1-1	Grid Spacer Model for Impact Analysis	D-10
Figure D.2.1-2	Boundary Condition of Grid Spacer Impact Analysis	D-11
Figure D.2.1-3	Time History of Reaction Force	D-12
Figure D.2.2.1-1	Grid Spacer Cell Rows Affecting Thimble Misalignment	D-16
Figure D.2.2.1-2	Possible Geometrical Patterns of Grid Spacer Deformation	D-17
Figure D.2.2.1-3	Shearing Force Distribution in Buckling Deformation of 5 th Row	D-18
Figure D.2.2.1-4	Shearing Force Distribution in Buckling Deformation of 7 th and 8 th Row	D-18
Figure D.2.2.1-5	Pattern Example for Excluding Deformation	D-19
Figure D.2.2.2-1	Deformation of a Fuel Rod Cell	D-22
Figure D.2.2.2-2	Displacement of Guide Thimbles (Pattern I through Pattern III)	D-23
Figure D.2.2.2-3	Displacement of Guide Thimbles (Pattern IV through Pattern VI)	D-24
Figure D.2.2.2-4	Displacement of Guide Thimbles (Pattern VII through Pattern IX)	D-25
Figure D.2.2.2-5	Grid Deformation Pattern in NUPEC Seismic Vibration Test (No.5 grid spacer deformation after 1.5 S2(1) vibration test)	D-26
Figure D.2.2.3-1	US-APWR Fuel Assembly Skeleton Model	D-29
Figure D.2.2.3-2	Addition of Grid Spacer Deformation in Analysis Case 1	D-30
Figure D.2.2.3-3	Addition of Grid Spacer Deformation in Analysis Case 2	D-30
Figure D.2.2.3-4	Case 1: Shearing Force Distribution of RCC Guide Thimble [8 th Grid]	D-31
Figure D.2.2.3-5	Case 1: Shearing Force Distribution of RCC Guide Thimble [7 th Grid]	D-31
Figure D.2.2.3-6	Case 2: Shearing Force Distribution of RCC Guide Thimble [3 rd Grid]	D-32
Figure D.2.2.3-7	Case 2: Shearing Force Distribution of RCC Guide Thimble [4 th Grid]	D-32
Figure D.2.3.2-1	Outline Drawing of Test Equipment	D-37
Figure D.2.3.3-1	Grid Spacer Deformation Patterns	D-38
Figure D.2.3.3-2	Schematic View of Thimble Array Fixture Grid Spacer Mock-Up	D-39
Figure D.2.3.4-1 (1/2)	Insertion Delay Time from Start of Control Rod Drop to Dashpot	

Entrance	D-41
Figure D.2.3.4-1 (2/2) Insertion Delay Time from Start of Control Rod Drop to Dashpot	
Entrance	D-42
Figure D.3.1-1 Maximum Credible Deformation of Grid Spacer Cell	D-46
Figure D.3.2-1 Sensitivity of the limiting PCT for Grid Deformation.....	D-48

Appendix E

FINDS RESULTS OF RESPONSE ANALYSIS FOR SEISMIC AND LOCA HORIZONTAL DIRECTION

December 2010

**© 2010 Mitsubishi Heavy Industries, Ltd.
All Rights Reserved**

Table of Contents

List of Tables	E-3
E.1.0 INTRODUCTION	E-4
E.2.0 CASE STUDY RESULTS FOR THE RESPONSE ANALYSIS FOR SEISMIC HORIZONTAL DIRECTION	E-5
E.2.1 BOL Condition	E-5
E.2.2 EOL Condition	E-13
E.2.3 Effect of Vibration Characteristics Uncertainty	E-29
E.3.0 CASE STUDY RESULTS FOR THE RESPONSE ANALYSIS FOR LOCA HORIZONTAL DIRECTION	E-34
E.3.1 EOL Condition	E-34
E.3.2 Effect of Vibration Characteristics Uncertainty	E-36
E.4.0 CONCLUSION	E-38

List of Tables

Table E.2.1-1	Response Analysis Results in SSE Horizontal Direction with BOL Condition	E-6
Table E.2.1-2	Response Analysis Results in 560-100 Wave Horizontal Direction with BOL Condition	E-10
Table E.2.2-1	Response Analysis Results in SSE Horizontal Direction with EOL Condition	E-14
Table E.2.2-2	Best estimated buckled grid number distribution for 270-200 wave.....	E-18
Table E.2.2-3	Best estimated buckled grid number distribution for 270-500 wave.....	E-19
Table E.2.2-4	Best estimated buckled grid number distribution for 560-100 wave.....	E-20
Table E.2.2-5	Best estimated buckled grid number distribution for 560-200 wave.....	E-21
Table E.2.2-6	Best estimated buckled grid number distribution for 560-500 wave.....	E-22
Table E.2.2-7	Best estimated buckled grid number distribution for 900-100 wave.....	E-23
Table E.2.2-8	Best estimated buckled grid number distribution for 900-200 wave.....	E-24
Table E.2.2-9	Best estimated buckled grid number distribution for 2032-100 wave....	E-25
Table E.2.2-10	Response Analysis Results in 560-100 Wave Horizontal Direction with EOL Condition	E-26
Table E.2.3-1	Required Cases for Uncertainty Analysis	E-30
Table E.2.3-2	Uncertainty Response Analysis Results (560-100 Wave)	E-31
Table E.3.1-1	Response Analysis Results in LOCA Horizontal Direction	E-35
Table E.3.2-1	Uncertainty Response Analysis Results (CLB 8B 102%LF Wave).....	E-37

E.1.0 INTRODUCTION

The response analysis result for the following SSE and LOCA events are described in this appendix.

SSE:

- 270-200
- 270-500
- 560-100
- 560-200
- 560-500
- 900-100
- 900-200
- 2032-100

LOCA:

- CLB 8B 102%LF
- HLB 10B 102%LF

- The frequency of () is considered as the uncertainty of the SSE acceleration wave.

- The fuel assembly vibration characteristics and the impact characteristics in the grid spacers are also conservatively considered in the model by choosing the most limiting combination of inputs for evaluation considering the varying characteristics of the fuel assembly over its lifetime. The detailed explanation of the EOL model is described in Appendix C. As shown in Appendix C of the report, although it is considered that the EOL condition when the damping becomes lower gives the larger displacement qualitatively, the BOL condition can give the larger displacement if the fuel assembly vibration characteristic at BOL condition synchronizes with the SSE acceleration wave. Therefore the response analyses are performed for both the BOL condition and the EOL condition and the condition giving the most limiting results is used.

- Concerning the LOCA event, only the most limiting fuel assembly condition (EOL) is used for the response analysis.

- In addition, the () cases for combining the uncertainties in the amplitude dependence of frequency and of damping, as shown in Table C.6.1-1 of Appendix C are considered to determine the most limiting case which gives the most limiting result.

- Concerning LOCA events only the most limiting of the () cases for evaluating SSE events is used in the response analysis.

E.2.0 CASE STUDY RESULTS FOR THE RESPONSE ANALYSIS FOR SEISMIC HORIZONTAL DIRECTION

E.2.1 BOL Condition

The maximum responses obtained with BOL conditions are shown in Table E.2.1-1 for 270-200, 270-500, 560-100, 560-200, 560-500, 900-100, 900-200 and 2032-100. From this table, with 560-100 having the maximum displacement of () inch () mm) in X direction and () inch () mm) in Z direction, it is the most limiting SSE wave with respect to the maximum displacement of the fuel assembly.

Concerning the uncertainty of the SSE acceleration wave, the maximum responses obtained with BOL conditions for 560-100 are shown in Table E.2.1-2. Here, the () frequency of 560-100, having the maximum displacement of () inch () mm) in X direction and the () frequency of 560-100, having the maximum displacement of () inch () mm) in Z direction, are the most limiting cases of the SSE wave uncertainty.

Table E.2.1-1 Response Analysis Results in SSE Horizontal Direction with BOL Condition

Wave	Units	270-200		270-500	
Direction	-	x	z	x	z
Maximum displacement	inch (mm)				
Time	s				
Fuel assembly number	-				
Grid number	-				
Maximum Impact force*	lbf (N)				
Time	s				
Fuel assembly number **	-				
Grid number	-				

* Buckling force of the grid spacer is () lbf () N) in the FINDS code

** NR refers to Neutron Reflector

Table E.2.1-1(continued) Response Analysis Results in SSE Horizontal Direction with BOL Condition

Wave	Units	560-100		560-200	
Direction	-	x	z	x	z
Maximum displacement	inch (mm)				
Time	s				
Fuel assembly number	-				
Grid number	-				
Maximum Impact force*	lbf (N)				
Time	s				
Fuel assembly number **	-				
Grid number	-				

* Buckling force of the grid spacer is () lbf () N in the FINDS code

** NR refers to Neutron Reflector

Table E.2.1-1(continued) Response Analysis Results in SSE Horizontal Direction with BOL Condition

Wave	Units	560-500		900-100	
Direction	-	x	z	x	z
Maximum displacement	inch (mm)				
Time	s				
Fuel assembly number	-				
Grid number	-				
Maximum Impact force*	lbf (N)				
Time	s				
Fuel assembly number **	-				
Grid number	-				

* Buckling force of the grid spacer is () lbf () N in the FINDS code

** NR refers to Neutron Reflector

Table E.2.1-1(continued) Response Analysis Results in SSE Horizontal Direction with BOL Condition

Wave	Units	900-200		2032-100	
Direction	-	x	z	x	z
Maximum displacement	inch (mm)				
Time	s				
Fuel assembly number	-				
Grid number	-				
Maximum Impact force*	lbf (N)				
Time	s				
Fuel assembly number **	-				
Grid number	-				

* Buckling force of the grid spacer is () lbf () N) in the FINDS code

** NR refers to Neutron Reflector

Table E.2.1-2 Response Analysis Results in 560-100 Wave Horizontal Direction with BOL Condition

Wave	Units	560-100
Variation of frequency	-	
Direction	-	
Maximum displacement	inch (mm)	
Time	s	
Fuel assembly number	-	
Grid number	-	
Maximum Impact force*	lbf (N)	
Time	s	
Fuel assembly number **	-	
Grid number	-	

* Buckling force of the grid spacer is () lbf () N) in the FINDS code

** NR refers to Neutron Reflector

Table E.2.1-2(continued) Response Analysis Results in 560-100 Wave Horizontal Direction with BOL Condition

Wave	Units	560-100
Variation of frequency	-	
Direction	-	
Maximum displacement	inch (mm)	
Time	s	
Fuel assembly number	-	
Grid number	-	
Maximum Impact force*	lbf (N)	
Time	s	
Fuel assembly number **	-	
Grid number	-	

* Buckling force of the grid spacer is () lbf () N in the FINDS code

** NR refers to Neutron Reflector

Table E.2.1-2(continued) Response Analysis Results in 560-100 Wave Horizontal Direction with BOL Condition

Wave	Units	560-100
Variation of frequency	-	
Direction	-	
Maximum displacement	inch (mm)	
Time	s	
Fuel assembly number	-	
Grid number	-	
Maximum Impact force*	lbf (N)	
Time	s	
Fuel assembly number **	-	
Grid number	-	

* Buckling force of the grid spacer is () lbf () N in the FINDS code

** NR refers to Neutron Reflector

E.2.2 EOL Condition

The maximum responses obtained with BOL conditions are shown in Table E.2.1-1 for 270-200, 270-500, 560-100, 560-200, 560-500, 900-100, 900-200 and 2032-100. From this table, with 560-100 having the maximum displacement of () inch (() mm) in X direction and () inch (() mm) in Z direction, it is the most limiting SSE wave with respect to the maximum displacement of the fuel assembly.

Table E.2.2-2 to Table E.2.2-9 show the buckled grid number distribution respectively for 270-200, 270-500, 560-100, 560-200, 560-500, 900-100, 900-200 and 2032-100 waves. The determination of grid spacer buckling is described in Section D.1.0 of Appendix D of this report. For this evaluation, as described below in E.2.3, CLB 8B 102%LF is chosen as the representative LOCA wave.

Concerning the uncertainty of the SSE acceleration wave, the maximum responses obtained with BOL conditions for 560-100 are shown in Table E.2.1-2. Here, the () frequency of 560-100, having the maximum displacement of () inch (() mm) in X direction and () inch (() mm) in Z direction, is the most limiting case of the SSE wave uncertainty. In addition, it is confirmed that EOL conditions result in a larger maximum displacement compared to the BOL conditions described in Section E.2.1. Therefore the EOL condition is the most limiting.

**Table E.2.2-1 Response Analysis Results in SSE Horizontal Direction
with EOL Condition**

Wave	Units	270-200		270-500	
Direction	-	x	z	x	z
Maximum displacement	inch (mm)				
Time	s				
Fuel assembly number	-				
Grid number	-				
Maximum Impact force*	lbf (N)				
Time	s				
Fuel assembly number **	-				
Grid number	-				

* Buckling force of the grid spacer is () lbf () N) in the FINDS code

** NR refers to Neutron Reflector

Table E.2.2-1(continued) Response Analysis Results in SSE Horizontal Direction with EOL Condition

Wave	Units	560-100		560-200	
Direction	-	x	z	x	z
Maximum displacement	inch (mm)				
Time	s				
Fuel assembly number	-				
Grid number	-				
Maximum Impact force*	lbf (N)				
Time	s				
Fuel assembly number **	-				
Grid number	-				

* Buckling force of the grid spacer is () lbf () N) in the FINDS code

** NR refers to Neutron Reflector

Table E.2.2-1(continued) Response Analysis Results in SSE Horizontal Direction with EOL Condition

Wave	Units	560-500		900-100	
Direction	-	x	z	x	z
Maximum displacement	inch (mm)				
Time	s				
Fuel assembly number	-				
Grid number	-				
Maximum Impact force*	lbf (N)				
Time	s				
Fuel assembly number **	-				
Grid number	-				

* Buckling force of the grid spacer is () lbf () N) in the FINDS code

** NR refers to Neutron Reflector

Table E.2.2-1(continued) Response Analysis Results in SSE Horizontal Direction with EOL Condition

Wave	Units	900-200		2032-100	
Direction	-	x	z	x	z
Maximum displacement	inch (mm)				
Time	s				
Fuel assembly number	-				
Grid number	-				
Maximum Impact force*	lbf (N)				
Time	s				
Fuel assembly number **	-				
Grid number	-				

* Buckling force of the grid spacer is () lbf () N in the FINDS code

** NR refers to Neutron Reflector

Table E.2.2-2 Best estimated buckled grid number distribution for 270-200 wave

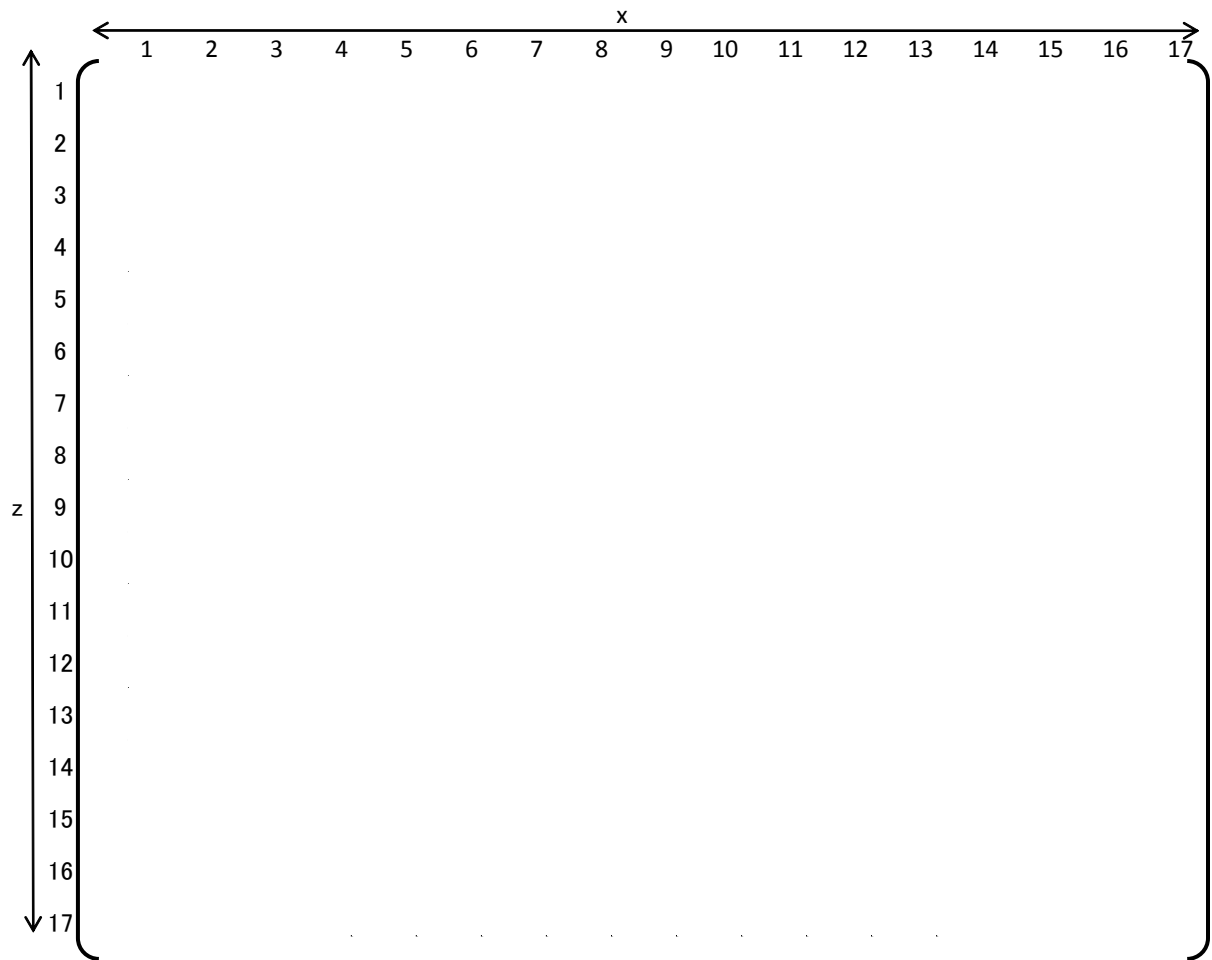


Table E.2.2-3 Best estimated buckled grid number distribution for 270-500 wave

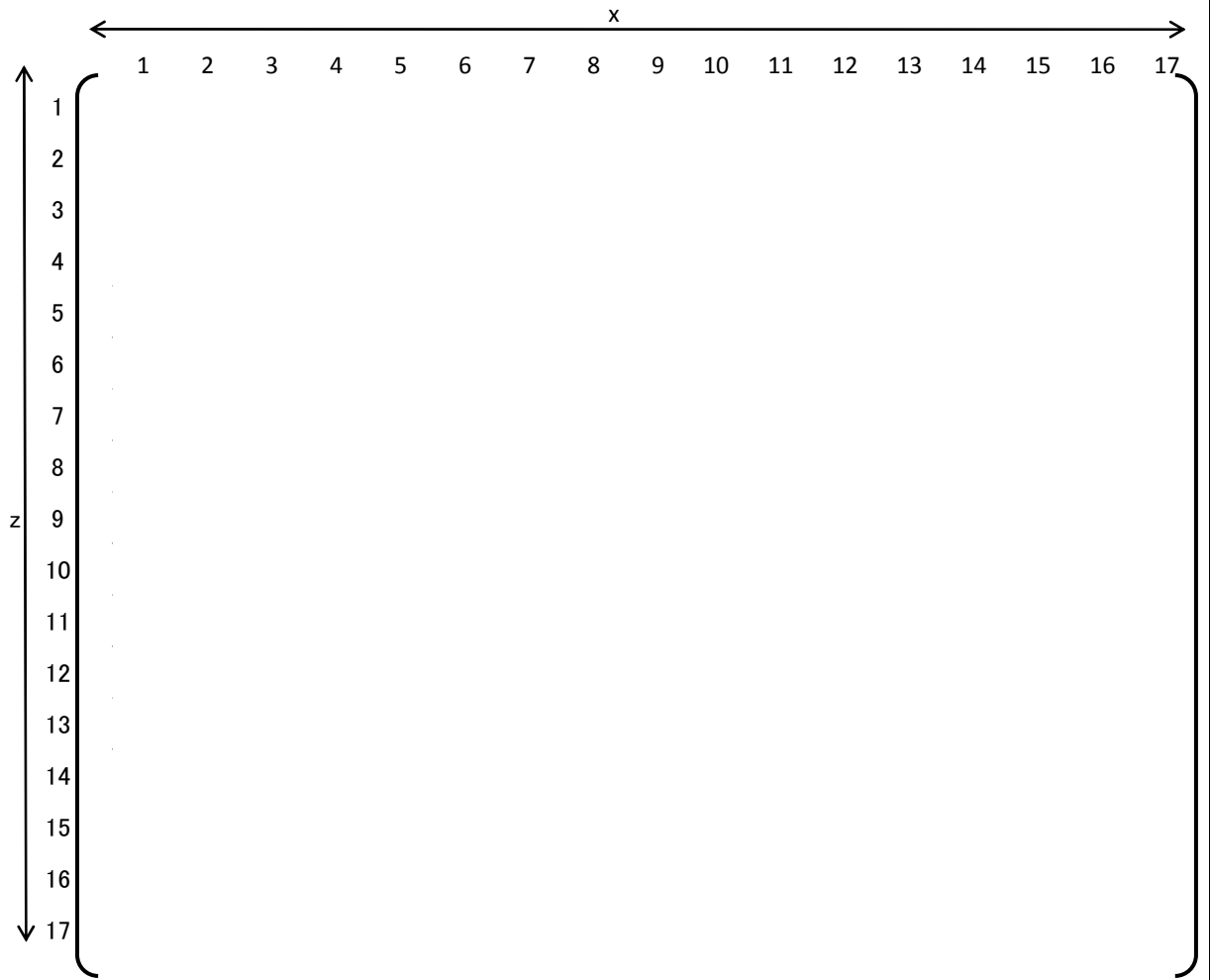


Table E.2.2-4 Best estimated buckled grid number distribution for 560-100 wave

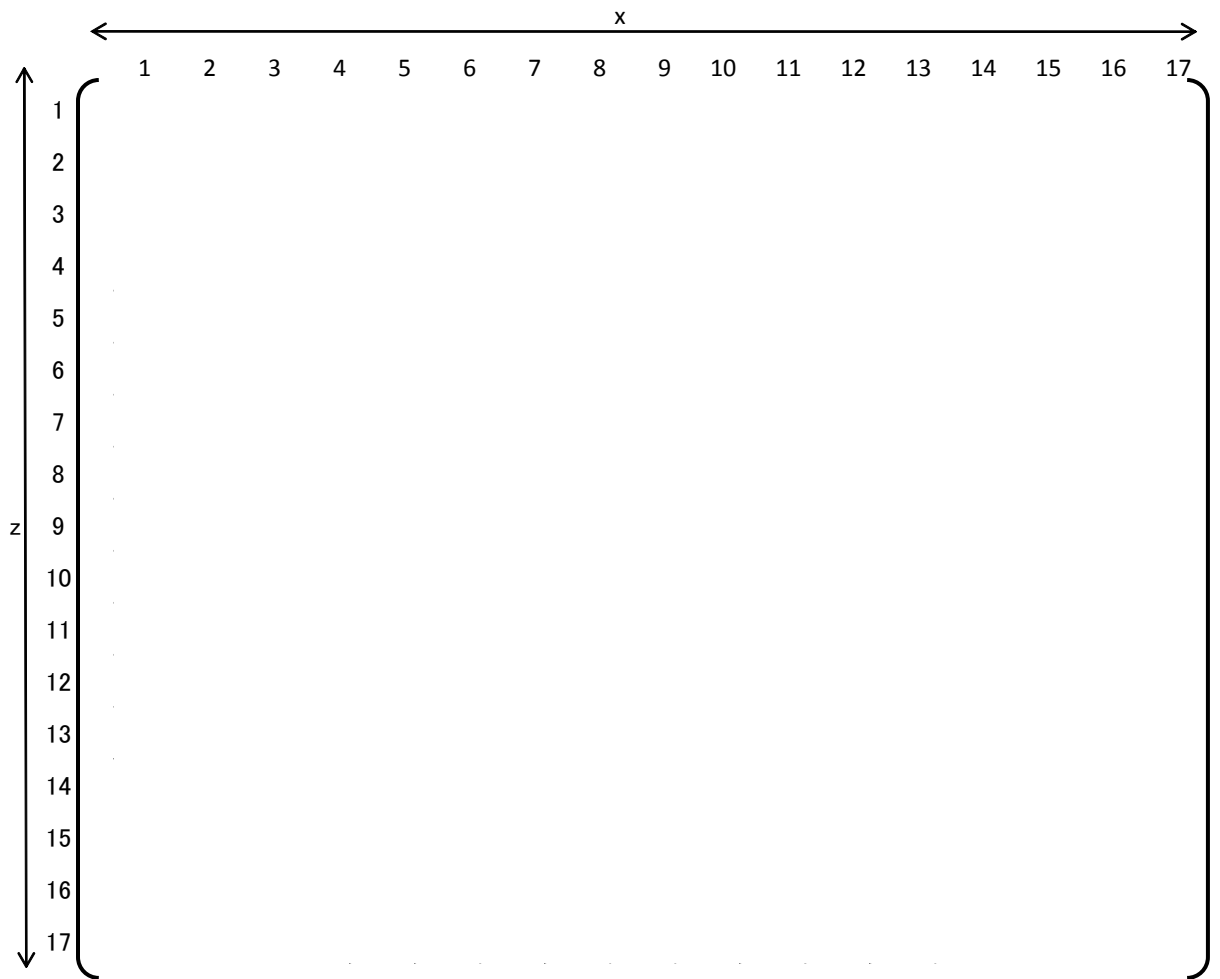


Table E.2.2-5 Best estimated buckled grid number distribution for 560-200 wave

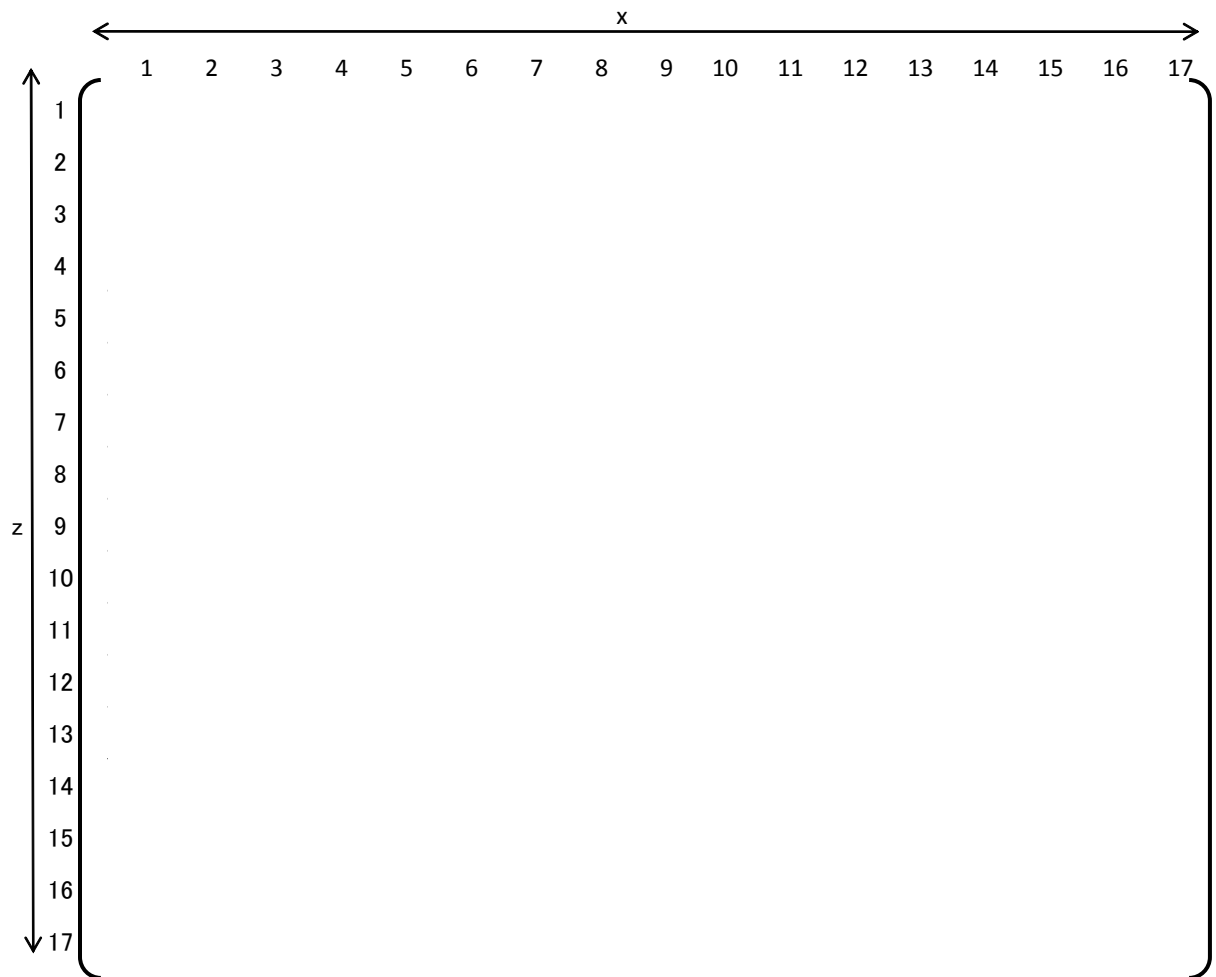


Table E.2.2-6 Best estimated buckled grid number distribution for 560-500 wave

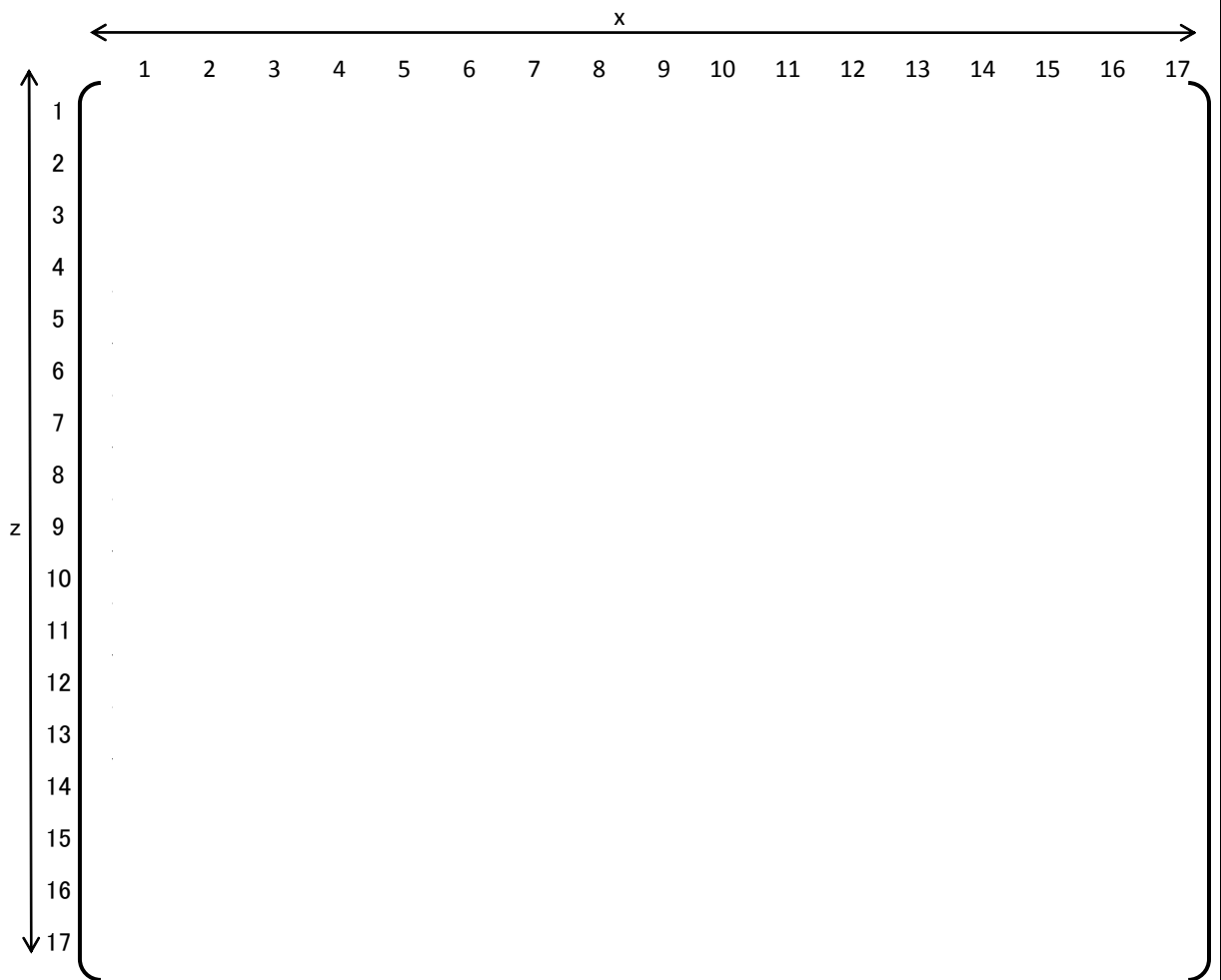


Table E.2.2-7 Best estimated buckled grid number distribution for 900-100 wave

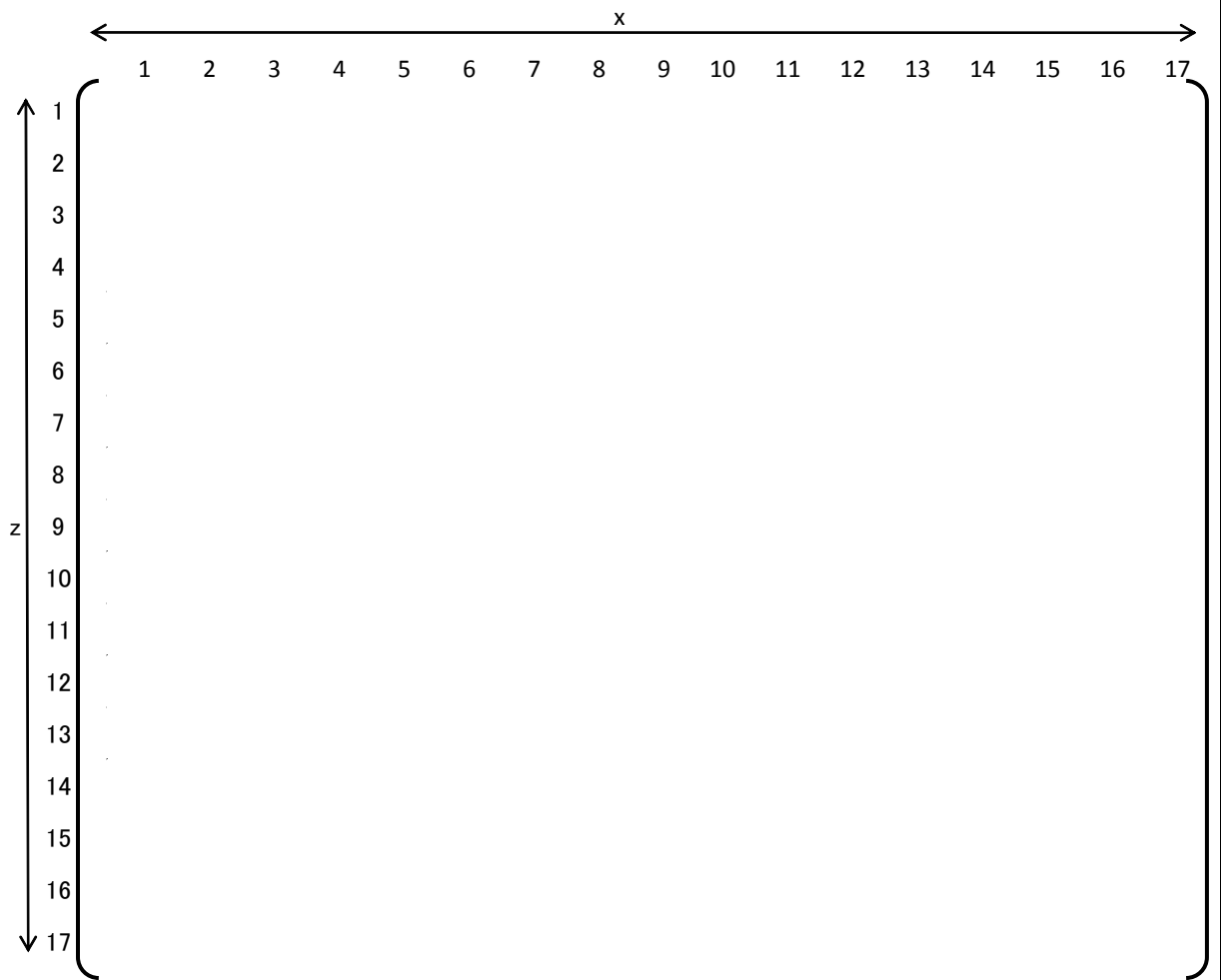


Table E.2.2-8 Best estimated buckled grid number distribution for 900-200 wave

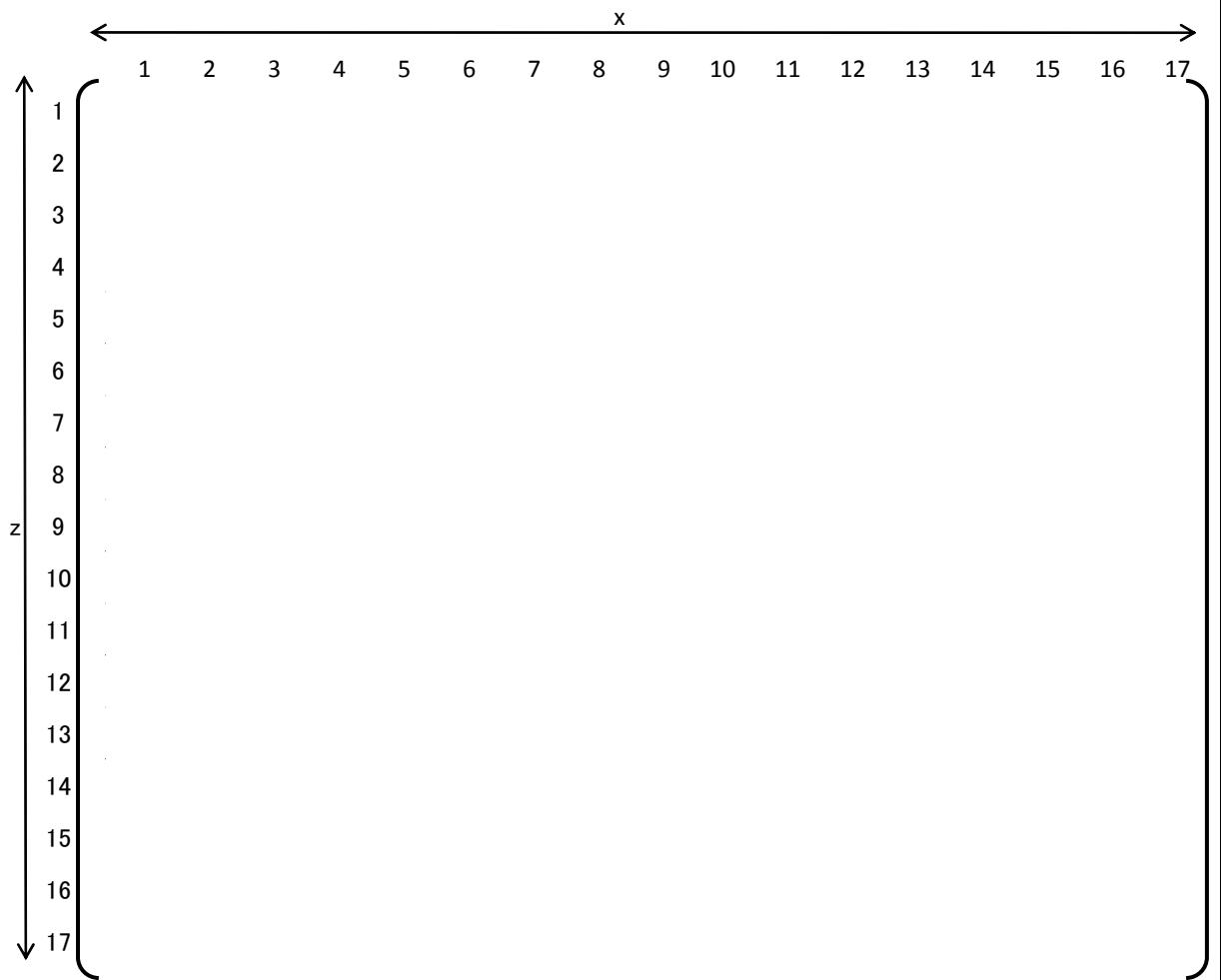
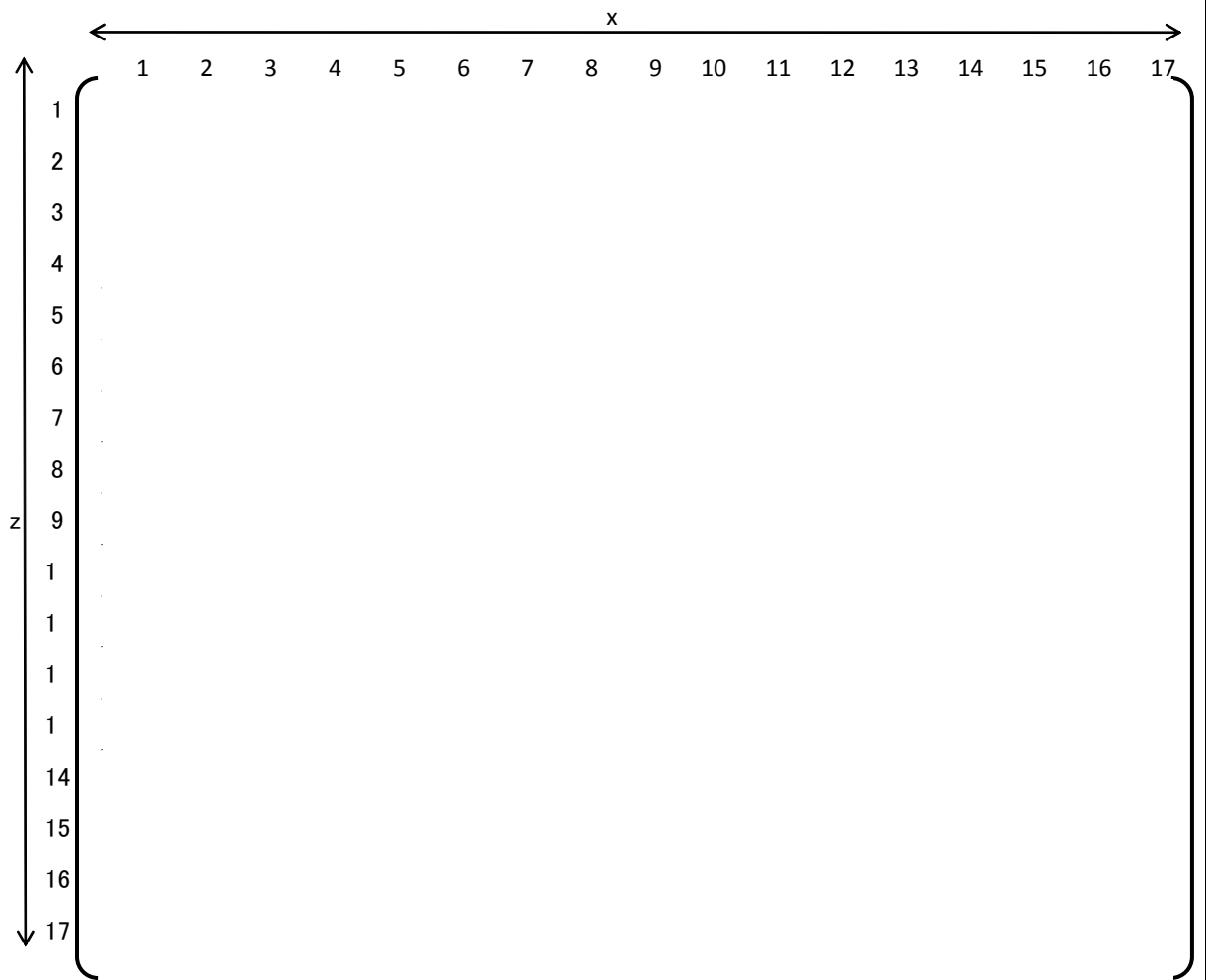


Table E.2.2-9 Best estimated buckled grid number distribution for 2032-100 wave



**Table E.2.2-10 Response Analysis Results in 560-100 Wave Horizontal Direction
with EOL Condition**

Wave	Units	560-100
Variation of frequency	-	
Direction	-	
Maximum displacement	inch (mm)	
Time	s	
Fuel assembly number	-	
Grid number	-	
Maximum Impact force*	lbf (N)	
Time	s	
Fuel assembly number **	-	
Grid number	-	

* Buckling force of the grid spacer is () lbf () N) in the FINDS code
 ** NR refers to Neutron Reflector

Table E.2.2-10(continued) Response Analysis Results in 560-100 Wave Horizontal Direction with EOL Condition

Wave	Units	560-100
Variation of frequency	-	
Direction	-	
Maximum displacement	inch (mm)	
Time	s	
Fuel assembly number	-	
Grid number	-	
Maximum Impact force*	lbf (N)	
Time	s	
Fuel assembly number **	-	
Grid number	-	

* Buckling force of the grid spacer is () lbf () N in the FINDS code
 ** NR refers to Neutron Reflector

Table E.2.2-10(continued) Response Analysis Results in 560-100 Wave Horizontal Direction with EOL Condition

Wave	Units	560-100
Variation of frequency	-	
Direction	-	
Maximum displacement	inch (mm)	
Time	s	
Fuel assembly number	-	
Grid number	-	
Maximum Impact force*	lbf (N)	
Time	s	
Fuel assembly number **	-	
Grid number	-	

* Buckling force of the grid spacer is () lbf () N in the FINDS code
 ** NR refers to Neutron Reflector

E.2.3 Effect of Vibration Characteristics Uncertainty

Since it is confirmed that the combination of Medium 1 and EOL conditions produces the most limiting results from the response analysis of Section E.2.1 and E.2.2, FINDS analyses are performed for () uncertainty cases for the Medium 1 and EOL conditions (all cases in Table E.2.3-1, except for the BE / BE combination) and the difference between the best estimate and each combination of uncertainties is considered to determine the effects of the uncertainty of the amplitude dependence of frequency and damping.

The maximum responses obtained with the combinations of the variation in frequency and damping factor are shown in Table E.2.3-2.

From Table E.2.3.2, the () combination, with the maximum displacement of () inch (() mm) in X direction and () inch (() mm) in Z direction, is the most limiting with respect to fuel assembly maximum displacement.

Table E.2.3-1 Required Cases for Uncertainty Analysis

		Damping	
Frequency			

**Table E.2.3-2 Uncertainty Response Analysis Results
(560-100 Wave)**

Wave	Units	560-100
Combination of Variation	-	
Direction	-	
Maximum displacement	inch (mm)	
Time	s	
Fuel assembly number	-	
Grid number	-	
Maximum Impact force *	lbf (N)	
Time	s	
Fuel assembly number **	-	
Grid number	-	

* Buckling force of the grid spacer is () lbf () N) in the FINDS code

** NR refers to Neutron Reflector

**Table E.2.3-2(continued) Uncertainty Response Analysis Results
(560-100 Wave)**

Wave	Units	560-100
Combination of Variation	-	
Direction	-	
Maximum displacement	inch (mm)	
Time	s	
Fuel assembly number	-	
Grid number	-	
Maximum Impact force *	lbf (N)	
Time	s	
Fuel assembly number **	-	
Grid number	-	

* Buckling force of the grid spacer is () lbf (() N) in the FINDS code

** NR refers to Neutron Reflector

**Table E.2.3-2(continued) Uncertainty Response Analysis Results
(560-100 Wave)**

Wave	Units	560-100
Combination of Variation	-	
Direction	-	
Maximum displacement	inch (mm)	
Time	s	
Fuel assembly number	-	
Grid number	-	
Maximum Impact force *	lbf (N)	
Time	s	
Fuel assembly number **	-	
Grid number	-	

* Buckling force of the grid spacer is () lbf () N) in the FINDS code

** NR refers to Neutron Reflector

E.3.0 CASE STUDY RESULTS FOR THE RESPONSE ANALYSIS FOR LOCA HORIZONTAL DIRECTION

E.3.1 EOL Condition

The response analysis for LOCA event is conducted using EOL conditions, which is confirmed to be the most limiting fuel assembly condition for the SSE, as described in Section E.2.0.

The maximum responses obtained with EOL conditions are shown in Table E.3.1-1 for CLB 8B 102%LF and Table E.3.1-2 for HLB 10B 102%LF.

From these tables, the CLB 8B 102%LF wave, with the maximum displacement of () inch () mm in X direction and () inch () mm in Z direction, is the most limiting LOCA event with respect to fuel assembly maximum displacement.

Table E.3.1-1 Response Analysis Results in LOCA Horizontal Direction

Wave	Units	CLB 8B 102%LF		HLB 10B 102%LF	
Direction	-	x	z	x	z
Maximum displacement	inch (mm)				
Time	s				
Fuel assembly number	-				
Grid number	-				
Maximum Impact force	lbf (N)				
Time	s				
Fuel assembly number *	-				
Grid number	-				

* NR means the Neutron reflector

E.3.2 Effect of Vibration Characteristics Uncertainty

Concerning LOCA event, the { } combination, shown to be the most limiting for the SSE, as described in Section E.2.3, is evaluated only for CLB 8B 102%LF, which was confirmed to be the most limiting as described in Section E.3.1.

The maximum responses obtained with the { } combination of the variation in frequency and damping factor are shown in Table E.3.2-1.

From Table E.3.2-1, the { } combination is shown to result in the maximum displacement of { } inch ({ } mm) in X direction and { } inch ({ } mm) in Z direction, while the nominal case maximum displacement is { } inch ({ } mm) in X direction and { } inch ({ } mm) in Z direction.

**Table E.3.2-1 Uncertainty Response Analysis Results
(CLB 8B 102%LF Wave)**

Wave	Units	CLB 8B 102%LF
Combination of Variation	-	
Direction	-	
Maximum displacement	inch (mm)	
Time	s	
Fuel assembly number	-	
Grid number	-	
Maximum Impact force	lbf (N)	
Time	s	
Fuel assembly number *	-	
Grid number	-	

* NR refers to Neutron Reflector

E.4.0 CONCLUSION

The response analysis result for the following SSE and LOCA events are described in this appendix.

SSE:

- 270-200
- 270-500
- 560-100
- 560-200
- 560-500
- 900-100
- 900-200
- 2032-100

LOCA:

- CLB 8B 102%LF
- HLB 10B 102%LF

As shown in Section E.2.0, the following were confirmed concerning the response analysis for the SSE event.

- 560-100 is the most limiting SSE wave for the fuel assembly.
- () frequency is the most limiting with respect to the SSE wave uncertainty.
- EOL conditions are the most limiting.
- () combination is the most limiting with respect to fuel assembly vibration characteristic's uncertainty.

As shown in Section E.3.0, the following were also confirmed concerning the response analysis for the LOCA event.

- CLB 8B 102%LF is the most limiting LOCA event for the fuel assembly.

Appendix F

WORST CASE RESULTS OF RESPONSE ANALYSIS FOR SEISMIC AND LOCA HORIZONTAL DIRECTION

December 2010

**© 2010 Mitsubishi Heavy Industries, Ltd.
All Rights Reserved**

Table of Contents

List of Tables	F-3
F.1.0 INTRODUCTION	F-8
F.2.0 WORST CASE RESULTS FOR THE SEISMIC HORIZONTAL DIRECTION RESPONSE ANALYSIS	F-9
F.2.1 Response to SSE Event	F-9
F.2.2 Response to SSE Event including the Uncertainty of SSE Wave	F-26
F.2.3 Response to SSE Event including the Uncertainty of Fuel Assembly Vibration	F-43
F.2.4 Response to LOCA Event	F-60
F.2.5 Response to LOCA Event including the Uncertainty of Fuel Assembly Vibration ...	F-77
F.3.0 WORST CASE RESULTS OF GRID SPACER BUCKLING EVALUATION	F-94
F.4.0 WORST CASE RESULTS OF STRESS ANALYSIS FOR SEISMIC AND LOCA HORIZONTAL DIRECTION	F-115
F.5.0 PARAMETRIC STUDY OF FINDS INPUT UNCERTAINTY	F-121
F.5.1 Introduction	F-121
F.5.2 Effect of FINDS input uncertainty	F-121
F.5.2.1 Effect of input acceleration amplitude uncertainty	F-121
F.5.2.2 Effect of frequency uncertainty	F-121
F.5.3 Conclusion	F-121
F.6.0 CONCLUSION	F-124
F.7.0 REFERENCES	F-124

List of Tables

Table F.2.1-1(a)	Maximum Displacement Results for 560-100 with EOL Condition (x direction of 17FA row).....	F-10
Table F.2.1-1(b)	Maximum Displacement Results for 560-100 with EOL Condition (z direction of 17FA row).....	F-11
Table F.2.1-1(c)	Maximum Impact Force Results for 560-100 with EOL Condition (x direction of 17FA row).....	F-12
Table F.2.1-1(d)	Maximum Impact Force Results for 560-100 with EOL Condition (z direction of 17FA row).....	F-13
Table F.2.1-2(a)	Maximum Displacement Results for 560-100 with EOL Condition (x direction of 15FA row).....	F-14
Table F.2.1-2(b)	Maximum Displacement Results for 560-100 with EOL Condition (z direction of 15FA row).....	F-15
Table F.2.1-2(c)	Maximum Impact Force Results for 560-100 with EOL Condition (x direction of 15FA row).....	F-16
Table F.2.1-2(d)	Maximum Impact Force Results for 560-100 with EOL Condition (z direction of 15FA row).....	F-17
Table F.2.1-3(a)	Maximum Displacement Results for 560-100 with EOL Condition (x direction of 13FA row).....	F-18
Table F.2.1-3(b)	Maximum Displacement Results for 560-100 with EOL Condition (z direction of 13FA row).....	F-19
Table F.2.1-3(c)	Maximum Impact Force Results for 560-100 with EOL Condition (x direction of 13FA row).....	F-20
Table F.2.1-3(d)	Maximum Impact Force Results for 560-100 with EOL Condition (z direction of 13FA row).....	F-21
Table F.2.1-4(a)	Maximum Displacement Results for 560-100 with EOL Condition (x direction of 9FA row).....	F-22
Table F.2.1-4(b)	Maximum Displacement Results for 560-100 with EOL Condition (z direction of 9FA row).....	F-23
Table F.2.1-4(c)	Maximum Impact Force Results for 560-100 with EOL Condition (x direction of 9FA row).....	F-24
Table F.2.1-4(d)	Maximum Impact Force Results for 560-100 with EOL Condition (z direction of 9FA row).....	F-25
Table F2.2-1(a)	Maximum Displacement Results for 560-100 including the Uncertainty of SSE Wave (x direction of 17FA row)	F-27
Table F2.2-1(b)	Maximum Displacement Results for 560-100 including the Uncertainty of SSE Wave (z direction of 17FA row)	F-28
Table F2.2-1(c)	Maximum Impact Force Results for 560-100 including the Uncertainty of SSE Wave (x direction of 17FA row)	F-29
Table F2.2-1(d)	Maximum Impact Force Results for 560-100 including the Uncertainty of SSE Wave (z direction of 17FA row)	F-30
Table F2.2-2(a)	Maximum Displacement Results for 560-100 including the Uncertainty of SSE Wave (x direction of 15FA row)	F-31
Table F2.2-2(b)	Maximum Displacement Results for 560-100 including the Uncertainty of SSE Wave (z direction of 15FA row)	F-32
Table F2.2-2(c)	Maximum Impact Force Results for 560-100	

	including the Uncertainty of SSE Wave (x direction of 15FA row)	F-33
Table F2.2-2(d)	Maximum Impact Force Results for 560-100 including the Uncertainty of SSE Wave (z direction of 15FA row)	F-34
Table F2.2-3(a)	Maximum Displacement Results for 560-100 including the Uncertainty of SSE Wave (x direction of 13FA row)	F-35
Table F2.2-3(b)	Maximum Displacement Results for 560-100 including the Uncertainty of SSE Wave (z direction of 13FA row)	F-36
Table F2.2-3(c)	Maximum Impact Force Results for 560-100 including the Uncertainty of SSE Wave (x direction of 13FA row)	F-37
Table F2.2-3(d)	Maximum Impact Force Results for 560-100 including the Uncertainty of SSE Wave (z direction of 13FA row)	F-38
Table F2.2-4(a)	Maximum Displacement Results for 560-100 including the Uncertainty of SSE Wave (x direction of 9FA row)	F-39
Table F2.2-4(b)	Maximum Displacement Results for 560-100 including the Uncertainty of SSE Wave (z direction of 9FA row)	F-40
Table F2.2-4(c)	Maximum Impact Force Results for 560-100 including the Uncertainty of SSE Wave (x direction of 9FA row)	F-41
Table F2.2-4(d)	Maximum Impact Force Results for 560-100 including the Uncertainty of SSE Wave (z direction of 9FA row)	F-42
Table F.2.3-1(a)	Maximum Displacement Results for 560-100 including the Uncertainty of Fuel Assembly Vibration (x direction of 17FA row)	F-44
Table F.2.3-1(b)	Maximum Displacement Results for 560-100 including the Uncertainty of Fuel Assembly Vibration (z direction of 17FA row)	F-45
Table F.2.3-1(c)	Maximum Impact Force Results for 560-100 including the Uncertainty of Fuel Assembly Vibration (x direction of 17FA row)	F-46
Table F.2.3-1(d)	Maximum Impact Force Results for 560-100 including the Uncertainty of Fuel Assembly Vibration (z direction of 17FA row)	F-47
Table F.2.3-2(a)	Maximum Displacement Results for 560-100 including the Uncertainty of Fuel Assembly Vibration (x direction of 15FA row)	F-48
Table F.2.3-2(b)	Maximum Displacement Results for 560-100 including the Uncertainty of Fuel Assembly Vibration (z direction of 15FA row)	F-49
Table F.2.3-2(c)	Maximum Impact Force Results for 560-100 including the Uncertainty of Fuel Assembly Vibration (x direction of 15FA row)	F-50
Table F.2.3-2(d)	Maximum Impact Force Results for 560-100 including the Uncertainty of Fuel Assembly Vibration (z direction of 15FA row)	F-51
Table F.2.3-3(a)	Maximum Displacement Results for 560-100 including the Uncertainty of Fuel Assembly Vibration (x direction of 13FA row)	F-52
Table F.2.3-3(b)	Maximum Displacement Results for 560-100 including the Uncertainty of Fuel Assembly Vibration (z direction of 13FA row)	F-53
Table F.2.3-3(c)	Maximum Impact Force Results for 560-100 including the Uncertainty of Fuel Assembly Vibration (x direction of 13FA row)	F-54
Table F.2.3-3(d)	Maximum Impact Force Results for 560-100 including the Uncertainty of Fuel Assembly Vibration (z direction of 13FA row)	F-55
Table F.2.3-4(a)	Maximum Displacement Results for 560-100 including the Uncertainty of Fuel Assembly Vibration (x direction of 9FA row)	F-56
Table F.2.3-4(b)	Maximum Displacement Results for 560-100 including the Uncertainty of Fuel Assembly Vibration (z direction of 9FA row)	F-57
Table F.2.3-4(c)	Maximum Impact Force Results for 560-100 including the Uncertainty of Fuel Assembly Vibration (x direction of 9FA row)	F-58
Table F.2.3-4(d)	Maximum Impact Force Results for 560-100 including the Uncertainty	

	of Fuel Assembly Vibration (z direction of 9FA row)	F-59
Table F2.4-1(a)	Maximum Displacement Results for CLB 8B 102%LF with EOL Condition (x direction of 17FA row).....	F-61
Table F2.4-1(b)	Maximum Displacement Results for CLB 8B 102%LF with EOL Condition (z direction of 17FA row).....	F-62
Table F2.4-1(c)	Maximum Impact Force Results for CLB 8B 102%LF with EOL Condition (x direction of 17FA row).....	F-63
Table F2.4-1(d)	Maximum Impact Force Results for CLB 8B 102%LF with EOL Condition (z direction of 17FA row).....	F-64
Table F2.4-2(a)	Maximum Displacement Results for CLB 8B 102%LF with EOL Condition (x direction of 15FA row).....	F-65
Table F2.4-2(b)	Maximum Displacement Results for CLB 8B 102%LF with EOL Condition (z direction of 15FA row).....	F-66
Table F2.4-2(c)	Maximum Impact Force Results for CLB 8B 102%LF with EOL Condition (x direction of 15FA row).....	F-67
Table F2.4-2(d)	Maximum Impact Force Results for CLB 8B 102%LF with EOL Condition (z direction of 15FA row).....	F-68
Table F2.4-3(a)	Maximum Displacement Results for CLB 8B 102%LF with EOL Condition (x direction of 13FA row).....	F-69
Table F2.4-3(b)	Maximum Displacement Results for CLB 8B 102%LF with EOL Condition (z direction of 13FA row).....	F-70
Table F2.4-3(c)	Maximum Impact Force Results for CLB 8B 102%LF with EOL Condition (x direction of 13FA row).....	F-71
Table F2.4-3(d)	Maximum Impact Force Results for CLB 8B 102%LF with EOL Condition (z direction of 13FA row).....	F-72
Table F2.4-4(a)	Maximum Displacement Results for CLB 8B 102%LF with EOL Condition (x direction of 9FA row).....	F-73
Table F2.4-4(b)	Maximum Displacement Results for CLB 8B 102%LF with EOL Condition (z direction of 9FA row).....	F-74
Table F2.4-4(c)	Maximum Impact Force Results for CLB 8B 102%LF with EOL Condition (x direction of 9FA row).....	F-75
Table F2.4-4(d)	Maximum Impact Force Results for CLB 8B 102%LF with EOL Condition (z direction of 9FA row).....	F-76
Table F2.5-1(a)	Maximum Displacement Results for CLB 8B 102%LF including the Uncertainty of Fuel Assembly Vibration (x direction of 17FA row)	F-78
Table F2.5-1(b)	Maximum Displacement Results for CLB 8B 102%LF including the Uncertainty of Fuel Assembly Vibration (z direction of 17FA row)	F-79
Table F2.5-1(c)	Maximum Impact Force Results for CLB 8B 102%LF including the Uncertainty of Fuel Assembly Vibration (x direction of 17FA row)	F-80
Table F2.5-1(d)	Maximum Impact Force Results for CLB 8B 102%LF including the Uncertainty of Fuel Assembly Vibration (z direction of 17FA row)	F-81
Table F2.5-2(a)	Maximum Displacement Results for CLB 8B 102%LF including the Uncertainty of Fuel Assembly Vibration (x direction of 15FA row)	F-82
Table F2.5-2(b)	Maximum Displacement Results for CLB 8B 102%LF including the Uncertainty of Fuel Assembly Vibration (z direction of 15FA row)	F-83
Table F2.5-2(c)	Maximum Impact Force Results for CLB 8B 102%LF including the Uncertainty of Fuel Assembly Vibration (x direction of 15FA row)	F-84
Table F2.5-2(d)	Maximum Impact Force Results for CLB 8B 102%LF including the Uncertainty of Fuel Assembly Vibration (z direction of 15FA row)	F-85
Table F2.5-3(a)	Maximum Displacement Results for CLB 8B 102%LF including the	

	Uncertainty of Fuel Assembly Vibration (x direction of 13FA row)	F-86
Table F2.5-3(b)	Maximum Displacement Results for CLB 8B 102%LF including the Uncertainty of Fuel Assembly Vibration (z direction of 13FA row)	F-87
Table F2.5-3(c)	Maximum Impact Force Results for CLB 8B 102%LF including the Uncertainty of Fuel Assembly Vibration (x direction of 13FA row)	F-88
Table F2.5-3(d)	Maximum Impact Force Results for CLB 8B 102%LF including the Uncertainty of Fuel Assembly Vibration (z direction of 13FA row)	F-89
Table F2.5-4(a)	Maximum Displacement Results for CLB 8B 102%LF including the Uncertainty of Fuel Assembly Vibration (x direction of 9FA row)	F-90
Table F2.5-4(b)	Maximum Displacement Results for CLB 8B 102%LF including the Uncertainty of Fuel Assembly Vibration (z direction of 9FA row)	F-91
Table F2.5-4(c)	Maximum Impact Force Results for CLB 8B 102%LF including the Uncertainty of Fuel Assembly Vibration (x direction of 9FA row)	F-92
Table F2.5-4(d)	Maximum Impact Force Results for CLB 8B 102%LF including the Uncertainty of Fuel Assembly Vibration (z direction of 9FA row)	F-93
Table F.3-1	Best Estimated Grid Spacer Buckling Evaluation Result for Grid No.2	F-95
Table F.3-2	Best Estimated Grid Spacer Buckling Evaluation Result for Grid No.3	F-96
Table F.3-3	Best Estimated Grid Spacer Buckling Evaluation Result for Grid No.4	F-97
Table F.3-4	Best Estimated Grid Spacer Buckling Evaluation Result for Grid No.5	F-98
Table F.3-5	Best Estimated Grid Spacer Buckling Evaluation Result for Grid No.6	F-99
Table F.3-6	Best Estimated Grid Spacer Buckling Evaluation Result for Grid No.7	F-100
Table F.3-7	Best Estimated Grid Spacer Buckling Evaluation Result for Grid No.8	F-101
Table F.3-8	Best Estimated Grid Spacer Buckling Evaluation Result for Grid No.9	F-102
Table F.3-9	Best Estimated Grid Spacer Buckling Evaluation Result for Grid No.10	F-103
Table F.3-10	Best Estimated Buckled Grid Spacer Number for Each Fuel Assembly Position	F-104
Table F.3-11	Grid Spacer Buckling Evaluation Result for Grid No.2 including Uncertainties	F-105
Table F.3-12	Grid Spacer Buckling Evaluation Result for Grid No.3 including Uncertainties	F-106
Table F.3-13	Grid Spacer Buckling Evaluation Result for Grid No.4 including Uncertainties	F-107
Table F.3-14	Grid Spacer Buckling Evaluation Result for Grid No.5 including Uncertainties	F-108
Table F.3-15	Grid Spacer Buckling Evaluation Result for Grid No.6 including Uncertainties	F-109
Table F.3-16	Grid Spacer Buckling Evaluation Result for Grid No.7 including Uncertainties	F-110
Table F.3-17	Grid Spacer Buckling Evaluation Result for Grid No.8 including Uncertainties	F-111
Table F.3-18	Grid Spacer Buckling Evaluation Result for Grid No.9	

	including Uncertainties	F-112
Table F.3-19	Grid Spacer Buckling Evaluation Result for Grid No.10 including Uncertainties	F-113
Table F.3-20	Buckled Grid Spacer Number for Each Fuel Assembly Position including Uncertainties	F-114
Table F.4-1	Best Estimated Bending Stress for Seismic and LOCA Horizontal Direction (Control Rod Guide Thimble).....	F-117
Table F.4-2	Best Estimated Bending Stress for Seismic and LOCA Horizontal Direction (Fuel Cladding)	F-118
Table F.4-3	Bending Stress for Seismic and LOCA Horizontal Direction (Control Rod Guide Thimble) including Uncertainties.....	F-119
Table F.4-4	Bending Stress for Seismic and LOCA Horizontal Direction (Fuel Cladding) including Uncertainties	F-120
Table F.5-1	Sensitivity Result for the Input Acceleration Amplitude (SSE 560-100 Wave).....	F-122
Table F.5-2	Sensitivity Result for the Input Acceleration Frequency (SSE 560-100 Wave).....	F-123

F.1.0 INTRODUCTION

The response analysis and stress analysis results due to the horizontal response for each core location due to the following conditions, confirmed to be the most limiting for the fuel assembly as shown in Appendix E of this report, is described in this appendix.

Safe shutdown earthquake (SSE):

- 560-100

LOCA:

- CLB 8B 102%LF

Fuel assembly vibrational characteristic (Most limiting condition)

- EOL condition

SSE wave Uncertainty

- Nominal case and () Frequency case

Fuel assembly vibration Uncertainty

- BE / BE case and () case

In addition, the sensitivity of the input uncertainties is discussed, in compliance with Section II.3 of Appendix A of Reference F-1.

F.2.0 WORST CASE RESULTS FOR THE SEISMIC HORIZONTAL DIRECTION RESPONSE ANALYSIS

F.2.1 Response to SSE Event

The maximum responses obtained for 560-100 with EOL BE/BE condition are shown in Table F.2.1-1 for the 17FA row, Table F.2.1-2 for the 15FA row, Table F.2.1-3 for the 13FA row and Table F.2.1-4 for the 9FA row, respectively.

The results are used in the fuel assembly stress analysis and the grid spacer buckling evaluation.

**Table F.2.1-1(a) Maximum Displacement Results for 560-100 with EOL Condition
(x direction of 17FA row)**

Condition	Units
Fuel Assembly Number	-
Maximum displacement	inch (mm)
Time	s
Grid number	-
Fuel Assembly Number	-
Maximum displacement	inch (mm)
Time	s
Grid number	-
Fuel Assembly Number	-
Maximum displacement	inch (mm)
Time	s
Grid number	-

**Table F.2.1-1(b) Maximum Displacement Results for 560-100 with EOL Condition
(z direction of 17FA row)**

Condition	Units
Fuel Assembly Number	-
Maximum displacement	inch (mm)
Time	s
Grid number	-
Fuel Assembly Number	-
Maximum displacement	inch (mm)
Time	s
Grid number	-
Fuel Assembly Number	-
Maximum displacement	inch (mm)
Time	s
Grid number	-

**Table F.2.1-1(c) Maximum Impact Force Results for 560-100 with EOL Condition
(x direction of 17FA row)**

Condition	Units
Fuel Assembly Number*	-
Maximum Impact force**	lbf (N)
Time	s
Grid number	-
Fuel Assembly Number*	-
Maximum Impact force**	lbf (N)
Time	s
Grid number	-
Fuel Assembly Number*	-
Maximum Impact force**	lbf (N)
Time	s
Grid number	-

* NR refers to Neutron Reflector

** Buckling force of the grid spacer is () lbf (() N) in the FINDS code

**Table F.2.1-1(d) Maximum Impact Force Results for 560-100 with EOL Condition
(z direction of 17FA row)**

Condition	Units
Fuel Assembly Number*	-
Maximum Impact force**	lbf (N)
Time	s
Grid number	-
Fuel Assembly Number*	-
Maximum Impact force**	lbf (N)
Time	s
Grid number	-
Fuel Assembly Number*	-
Maximum Impact force**	lbf (N)
Time	s
Grid number	-

* NR refers to Neutron Reflector

** Buckling force of the grid spacer is () lbf (() N) in the FINDS code

**Table F.2.1-2(a) Maximum Displacement Results for 560-100 with EOL Condition
(x direction of 15FA row)**

Condition	Units
Fuel Assembly Number	-
Maximum displacement	inch (mm)
Time	s
Grid number	-
Fuel Assembly Number	-
Maximum displacement	inch (mm)
Time	s
Grid number	-
Fuel Assembly Number	-
Maximum displacement	inch (mm)
Time	s
Grid number	-

**Table F.2.1-2(b) Maximum Displacement Results for 560-100 with EOL Condition
(z direction of 15FA row)**

Condition	Units
Fuel Assembly Number	-
Maximum displacement	inch (mm)
Time	s
Grid number	-
Fuel Assembly Number	-
Maximum displacement	inch (mm)
Time	s
Grid number	-
Fuel Assembly Number	-
Maximum displacement	inch (mm)
Time	s
Grid number	-

**Table F.2.1-2(c) Maximum Impact Force Results for 560-100 with EOL Condition
(x direction of 15FA row)**

Condition	Units
Fuel Assembly Number*	-
Maximum Impact force**	lbf (N)
Time	s
Grid number	-
Fuel Assembly Number*	-
Maximum Impact force**	lbf (N)
Time	s
Grid number	-
Fuel Assembly Number*	-
Maximum Impact force**	lbf (N)
Time	s
Grid number	-

* NR refers to Neutron Reflector

** Buckling force of the grid spacer is () lbf (() N) in the FINDS code

**Table F.2.1-2(d) Maximum Impact Force Results for 560-100 with EOL Condition
(z direction of 15FA row)**

Condition	Units
Fuel Assembly Number*	-
Maximum Impact force**	lbf (N)
Time	s
Grid number	-
Fuel Assembly Number*	-
Maximum Impact force**	lbf (N)
Time	s
Grid number	-
Fuel Assembly Number*	-
Maximum Impact force**	lbf (N)
Time	s
Grid number	-

* NR refers to Neutron Reflector

** Buckling force of the grid spacer is () lbf (() N) in the FINDS code

**Table F.2.1-3(a) Maximum Displacement Results for 560-100 with EOL Condition
(x direction of 13FA row)**

Condition	Units
Fuel Assembly Number	-
Maximum displacement	inch (mm)
Time	s
Grid number	-
Fuel Assembly Number	-
Maximum displacement	inch (mm)
Time	s
Grid number	-
Fuel Assembly Number	-
Maximum displacement	inch (mm)
Time	s
Grid number	-

**Table F.2.1-3(b) Maximum Displacement Results for 560-100 with EOL Condition
(z direction of 13FA row)**

Condition	Units
Fuel Assembly Number	-
Maximum displacement	inch (mm)
Time	s
Grid number	-
Fuel Assembly Number	-
Maximum displacement	inch (mm)
Time	s
Grid number	-
Fuel Assembly Number	-
Maximum displacement	inch (mm)
Time	s
Grid number	-

**Table F.2.1-3(c) Maximum Impact Force Results for 560-100 with EOL Condition
(x direction of 13FA row)**

Condition	Units
Fuel Assembly Number*	-
Maximum Impact force**	lbf (N)
Time	s
Grid number	-
Fuel Assembly Number*	-
Maximum Impact force**	lbf (N)
Time	s
Grid number	-
Fuel Assembly Number*	-
Maximum Impact force**	lbf (N)
Time	s
Grid number	-

* NR refers to Neutron Reflector

** Buckling force of the grid spacer is () lbf (() N) in the FINDS code

**Table F.2.1-3(d) Maximum Impact Force Results for 560-100 with EOL Condition
(z direction of 13FA row)**

Condition	Units
Fuel Assembly Number*	-
Maximum Impact force**	lbf (N)
Time	s
Grid number	-
Fuel Assembly Number*	-
Maximum Impact force**	lbf (N)
Time	s
Grid number	-
Fuel Assembly Number*	-
Maximum Impact force**	lbf (N)
Time	s
Grid number	-

* NR refers to Neutron Reflector

** Buckling force of the grid spacer is () lbf (() N) in the FINDS code

**Table F.2.1-4(a) Maximum Displacement Results for 560-100 with EOL Condition
(x direction of 9FA row)**

Condition	Units
Fuel Assembly Number	-
Maximum displacement	inch (mm)
Time	s
Grid number	-
Fuel Assembly Number	-
Maximum displacement	inch (mm)
Time	s
Grid number	-

**Table F.2.1-4(b) Maximum Displacement Results for 560-100 with EOL Condition
(z direction of 9FA row)**

Condition	Units
Fuel Assembly Number	-
Maximum displacement	inch (mm)
Time	s
Grid number	-
Fuel Assembly Number	-
Maximum displacement	inch (mm)
Time	s
Grid number	-

**Table F.2.1-4(c) Maximum Impact Force Results for 560-100 with EOL Condition
(x direction of 9FA row)**

Condition	Units
Fuel Assembly Number*	-
Maximum Impact force**	lbf (N)
Time	s
Grid number	-
Fuel Assembly Number*	-
Maximum Impact force**	lbf (N)
Time	s
Grid number	-

* NR refers to Neutron Reflector

** Buckling force of the grid spacer is () lbf (() N) in the FINDS code

**Table F.2.1-4(d) Maximum Impact Force Results for 560-100 with EOL Condition
(z direction of 9FA row)**

Condition	Units
Fuel Assembly Number*	-
Maximum Impact force**	lbf (N)
Time	s
Grid number	-
Fuel Assembly Number*	-
Maximum Impact force**	lbf (N)
Time	s
Grid number	-

* NR refers to Neutron Reflector

** Buckling force of the grid spacer is () lbf (() N) in the FINDS code

F.2.2 Response to SSE Event including the Uncertainty of SSE Wave

The maximum responses obtained with the 560-100() frequency wave and EOL BE/BE condition are shown in Table F.2.2-1 for the 17FA row, Table F.2.2-2 for the 15FA row, Table F.2.2-3 for the 13FA row and Table F.2.2-4 for the 9FA row, respectively, in the same way as described in Section F.2.1.

The results are used in the fuel assembly stress analysis and the grid spacer buckling evaluation.

Table F2.2-1(a) Maximum Displacement Results for 560-100 including the Uncertainty of SSE Wave (x direction of 17FA row)

Condition	Units
Fuel Assembly Number	-
Maximum displacement	inch (mm)
Time	s
Grid number	-
Fuel Assembly Number	-
Maximum displacement	inch (mm)
Time	s
Grid number	-
Fuel Assembly Number	-
Maximum displacement	inch (mm)
Time	s
Grid number	-

Table F2.2-1(b) Maximum Displacement Results for 560-100 including the Uncertainty of SSE Wave (z direction of 17FA row)

Condition	Units
Fuel Assembly Number	-
Maximum displacement	inch (mm)
Time	s
Grid number	-
Fuel Assembly Number	-
Maximum displacement	inch (mm)
Time	s
Grid number	-
Fuel Assembly Number	-
Maximum displacement	inch (mm)
Time	s
Grid number	-

Table F2.2-1(c) Maximum Impact Force Results for 560-100 including the Uncertainty of SSE Wave (x direction of 17FA row)

Condition	Units
Fuel Assembly Number*	-
Maximum Impact force**	lbf (N)
Time	s
Grid number	-
Fuel Assembly Number*	-
Maximum Impact force**	lbf (N)
Time	s
Grid number	-
Fuel Assembly Number*	-
Maximum Impact force**	lbf (N)
Time	s
Grid number	-

* NR refers to Neutron Reflector

** Buckling force of the grid spacer is () lbf (() N) in the FINDS code

Table F2.2-1(d) Maximum Impact Force Results for 560-100 including the Uncertainty of SSE Wave (z direction of 17FA row)

Condition	Units
Fuel Assembly Number*	-
Maximum Impact force**	lbf (N)
Time	s
Grid number	-
Fuel Assembly Number*	-
Maximum Impact force**	lbf (N)
Time	s
Grid number	-
Fuel Assembly Number*	-
Maximum Impact force**	lbf (N)
Time	s
Grid number	-

* NR refers to Neutron Reflector

** Buckling force of the grid spacer is () lbf (() N) in the FINDS code

Table F2.2-2(a) Maximum Displacement Results for 560-100 including the Uncertainty of SSE Wave (x direction of 15FA row)

Condition	Units
Fuel Assembly Number	-
Maximum displacement	inch (mm)
Time	s
Grid number	-
Fuel Assembly Number	-
Maximum displacement	inch (mm)
Time	s
Grid number	-
Fuel Assembly Number	-
Maximum displacement	inch (mm)
Time	s
Grid number	-

Table F2.2-2(b) Maximum Displacement Results for 560-100 including the Uncertainty of SSE Wave (z direction of 15FA row)

Condition	Units
Fuel Assembly Number	-
Maximum displacement	inch (mm)
Time	s
Grid number	-
Fuel Assembly Number	-
Maximum displacement	inch (mm)
Time	s
Grid number	-
Fuel Assembly Number	-
Maximum displacement	inch (mm)
Time	s
Grid number	-

Table F2.2-2(c) Maximum Impact Force Results for 560-100 including the Uncertainty of SSE Wave (x direction of 15FA row)

Condition	Units
Fuel Assembly Number*	-
Maximum Impact force**	lbf (N)
Time	s
Grid number	-
Fuel Assembly Number*	-
Maximum Impact force**	lbf (N)
Time	s
Grid number	-
Fuel Assembly Number*	-
Maximum Impact force**	lbf (N)
Time	s
Grid number	-

* NR refers to Neutron Reflector

** Buckling force of the grid spacer is () lbf (() N) in the FINDS code

Table F2.2-2(d) Maximum Impact Force Results for 560-100 including the Uncertainty of SSE Wave (z direction of 15FA row)

Condition	Units
Fuel Assembly Number*	-
Maximum Impact force**	lbf (N)
Time	s
Grid number	-
Fuel Assembly Number*	-
Maximum Impact force**	lbf (N)
Time	s
Grid number	-
Fuel Assembly Number*	-
Maximum Impact force**	lbf (N)
Time	s
Grid number	-

* NR refers to Neutron Reflector

** Buckling force of the grid spacer is () lbf (() N) in the FINDS code

Table F2.2-3(a) Maximum Displacement Results for 560-100 including the Uncertainty of SSE Wave (x direction of 13FA row)

Condition	Units
Fuel Assembly Number	-
Maximum displacement	inch (mm)
Time	s
Grid number	-
Fuel Assembly Number	-
Maximum displacement	inch (mm)
Time	s
Grid number	-
Fuel Assembly Number	-
Maximum displacement	inch (mm)
Time	s
Grid number	-

Table F2.2-3(b) Maximum Displacement Results for 560-100 including the Uncertainty of SSE Wave (z direction of 13FA row)

Condition	Units
Fuel Assembly Number	-
Maximum displacement	inch (mm)
Time	s
Grid number	-
Fuel Assembly Number	-
Maximum displacement	inch (mm)
Time	s
Grid number	-
Fuel Assembly Number	-
Maximum displacement	inch (mm)
Time	s
Grid number	-

Table F2.2-3(c) Maximum Impact Force Results for 560-100 including the Uncertainty of SSE Wave (x direction of 13FA row)

Condition	Units
Fuel Assembly Number*	-
Maximum Impact force**	lbf (N)
Time	s
Grid number	-
Fuel Assembly Number*	-
Maximum Impact force**	lbf (N)
Time	s
Grid number	-
Fuel Assembly Number*	-
Maximum Impact force**	lbf (N)
Time	s
Grid number	-

* NR refers to Neutron Reflector

** Buckling force of the grid spacer is () lbf (() N) in the FINDS code

Table F2.2-3(d) Maximum Impact Force Results for 560-100 including the Uncertainty of SSE Wave (z direction of 13FA row)

Condition	Units
Fuel Assembly Number*	-
Maximum Impact force**	lbf (N)
Time	s
Grid number	-
Fuel Assembly Number*	-
Maximum Impact force**	lbf (N)
Time	s
Grid number	-
Fuel Assembly Number*	-
Maximum Impact force**	lbf (N)
Time	s
Grid number	-

* NR refers to Neutron Reflector

** Buckling force of the grid spacer is () lbf (() N) in the FINDS code

Table F2.2-4(a) Maximum Displacement Results for 560-100 including the Uncertainty of SSE Wave (x direction of 9FA row)

Condition	Units
Fuel Assembly Number	-
Maximum displacement	inch (mm)
Time	s
Grid number	-
Fuel Assembly Number	-
Maximum displacement	inch (mm)
Time	s
Grid number	-

Table F2.2-4(b) Maximum Displacement Results for 560-100 including the Uncertainty of SSE Wave (z direction of 9FA row)

Condition	Units
Fuel Assembly Number	-
Maximum displacement	inch (mm)
Time	s
Grid number	-
Fuel Assembly Number	-
Maximum displacement	inch (mm)
Time	s
Grid number	-

Table F2.2-4(c) Maximum Impact Force Results for 560-100 including the Uncertainty of SSE Wave (x direction of 9FA row)

Condition	Units
Fuel Assembly Number*	-
Maximum Impact force**	lbf (N)
Time	s
Grid number	-
Fuel Assembly Number*	-
Maximum Impact force**	lbf (N)
Time	s
Grid number	-

* NR refers to Neutron Reflector

** Buckling force of the grid spacer is () lbf (() N) in the FINDS code

Table F2.2-4(d) Maximum Impact Force Results for 560-100 including the Uncertainty of SSE Wave (z direction of 9FA row)

Condition	Units
Fuel Assembly Number*	-
Maximum Impact force**	lbf (N)
Time	s
Grid number	-
Fuel Assembly Number*	-
Maximum Impact force**	lbf (N)
Time	s
Grid number	-

* NR refers to Neutron Reflector

** Buckling force of the grid spacer is () lbf (() N) in the FINDS code

F.2.3 Response to SSE Event including the Uncertainty of Fuel Assembly Vibration

The maximum responses obtained with the 560-100 wave and the EOL () condition are shown in Table F.2.3-1 for the 17FA row, Table F.2.3-2 for the 15FA row, Table F.2.3-3 for the 13FA row and Table F.2.3-4 for the 9FA row, respectively, in the same way as described in Section F.2.1.

The results are used in the fuel assembly stress analysis and the grid spacer buckling evaluation.

Table F.2.3-1(a) Maximum Displacement Results for 560-100 including the Uncertainty of Fuel Assembly Vibration (x direction of 17FA row)

Condition	Units
Fuel Assembly Number	-
Maximum displacement	inch (mm)
Time	s
Grid number	-
Fuel Assembly Number	-
Maximum displacement	inch (mm)
Time	s
Grid number	-
Fuel Assembly Number	-
Maximum displacement	inch (mm)
Time	s
Grid number	-

Table F.2.3-1(b) Maximum Displacement Results for 560-100 including the Uncertainty of Fuel Assembly Vibration (z direction of 17FA row)

Condition	Units
Fuel Assembly Number	-
Maximum displacement	inch (mm)
Time	s
Grid number	-
Fuel Assembly Number	-
Maximum displacement	inch (mm)
Time	s
Grid number	-
Fuel Assembly Number	-
Maximum displacement	inch (mm)
Time	s
Grid number	-

Table F.2.3-1(c) Maximum Impact Force Results for 560-100 including the Uncertainty of Fuel Assembly Vibration (x direction of 17FA row)

Condition	Units
Fuel Assembly Number*	-
Maximum Impact force**	lbf (N)
Time	s
Grid number	-
Fuel Assembly Number*	-
Maximum Impact force**	lbf (N)
Time	s
Grid number	-
Fuel Assembly Number*	-
Maximum Impact force**	lbf (N)
Time	s
Grid number	-

* NR refers to Neutron Reflector

** Buckling force of the grid spacer is () lbf (() N) in the FINDS code

Table F.2.3-1(d) Maximum Impact Force Results for 560-100 including the Uncertainty of Fuel Assembly Vibration (z direction of 17FA row)

Condition	Units
Fuel Assembly Number*	-
Maximum Impact force**	lbf (N)
Time	s
Grid number	-
Fuel Assembly Number*	-
Maximum Impact force**	lbf (N)
Time	s
Grid number	-
Fuel Assembly Number*	-
Maximum Impact force**	lbf (N)
Time	s
Grid number	-

* NR refers to Neutron Reflector

** Buckling force of the grid spacer is () lbf (() N) in the FINDS code

Table F.2.3-2(a) Maximum Displacement Results for 560-100 including the Uncertainty of Fuel Assembly Vibration (x direction of 15FA row)

Condition	Units
Fuel Assembly Number	-
Maximum displacement	inch (mm)
Time	s
Grid number	-
Fuel Assembly Number	-
Maximum displacement	inch (mm)
Time	s
Grid number	-
Fuel Assembly Number	-
Maximum displacement	inch (mm)
Time	s
Grid number	-

Table F.2.3-2(b) Maximum Displacement Results for 560-100 including the Uncertainty of Fuel Assembly Vibration (z direction of 15FA row)

Condition	Units
Fuel Assembly Number	-
Maximum displacement	inch (mm)
Time	s
Grid number	-
Fuel Assembly Number	-
Maximum displacement	inch (mm)
Time	s
Grid number	-
Fuel Assembly Number	-
Maximum displacement	inch (mm)
Time	s
Grid number	-

Table F.2.3-2(c) Maximum Impact Force Results for 560-100 including the Uncertainty of Fuel Assembly Vibration (x direction of 15FA row)

Condition	Units
Fuel Assembly Number*	-
Maximum Impact force**	lbf (N)
Time	s
Grid number	-
Fuel Assembly Number*	-
Maximum Impact force**	lbf (N)
Time	s
Grid number	-
Fuel Assembly Number*	-
Maximum Impact force**	lbf (N)
Time	s
Grid number	-

* NR refers to Neutron Reflector

** Buckling force of the grid spacer is () lbf (() N) in the FINDS code

Table F.2.3-2(d) Maximum Impact Force Results for 560-100 including the Uncertainty of Fuel Assembly Vibration (z direction of 15FA row)

Condition	Units
Fuel Assembly Number*	-
Maximum Impact force**	lbf (N)
Time	s
Grid number	-
Fuel Assembly Number*	-
Maximum Impact force**	lbf (N)
Time	s
Grid number	-
Fuel Assembly Number*	-
Maximum Impact force**	lbf (N)
Time	s
Grid number	-

* NR refers to Neutron Reflector

** Buckling force of the grid spacer is () lbf (() N) in the FINDS code

Table F.2.3-3(a) Maximum Displacement Results for 560-100 including the Uncertainty of Fuel Assembly Vibration (x direction of 13FA row)

Condition	Units
Fuel Assembly Number	-
Maximum displacement	inch (mm)
Time	s
Grid number	-
Fuel Assembly Number	-
Maximum displacement	inch (mm)
Time	s
Grid number	-
Fuel Assembly Number	-
Maximum displacement	inch (mm)
Time	s
Grid number	-

Table F.2.3-3(b) Maximum Displacement Results for 560-100 including the Uncertainty of Fuel Assembly Vibration (z direction of 13FA row)

Condition	Units
Fuel Assembly Number	-
Maximum displacement	inch (mm)
Time	s
Grid number	-
Fuel Assembly Number	-
Maximum displacement	inch (mm)
Time	s
Grid number	-
Fuel Assembly Number	-
Maximum displacement	inch (mm)
Time	s
Grid number	-

Table F.2.3-3(c) Maximum Impact Force Results for 560-100 including the Uncertainty of Fuel Assembly Vibration (x direction of 13FA row)

Condition	Units
Fuel Assembly Number*	-
Maximum Impact force**	lbf (N)
Time	s
Grid number	-
Fuel Assembly Number*	-
Maximum Impact force**	lbf (N)
Time	s
Grid number	-
Fuel Assembly Number*	-
Maximum Impact force**	lbf (N)
Time	s
Grid number	-

* NR refers to Neutron Reflector

** Buckling force of the grid spacer is () lbf (() N) in the FINDS code

Table F.2.3-3(d) Maximum Impact Force Results for 560-100 including the Uncertainty of Fuel Assembly Vibration (z direction of 13FA row)

Condition	Units
Fuel Assembly Number*	-
Maximum Impact force**	lbf (N)
Time	s
Grid number	-
Fuel Assembly Number*	-
Maximum Impact force**	lbf (N)
Time	s
Grid number	-
Fuel Assembly Number*	-
Maximum Impact force**	lbf (N)
Time	s
Grid number	-

* NR refers to Neutron Reflector

** Buckling force of the grid spacer is () lbf (() N) in the FINDS code

Table F.2.3-4(a) Maximum Displacement Results for 560-100 including the Uncertainty of Fuel Assembly Vibration (x direction of 9FA row)

Condition	Units
Fuel Assembly Number	-
Maximum displacement	inch (mm)
Time	s
Grid number	-
Fuel Assembly Number	-
Maximum displacement	inch (mm)
Time	s
Grid number	-

Table F.2.3-4(b) Maximum Displacement Results for 560-100 including the Uncertainty of Fuel Assembly Vibration (z direction of 9FA row)

Condition	Units
Fuel Assembly Number	-
Maximum displacement	inch (mm)
Time	s
Grid number	-
Fuel Assembly Number	-
Maximum displacement	inch (mm)
Time	s
Grid number	-

Table F.2.3-4(c) Maximum Impact Force Results for 560-100 including the Uncertainty of Fuel Assembly Vibration (x direction of 9FA row)

Condition	Units
Fuel Assembly Number*	-
Maximum Impact force**	lbf (N)
Time	s
Grid number	-
Fuel Assembly Number*	-
Maximum Impact force**	lbf (N)
Time	s
Grid number	-

* NR refers to Neutron Reflector

** Buckling force of the grid spacer is () lbf (() N) in the FINDS code

Table F.2.3-4(d) Maximum Impact Force Results for 560-100 including the Uncertainty of Fuel Assembly Vibration (z direction of 9FA row)

Condition	Units
Fuel Assembly Number*	-
Maximum Impact force**	lbf (N)
Time	s
Grid number	-
Fuel Assembly Number*	-
Maximum Impact force**	lbf (N)
Time	s
Grid number	-

* NR refers to Neutron Reflector

** Buckling force of the grid spacer is () lbf (() N) in the FINDS code

F.2.4 Response to LOCA Event

The maximum responses obtained with the CLB 8B 102%LF input and EOL BE/BE condition are shown in Table F.2.4-1 for the 17FA row, Table F.2.4-2 for the 15FA row, Table F.2.4-3 for the 13FA row and Table F.2.4-4 for the 9FA row, respectively, in the same way as described in Section F.2.1.

The results obtained are used in the fuel assembly stress analysis and the grid spacer buckling evaluation.

**Table F2.4-1(a) Maximum Displacement Results for CLB 8B 102%LF with EOL
Condition (x direction of 17FA row)**

Condition	Units
Fuel Assembly Number	-
Maximum displacement	inch (mm)
Time	s
Grid number	-
Fuel Assembly Number	-
Maximum displacement	inch (mm)
Time	s
Grid number	-
Fuel Assembly Number	-
Maximum displacement	inch (mm)
Time	s
Grid number	-

Table F2.4-1(b) Maximum Displacement Results for CLB 8B 102%LF with EOL Condition (z direction of 17FA row)

Condition	Units
Fuel Assembly Number	-
Maximum displacement	inch (mm)
Time	s
Grid number	-
Fuel Assembly Number	-
Maximum displacement	inch (mm)
Time	s
Grid number	-
Fuel Assembly Number	-
Maximum displacement	inch (mm)
Time	s
Grid number	-

**Table F2.4-1(c) Maximum Impact Force Results for CLB 8B 102%LF with EOL Condition
(x direction of 17FA row)**

Condition	Units
Fuel Assembly Number*	-
Maximum Impact force**	lbf (N)
Time	s
Grid number	-
Fuel Assembly Number*	-
Maximum Impact force**	lbf (N)
Time	s
Grid number	-
Fuel Assembly Number*	-
Maximum Impact force**	lbf (N)
Time	s
Grid number	-

* NR refers to Neutron Reflector

** Buckling force of the grid spacer is () lbf (() N) in the FINDS code

**Table F2.4-1(d) Maximum Impact Force Results for CLB 8B 102%LF with EOL Condition
(z direction of 17FA row)**

Condition	Units
Fuel Assembly Number*	-
Maximum Impact force**	lbf (N)
Time	s
Grid number	-
Fuel Assembly Number*	-
Maximum Impact force**	lbf (N)
Time	s
Grid number	-
Fuel Assembly Number*	-
Maximum Impact force**	lbf (N)
Time	s
Grid number	-

* NR refers to Neutron Reflector

** Buckling force of the grid spacer is () lbf (() N) in the FINDS code

**Table F2.4-2(a) Maximum Displacement Results for CLB 8B 102%LF with EOL
Condition (x direction of 15FA row)**

Condition	Units
Fuel Assembly Number	-
Maximum displacement	inch (mm)
Time	s
Grid number	-
Fuel Assembly Number	-
Maximum displacement	inch (mm)
Time	s
Grid number	-
Fuel Assembly Number	-
Maximum displacement	inch (mm)
Time	s
Grid number	-

Table F2.4-2(b) Maximum Displacement Results for CLB 8B 102%LF with EOL Condition (z direction of 15FA row)

Condition	Units
Fuel Assembly Number	-
Maximum displacement	inch (mm)
Time	s
Grid number	-
Fuel Assembly Number	-
Maximum displacement	inch (mm)
Time	s
Grid number	-
Fuel Assembly Number	-
Maximum displacement	inch (mm)
Time	s
Grid number	-

**Table F2.4-2(c) Maximum Impact Force Results for CLB 8B 102%LF with EOL Condition
(x direction of 15FA row)**

Condition	Units
Fuel Assembly Number*	-
Maximum Impact force**	lbf (N)
Time	s
Grid number	-
Fuel Assembly Number*	-
Maximum Impact force**	lbf (N)
Time	s
Grid number	-
Fuel Assembly Number*	-
Maximum Impact force**	lbf (N)
Time	s
Grid number	-

* NR refers to Neutron Reflector

** Buckling force of the grid spacer is () lbf (() N) in the FINDS code

Table F2.4-2(d) Maximum Impact Force Results for CLB 8B 102%LF with EOL Condition
(z direction of 15FA row)

Condition	Units
Fuel Assembly Number*	-
Maximum Impact force**	lbf (N)
Time	s
Grid number	-
Fuel Assembly Number*	-
Maximum Impact force**	lbf (N)
Time	s
Grid number	-
Fuel Assembly Number*	-
Maximum Impact force**	lbf (N)
Time	s
Grid number	-

* NR refers to Neutron Reflector

** Buckling force of the grid spacer is () lbf (() N) in the FINDS code

**Table F2.4-3(a) Maximum Displacement Results for CLB 8B 102%LF with EOL
Condition (x direction of 13FA row)**

Condition	Units
Fuel Assembly Number	-
Maximum displacement	inch (mm)
Time	s
Grid number	-
Fuel Assembly Number	-
Maximum displacement	inch (mm)
Time	s
Grid number	-
Fuel Assembly Number	-
Maximum displacement	inch (mm)
Time	s
Grid number	-

Table F2.4-3(b) Maximum Displacement Results for CLB 8B 102%LF with EOL Condition (z direction of 13FA row)

Condition	Units
Fuel Assembly Number	-
Maximum displacement	inch (mm)
Time	s
Grid number	-
Fuel Assembly Number	-
Maximum displacement	inch (mm)
Time	s
Grid number	-
Fuel Assembly Number	-
Maximum displacement	inch (mm)
Time	s
Grid number	-

**Table F2.4-3(c) Maximum Impact Force Results for CLB 8B 102%LF with EOL Condition
(x direction of 13FA row)**

Condition	Units
Fuel Assembly Number*	-
Maximum Impact force**	lbf (N)
Time	s
Grid number	-
Fuel Assembly Number*	-
Maximum Impact force**	lbf (N)
Time	s
Grid number	-
Fuel Assembly Number*	-
Maximum Impact force**	lbf (N)
Time	s
Grid number	-

* NR refers to Neutron Reflector

** Buckling force of the grid spacer is () lbf (() N) in the FINDS code

Table F2.4-3(d) Maximum Impact Force Results for CLB 8B 102%LF with EOL Condition
(z direction of 13FA row)

Condition	Units
Fuel Assembly Number*	-
Maximum Impact force**	lbf (N)
Time	s
Grid number	-
Fuel Assembly Number*	-
Maximum Impact force**	lbf (N)
Time	s
Grid number	-
Fuel Assembly Number*	-
Maximum Impact force**	lbf (N)
Time	s
Grid number	-

* NR refers to Neutron Reflector

** Buckling force of the grid spacer is () lbf (() N) in the FINDS code

Table F2.4-4(a) Maximum Displacement Results for CLB 8B 102%LF with EOL Condition (x direction of 9FA row)

Condition	Units
Fuel Assembly Number	-
Maximum displacement	inch (mm)
Time	s
Grid number	-
Fuel Assembly Number	-
Maximum displacement	inch (mm)
Time	s
Grid number	-

Table F2.4-4(b) Maximum Displacement Results for CLB 8B 102%LF with EOL Condition (z direction of 9FA row)

Condition	Units
Fuel Assembly Number	-
Maximum displacement	inch (mm)
Time	s
Grid number	-
Fuel Assembly Number	-
Maximum displacement	inch (mm)
Time	s
Grid number	-

**Table F2.4-4(c) Maximum Impact Force Results for CLB 8B 102%LF with EOL Condition
(x direction of 9FA row)**

Condition	Units
Fuel Assembly Number*	-
Maximum Impact force**	lbf (N)
Time	s
Grid number	-
Fuel Assembly Number*	-
Maximum Impact force**	lbf (N)
Time	s
Grid number	-

* NR refers to Neutron Reflector

** Buckling force of the grid spacer is () lbf (() N) in the FINDS code

**Table F2.4-4(d) Maximum Impact Force Results for CLB 8B 102%LF with EOL Condition
(z direction of 9FA row)**

Condition	Units
Fuel Assembly Number*	-
Maximum Impact force**	lbf (N)
Time	s
Grid number	-
Fuel Assembly Number*	-
Maximum Impact force**	lbf (N)
Time	s
Grid number	-

* NR refers to Neutron Reflector

** Buckling force of the grid spacer is () lbf (() N) in the FINDS code

F.2.5 Response to LOCA Event including the Uncertainty of Fuel Assembly Vibration

The maximum responses obtained with the CLB 8B 102%LF input and EOL () condition are shown in Table F.2.5-1 for the 17FA row, Table F.2.5-2 for the 15FA row, Table F.2.5-3 for the 13FA row and Table F.2.5-4 for the 9FA row, respectively, in the same way as described in Section F.2.1.

The results are used in the fuel assembly stress analysis and the grid spacer buckling evaluation.

Table F2.5-1(a) Maximum Displacement Results for CLB 8B 102%LF including the Uncertainty of Fuel Assembly Vibration (x direction of 17FA row)

Condition	Units
Fuel Assembly Number	-
Maximum displacement	inch (mm)
Time	s
Grid number	-
Fuel Assembly Number	-
Maximum displacement	inch (mm)
Time	s
Grid number	-
Fuel Assembly Number	-
Maximum displacement	inch (mm)
Time	s
Grid number	-

Table F2.5-1(b) Maximum Displacement Results for CLB 8B 102%LF including the Uncertainty of Fuel Assembly Vibration (z direction of 17FA row)

Condition	Units
Fuel Assembly Number	-
Maximum displacement	inch (mm)
Time	s
Grid number	-
Fuel Assembly Number	-
Maximum displacement	inch (mm)
Time	s
Grid number	-
Fuel Assembly Number	-
Maximum displacement	inch (mm)
Time	s
Grid number	-

Table F2.5-1(c) Maximum Impact Force Results for CLB 8B 102%LF including the Uncertainty of Fuel Assembly Vibration (x direction of 17FA row)

Condition	Units
Fuel Assembly Number*	-
Maximum Impact force**	lbf (N)
Time	s
Grid number	-
Fuel Assembly Number*	-
Maximum Impact force**	lbf (N)
Time	s
Grid number	-
Fuel Assembly Number*	-
Maximum Impact force**	lbf (N)
Time	s
Grid number	-

* NR refers to Neutron Reflector

** Buckling force of the grid spacer is () lbf (() N) in the FINDS code

Table F2.5-1(d) Maximum Impact Force Results for CLB 8B 102%LF including the Uncertainty of Fuel Assembly Vibration (z direction of 17FA row)

Condition	Units
Fuel Assembly Number*	-
Maximum Impact force**	lbf (N)
Time	s
Grid number	-
Fuel Assembly Number*	-
Maximum Impact force**	lbf (N)
Time	s
Grid number	-
Fuel Assembly Number*	-
Maximum Impact force**	lbf (N)
Time	s
Grid number	-

* NR refers to Neutron Reflector

** Buckling force of the grid spacer is () lbf (() N) in the FINDS code

Table F2.5-2(a) Maximum Displacement Results for CLB 8B 102%LF including the Uncertainty of Fuel Assembly Vibration (x direction of 15FA row)

Condition	Units
Fuel Assembly Number	-
Maximum displacement	inch (mm)
Time	s
Grid number	-
Fuel Assembly Number	-
Maximum displacement	inch (mm)
Time	s
Grid number	-
Fuel Assembly Number	-
Maximum displacement	inch (mm)
Time	s
Grid number	-

Table F2.5-2(b) Maximum Displacement Results for CLB 8B 102%LF including the Uncertainty of Fuel Assembly Vibration (z direction of 15FA row)

Condition	Units
Fuel Assembly Number	-
Maximum displacement	inch (mm)
Time	s
Grid number	-
Fuel Assembly Number	-
Maximum displacement	inch (mm)
Time	s
Grid number	-
Fuel Assembly Number	-
Maximum displacement	inch (mm)
Time	s
Grid number	-

Table F2.5-2(c) Maximum Impact Force Results for CLB 8B 102%LF including the Uncertainty of Fuel Assembly Vibration (x direction of 15FA row)

Condition	Units
Fuel Assembly Number*	-
Maximum Impact force**	lbf (N)
Time	s
Grid number	-
Fuel Assembly Number*	-
Maximum Impact force**	lbf (N)
Time	s
Grid number	-
Fuel Assembly Number*	-
Maximum Impact force**	lbf (N)
Time	s
Grid number	-

* NR refers to Neutron Reflector

** Buckling force of the grid spacer is () lbf (() N) in the FINDS code

Table F2.5-2(d) Maximum Impact Force Results for CLB 8B 102%LF including the Uncertainty of Fuel Assembly Vibration (z direction of 15FA row)

Condition	Units
Fuel Assembly Number*	-
Maximum Impact force**	lbf (N)
Time	s
Grid number	-
Fuel Assembly Number*	-
Maximum Impact force**	lbf (N)
Time	s
Grid number	-
Fuel Assembly Number*	-
Maximum Impact force**	lbf (N)
Time	s
Grid number	-

* NR refers to Neutron Reflector

** Buckling force of the grid spacer is () lbf (() N) in the FINDS code

Table F2.5-3(a) Maximum Displacement Results for CLB 8B 102%LF including the Uncertainty of Fuel Assembly Vibration (x direction of 13FA row)

Condition	Units
Fuel Assembly Number	-
Maximum displacement	inch (mm)
Time	s
Grid number	-
Fuel Assembly Number	-
Maximum displacement	inch (mm)
Time	s
Grid number	-
Fuel Assembly Number	-
Maximum displacement	inch (mm)
Time	s
Grid number	-

Table F2.5-3(b) Maximum Displacement Results for CLB 8B 102%LF including the Uncertainty of Fuel Assembly Vibration (z direction of 13FA row)

Condition	Units
Fuel Assembly Number	-
Maximum displacement	inch (mm)
Time	s
Grid number	-
Fuel Assembly Number	-
Maximum displacement	inch (mm)
Time	s
Grid number	-
Fuel Assembly Number	-
Maximum displacement	inch (mm)
Time	s
Grid number	-

Table F2.5-3(c) Maximum Impact Force Results for CLB 8B 102%LF including the Uncertainty of Fuel Assembly Vibration (x direction of 13FA row)

Condition	Units
Fuel Assembly Number*	-
Maximum Impact force**	lbf (N)
Time	s
Grid number	-
Fuel Assembly Number*	-
Maximum Impact force**	lbf (N)
Time	s
Grid number	-
Fuel Assembly Number*	-
Maximum Impact force**	lbf (N)
Time	s
Grid number	-

* NR refers to Neutron Reflector

** Buckling force of the grid spacer is () lbf (() N) in the FINDS code

Table F2.5-3(d) Maximum Impact Force Results for CLB 8B 102%LF including the Uncertainty of Fuel Assembly Vibration (z direction of 13FA row)

Condition	Units
Fuel Assembly Number*	-
Maximum Impact force**	lbf (N)
Time	s
Grid number	-
Fuel Assembly Number*	-
Maximum Impact force**	lbf (N)
Time	s
Grid number	-
Fuel Assembly Number*	-
Maximum Impact force**	lbf (N)
Time	s
Grid number	-

* NR refers to Neutron Reflector

** Buckling force of the grid spacer is () lbf (() N) in the FINDS code

Table F2.5-4(a) Maximum Displacement Results for CLB 8B 102%LF including the Uncertainty of Fuel Assembly Vibration (x direction of 9FA row)

Condition	Units
Fuel Assembly Number	-
Maximum displacement	inch (mm)
Time	s
Grid number	-
Fuel Assembly Number	-
Maximum displacement	inch (mm)
Time	s
Grid number	-

Table F2.5-4(b) Maximum Displacement Results for CLB 8B 102%LF including the Uncertainty of Fuel Assembly Vibration (z direction of 9FA row)

Condition	Units
Fuel Assembly Number	-
Maximum displacement	inch (mm)
Time	s
Grid number	-
Fuel Assembly Number	-
Maximum displacement	inch (mm)
Time	s
Grid number	-

Table F2.5-4(c) Maximum Impact Force Results for CLB 8B 102%LF including the Uncertainty of Fuel Assembly Vibration (x direction of 9FA row)

Condition	Units
Fuel Assembly Number*	-
Maximum Impact force**	lbf (N)
Time	s
Grid number	-
Fuel Assembly Number*	-
Maximum Impact force**	lbf (N)
Time	s
Grid number	-

* NR refers to Neutron Reflector

** Buckling force of the grid spacer is () lbf (() N) in the FINDS code

Table F2.5-4(d) Maximum Impact Force Results for CLB 8B 102%LF including the Uncertainty of Fuel Assembly Vibration (z direction of 9FA row)

Condition	Units
Fuel Assembly Number*	-
Maximum Impact force**	lbf (N)
Time	s
Grid number	-
Fuel Assembly Number*	-
Maximum Impact force**	lbf (N)
Time	s
Grid number	-

* NR refers to Neutron Reflector

** Buckling force of the grid spacer is () lbf (() N) in the FINDS code

F.3.0 WORST CASE RESULTS OF GRID SPACER BUCKLING EVALUATION

From the results obtained in Section F.2.0, the grid spacer buckling evaluation is conducted, which is used to determine the RCCA insertability and reactor coolability (PCT).

The determination of grid spacer buckling is described in Section D.1.0 of Appendix D of this report.

The impact force results include the uncertainty effects as defined by the following equation. It is also applied to the z direction.

The results for grid spacers No.2 to No.10 without considering uncertainties are shown in Table F.3-1 to F.3-9, respectively. It is noted that corrosion does not occur at grid spacer No.1 and No.11. The number of buckled grid spacers in each fuel assembly without uncertainties, based on the impact force greater than () N is shown in Table F.3-10.

The results for grid spacers No.2 to No.10 with uncertainties are shown in Table F.3-11 to F.3-19, respectively. It is noted that corrosion does not occur at grid spacer No.1 and No.11. The number of buckled grid spacers in each fuel assembly with uncertainties, based on the impact force greater than () N is shown in Table F.3-20.

The results with uncertainties are used in the RCCA insertability and reactor coolability (PCT) evaluation conservatively.

Table F.3-1 Best Estimated Grid Spacer Buckling Evaluation Result for Grid No.2

(Unit: N)																	
	X-1	X-2	X-3	X-4	X-5	X-6	X-7	X-8	X-9	X-10	X-11	X-12	X-13	X-14	X-15	X-16	X-17
Z-1																	
Z-2																	
Z-3																	
Z-4																	
Z-5																	
Z-6																	
Z-7																	
Z-8																	
Z-9																	
Z-10																	
Z-11																	
Z-12																	
Z-13																	
Z-14																	
Z-15																	
Z-16																	
Z-17																	

Table F.3-2 Best Estimated Grid Spacer Buckling Evaluation Result for Grid No.3

(Unit: N)		X-1	X-2	X-3	X-4	X-5	X-6	X-7	X-8	X-9	X-10	X-11	X-12	X-13	X-14	X-15	X-16	X-17
Z-1																		
Z-2																		
Z-3																		
Z-4																		
Z-5																		
Z-6																		
Z-7																		
Z-8																		
Z-9																		
Z-10																		
Z-11																		
Z-12																		
Z-13																		
Z-14																		
Z-15																		
Z-16																		
Z-17																		

Table F.3-3 Best Estimated Grid Spacer Buckling Evaluation Result for Grid No.4

(Unit: N)	
X-1	X-17
X-2	X-16
X-3	X-15
X-4	X-14
X-5	X-13
X-6	X-12
X-7	X-11
X-8	X-10
X-9	X-9
X-10	X-8
X-11	X-7
X-12	X-6
X-13	X-5
X-14	X-4
X-15	X-3
X-16	X-2
X-17	X-1

Z-1
Z-2
Z-3
Z-4
Z-5
Z-6
Z-7
Z-8
Z-9
Z-10
Z-11
Z-12
Z-13
Z-14
Z-15
Z-16
Z-17

Table F.3-4 Best Estimated Grid Spacer Buckling Evaluation Result for Grid No.5

(Unit: N)		X-1	X-2	X-3	X-4	X-5	X-6	X-7	X-8	X-9	X-10	X-11	X-12	X-13	X-14	X-15	X-16	X-17
Z-1																		
Z-2																		
Z-3																		
Z-4																		
Z-5																		
Z-6																		
Z-7																		
Z-8																		
Z-9																		
Z-10																		
Z-11																		
Z-12																		
Z-13																		
Z-14																		
Z-15																		
Z-16																		
Z-17																		

Table F.3-5 Best Estimated Grid Spacer Buckling Evaluation Result for Grid No.6

(Unit: N)	
X-1	X-17
X-2	X-16
X-3	X-15
X-4	X-14
X-5	X-13
X-6	X-12
X-7	X-11
X-8	X-10
X-9	X-9
X-10	X-8
X-11	X-7
X-12	X-6
X-13	X-5
X-14	X-4
X-15	X-3
X-16	X-2
X-17	X-1

Table F.3-6 Best Estimated Grid Spacer Buckling Evaluation Result for Grid No.7

(Unit: N)		X-1	X-2	X-3	X-4	X-5	X-6	X-7	X-8	X-9	X-10	X-11	X-12	X-13	X-14	X-15	X-16	X-17
Z-1																		
Z-2																		
Z-3																		
Z-4																		
Z-5																		
Z-6																		
Z-7																		
Z-8																		
Z-9																		
Z-10																		
Z-11																		
Z-12																		
Z-13																		
Z-14																		
Z-15																		
Z-16																		
Z-17																		

Table F.3-7 Best Estimated Grid Spacer Buckling Evaluation Result for Grid No.8

(Unit: N)		X-1	X-2	X-3	X-4	X-5	X-6	X-7	X-8	X-9	X-10	X-11	X-12	X-13	X-14	X-15	X-16	X-17
Z-1																		
Z-2																		
Z-3																		
Z-4																		
Z-5																		
Z-6																		
Z-7																		
Z-8																		
Z-9																		
Z-10																		
Z-11																		
Z-12																		
Z-13																		
Z-14																		
Z-15																		
Z-16																		
Z-17																		

Table F.3-8 Best Estimated Grid Spacer Buckling Evaluation Result for Grid No.9

(Unit: N)	
X-1	X-17
X-2	X-16
X-3	X-15
X-4	X-14
X-5	X-13
X-6	X-12
X-7	X-11
X-8	X-10
X-9	X-9
X-10	X-8
X-11	X-7
X-12	X-6
X-13	X-5
X-14	X-4
X-15	X-3
X-16	X-2
X-17	X-1

Z-1
Z-2
Z-3
Z-4
Z-5
Z-6
Z-7
Z-8
Z-9
Z-10
Z-11
Z-12
Z-13
Z-14
Z-15
Z-16
Z-17

Table F.3-9 Best Estimated Grid Spacer Buckling Evaluation Result for Grid No.10

(Unit: N)	
X-1	X-17
X-2	X-16
X-3	X-15
X-4	X-14
X-5	X-13
X-6	X-12
X-7	X-11
X-8	X-10
X-9	X-9
X-10	X-8
X-11	X-7
X-12	X-6
X-13	X-5
X-14	X-4
X-15	X-3
X-16	X-2
X-17	X-1

Z-1
Z-2
Z-3
Z-4
Z-5
Z-6
Z-7
Z-8
Z-9
Z-10
Z-11
Z-12
Z-13
Z-14
Z-15
Z-16
Z-17

Table F.3-10 Best Estimated Buckled Grid Spacer Number for Each Fuel Assembly Position

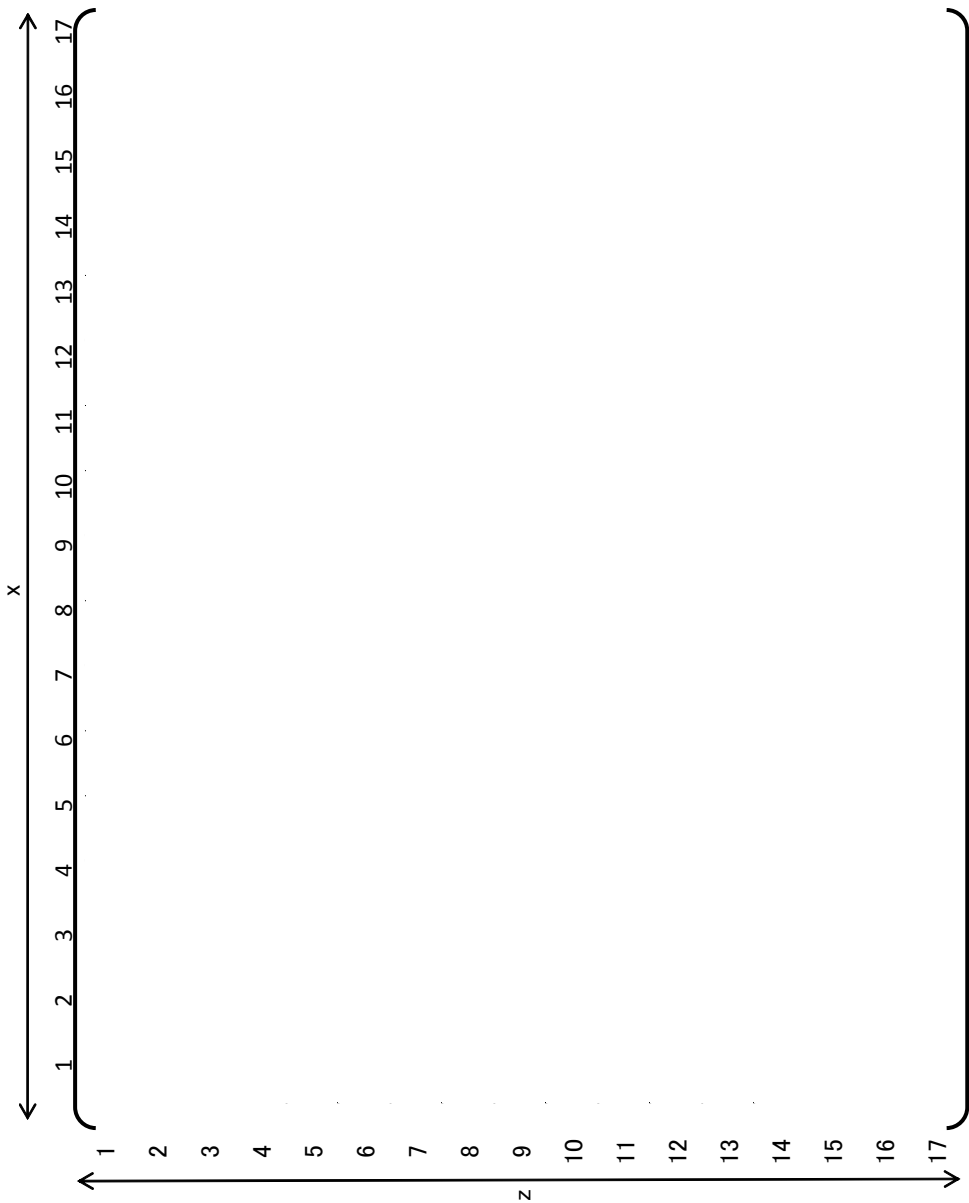


Table F.3-11 Grid Spacer Buckling Evaluation Result for Grid No.2 including Uncertainties

(Unit: N)		X-1	X-2	X-3	X-4	X-5	X-6	X-7	X-8	X-9	X-10	X-11	X-12	X-13	X-14	X-15	X-16	X-17
Z-1																		
Z-2																		
Z-3																		
Z-4																		
Z-5																		
Z-6																		
Z-7																		
Z-8																		
Z-9																		
Z-10																		
Z-11																		
Z-12																		
Z-13																		
Z-14																		
Z-15																		
Z-16																		
Z-17																		

Table F.3-12 Grid Spacer Buckling Evaluation Result for Grid No.3 including Uncertainties

(Unit: N)		X-1	X-2	X-3	X-4	X-5	X-6	X-7	X-8	X-9	X-10	X-11	X-12	X-13	X-14	X-15	X-16	X-17
Z-1																		
Z-2																		
Z-3																		
Z-4																		
Z-5																		
Z-6																		
Z-7																		
Z-8																		
Z-9																		
Z-10																		
Z-11																		
Z-12																		
Z-13																		
Z-14																		
Z-15																		
Z-16																		
Z-17																		

Table F.3-13 Grid Spacer Buckling Evaluation Result for Grid No.4 including Uncertainties

(Unit: N)		X-1	X-2	X-3	X-4	X-5	X-6	X-7	X-8	X-9	X-10	X-11	X-12	X-13	X-14	X-15	X-16	X-17
Z-1																		
Z-2																		
Z-3																		
Z-4																		
Z-5																		
Z-6																		
Z-7																		
Z-8																		
Z-9																		
Z-10																		
Z-11																		
Z-12																		
Z-13																		
Z-14																		
Z-15																		
Z-16																		
Z-17																		

Table F.3-14 Grid Spacer Buckling Evaluation Result for Grid No.5 including Uncertainties

(Unit: N)		X-1	X-2	X-3	X-4	X-5	X-6	X-7	X-8	X-9	X-10	X-11	X-12	X-13	X-14	X-15	X-16	X-17
Z-1																		
Z-2																		
Z-3																		
Z-4																		
Z-5																		
Z-6																		
Z-7																		
Z-8																		
Z-9																		
Z-10																		
Z-11																		
Z-12																		
Z-13																		
Z-14																		
Z-15																		
Z-16																		
Z-17																		

Table F.3-15 Grid Spacer Buckling Evaluation Result for Grid No.6 including Uncertainties

(Unit: N)																	
	X-1	X-2	X-3	X-4	X-5	X-6	X-7	X-8	X-9	X-10	X-11	X-12	X-13	X-14	X-15	X-16	X-17
Z-1																	
Z-2																	
Z-3																	
Z-4																	
Z-5																	
Z-6																	
Z-7																	
Z-8																	
Z-9																	
Z-10																	
Z-11																	
Z-12																	
Z-13																	
Z-14																	
Z-15																	
Z-16																	
Z-17																	

Table F.3-16 Grid Spacer Buckling Evaluation Result for Grid No.7 including Uncertainties

	X-1	X-2	X-3	X-4	X-5	X-6	X-7	X-8	X-9	X-10	X-11	X-12	X-13	X-14	X-15	X-16	X-17	(Unit: N)
Z-1																		
Z-2																		
Z-3																		
Z-4																		
Z-5																		
Z-6																		
Z-7																		
Z-8																		
Z-9																		
Z-10																		
Z-11																		
Z-12																		
Z-13																		
Z-14																		
Z-15																		
Z-16																		
Z-17																		

Table F.3-17 Grid Spacer Buckling Evaluation Result for Grid No.8 including Uncertainties

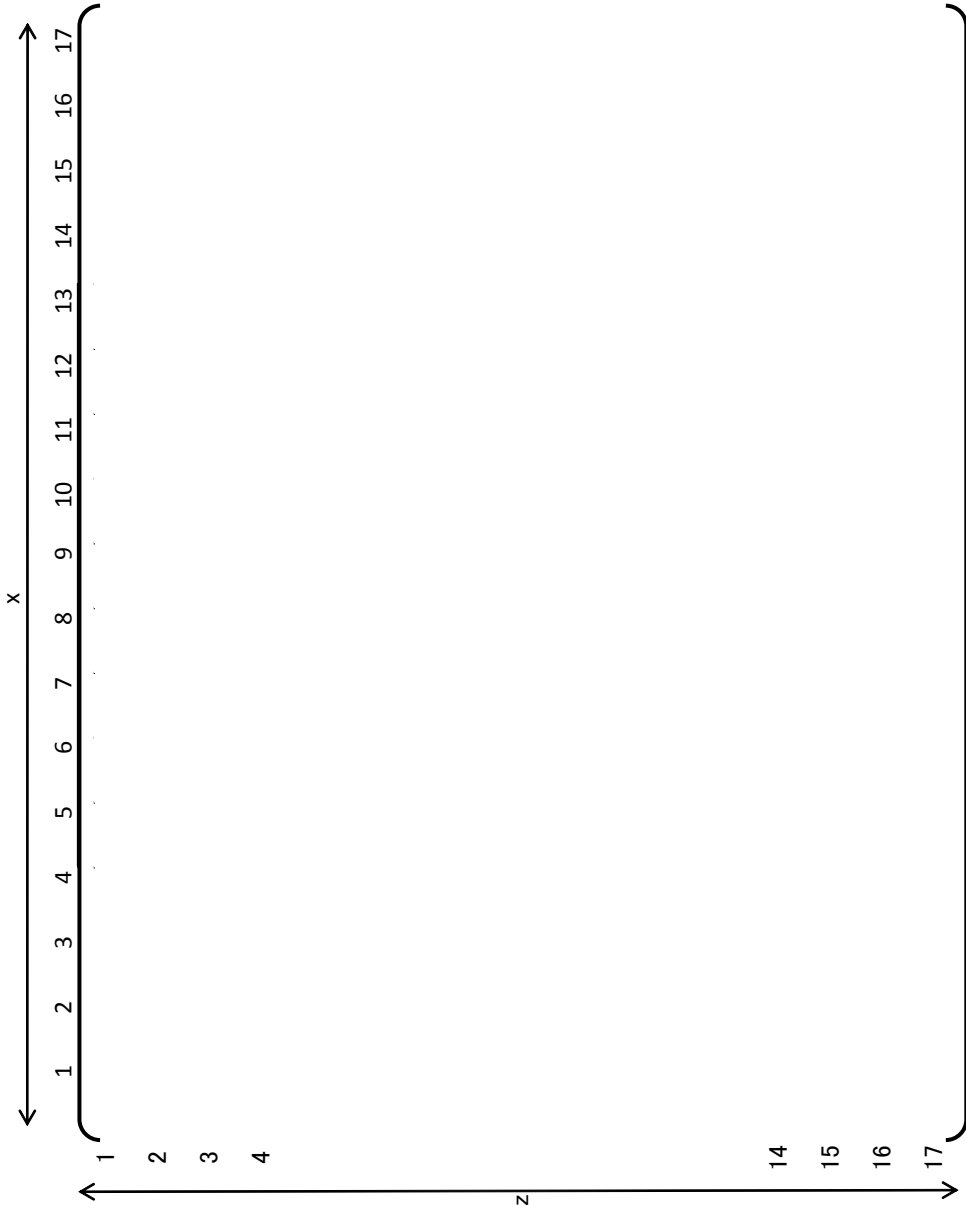
(Unit: N)																	
	X-1	X-2	X-3	X-4	X-5	X-6	X-7	X-8	X-9	X-10	X-11	X-12	X-13	X-14	X-15	X-16	X-17
Z-1																	
Z-2																	
Z-3																	
Z-4																	
Z-5																	
Z-6																	
Z-7																	
Z-8																	
Z-9																	
Z-10																	
Z-11																	
Z-12																	
Z-13																	
Z-14																	
Z-15																	
Z-16																	
Z-17																	

Table F.3-18 Grid Spacer Buckling Evaluation Result for Grid No.9 including Uncertainties

	X-1	X-2	X-3	X-4	X-5	X-6	X-7	X-8	X-9	X-10	X-11	X-12	X-13	X-14	X-15	X-16	X-17	(Unit: N)
Z-1																		
Z-2																		
Z-3																		
Z-4																		
Z-5																		
Z-6																		
Z-7																		
Z-8																		
Z-9																		
Z-10																		
Z-11																		
Z-12																		
Z-13																		
Z-14																		
Z-15																		
Z-16																		
Z-17																		

Table F.3-19 Grid Spacer Buckling Evaluation Result for Grid No.10 including Uncertainties																	(Unit: N)
	X-1	X-2	X-3	X-4	X-5	X-6	X-7	X-8	X-9	X-10	X-11	X-12	X-13	X-14	X-15	X-16	X-17
Z-1																	
Z-2																	
Z-3																	
Z-4																	
Z-5																	
Z-6																	
Z-7																	
Z-8																	
Z-9																	
Z-10																	
Z-11																	
Z-12																	
Z-13																	
Z-14																	
Z-15																	
Z-16																	
Z-17																	

Table F.3-20 Buckled Grid Spacer Number for Each Fuel Assembly Position including Uncertainties



F.4.0 WORST CASE RESULTS OF STRESS ANALYSIS FOR SEISMIC AND LOCA HORIZONTAL DIRECTION

From the results obtained in Section F.2.0, the stress evaluation is conducted. The stress without uncertainties is calculated by the following equation.

$$\sigma = \frac{F}{A} \quad (F.4.1)$$

The stress results include the uncertainty effect defined by the following equation. It is also applied to the z direction.

$$\sigma = \frac{F}{A} \times \left(1 + \frac{\sigma_{\text{unc}}}{\sigma} \right) \quad (F.4.2)$$

The maximum bending stress of the control rod guide thimble and fuel cladding without uncertainties at each core location is shown in Table F.4-1 and Table F.4.-2, respectively. As shown in both tables, {

The maximum bending stress of the control rod guide thimble and fuel cladding with uncertainties at each core location is shown in Table F.4-3 and Table F.4.-4, respectively. As shown in both tables, {

The stress obtained is used in the stress evaluation by being combined with the stress due to the vertical response and the stress due to normal operation.

Table F.4-1 Best Estimated Bending Stress for Seismic and LOCA Horizontal Direction
(Control Rod Guide Thimble)

(Unit: MPa)

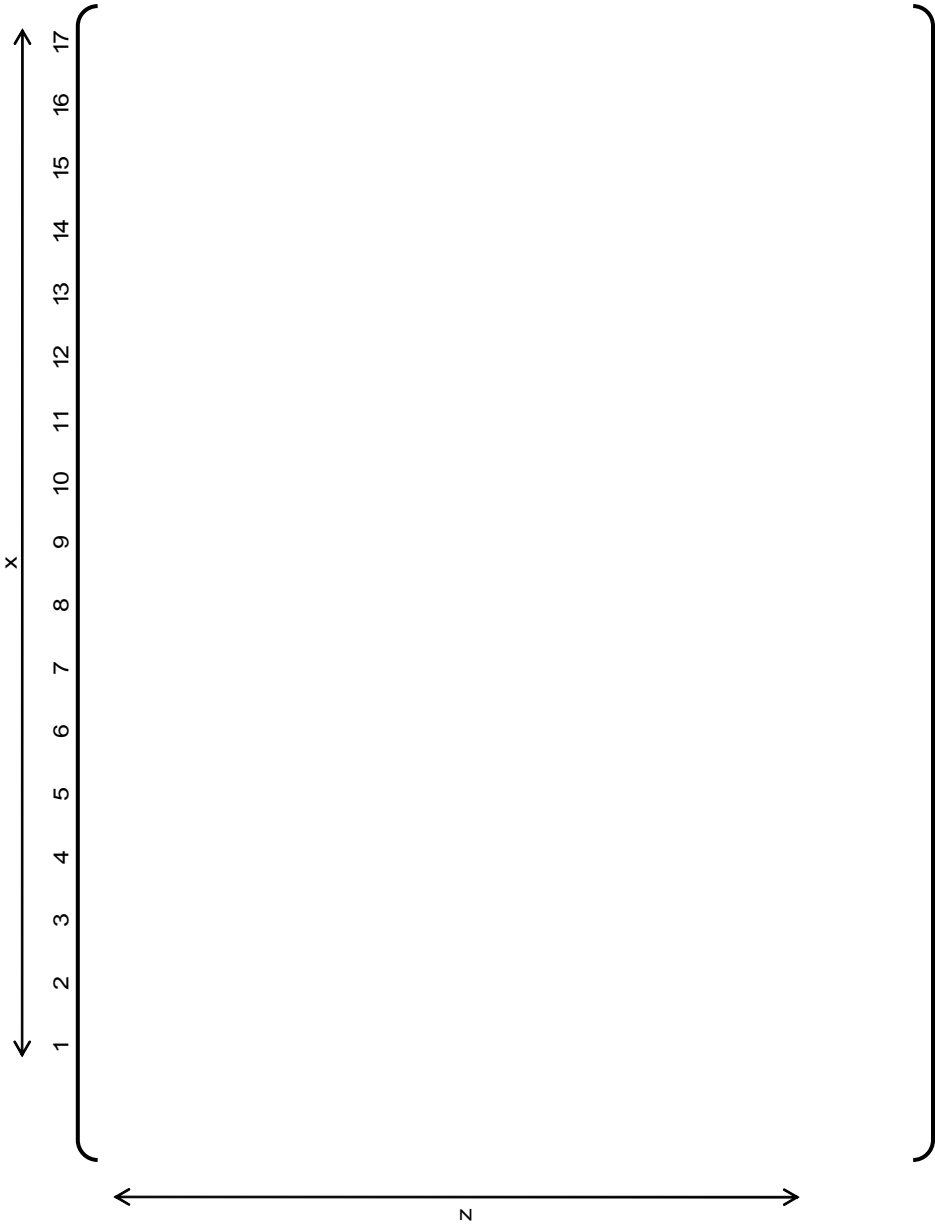


Table F.4-2 Best Estimated Bending Stress for Seismic and LOCA Horizontal Direction
(Fuel Cladding)

(Unit: MPa)

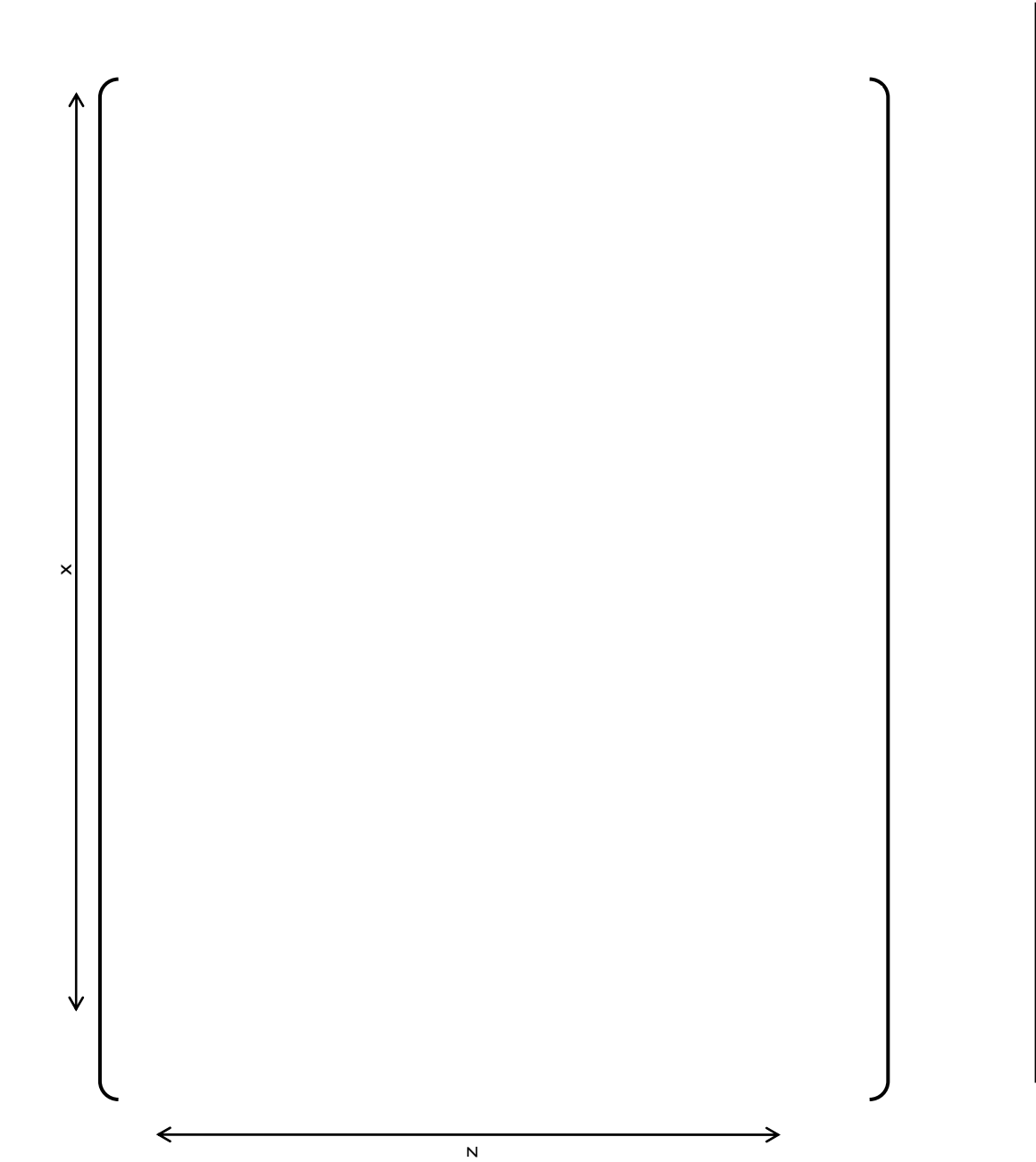


Table F.4-3 Bending Stress for Seismic and LOCA Horizontal Direction
(Control Rod Guide Thimble) including Uncertainties

(Unit: MPa)

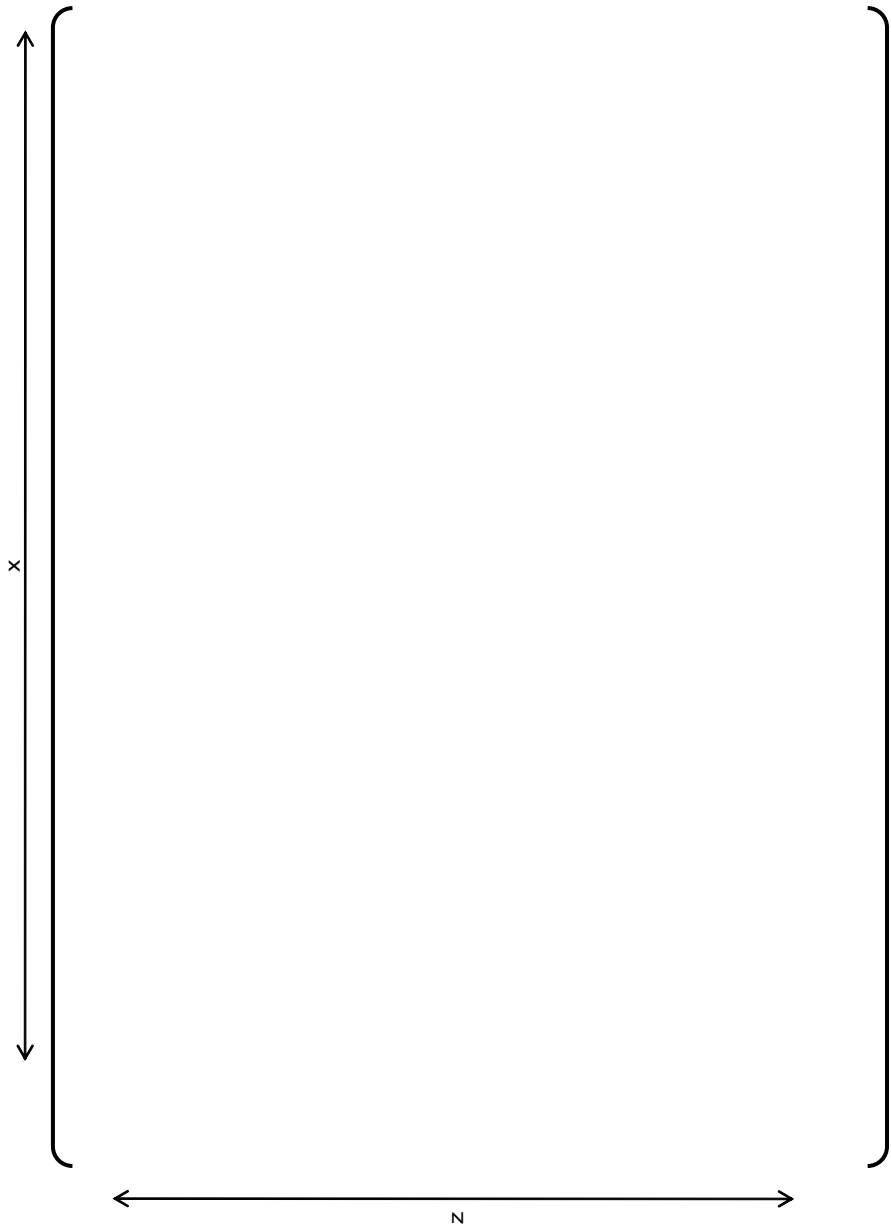
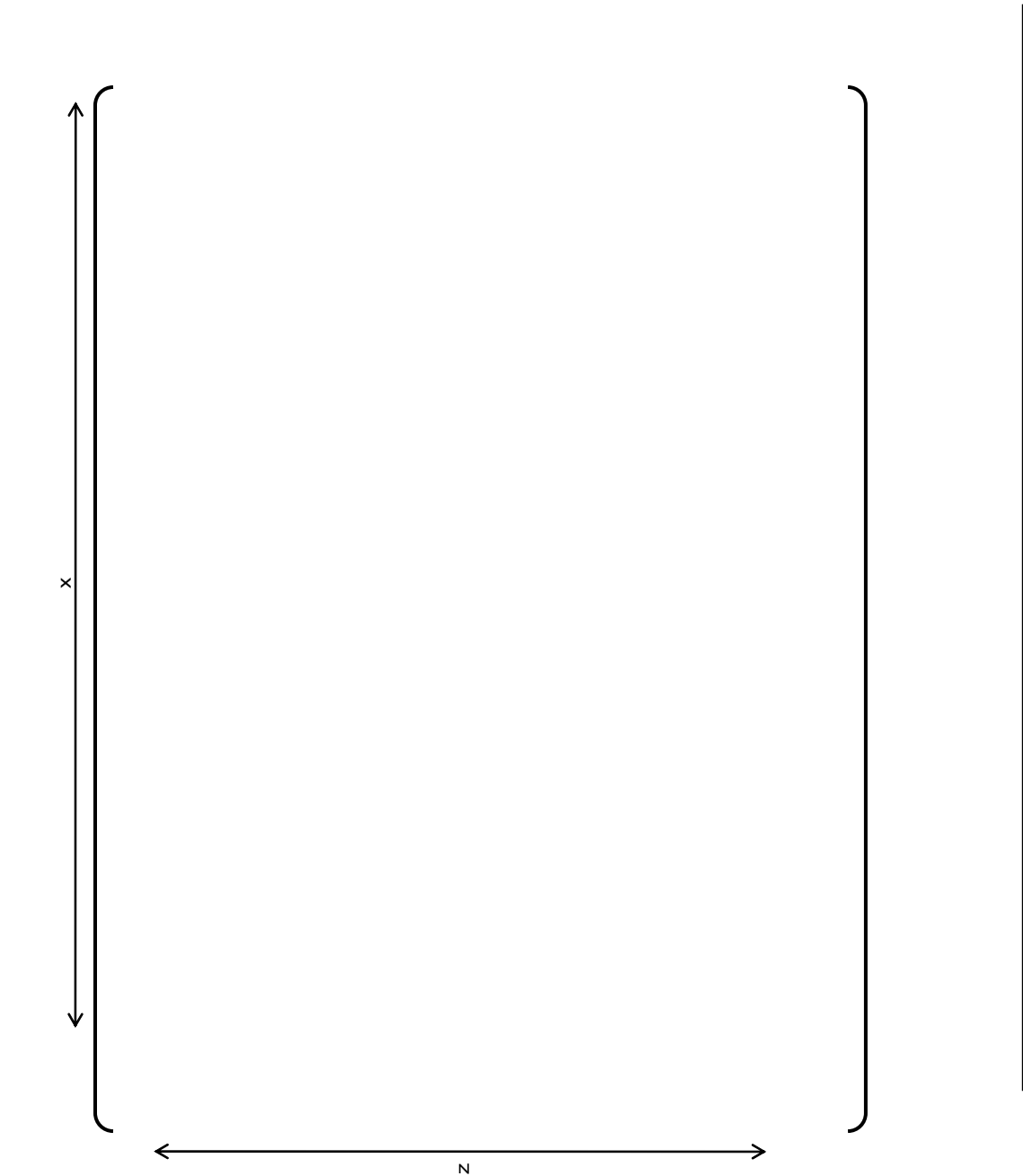


Table F.4-4 Bending Stress for Seismic and LOCA Horizontal Direction
(Fuel Cladding) including Uncertainties

(Unit: MPa)



F.5.0 PARAMETRIC STUDY OF FINDS INPUT UNCERTAINTY

F.5.1 Introduction

A parametric study is performed to determine the sensitivity of FINDS results to the variations in input amplitude and frequency, using the representative US-APWR plant acceleration wave with the nominal input for the EOL condition, which was confirmed to be the limiting condition.

The variations in input amplitude and frequency of 10 percent respectively can be considered as the uncertainty evaluation in compliance with the Appendix A Section II.3 of Reference F-1.

F.5.2 Effect of FINDS input uncertainty

F.5.2.1 Effect of input acceleration amplitude uncertainty

In this section, the effect of variation in input acceleration amplitude by 10 percent is discussed, consistent with Appendix A Section II.3 of Reference F-1.

The FINDS dynamic analysis is performed using 1.1 times the original 560-100 wave amplitude and the analysis results are shown in Table F.5-1. The analysis is performed using the 560-100 wave which gives the maximum fuel assembly deflection. The results are compared with the original results in the x and the z direction to quantify the effect of the amplitude variation.

Since a 10 percent change in input amplitude only resulted in a () percent increase (compared to the allowable of 15%) in the fuel assembly response, acceptable model sensitivity exists. Therefore no sensitivity factor due to input acceleration amplitude variation needs to be applied to the fuel assembly analysis results.

F.5.2.2 Effect of frequency uncertainty

In this section, the effect of variation in input acceleration frequency by ± 10 percent is discussed, consistent with Appendix A Section II.3 of Reference F-1.

The sensitivity analysis of the input acceleration frequency is performed using 1.1 and 0.9 times the original 560-100 wave frequencies and the results are shown in Table F.5-2 for the x and z direction.

Since a ± 10 percent change in frequency only resulted in a () percent increase in the fuel assembly response, acceptable model sensitivity exists. Therefore no sensitivity factor due to input frequency variation needs to be applied to the fuel assembly response standard analysis results.

F.5.3 Conclusion

The effect of the input uncertainties is discussed and the sensitivity of these uncertainties when using the representative US-APWR plant acceleration wave is confirmed to be less than the allowable variation of 15 percent.

**Table F.5-1 Sensitivity Result for the Input Acceleration Amplitude
(SSE 560-100 Wave)**

Wave	Units	SSE 560-100			
Variation	-	amplitude of +10%		standard	
Direction	-	x	z	x	z
Maximum displacement					
Time					
Fuel assembly number					
Grid number					
Maximum Impact force*					
Time					
Fuel assembly number **					
Grid number					

* Buckling force of the grid spacer is () lbf () N) in the FINDS code
 ** NR refers to the Neutron Reflector

**Table F.5-2 Sensitivity Result for the Input Acceleration Frequency
(SSE 560-100 Wave)**

Wave	Units	SSE 560-100					
Variation	-	frequency of +10%		frequency of -10%		standard	
Direction	-	x	z	x	z	x	z
Maximum displacement	inch (mm)						
Time	s						
Fuel assembly number	-						
Grid number	-						
Maximum Impact force*	lbf (N)						
Time	s						
Fuel assembly number **	-						
Grid number	-						

* Buckling force of the grid spacer is () lbf () N) in the FINDS code

** NR refers to the Neutron Reflector

F.6.0 CONCLUSION

The response analysis result and the stress analysis result due to the horizontal response for each core location for the following condition, confirmed to be the severest for the fuel assembly as shown in Appendix E of this report, was described in this appendix.

Safe shutdown earthquake (SSE):

- 560-100 (M1)

LOCA:

- CLB 8B 102%LF

Fuel assembly vibration characteristic (Most limiting case)

- EOL condition

Seismic wave uncertainty

- Nominal case and () Frequency case

Fuel assembly vibration uncertainty

- BE / BE case and () case

The number of buckled grid spacers in each assembly, shown in Table F.3-10, is used for the RCCA insertability and reactor coolability evaluation.

The maximum bending stress of the control rod guide thimble and fuel cladding due to the horizontal response including uncertainties in the core is obtained as shown in Table F.4-3 and Table F.4.-4, respectively. This stress is combined with the stress due to the vertical response and the stress due to normal operation.

F.7.0 REFERENCES

- (F-1) U.S. Nuclear Regulatory Commission, Standard Review Plan (NUREG-0800) Section 4.2, March 2007